



WILEY

# CATALYSTS FOR FINE CHEMICAL SYNTHESIS

Micro and  
Mesoporous  
Solid Catalysts

4

Eric G. Derouane

---

# Catalysts for Fine Chemical Synthesis

---

Volume 4

# Catalysts for Fine Chemical Synthesis

Series Editors

**Stanley M. Roberts, Ivan V. Kozhevnikov**

*University of Manchester, UK, University of Liverpool, UK*

**Eric G. Derouane**

*Universidade do Algarve, Faro, Portugal*

Previously Published Books in this Series

## **Volume 1: Hydrolysis, Oxidation and Reduction**

Edited by Stanley M. Roberts and Geraldine Poignant, *University of Liverpool, UK*

ISBN: 0 471 98123 0

## **Volume 2: Catalysis by Polyoxometalates**

Edited by Ivan K. Kozhevnikov, *University of Liverpool, UK*

ISBN: 0 471 62381 4

## **Volume 3: Metal Catalysed Carbon–Carbon Bond–Forming Reactions**

Edited by Stanley M. Roberts and Jianliang Xiao, *University of Liverpool, UK* and John Whittall and Tom E. Pickett, *The Heath, Runcorn Stylacats Ltd, UK*

ISBN: 0 470 861991

## **Volume 4: Microporous and Mesoporous Solid Catalysts**

Edited by Eric G. Derouane, *Universidade do Algarve, Faro, Portugal* and *Instituto Superior Técnico, Lisbon, Portugal*

ISBN: 0 471 49054 7

Forthcoming Books in this Series

## **Volume 5: Regio- and Stereo-Controlled Oxidations and Reductions**

Edited by Stanley M. Roberts and John Whittall, *University of Manchester, UK*

ISBN: 0 470 09022 7

---

# Catalysts for Fine Chemical Synthesis

---

Volume 4

# Microporous and Mesoporous Solid Catalysts

*Edited by*

**Eric G. Derouane**

*Universidade do Algarve, Faro, Portugal and  
Instituto Superior Técnico, Lisbon, Portugal*



John Wiley & Sons, Ltd

Copyright © 2006 John Wiley & Sons Ltd, The Atrium, Southern Gate, Chichester,  
West Sussex PO19 8SQ, England

Telephone (+44) 1243 779777

Email (for orders and customer service enquiries): [cs-books@wiley.co.uk](mailto:cs-books@wiley.co.uk)  
Visit our Home Page on [www.wileyeurope.com](http://www.wileyeurope.com) or [www.wiley.com](http://www.wiley.com)

All Rights Reserved. No part of this publication may be reproduced, stored in a retrieval system or transmitted in any form or by any means, electronic, mechanical, photocopying, recording, scanning or otherwise, except under the terms of the Copyright, Designs and Patents Act 1988 or under the terms of a licence issued by the Copyright Licensing Agency Ltd, 90 Tottenham Court Road, London W1T 4LP, UK, without the permission in writing of the Publisher. Requests to the Publisher should be addressed to the Permissions Department, John Wiley & Sons Ltd, The Atrium, Southern Gate, Chichester, West Sussex PO19 8SQ, England, or emailed to [permreq@wiley.co.uk](mailto:permreq@wiley.co.uk), or faxed to (+44) 1243 770620.

Designations used by companies to distinguish their products are often claimed as trademarks. All brand names and product names used in this book are trade names, service marks, trademarks or registered trademarks of their respective owners. The Publisher is not associated with any product or vendor mentioned in this book.

This publication is designed to provide accurate and authoritative information in regard to the subject matter covered. It is sold on the understanding that the Publisher is not engaged in rendering professional services. If professional advice or other expert assistance is required, the services of a competent professional should be sought.

The publisher and the author make no representations or warranties with respect to the accuracy or completeness of the contents of this work and specifically disclaim all warranties, including without limitation any implied warranties of fitness for a particular purpose. This work is sold with the understanding that the publisher is not engaged in rendering professional services. The advice and strategies contained herein may not be suitable for every situation. In view of ongoing research, equipment modifications, changes in governmental regulations, and the constant flow of information relating to the use of experimental reagents, equipment, and devices, the reader is urged to review and evaluate the information provided in the package insert or instructions for each chemical, piece of equipment, reagent, or device for, among other things, any changes in the instructions or indication of usage and for added warnings and precautions. The fact that an organization or Website is referred to in this work as a citation and/or a potential source of further information does not mean that the author or the publisher endorses the information the organization or Website may provide or recommendations it may make. Further, readers should be aware that Internet Websites listed in this work may have changed or disappeared between when this work was written and when it is read. No warranty may be created or extended by any promotional statements for this work. Neither the publisher nor the author shall be liable for any damages arising herefrom.

#### ***Other Wiley Editorial Offices***

John Wiley & Sons Inc., 111 River Street, Hoboken, NJ 07030, USA

Jossey-Bass, 989 Market Street, San Francisco, CA 94103-1741, USA

Wiley-VCH Verlag GmbH, Boschstr. 12, D-69469 Weinheim, Germany

John Wiley & Sons Australia Ltd, 42 McDougall Street, Milton, Queensland 4064, Australia

John Wiley & Sons (Asia) Pte Ltd, 2 Clementi Loop #02-01, Jin Xing Distripark, Singapore 129809

John Wiley & Sons Canada Ltd, 6045 Freemont Blvd, Mississauga, Ontario L5R 4J3, Canada

Wiley also publishes its books in a variety of electronic formats. Some content that appears in print may not be available in electronic books.

#### ***Library of Congress Cataloging-in-Publication Data***

Microporous and mesoporous solid catalysts / edited by Eric G. Derouane.

p. cm. – (Catalysts for fine chemical synthesis; v. 4)

Includes bibliographical references and index.

ISBN-13: 978-0-471-49054-8 (acid-free paper)

ISBN-10: 0-471-49054-7 (acid-free paper)

1. Catalysts—Textbooks. 2. Silica-alumina catalysts—Textbooks.

3. Zeolites—Textbooks. I. Derouane, E. G. II. Title. III. Series.

TP159.C3.M53 2006

660'.2995—dc22

2006012611

#### ***British Library Cataloguing in Publication Data***

A catalogue record for this book is available from the British Library

ISBN-13 978-0-471-49054-8

ISBN-10 0-471-49054-7

Typeset in 10/12pt Times by Thomson Digital

Printed and bound in Great Britain by TJ International Ltd, Padstow, Cornwall

This book is printed on acid-free paper responsibly manufactured from sustainable forestry in which at least two trees are planted for each one used for paper production.

---

# Contents

---

Series Preface. . . . .	ix
Preface to Volume 4 . . . . .	xi
Abbreviations . . . . .	xiii
<b>1 An Overview of Zeolite, Zeotype and Mesoporous Solids Chemistry: Design, Synthesis and Catalytic Properties . . . . .</b>	<b>1</b>
<i>Thomas Maschmeyer and Leon van de Water</i>	
1.1 Zeolites, zeotypes and mesoporous solids: synthetic aspects . . . . .	1
1.1.1 Introduction . . . . .	1
1.1.2 Synthetic aspects: template theory for zeolite synthesis . . . . .	2
1.1.3 Synthetic aspects: template theory for mesoporous oxides synthesis. . . . .	7
1.2 Design of extra-large pore zeolites and other micro- and mesoporous catalysts . . . . .	11
1.2.1 Introduction . . . . .	11
1.2.2 Extra-large pore zeolites. . . . .	11
1.2.3 Hierarchical pore architectures: combining micro- and mesoporosity. . . . .	13
1.3 Potential of post-synthesis functionalized micro- and mesoporous solids as catalysts for fine chemical synthesis. . . . .	19
1.3.1 Introduction . . . . .	19
1.3.2 Covalent functionalization . . . . .	20
1.3.3 Noncovalent immobilization approaches. . . . .	25
1.3.4 Single-site catalysts inspired by natural systems . . . . .	29
References . . . . .	30
<b>2 Problems and Pitfalls in the Applications of Zeolites and other Microporous and Mesoporous Solids to Catalytic Fine Chemical Synthesis . . . . .</b>	<b>39</b>
<i>Michel Guisnet and Matteo Guidotti</i>	
2.1 Introduction . . . . .	39
2.2 Zeolite catalysed organic reactions . . . . .	42
2.2.1 Fundamental and practical differences with homogeneous reactions . . . . .	42
2.2.2 Batch mode catalysis . . . . .	45
2.2.3 Continuous flow mode catalysis . . . . .	51
2.2.4 Competition for adsorption: influence on reaction rate, stability and selectivity . . . . .	53

2.2.5	Catalyst deactivation . . . . .	61
2.3	General conclusions . . . . .	63
	References . . . . .	64
<b>3</b>	<b>Aromatic Acetylation . . . . .</b>	<b>69</b>
	<i>Michel Guisnet and Matteo Guidotti</i>	
3.1	Aromatic acetylation . . . . .	69
3.1.1	Acetylation with Acetic Anhydride . . . . .	70
3.1.2	Acetylation with Acetic Acid . . . . .	82
3.2	Procedures and protocols . . . . .	89
3.2.1	Selective synthesis of acetophenones in batch reactors through acetylation with acetic anhydride . . . . .	89
3.2.2	Selective synthesis of acetophenones in fixed bed reactors through acetylation with acetic anhydride . . . . .	90
	References . . . . .	91
<b>4</b>	<b>Aromatic Benzoylation . . . . .</b>	<b>95</b>
	<i>Patrick Geneste and Annie Finiels</i>	
4.1	Aromatic benzoylation . . . . .	95
4.1.1	Effect of the zeolite . . . . .	96
4.1.2	Effect of the acylating agent . . . . .	97
4.1.3	Effect of the solvent. . . . .	97
4.1.4	Benzoylation of phenol and the Fries rearrangement . . . . .	97
4.1.5	Kinetic law . . . . .	99
4.1.6	Substituent effect. . . . .	100
4.1.7	Experimental. . . . .	101
4.2	Acylation of anisole over mesoporous aluminosilicates. . . . .	102
	References . . . . .	103
<b>5</b>	<b>Nitration of Aromatic Compounds . . . . .</b>	<b>105</b>
	<i>Avelino Corma and Sara Iborra</i>	
5.1	Introduction. . . . .	105
5.2	Reaction mechanism. . . . .	106
5.3	Nitration of aromatic compounds using zeolites as catalysts . . . . .	107
5.3.1	Nitration in liquid phase. . . . .	107
5.3.2	Vapour phase nitration . . . . .	116
5.4	Conclusions. . . . .	118
	References . . . . .	118
<b>6</b>	<b>Oligomerization of Alkenes. . . . .</b>	<b>125</b>
	<i>Avelino Corma and Sara Iborra</i>	
6.1	Introduction. . . . .	125
6.2	Reaction mechanisms . . . . .	126
6.3	Acid zeolites as catalysts for oligomerization of alkenes . . . . .	127
6.3.1	Medium pore zeolites: influence of crystal size and acid site density. . . . .	127
6.3.2	Use of large pore zeolites. . . . .	130
6.3.3	Catalytic membranes for olefin oligomerization. . . . .	131
6.4	Mesoporous aluminosilicates as oligomerization catalysts. . . . .	131
6.5	Nickel supported aluminosilicates as catalysts . . . . .	132
	References . . . . .	136

<b>7 Microporous and Mesoporous Catalysts for the Transformation of Carbohydrates</b> . . . . .	141
<i>Claude Moreau</i>	
7.1 Introduction . . . . .	141
7.2 Hydrolysis of sucrose in the presence of H-form zeolites . . . . .	142
7.3 Hydrolysis of fructose and glucose precursors . . . . .	143
7.4 Isomerization of glucose into fructose . . . . .	144
7.5 Dehydration of fructose and fructose-precursors. . . . .	145
7.6 Dehydration of xylose. . . . .	146
7.7 Synthesis of alkyl-D-glucosides . . . . .	147
7.7.1 Synthesis of butyl-D-glucosides . . . . .	147
7.7.2 Synthesis of long-chain alkyl-D-glucosides . . . . .	150
7.8 Synthesis of alkyl-D-fructosides . . . . .	151
7.9 Hydrogenation of glucose . . . . .	151
7.10 Oxidation of glucose . . . . .	153
7.11 Conclusions . . . . .	154
References . . . . .	154
<b>8 One-pot Reactions on Bifunctional Catalysts</b> . . . . .	157
<i>Michel Guisnet and Matteo Guidotti</i>	
8.1 Introduction . . . . .	157
8.2 Examples . . . . .	158
8.2.1 One-pot transformations involving successive hydrogenation and acid–base steps. . . . .	158
8.2.2 One-pot transformations involving successive oxidation and acid–base steps . . . . .	166
References . . . . .	168
<b>9 Base-type Catalysis</b> . . . . .	171
<i>Didier Tichit, Sara Iborra, Avelino Corma and Daniel Brunel</i>	
9.1 Introduction . . . . .	171
9.2 Characterization of solid bases. . . . .	172
9.2.1 Test reactions . . . . .	172
9.2.2 Probe molecules combined with spectroscopic methods . . . . .	174
9.3 Solid base catalysts . . . . .	175
9.3.1 Alkaline earth metal oxides. . . . .	175
9.3.2 Catalysis on alkaline earth metal oxides . . . . .	177
9.3.3 Hydrotalcites and related compounds . . . . .	183
9.3.4 Organic base-supported catalysts . . . . .	187
9.4 Conclusions . . . . .	195
References . . . . .	195
<b>10 Hybrid Oxidation Catalysts from Immobilized Complexes on Inorganic Microporous Supports</b> . . . . .	207
<i>Dirk De Vos, Ive Hermans, Bert Sels and Pierre Jacobs</i>	
10.1 Introduction and scope . . . . .	207
10.2 Oxygenation potential of heme-type complexes in zeolite. . . . .	211
10.2.1 Metallo-phthalocyanines encapsulated in the cages of faujasite-type zeolites . . . . .	211
10.2.2 Oxygenation potential of metallo-phthalocyanines encapsulated in the mesopores of VPI-5 $\text{AlPO}_4$ . . . . .	215



10.2.3	Oxygenation potential of zeolite encapsulated metallo-porphyrins . . . . .	216
10.3	Oxygenation potential of zeolite encapsulated nonheme complexes . . . .	220
10.3.1	Immobilization of <i>N,N'</i> -bidentate complexes in zeolite Y . . . .	220
10.3.2	Ligation of zeolite exchanged transition ions with bidentate aza ligands . . . . .	224
10.3.3	Ligation of zeolite exchanged transition ions with tri- and tetra-aza(cyclo)alkane ligands . . . . .	225
10.3.4	Ligation of zeolite exchanged transition ions with Schiff base-type ligands . . . . .	228
10.3.5	Zeolite effects with <i>N,N'</i> -bis(2-pyridinecarboxamide) complexes of Mn and Fe in zeolite Y . . . . .	231
10.3.6	Zeolite encapsulated chiral oxidation catalysts . . . . .	233
10.4	Conclusions . . . . .	235
	Acknowledgements . . . . .	235
	References . . . . .	235
	Subject Index . . . . .	241

---

# Catalysts for Fine Chemical Synthesis Series Preface

---

During the early-to-mid 1990s we published a wide range of protocols, detailing the use of biotransformations in synthetic organic chemistry. The procedures were first published in the form of a loose-leaf laboratory manual and, recently, all the protocols have been collected together and published in book form (*Preparative Biotransformations*, John Wiley & Sons, Ltd, Chichester, 1999).

Over the past few years the employment of enzymes and whole cells to carry out selected organic reactions has become much more commonplace. Very few research groups would now have any reservations about using commercially available biocatalysts such as lipases. Biotransformations have become accepted as powerful methodologies in synthetic organic chemistry.

Perhaps less clear to a newcomer to a particular area of chemistry is when to use biocatalysis as a key step in a synthesis, and when it is better to use one of the alternative non-natural catalysts that may be available. Therefore we set out to extend the objective of *Preparative Biotransformations*, so as to cover the whole panoply of catalytic methods available to the synthetic chemist, incorporating biocatalytic procedures where appropriate.

In keeping with the earlier format we aim to provide the readership with sufficient practical details for the preparation and successful use of the relevant catalyst. Coupled with these specific examples, a selection of the products that may be obtained by a particular technology will be reviewed.

In the different volumes of this new series we will feature catalysts for oxidation and reduction reactions, hydrolysis protocols and catalytic systems for carbon-carbon bond formation *inter alia*. Many of the catalysts featured will be chiral, given the present day interest in the preparation of single-enantiomer fine chemicals. When appropriate, a catalyst type that is capable of a wide range of transformations will be featured. In these volumes the amount of practical data that is described will be proportionately less, and attention will be focused on the past uses of the system and its future potential.

Newcomers to a particular area of catalysis may use these volumes to validate their techniques, and, when a choice of methods is available, use the background

information better to delineate the optimum strategy to try to accomplish a previously unknown conversion.

**S. M. ROBERTS**  
**I. KOZHEVNIKOV**  
**E. G. DEROUANE**  
**Liverpool, 2002**

---

# Preface to Volume 4: Microporous and Mesoporous Solid Catalysts

---

Previous Volumes in this Series have described, in general, practical tips for performing topical reactions. Volume 2 was however dedicated specifically to 'Catalysis by Polyoxometalates'. The present Volume features recent advances in the application of microporous and mesoporous solid catalysts to fine chemical synthesis, a field that is receiving increasing attention because of its high potential for the development of 'green' processes for the synthesis of fine chemicals.

Reactions for the synthesis of fine chemicals differ in many aspects from the hydrocarbon reactions that constitute today the major application of zeolites and other micro- or mesoporous catalysts, as they often involve the transformation of molecules with several functional groups. Chemoselectivity is therefore of prime importance. These reactions are generally operated in rather mild conditions and condensed media (rather than vapour phase) to avoid undesired secondary reactions. The use of solvents can have major impacts on the activity and selectivity of these catalysts as they may affect the adsorption and desorption of reactants and products on these catalysts.

The unique properties of zeolites and other micro- or mesoporous solids that may favour their application to fine chemical synthesis are: (1) the compatibility between the size and shape of their channels or cavities with the size of the reactants and/or products (generally referred to as molecular shape selectivity) that may direct the reaction away from the thermodynamically favoured route; (2) the occurrence of confinement effects increasing the concentration of reactants near the catalytic sites; and (3) the ability to tune their catalytic properties (acidic, basic, or other) via various treatments as described in this Volume.

Several excellent and exhaustive reviews of organic reactions catalysed by zeolites and mesoporous solids have been published. They are cited appropriately in the various chapters of this Volume that, instead of aiming for completeness, is focusing on a general illustration of the effects that such catalysts can have on fine chemical transformations.

Chapter 1 is a general overview of zeolite, zeotype and mesoporous solids chemistry, including their design, synthesis and general catalytic properties. Chapter 2 deals with the problems and pitfalls that may occur in the applications of zeolites and other microporous and mesoporous solids to fine chemical synthesis. The remaining chapters deal with specific applications of these catalysts to fine chemical synthesis.

The Editors, last but not least, wish to thank all the authors who have contributed to this Volume for the high quality of their respective Chapters. We hope that this Volume will trigger the interest and allow other scientists to enter a research field that is exciting and is proving to be more and more important for sustainable fine chemical synthesis.

**ERIC G. DEROUANE**

**Lisbon and Faro, 2005**

---

# Abbreviations

---

AFM	atomic force microscopy
BET	Brunauer–Emmett–Teller
cod	1,5-cyclooctadiene (ligand)
CP-MAS	cross-polarization magic-angle spinning
ee	enantiomeric excess
EPR	electron paramagnetic resonance
ESR	electron spin resonance
EXAFS	extended X-ray absorption fine structure
FID	flame ionization detector
FTIR	Fourier transform infrared spectroscopy
GC	gas chromatography
HOMO	highest occupied molecular orbital
HR-TEM	high resolution transmission electron microscopy
IR	infrared spectroscopy
LUMO	lowest unoccupied molecular orbital
MLCT	metal-to-ligand charge transfer
NMR	nuclear magnetic resonance
PTFE	poly(tetrafluoroethylene)
salen	1,6-bis(2-hydroxyphenyl)-2,5-diaza-1,5-hexadiene (ligand)
SAXS	small-angle X-ray scattering
SDA	structural directing agent
SQUID	superconducting quantum interference device
TG	thermogravimetry
TGA	thermogravimetric analysis
TOF	turnover frequency
UV	ultraviolet
vis	visible
WAXS	wide-angle X-ray scattering
XAS	X-ray absorption spectroscopy
XPS	X-ray photoelectron spectroscopy
XRD	X-ray diffraction



---

# 1 An Overview of Zeolite, Zeotype and Mesoporous Solids Chemistry: Design, Synthesis and Catalytic Properties

---

THOMAS MASCHMEYER AND LEON VAN DE WATER

*Laboratory of Advanced Catalysis for Sustainability, School of Chemistry – F11,  
The University of Sydney, NSW 2006, Australia*

## CONTENTS

1.1	ZEOLITES, ZEOTYPES AND MESOPOROUS SOLIDS: SYNTHETIC ASPECTS . . . . .	1
1.1.1	Introduction . . . . .	1
1.1.2	Synthetic aspects: template theory for zeolite synthesis . . . . .	2
1.1.3	Synthetic aspects: template theory for mesoporous oxides synthesis . . . . .	7
1.2	DESIGN OF EXTRA-LARGE PORE ZEOLITES AND OTHER MICROPOROUS AND MESOPOROUS CATALYSTS	11
1.2.1	Introduction . . . . .	11
1.2.2	Extra-large pore zeolites . . . . .	11
1.2.3	Hierarchical pore architectures: combining microporous and mesoporosity	13
1.3	POTENTIAL OF POST-SYNTHESIS FUNCTIONALIZED MICROPOROUS AND MESOPOROUS SOLIDS AS CATALYSTS FOR FINE CHEMICAL SYNTHESIS . . . . .	19
1.3.1	Introduction . . . . .	19
1.3.2	Covalent functionalization . . . . .	20
1.3.3	Noncovalent immobilization approaches . . . . .	25
1.3.4	Single-site catalysts inspired by natural systems . . . . .	29
	REFERENCES . . . . .	30

## 1.1 ZEOLITES, ZEOTYPES AND MESOPOROUS SOLIDS: SYNTHETIC ASPECTS

### 1.1.1 INTRODUCTION

The role that porous catalytic solids play in the production of a diverse range of everyday items, such as plastics, washing powders, fuels or pharmaceuticals, can hardly be overestimated. However, not all manufacturing processes rely on catalytic



technology at every step. Particularly fine chemicals and pharmaceuticals synthesis still employ classic stoichiometric approaches to a significant extent. Therefore, the development of new catalysts with even better characteristics in terms of activity, selectivity and stability is an on-going challenge. Initially, we will address the principles underlying the preparation of catalytically relevant microporous and mesoporous oxidic materials. Subsequently several sections deal with the various methods currently available to modify as-synthesized materials into single-site catalysts with well-defined properties.

Porous oxide catalytic materials are commonly subdivided into microporous (pore diameter  $<2$  nm) and mesoporous (2–50 nm) materials. Zeolites are aluminosilicates with pore sizes in the range of 0.3–1.2 nm. Their high acidic strength, which is the consequence of the presence of aluminium atoms in the framework, combined with a high surface area and small pore-size distribution, has made them valuable in applications such as shape-selective catalysis and separation technology. The introduction of redox-active heteroatoms has broadened the applicability of crystalline microporous materials towards reactions other than acid-catalysed ones.

Since mesoporous materials contain pores from 2 nm upwards, these materials are not restricted to the catalysis of small molecules only, as is the case for zeolites. Therefore, mesoporous materials have great potential in catalytic/separation technology applications in the fine chemical and pharmaceutical industries. The first mesoporous materials were pure silicates and aluminosilicates. More recently, the addition of key metallic or molecular species into or onto the siliceous mesoporous framework, and the synthesis of various other mesoporous transition metal oxide materials, has extended their applications to very diverse areas of technology. Potential uses for mesoporous ‘smart’ materials in sensors, solar cells, nanoelectrodes, optical devices, batteries, fuel cells and electrochromic devices, amongst other applications, have been suggested in the literature.<sup>[1–5]</sup>

### 1.1.2 SYNTHETIC ASPECTS: TEMPLATE THEORY FOR ZEOLITE SYNTHESIS

Aluminosilicate zeolites have been produced synthetically since the 1950s. In the 1960s tetraalkylammonium ions were added to zeolite synthesis gels, resulting in the synthesis of new structures such as the ZSM-5 family of zeolites.<sup>[6]</sup> ‘Template Theory’ evolved to explain the structure-directing effects of organic species in zeolite synthesis gels.<sup>[7]</sup> Charge distribution, size and geometric shape of the template species were believed to be the main causes of the structure-directing process. Factors such as pH, concentration,  $\text{SiO}_2/\text{Al}_2\text{O}_3$  ratio, ageing, agitation and temperature were considered to be the main determinants of the gel chemistry that influence the outcome of the zeolite crystallization process. However, addition of organic template species affected the gel chemistry of zeolite synthesis mixtures also and it was not clear which factors dominated, template activity or gel chemistry, in the determination as to which product formed.<sup>[8]</sup> Although at first glance it may have appeared that there was a good correlation between template

structure and pore architecture, the development of new synthetic procedures for making zeolites using organic templates has been, and still is, conducted chiefly by trial and error.<sup>[9]</sup>

Generally, zeolite synthesis mixtures contain a silicon (and aluminium) precursor, a template species (alternatively called structure-directing agent, SDA) which can be either an organic species or an alkali metal ion, water, and a so-called mineralizing agent. This mineralizing agent, usually  $\text{OH}^-$ , or  $\text{F}^-$  in some more recent studies,<sup>[10]</sup> leads to the partial dissolution of any silica network formed, thereby making the zeolite formation process reversible and steering it away from very unstable structures for any given set of synthesis conditions. This is important as less regular phases and phase mixtures would otherwise be the result. The relation between SDA and the framework structure formed has been thoroughly investigated. For example, the group of Zones and Davis systematically probed the effect of rigid, bulky organocationic SDAs on the final zeolite structures obtained.<sup>[11]</sup> The SDAs were designed to destabilize the structure of commonly occurring competing phases, and three new zeolitic phases were indeed reported from this study. Molecular modelling confirmed the correlation between the structure of the SDA and that of the observed zeolite phase. However, in contrast to the results from this study, it is in most cases not possible to derive a one-to-one relationship between template and framework structure. Despite the progress made, the question why certain templates induce certain zeolite structures still remains largely unanswered, especially in the case of the smaller, less rigid tetraalkylammonium templates. Zeolite crystallization appears largely kinetically controlled, which means that instead of the thermodynamically most stable product often the species that nucleates most easily is formed.<sup>[9]</sup> Therefore, the term 'template' should be used only in those cases where a true one-to-one relationship between organic species and inorganic framework structure exists. Often, one might view the 'template' rather acting as a crystal growth moderator (nucleation and/or retardation) than as a true template.

The development of the understanding of the underlying principles of zeolite synthesis has been reviewed recently by Cundy and Cox.<sup>[12]</sup> The initial stages of the organization of the silica precursor around the template molecules have been studied by many authors. In most cases, the tetrapropylammonium hydroxide (TPAOH)–tetraethoxy silane (TEOS)–water system has been the subject of these fundamental studies. Burkett and Davis<sup>[13,14]</sup> described the organization of the silicon source and the organic template species as the result of van der Waals interactions, where hydrophobic alkyl chains of the template and hydrophobic silicon atoms closely interact. It is proposed that an organized, hydrophobic water layer is formed around the alkyl chains, which can be considered as an organized hydration mantle (Figure 1.1).

A similar organized solvent mantle is proposed to be present around the silicate species and a displacement of the hydration mantle around the SDA by the silicate species is the origin of the SDA–silicate interaction. Long-range order is attained in a consecutive layer-by-layer zeolite growth step. This proposed formation mechanism is in agreement with results of an *in situ* SAXS and WAXS study by de Moor *et al.*<sup>[15]</sup> of the same system. Their results show the initial formation of colloidal

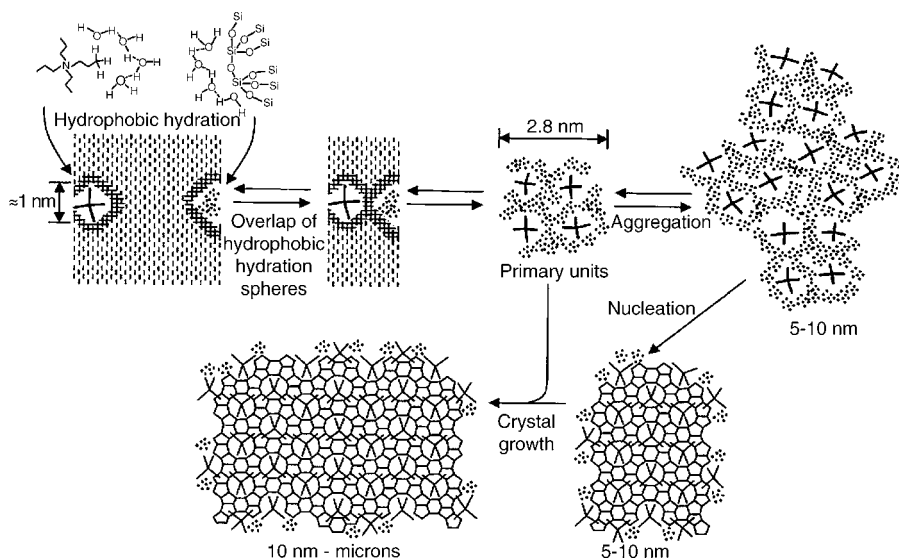


**Figure 1.1** Scheme for the crystallization mechanism of Si-TPA-MFI. Reproduced from Corma and Davis<sup>[28]</sup> by permission of Wiley-VCH

amorphous aggregates, which are not organized further in a secondary aggregation step, but instead, redissolve and act as a source of nutrients for the growing crystallites. It was also found that the alkalinity of the clear synthesis gel solution plays an important role in the size of the final crystal: at higher alkalinity a smaller number of viable nuclei are being formed, giving rise to larger crystals. In contrast to this formation mechanism, other authors have suggested the formation of small, highly organized silicate–SDA clusters, so-called secondary building units, a concept already proposed by one of the founding fathers of zeolite chemistry.<sup>[16]</sup> According to the research group in Leuven, these building blocks form during the earliest stages of zeolite preparation, i.e. already during the mixing of the silicon precursor, the TPAOH template and water at ambient temperature and pressure. These precursor species, with dimensions of  $1.3 \times 4.0 \times 4.0$  nm (‘nanoblocks’ or ‘nanoslabs’), contain features specific for the MFI structure, as was concluded from IR data.<sup>[17]</sup> It was also found that this species contains TPA in the channel intersections. In a subsequent paper the same authors show, on the basis of a  $^{29}\text{Si}$  NMR study, that TPA cations are present at the liquid–liquid TEOS–water interface, with their propyl chains pointing into the TEOS layer.<sup>[18]</sup> The hydrolysis–condensation reactions of the TEOS molecules require close contacts with the template, indicating that the structure direction by the template and the hydrolysis take place simultaneously. Initially, tetracyclic undecamers are formed, and after 45 min at room temperature trimers of this entity (i.e. 33-mers) were observed (Figure 1.2). This species contains hydroxyl groups on its outer surface, allowing migration into the aqueous layer.<sup>[18]</sup> Aggregation of these building blocks occurs very slowly due to electrostatic repulsion between the negatively charged silicate entities. This charge

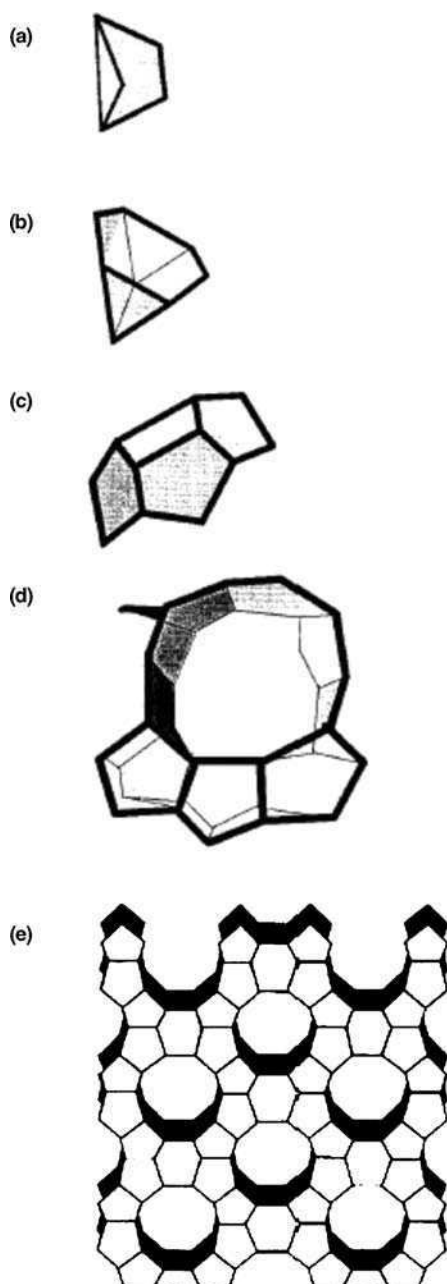


**Figure 1.2** Siliceous entities occurring in the TPAOH-TEOS system: (a) bicyclic pentamer; (b) pentacyclic octamer; (c) tetracyclic undecamer; (d) 'trimer' in mixtures with composition  $(\text{TPAOH})_{0.36}(\text{TEOS})(\text{H}_2\text{O})_{6.0}$ , (e) nanoslab in mixtures with composition  $(\text{TPAOH})_{0.36}(\text{TEOS})(\text{H}_2\text{O})_{17.5}$ . Reproduced from Kirschhock *et al.*, *J. Phys. Chem. B*, **1999**, *103*, 4972-4978 by permission of American Chemical Society

is compensated by the  $\text{TPA}^+$  template species, which explains their structure-directing effect upon condensation of the zeolite framework around it.

Bu *et al.* investigated the role of methyl amine as the organic template in the synthesis of a series of zeotype germanates. In the absence of the template a two-dimensional layered structure was formed. In contrast, in the presence of methylamine a three-dimensional framework evolved from these sheets.<sup>[19]</sup>

The presence of (quaternized) amines is not a prerequisite for the formation of a zeolite. Some zeolites can be prepared by using an alkali metal ion species as the SDA, examples being zeolites A, X, and Y (for details see International Zeolite Association website, <http://www.izasyntesis.org/>). The formation mechanism of these zeolites has not been investigated in great detail. Atomic force microscopy (AFM) was used to study the role of defects on the growth process of zeolites Y, A, and Silicalite-1.<sup>[20]</sup> It was found that the surface of the growing crystals in zeolite Y is composed of terraces with a height of 15 Å, corresponding to the height of a faujasite sheet. Similarly, a terrace height of 12 Å was observed for zeolite A, which corresponds to the size of a sodalite cage. These observations have been explained by assuming a layer-by-layer growth process, where template ions decorate the surface of the negatively charged growing zeolite crystal. However, the role that alkali metal ions play in the growth process was not elucidated in this study. This ‘terrace-ledge-kink’ growth mechanism is in agreement with a study by Bosnar *et al.*<sup>[21]</sup> who investigated the role of  $\text{Na}^+$  concentration on the growth rate of zeolite A. It was found that the  $\text{Na}^+$  ions take part in the surface reaction by balancing the surface charge. The growth rate was found to increase with increasing  $\text{Na}^+$  concentration.

It is clear that for a better understanding of the zeolite formation mechanism, *in situ* characterization techniques are essential. The aforementioned studies involve *in situ* IR,  $^{29}\text{Si}$  NMR and X-ray scattering techniques,<sup>[13–15,17]</sup> although only the gel stage of the zeolite formation process was covered in these cases. The next step is the study of the crystallization process for these microporous materials, and indeed several research groups have reported such *in situ* investigations.<sup>[15,22,23]</sup> Unfortunately, only one analytical technique was used in each of these studies, which makes it difficult to obtain information on all aspects of the crystal growth process. Very recently, Grandjean *et al.* reported the combination of multiple time-resolved *in situ* techniques, namely SAXS–WAXS, UV–vis, Raman and XAS, for probing the crystallization of a cobalt-modified aluminophosphate material, Co-APO-5.<sup>[24]</sup> This study showed that the alumina and phosphoric acid precursors react instantaneously after mixing to form Al–O–P chains (Raman data). These largely covalent polymeric structures are then thought to agglomerate, in a similar way to the nanoslabs as introduced by Ravishankar *et al.*<sup>[17]</sup> and Kirschhock *et al.*<sup>[18]</sup> In the Co-APO-5 study it was shown that the size of these primary particles increases from 7 nm in the very beginning of the heating process to 20 nm just before the start of the crystallization. The coordination number of about half of the  $\text{Co}^{2+}$  ions in the mixture changes slowly from 6 to 4 in the heating stage prior to crystallization (EXAFS data). The crystallization abruptly begins at around 155–160 °C, which was derived from the rapid transformation of the remaining octahedral  $\text{Co}^{2+}$  to tetrahedral coordination, as observed with EXAFS and UV–vis spectroscopies.

However, the structure-directing effect of the template on the final framework structure was not elucidated even in this study. *In situ* studies into the structural features of the template species at the gel stage and during crystallization are needed to shed more light on this issue.

In recent years, some progress has been made in understanding zeolite templating by using computer modelling. Attempts have been made to predict the templates required for certain zeolite syntheses by Lewis *et al.*<sup>[25,26]</sup> Both known templates and a new one, which was subsequently proven experimentally to direct a certain zeolite structure, were generated by the model. However, the interactions between template and silicate host are often more complex than this space-filling approach assumes and further fine-tuning is needed.<sup>[9]</sup>

The zeolite framework type that is formed during hydrothermal treatment is not only a function of the applied SDA. The introduction of heteroatoms other than silicon or aluminium in the framework may stabilize certain structural features, thereby allowing the formation of zeolite structures that are not attainable otherwise. Blasco *et al.* used Hartree–Fock *ab initio* methods to discover that the presence of small amounts of Ge<sup>4+</sup> in the silica framework stabilizes double four-membered rings (D4MR), cubic subunits formed by two rings each containing four silicon atoms.<sup>[27]</sup> D4MR are absent in most known silicate frameworks,<sup>[28]</sup> as the strain present in this arrangement makes them highly unstable. By replacing some of the Si–O–Si linkages by Si–O–Ge, some of the strain can be released. This stabilizing effect has been successfully applied by the same authors to synthesize a hitherto unknown polymorph of zeolite Beta, polymorph C, which can only be made by introducing a germanium precursor to the synthesis gel.<sup>[29]</sup> This study shows that in some cases computational techniques can be successfully applied to predict the beneficial effect of this type of isomorphous substitution.

### 1.1.3 SYNTHETIC ASPECTS: TEMPLATE THEORY FOR MESOPOROUS OXIDES SYNTHESIS

Mesoporous oxides are formed in the presence of surfactant-type template molecules. These species form micelle aggregates in aqueous environments. The organization mechanism of the monomeric silica species around these ‘micellar rods’ was coined the ‘Liquid Crystal Templating’ (LCT) mechanism. Subsequent hydrothermal treatment and calcination leads to condensation of the silica species and removal of the organic template species, respectively. The concurrent discovery of M41S materials by Mobil scientists in 1992 and the discovery of the very similar material FSM-16 (formed by recrystallization of kanemite after ion exchange of the Na<sup>+</sup> ions for tetraalkyl ammonium ions) by Inagaki *et al.* in 1994 mark the beginning of the new era of well-defined, periodic mesoporous oxides.<sup>[30–33]</sup> A great deal of work has been directed towards refining the dilute regime synthetic procedure and improving the properties of the resulting mesoporous materials since. Mesoporous materials are generally synthesized at low temperatures (25–100 °C) so that the condensation reactions are predominantly kinetically controlled.<sup>[34]</sup> The silica

mesopore walls in these materials are amorphous on an atomic scale, which means that they are thermodynamically less stable than the metastable zeolite frameworks. Quartz is thermodynamically the most stable form of silica and prolonged high temperature heating of either mesoporous silica or all silica zeolites would eventually lead to its formation.

In the original papers describing the synthesis of M41S materials,<sup>[30,31]</sup> the pore diameters of the mesoporous materials were determined by the choice of surfactant template, and also by the use of an auxiliary organic molecule, mesitylene (1,3,5-trimethylbenzene). Pore diameters ranging between 20 and 100 Å were obtained. Further investigations by the same research group revealed that with the same synthesis, different mesophases could be produced. Apart from MCM-41, which forms around rod-like micellar surfactant aggregates, a cubic phase with a three-dimensional pore system, MCM-48, was observed when a spherical organization of the surfactant species, instead of a rod-like one, occurs. It was reported that the surfactant to silica ratio was the crucial parameter in determining the shape of the micelle aggregates.<sup>[35]</sup> More recently, *n*-alkanes of different chain lengths were used as swelling agents for the mesoporous products.<sup>[36]</sup> The pore diameters of the products increased proportionally with the length of the *n*-alkanes, containing up to 15 carbon atoms. The pore diameter of mesoporous products has also been controlled by adjusting the synthesis gel and crystallization variables. In the presence of tetramethyl ammonium cations, mesoporous products were formed after 24 h, and the pore size increased with longer crystallization times.<sup>[37]</sup> Similar results were obtained by Cheng *et al.*, where the pure silica MCM-41 channel diameter was varied between 26.1 and 36.5 Å, and the wall thickness was varied between 13.4 and 26.8 Å, simply by using different synthesis temperatures (70–200 °C) and/or reaction times.<sup>[38]</sup> In general, MCM-41 with wider pores, thicker walled channels and higher degrees of polymerization were obtained for longer reaction times. The MCM-41 structure with the thickest walls (26.8 Å) could withstand temperatures as high as 1000 °C without disintegration. The suggested explanation for the pore expansion with increasing reaction time was as follows: as reaction times are increased, the pore size of the MCM-41 product increased, reaching an upper limit very close to the diameter of a cetyltrimethyl ammonium bromide (CTAB) micelle. At high temperatures (165 °C in the work of Cheng *et al.*), some surfactant cations decompose to neutral C<sub>16</sub>H<sub>33</sub>(CH<sub>3</sub>)<sub>2</sub>N molecules, which locate themselves in the hydrocarbon core of the micelle. This has the effect of increasing the micelle diameter, and therefore the MCM-41 pore size. There is, however, an upper limit to the number of neutral amine molecules the micelles can accommodate in their core, leading to an upper limit in the swelling effect.<sup>[38]</sup>

Particle size is of particular importance for mesoporous materials containing unidirectional channels, such as MCM-41. If the mesopores are long, which might be the case in large particles, diffusion limitations could occur and in these cases it is preferable to have a very small particle size. Small particles of MCM-41 are obtained if reaction times are kept short, i.e. the mesoporous product nucleates, but has little time to grow into larger particles. Cutting the reaction times short can, however, jeopardize the silica condensation process, leading to poorly polymerized

products. Microwave heating overcomes this problem by speeding up the condensation step, allowing high quality products to form in times as short as 1 h at 150 °C.<sup>[39–42]</sup> The resulting MCM-41 crystallites are very small (approximately 100 nm in diameter).

Virtually at the same time as M41S mesoporous silicas were first being synthesized, Inagaki *et al.*<sup>[32,33]</sup> reported the synthesis of hexagonally packed channels from layered polysilicate kanemite. The mechanism for the formation of this material, FSM-16, is very different from the silicate anion-initiated MCM-41 synthesis and has been shown to occur via intercalation of the kanemite layers with surfactant molecules. Kanemite consists of flexible, poorly polymerized silicate layers which buckle around the intercalated surfactant molecules. Vartuli *et al.*<sup>[43]</sup> compared M41S materials generated from the ligand charge transfer (LCT) method with the products resulting from intercalation of layered polysilicates. Both methods used alkyl trimethylammonium surfactants as templates, but the mechanisms of formation, silicate anion initiated LCT and intercalation were very distinct. The MCM-41 synthesized using the LCT method was found to have five times the internal pore volume of the layered silicate-derived material, and the pore-size distribution was found to be sharper than for FSM-16.

Based on the same LCT mechanism, other mesoporous silicate materials have been developed since. Some of these newer materials have improved characteristics such as a higher thermal stability, which is known to be limited in the case of MCM-41.<sup>[44]</sup> Apart from the low thermal stability, the one-dimensional pore structure of MCM-41 poses limitations to its applications. The field of mesoporous oxide materials was further extended by Pinnavaia and co-workers, who used nonionic poly(ethylene oxide) template molecules.<sup>[45]</sup> The low cost and nontoxicity of this type of surfactant was reported to be the main advantage. The silica framework was formed around the rod- or worm-like micelles formed, where the channels in the three-dimensional structure showed diameters between 20 and 58 Å. More recently, in 1998, ultra-large pore hexagonal and cubic mesoporous products were synthesized using nonionic poly(alkylene oxide) triblock copolymers as structure directing agents and tetraalkoxysilane silica sources, in acidic media (pH < 1).<sup>[46]</sup> This work is related to the work reported by Pinnavaia's group, where the larger size of the structure-directing agent species allows pore sizes of up to 300 Å in the products. The hexagonal SBA-15 product was synthesized with a wide range of uniform pore sizes and pore wall thicknesses at low temperature (35–80 °C) using triblock copolymers, such as poly(ethylene oxide)-poly(propylene oxide)-poly(ethylene oxide), PEO-PPO-PEO. The method was found to be very versatile: structured products were obtained using (TMOS, TEOS and TPOS) as silica sources, and a whole range of acids were used to obtain the required synthesis gel pH (HCl, HBr, HI, HNO<sub>3</sub>, H<sub>2</sub>SO<sub>4</sub> or H<sub>3</sub>PO<sub>4</sub>). More recently, the synthesis of SBA-15 materials has been conducted by the same authors in a confined environment, in porous alumina nanochannels. In contrast to synthesizing the material on flat surfaces, where thin films of two-dimensional mesostructures are formed, the confinement of the synthesis causes the sheets to roll up in the cylindrical space. Amongst other structural motifs, the resulting structures exhibit chiral (although



racemic) double-helical channels.<sup>[47]</sup> It was shown to be possible to modify the exact morphology by changing the dimensions of the alumina channels.

Following similar principles of combining the aggregate-forming properties of bifunctional molecules with low cost and low toxicity, a mesoporous silica material with a three-dimensional worm-like pore system was reported. Triethanol amine (TEA) was used as the SDA and TEOS as the silica source in this mesoporous silica, TUD-1.<sup>[48]</sup> The formation mechanism is depicted in Figure 1.3(a). The properties of the material can be easily tuned by modifications in the synthesis procedure, for example, the pore size of the material was found to be proportional to

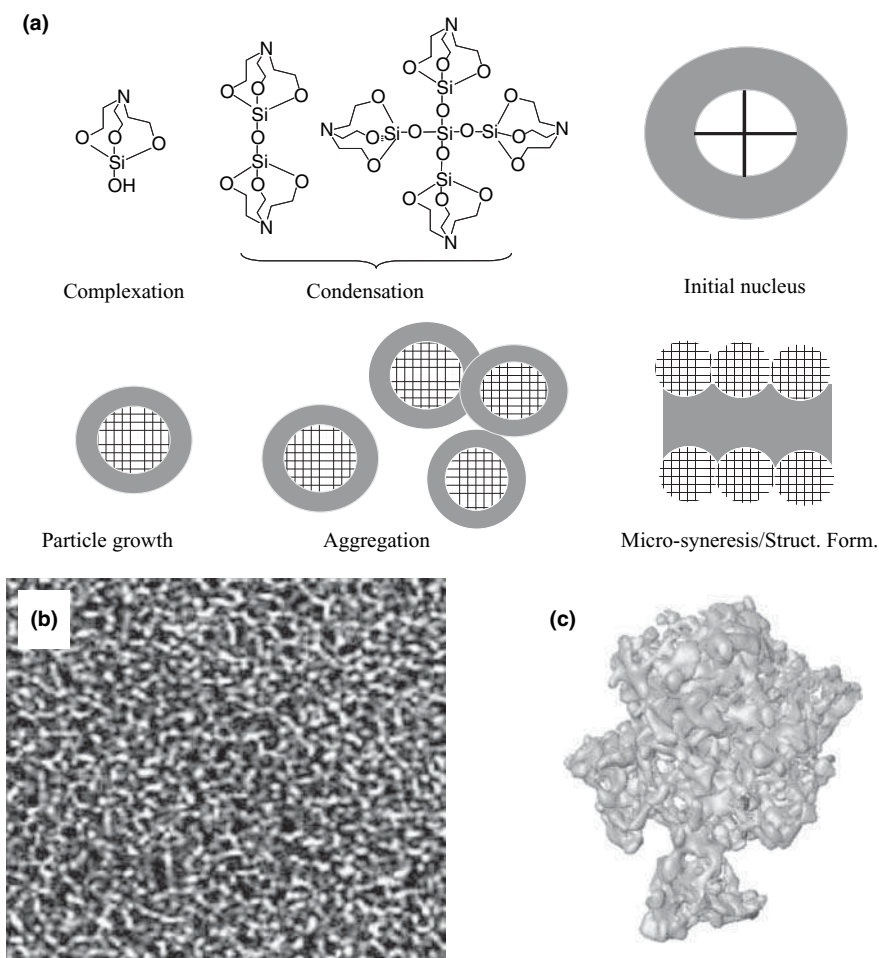


**Figure 1.3** (a) TUD-1 synthesis path, grey shading indicates aggregation of TEA, hatched area indicates silica. (b) HR-TEM image of the mesoporous, foam-like structure. (c) three-dimensional representation of TUD-1 particle, based on a series of HR-TEM images, created under the supervision of Prof. K. P. de Jong, Utrecht University, The Netherlands

the hydrothermal heating time, and is typically in the range of 25–500 Å.<sup>[49]</sup> BET surface areas can be as high as 1000 m<sup>2</sup> g<sup>-1</sup>, and the material exhibits a high thermal and hydrothermal stability. A high resolution transition electron microscopy (HR-TEM) image and a representation based on three-dimensional HR-TEM images of the material are also shown in Figure 1.3.

The field of mesoporous materials has developed rapidly since the first reports on these materials in 1992, as these last examples show. The trend is to utilize inexpensive, multifunctional micelle- or aggregate-forming surfactants or templates which may adopt many different liquid crystal-like configurations in aqueous solution. Formation of a silicate structure with well-defined pore dimensions and connectivity may then be accomplished by the appropriate choice of the synthetic conditions. Additional microporous and macroporosity may be incorporated by using macroporous host materials, as in the case of Stucky of the work by and co-workers, who created mesophases with unprecedented architecture.<sup>[47]</sup>

## 1.2 DESIGN OF EXTRA-LARGE PORE ZEOLITES AND OTHER MICROPOROUS AND MESOPOROUS CATALYSTS

### 1.2.1 INTRODUCTION

The utility of the currently available catalytic microporous and mesoporous oxide materials is limited by their attainable pore sizes, pore architectures, the uniformity of the structures and the extent to which catalytically active heteroatoms can be introduced.<sup>[28]</sup> In the case of zeolites, the small size of the pores is the main limitation to their use in fine chemical or pharmaceutical synthetic applications, as most substrate and product molecules are too large to enter or leave the pore system. Also, in applications such as hydrocracking in oil refineries, the substrate species are often too large to make use of the internal surface of zeolite catalysts (other than in pore-mouth catalysis). Mesoporous materials, on the other hand, have as a main disadvantage their noncrystallinity, resulting in lower thermal and mechanical stability and in broader pore-size distributions and, hence, lower substrate/product selectivities compared with those found for zeolites. Moreover, the lack of crystallinity means a high concentration of structural defects, i.e. the presence of a high degree of surface silanol groups. For mesoporous aluminosilicates, an incomplete incorporation of aluminium into the framework and a less rigid lattice environment means that their acidity is considerably lower than for zeolites, which limits their use as acid catalyst in reactions with large substrate species. In the following sections, approaches to close the gap between zeolites and mesoporous materials as catalysts are discussed.

### 1.2.2 EXTRA-LARGE PORE ZEOLITES

A great demand exists for (hydro)thermally stable, crystalline structures with pore sizes in the 10–20 Å size range that feature tetrahedral frameworks to allow

incorporation of heteroatoms like Al to generate a framework charge imbalance and, thus, impart the material with a high acidic strength.<sup>[50]</sup> Although some progress has been made in recent years, the crystallization of extra-large pore zeolites (containing 12-membered or larger rings) has been and continues to be a great challenge. Many of the reported extra-large pore crystalline structures are aluminophosphates, rather than silica-based materials. The first example of this class, VPI-5, was reported in 1988 and features one-dimensional channels with 18-membered rings (pore diameter of 12 Å).<sup>[51]</sup> These aluminophosphates, however, often suffer from low thermal stability due to the presence of substantial amounts of terminal OH groups and extra-framework octahedral T-atoms. The extra-large pore SiO<sub>2</sub> materials, UTD-1,<sup>[52,53]</sup> CIT-5<sup>[54]</sup> and the germanosilicate IM-12,<sup>[55]</sup> which contains 12- and 14-membered rings with internal free diameters of 8.5 × 5.5 Å and 9.5 × 7.1 Å, all contain 14-membered rings in their largest channels, but the pore diameters of these materials do not exceed 10 Å. Corma *et al.* reported the crystallization of ITQ-15, containing a two-dimensional channel system of interconnected 12- and 14-ring channels (pore dimensions 8.4 × 5.8 Å and 10 × 6.7 Å, respectively),<sup>[56]</sup> and of ITQ-21, which contains a three-dimensional channel system of 12-membered rings with a diameter of 7.4 Å and cavities with a dimension of 11.8 Å.<sup>[57]</sup> These ITQ materials were tested in cracking experiments involving large substrate species and, indeed, they were found to exhibit higher activities than catalysts with smaller channel dimensions or lower pore dimensionality. In all these cases, however, very costly cationic ammonium species were used as the SDAs. The largest rings reported for silica-based materials are those of the thermally stable gallosilicate ECR-34, which requires a mixture of alkali ions and tetraethyl ammonium ions as the structure-directing species. Although this material contains a one-dimensional pore structure featuring useful 18-membered rings with a large diameter of 10.1 Å,<sup>[58]</sup> it does not contain strongly acidic sites, limiting its application. Very recently, a mesoporous crystalline germanium oxide material was reported, with channels composed of an unusually large ring size of 30, with a pore size of 12 Å and 25 Å cavities.<sup>[59]</sup> Mixed organic–inorganic framework species can adopt even more open structures, as was recently illustrated by the chromium terephthalate species MIL-101. This porous coordination compound consists of chromate trimers which are linked by terephthalate ligands to form ‘super-tetrahedra’, which are further organized to form two types of mesoporous cages with internal free diameters of 29 and 34 Å, respectively, and with windows of 12 and 14.5 by 16 Å, respectively.<sup>[60]</sup>

Synthetic approaches towards zeolites with large pore sizes may benefit from the introduction of small rings, as an experimental correlation between framework density and the smallest ring size within a structure has been discovered.<sup>[61]</sup> Similar conclusions were drawn from computational studies by Zwijnenburg *et al.*<sup>[62]</sup> who showed that the presence of a small amount of small rings (e.g. three-membered rings) may aid the stabilization of structures containing large pores and that synthetic efforts should be directed towards synthesizing building blocks containing three-membered rings. Such three-membered rings are known to exist in minerals such as phenakite and euclase,<sup>[63]</sup> where Be atoms are present in these small rings.

Annen *et al.* discovered that it was possible to substitute this toxic heteroatom for Zn, and the first synthetic zincosilicate containing three-membered rings, VPI-7, was reported in 1991.<sup>[64]</sup> Rietveld refinement of this structure revealed the presence of a three-dimensional channel system comprising eight- and nine-membered rings.<sup>[65]</sup> The three-membered rings are formed by 2 Si and 1 Zn atom, illustrating the need for atoms other than Si and Al to make small T-O-T angles possible. Cheetham *et al.* reported the preparation of a beryllsilicate, being the only one example of a framework containing three-membered rings combined with extra large pores (14-membered rings).<sup>[66]</sup>

The presence of three-membered rings has also been suggested to be advantageous in the quest for crystalline mesoporous materials.<sup>[50]</sup> The lack of crystallinity, which is a general feature of this class of materials, has been ascribed to their low framework density. For a range of crystalline framework materials a correlation between the framework density and the size of the smallest ring size in the structure has been established.<sup>[61]</sup> If this correlation is applied to mesoporous materials, which have typical void fractions  $>0.5$ , then the presence of three-membered rings becomes clearly beneficial in the quest to render these structures crystalline.

### 1.2.3 HIERARCHICAL PORE ARCHITECTURES: COMBINING MICROPOROUS AND MESOPOROSITY

The inherent limitations of the use of zeolites as catalysts, i.e. their small pore sizes and long diffusion paths, have been addressed extensively. Corma reviewed the area of mesopore-containing microporous oxides,<sup>[67]</sup> with emphasis on extra-large pore zeolites and pillared-layered clay-type structures. Here we present a brief overview of different approaches to overcoming the limitations regarding the accessibility of catalytic sites in microporous oxide catalysts. In the first part, structures with hierarchical pore architectures, i.e. containing both microporous and mesoporous domains, are discussed. This is followed by a section on the modification of mesoporous host materials with nanometre-sized catalytically active metal oxide particles.

The introduction of a certain degree of mesoporosity into zeolite crystals in order to improve their diffusional properties is a straightforward idea with obvious benefits that has been explored for some time. Different strategies to introduce mesoporosity into zeolites have been reviewed in 2003,<sup>[68]</sup> and more recently by Pérez-Pariente *et al.*<sup>[69]</sup> The traditional way of generating mesoporous defects in a zeolite structure is by means of steam treatment. This treatment results in the selective removal of  $\text{Al}^{3+}$  from the framework, yielding so-called hydroxyl nests. Rearrangement of the structure often occurs, leading to healing of the structure in some places, and to the formation of larger cavities in other places.<sup>[70]</sup> Although the additional mesoporosity thus created may be beneficial in terms of the overall diffusional properties of the solid, the decrease in crystallinity of the structure and the deposition of the removed material on the outer surface of the crystals are serious drawbacks. Acid leaching is an alternative method to remove framework

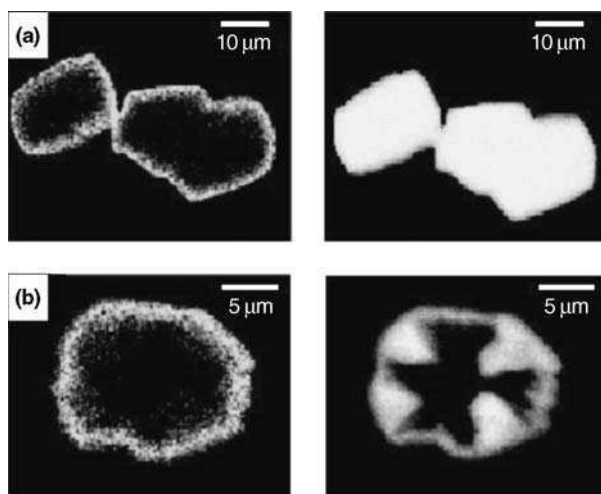


**Figure 1.4** SEM-EDX images of polished nontreated (a) and alkaline-treated (b) ZSM-5 crystals. Desilication predominantly occurs in the core, where the Al concentration is lowest. Reproduced from Groen *et al.*<sup>[74]</sup> by permission of American Chemical Society

aluminium. Mineral acids are routinely used for this purpose, which has as its main drawback the detrimental effect on the framework acidity (Al is removed or becomes partially extra-framework). Secondly, this technique is only applicable for high-alumina zeolites. Alkaline treatment of zeolites has been reported to dissolve siliceous species from the framework, thereby producing regular mesopores and leaving the microporous framework intact.<sup>[71,72]</sup> The mechanism of alkaline desilication of ZSM-5 has been studied in detail and it was found that desilication is directed by framework  $\text{Al}^{3+}$ , and an optimal Si/Al range of 25–50 was established. Desilication results in mesopore surface areas (as analysed by  $\text{N}_2$  physisorption) as large as  $200 \text{ m}^2/\text{g}$ , coupled with a loss in micropore volume of less than 25%.<sup>[73]</sup> Large ZSM-5 crystals, with a high Al concentration near the outer surface of the crystals, could even be selectively desilicated in the core of the crystals, leading to hollow ZSM-5 crystals. This illustrates the influence of Al to Si extraction. Advanced three-dimensional TEM techniques were used to visualize the mesoporosity distribution (Figure 1.4).<sup>[74]</sup>

A different approach towards zeolites containing mesopores involves the incorporation of a template with mesoscopic dimensions into the zeolite synthetic procedure. Carbon spheres and carbon nanotubes have been used for this purpose,<sup>[75]</sup> the latter with a typical diameter of 12 nm and several micrometres long. The synthesis of mesoporous silicalite-I, which is reported in this paper, simply involves the incorporation of the carbon nanotubes into the synthesis gel also containing TPAOH and TEOS. After combustion of the carbon template material, the product consists of single crystals with straight channels in the mesoporous size range penetrating the crystal (Figure 1.5).

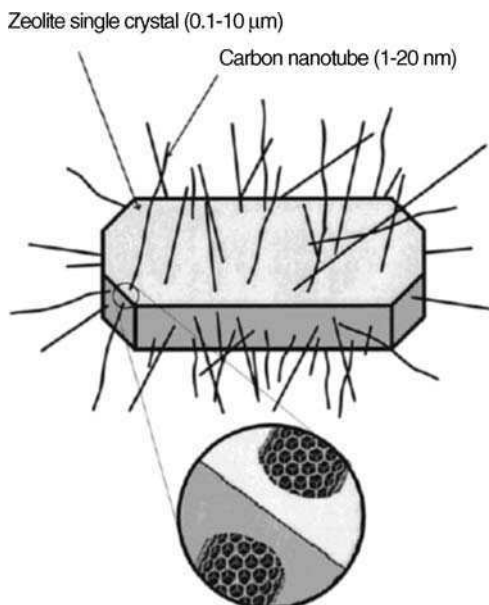


**Figure 1.5** Schematic illustration of the synthesis principle for crystallization of mesoporous zeolite single crystals. The individual zeolite crystals partially encapsulate the nanotubes during growth. Selective removal of the nanotubes by combustion leads to formation of intracrystalline mesopores. Reproduced from Schmidt *et al.*<sup>[75]</sup> by permission of American Chemical Society

Van de Water *et al.* reported that the introduction of small amounts of germanium into the synthesis gel of ZSM-5 changes its crystallization behaviour, resulting in increased mesoporosity.<sup>[76]</sup> A possible explanation for the increased mesoporous and macroporous surface area is that germanium enhances the nucleation rate, thereby generating a larger number of very small primary crystals inside a synthesis-gel sphere. These primary crystals then aggregate immediately, resulting in an imperfect intergrowth with a high number of interfaces, which is the origin of the observed mesoporosity. The typical elongated prismatic crystal shape, characteristic of ZSM-5 (Figure 1.6a), is lost upon increasing the germanium content of the gel. Long, rectangular blocks are formed upon increasing the germanium content, which, in turn, form spherical aggregates with the crystallites being connected to each other in the centre of these spheres (Figure 1.6b).

Nitrogen physisorption of the Ge-ZSM-5 sample revealed a considerable contribution of mesopores to the total pore volume, accompanied by a drop in micropore volume of 20%. In a study of the catalytic activity of these materials it was found that the increased mesoporosity of Ge-ZSM-5 had a beneficial effect on the catalytic activity in a series of acid-catalysed reactions.<sup>[77]</sup> It was observed that the presence of germanium in the framework does not change the strength of the acid sites but, instead, decreases the extent of deactivation from coke residues formed upon reaction. The microporous domains only have short diffusional lengths, but the shape selectivity ascribed to the zeolitic channels is still fully

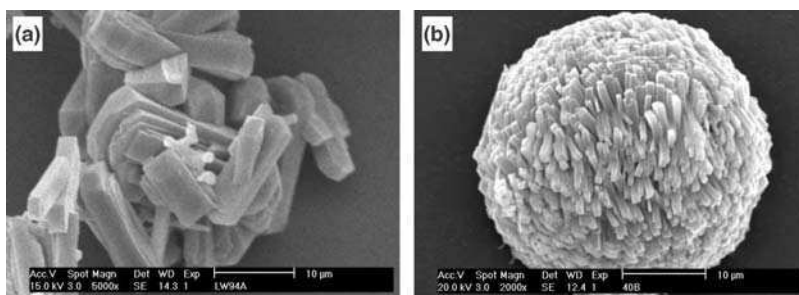


**Figure 1.6** SEM picture of ZSM-5 (a) and Ge-ZSM-5 with a Ge/(Ge + Si) ratio of 0.17 (b). Reproduced from van de Water *et al.*<sup>[76]</sup> by permission of American Chemical Society

effective. This was illustrated by the product distribution of the acetylation reaction of anisole, where it was reported that >99% *para*-product was formed.

A completely different approach to combining zeolite micropores with meso- and even macroporosity has been published by Li and co-workers.<sup>[78]</sup> They prepared self-supporting zeolite monoliths in a multi-step synthetic procedure. In the final material, micropores inside the zeolite nanocrystals (30–40 nm) are combined with a mesopore system formed by the packing of the nanoparticles, and a macropore system on the monolith level. Yet one step further towards improving the accessibility of the active sites of zeolites is to use two-dimensional zeolite *layers*, rather than three-dimensional frameworks, which would result in the ultimate reduction of the diffusion path length. Corma *et al.* reported on the delamination of a zeolite precursor with a clay-type layered structure, resulting in zeolite sheets with a layer thickness of around 25 Å.<sup>[79]</sup> The layers consist of a hexagonal array of ‘cups’ with a 10-membered channel system running through the sheets. Clearly, all (framework-related) acid sites are accessible to substrate molecules which would be too large to fit in the channels of a corresponding three-dimensional material. Indeed, the authors showed that the catalytic cracking of *n*-decane over the delaminated material (ITQ-2) shows a similar rate constant compared with the MWW-type zeolite reference material, which represents a three-dimensional analogue of the layered material. Interestingly, the products isolated from the reaction over ITQ-2 contain a smaller amount of gaseous products than those over MWW, indicating that fewer consecutive reaction steps occurred on ITQ-2. This is attributed to the shorter diffusion path into and out of ITQ-2. A large activity enhancement was found for ITQ-2 in cracking experiments involving vacuum gas oil, which was attributed to the better accessibility of the active sites in ITQ-2, compared with MWW (Figure 1.7).

The combination of micelle-forming species used in the preparation of mesoporous materials with silicate precursors of a variety of zeolites is a promising strategy to obtain mesoporous materials with zeolite-like acidity.<sup>[69]</sup> Although some progress has been made in this field, it has yet to be proven that catalytic materials with improved performance can be obtained in this manner. Strong evidence of the presence of crystallinity in the mesopore walls, combined with an increased acidic

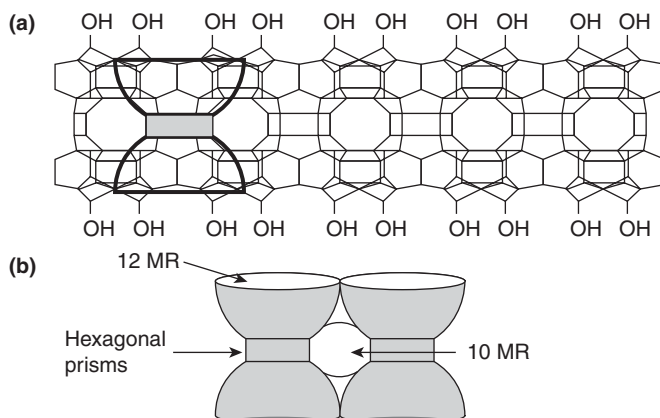


**Figure 1.7** (a) Proposed structure for the ITQ-2 layer showing the characteristic 10-membered ring separating arrays of ‘chalices’ perpendicular to (001), with an artist’s impression of one of the chalices included. (b) Artist’s impression of two fused chalices, each made of two ‘cups’, connected by a nonshared six-membered ring at the bottom, and with a 12-membered ring (12 MR) at their open top. The two fused chalices enclose a 10-membered ring (10 MR), which forms parts of the channel running between the cups inside the sheet. Reproduced from Corma *et al.*<sup>[79]</sup> by permission of Macmillan Publishers Ltd

strength and catalytic activity and stability, has yet to be reported. In this respect, the assembly of so-called ‘nanoslabs’, as discussed in Section 1.1.2, into higher order structures is an exciting direction. One of the current theories regarding the early stages of zeolite framework formation comprises the aggregation of TEOS and TPA species into nm-sized nanoslabs (with dimensions of  $1.3 \times 4.0 \times 4.0$  nm), which can be viewed as the building blocks from which the final zeolite structure is constructed. The organization of these building blocks into structures with mesoscopic dimensions would be a very attractive concept, indeed. However, the thickness of the crystalline nanoslabs (1.3 nm) is larger than the amorphous walls present in MCM-41 (1.0 nm), which would cause problems in view of the curvature of the channel walls. Despite this, the Leuven research group has very recently shown that it is possible to organize the nanometer-sized crystalline building blocks into hexagonally oriented so-called zeogrids and zeotiles.<sup>[80]</sup> The assembly process of the zeolite blocks was interrupted by adding surfactant species such as cetyltrimethylammonium bromide, which is used as the micelle-forming species in the synthesis of M41S materials. This results in the organization of the nanoslabs into a mesoporous superstructure, where the walls are thought to consist of the microporous crystalline Silicalite-1 material.

Instead of introducing a degree of mesoporosity into a microporous catalyst, the problem can also be approached from the opposite direction. Kloetstra *et al.* reported the introduction of crystalline microporous domains inside mesoporous MCM-41 by the partial recrystallization of the pore walls.<sup>[81]</sup> The mesoporous host can be regarded as the aluminium and silicon source for the zeolite crystallization.



The starting material comprises Al-containing MCM-41, allowing for the formation of zeolite-like microporous domains after recrystallization of some of the MCM-41 pore wall material. These sites are expected to exhibit strongly acidic properties related to the now zeolitic framework Al sites. Secondly, the Al present in the MCM-41 parent material allows the introduction of TPA<sup>+</sup> cations, which is the template for ZSM-5, via an ion exchange step. On the basis of IR (the appearance of a band at 550 cm<sup>-1</sup>, characteristic of the five-membered rings present in the MFI structure) and <sup>27</sup>Al NMR (an increase in the signal related to tetrahedrally coordinated Al), it was concluded that part of the MCM-41 silicate material was, indeed, converted into 'embryonic' ZSM-5 domains. The catalytic activity was compared with that of the parent MCM-41 and it appeared that the modified material had a significantly higher activity in the cracking of cumene.

Zhang and co-workers reported partial conversion of a mesoporous starting material (SBA-15) into a mesoporous aluminosilicate with zeolitic characteristics in a so-called vapour phase transport method.<sup>[82]</sup> In this process, Al is firstly introduced onto the mesoporous surface, followed by a filling of the mesopores with a carbonaceous species, and finally a partial recrystallization of aluminosilicate in the vapour of the SDA is conducted. The advantage of this method, compared with the hydrothermal recrystallization method of Kloetstra *et al.*, lies in the fact that the mesopore structure collapses to a lesser extent as the crystallization is limited to the surface of the mesoporous precursor.

Nanometre-sized catalytic species may be dispersed into the pores of a mesoporous host material in order to maximize the available surface area of that catalytic species and to prevent sintering at elevated temperatures. In this respect, zeolite crystallites, metal oxide species and even nanometre-sized metal particles may be introduced into a mesoporous host. Zeolite Beta crystallites (40 nm) have been introduced by Waller *et al.* into the mesoporous silica host TUD-1 by blending preformed zeolite crystallites into the synthesis mixture of the mesoporous carrier. As such, the zeolite crystallites were 'frozen' in the TUD-1 synthesis mixture during its gelation step.<sup>[83]</sup> The Zeolite Beta present in this composite material exhibits a higher activity in the cracking of *n*-hexane than does the equivalent amount of pure zeolite. The difference is ascribed to the fact that aggregation of the 40 nm particles occurs in the case of the pure zeolite, whereas in the composite material these particles are stabilized by the mesoporous host material. The accessibility of the active sites is improved in this way and the mesoporous pore system significantly reduced diffusion limitations on the reactant and product species of the reaction. Furthermore, the intergrowth region exhibits unusual acid sites, resulting from a twisted and strained surface, giving rise to high-energy surface siloxane two-rings which subsequently open to yield highly reactive silanols (as proven by *in situ* NH<sub>3</sub> adsorption FTIR studies reported in the same paper). A similar one-pot synthesis approach was applied to introduce nanometre-sized oxide particles of metallic species, such as titanium, cobalt, iron, vanadium and molybdenum into the TUD-1 host.<sup>[84]</sup> It was found that the particle size of these metal oxides was tunable by small changes in the preparation procedure, where the upper limit of their size is defined by the TUD-1 mesopore size and the lower limit can be

controlled by the concentration of the heteroatom species as well as the precise synthetic sequence (either inducing or avoiding heteroatom oxide particle formation). In some cases, i.e. in the case of titanium, even perfectly isolated tetrahedral metal atoms were present in the framework. The fate of the titanium species and its location could be tracked by *in situ* FTIR throughout the synthesis, thereby indirectly confirming the postulated formation mechanism of TUD-1.<sup>[85]</sup> The immobilization of gold nanoparticles onto mesoporous silica and titania hosts in a one-pot synthesis has been achieved by adding phosphine-stabilized gold particles (with a diameter in the range of 5–10 nm) to the synthesis mixture of mesoporous silica or titania materials.<sup>[86]</sup>

### 1.3 POTENTIAL OF POST-SYNTHESIS FUNCTIONALIZED MICROPOROUS AND MESOPOROUS SOLIDS AS CATALYSTS FOR FINE CHEMICAL SYNTHESIS

#### 1.3.1 INTRODUCTION

Whilst microporous and mesoporous materials in themselves can be catalytically active materials, as outlined in the previous sections, great potential lies in the possibility of their functionalization. Both homogeneous and heterogeneous catalysts have a great number of pros and cons, ranging from environmental and resource concerns (regarding the potential to recycle these materials), to the efficiency and effectiveness of the actual catalytic species. One area of mutual advancement for both these fields is in their combination, i.e. in the heterogenization of homogeneous catalysts. Microporous and mesoporous materials can provide the perfect supports for known homogeneous catalysts to facilitate this. In the following section the issues surrounding such composite materials are discussed.

The use, the development and the scope of individual microporous and mesoporous solids has been discussed in-depth in the previous section. The immobilization of further groups onto or into these hosts to provide the actual catalytic sites is a further sophistication in catalyst design. Incorporating catalytic species into the framework has disadvantages in that there are inherent structural irregularities, i.e. the preparation of a material with identical properties throughout in terms of the local environment of the catalytic sites cannot always be easily repeated. In contrast, immobilizing well-defined molecular catalysts provides identical single catalytic sites.<sup>[9,87]</sup>

There are several different approaches to fixing a molecular catalyst into a host material, some of these methods have been reviewed recently by On *et al.*<sup>[88]</sup> in 2001 and by De Vos *et al.*<sup>[89]</sup> Reviews from the perspective of chiral catalysis appeared in 2002 by Song and Lee,<sup>[90]</sup> and in 2004 by Li,<sup>[91]</sup> and noncovalently bound catalytic species on solid supports have been reviewed in 2004 by Horn *et al.*<sup>[92]</sup> This section is intended to complement these recent reviews and highlight as well as define the approaches encountered and to update some of the latest developments in this field.

### 1.3.2 COVALENT FUNCTIONALIZATION

The covalent binding of a metal complex to a solid support is the most commonly applied technique of functionalizing a microporous or mesoporous material. In essence, this technique can be further categorized into two subsections: (1) grafting, this is the direct attachment of a metal complex to the silica framework of the material; and (2) tethering, whereby a spacer ('tether') is used between the wall of the material and the metal complex.

#### Grafting of Metal Complexes

The first example of the direct grafting of truly isolated metal species onto a periodic mesoporous silica framework was reported in 1995 by Maschmeyer *et al.*<sup>[93]</sup> This involved the reaction of a titanocene-derivative with the walls of MCM-41. After grafting the titanocene onto the surface of the mesoporous host, the ligand was removed by calcination, thereby revealing the catalytically active  $Ti^{4+}$  species (Figure 1.8). Prior to this publication, the nature of research was dominated by attempts to incorporate isolated titanium atoms into the framework of microporous and mesoporous materials. This paper reported the highest TOFs using Ti-containing mesoporous materials in the epoxidation of alkenes openly published at the time. Regeneration after eventual deactivation of the catalyst was achieved without loss of activity and these first results opened the path for greater exploration of these types of well-defined site-specific catalytic materials.

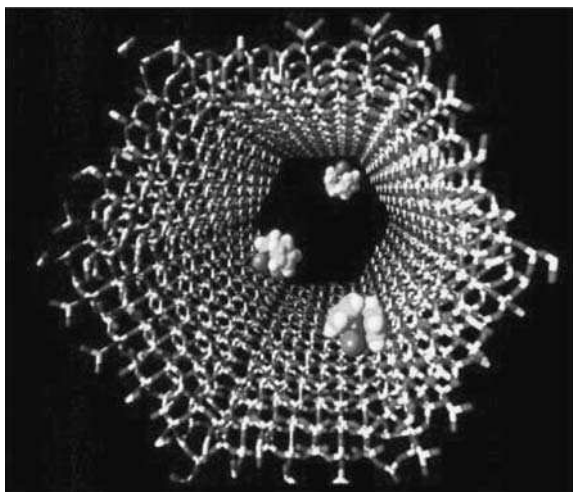


**Figure 1.8** Computer-generated illustration of the accommodation (diffusion / adsorption) of molecules of titanocene dichloride inside a pore (30 Å diameter) of siliceous MCM-41. For simplicity, none of the pendant Si-OH (silanol) groups, that make it possible to graft organometallic moieties inside the mesoporous host, are shown. Reproduced from Maschmeyer *et al.*<sup>[93]</sup> by permission of Macmillan Publishers Ltd

Subsequently, a range of other metal species has been introduced onto the surfaces of mesoporous materials. These have often involved small metal complexes, the ligands of which were removed by calcination after being grafted onto the walls.<sup>[88]</sup> Some recent examples of MCM-41 based materials are the Sn(IV) Lewis acids by Corma *et al.*,<sup>[94]</sup> vanadium-containing species by Singh *et al.*,<sup>[95,96]</sup> and a luminescent europium complex by Fernandes *et al.*<sup>[97]</sup> Rhodium and molybdenum complexes have been given attention by Pillinger *et al.* in analogous procedures, whereby bimetallic acetonitrile complexes have been grafted onto MCM-41.<sup>[98,99]</sup> These complexes have been shown to be sensitive to air, undergoing dissociation to create a mononuclear species in the case of Rh.

Mono-<sup>[100]</sup> and bimetallic<sup>[101]</sup> nanoparticles have been deposited inside the pores of mesoporous silicas in a two-step reaction. For example, the anionic metal carbonyl cluster  $[\text{Ru}_6\text{C}(\text{CO})_{16}]^{2-}$  [in the presence of bis(triphenylphosphino)iminium ( $\text{PPN}^+$ ) counterions] has been immobilized by incorporation into the pores of the host by impregnation. The carbonyl ligands are removed in a subsequent step by gentle thermolysis, yielding nm-sized metal particles grafted onto the walls of the MCM-41 host material. In the case of a Cu-Ru bimetallic cluster<sup>[102]</sup> the bridging chloride ligands react with the surface silanols and covalent Si-O-Cu bonds were formed, anchoring the particle firmly to the surface. EXAFS revealed this anchoring process as well as the structural changes due to the removal of the carbonyl ligands (Figure 1.9). The very high dispersion of the metallic species thus obtained results in good activity in hydrogenation test reactions.

In comparison to the mesoporous materials, less research has been published on the functionalization of microporous materials by direct grafting (excluding various types of ion exchange). It has been stated that some of the newly modified mesoporous materials suffer from the adsorption of products and by-products onto the amorphous walls of the support structure.<sup>[103]</sup> Microporous zeolitic

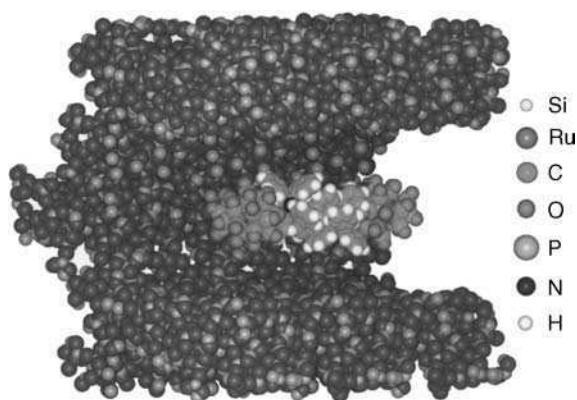


**Figure 1.9** Van der Waals surface interactions of two  $[\text{H}_2\text{Ru}_{10}(\text{CO})_{25}]^{2-}$  and two  $\text{PPN}^+$  molecules packing along a single mesopore. Reproduced from Zhou *et al.*<sup>[100]</sup> by permission of AAAS

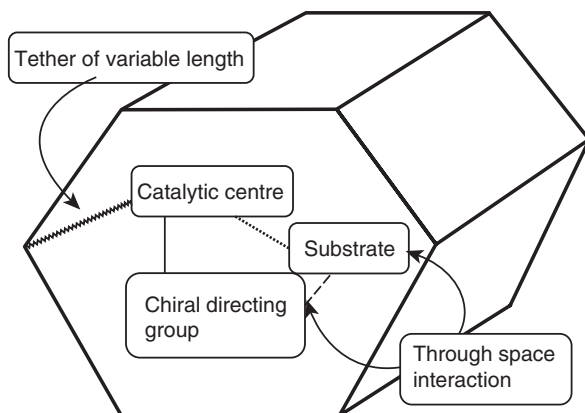


**Figure 1.10** Schematic representation of the confinement concept. Reproduced from Thomas *et al.*<sup>[105]</sup> by permission of Elsevier

materials possess better defined structures and may reduce the extent of such interactions: Sakthivel *et al.* reported the successful grafting of cyclopentadienyl molybdenum complexes onto H-zeolite Beta and H-zeolite-Y.<sup>[104]</sup> However, even though the product adsorption issues were reduced, the relatively low selectivity combined with the poor TOF, leaching problems and deactivation of the catalytic species due to contamination by a by-product lead to the conclusion that the small pore size unduly affects the catalytic system in this case.

### Tethering of Metal Complexes

The linking of a single-site transition metal complex catalyst to a mesoporous material via a spacer chain has become a popular method of heterogenizing a homogeneous complex. A schematic to describe this procedure is shown in Figure 1.10.<sup>[105]</sup> In this manner, the induction of desired chirality can also be introduced, using appropriate directing ligands attached to the active catalytic species. This results in catalytic materials that may be particularly interesting for the pharmaceutical industry and asymmetric catalysis is perhaps the biggest area of interest in the tethering of metal complexes to solid host materials.<sup>[90,105]</sup> The tether itself can be of varied length linked to the catalytic complex either directly via the metal centre or via a ligand attached to that metal, or even, in particular cases, via both the ligand and the transition metal.<sup>[106]</sup> The vast majority of publications following this approach involve mesoporous oxide host materials. In one of the first examples of this type of tethering, reported by Maschmeyer *et al.*, MCM-41 was functionalized with glycine to provide an anchor point for a cobalt(III) complex.<sup>[107]</sup> The Si-OH bonds were first functionalized with an alkyl bromide before the bromide end of the linker was reacted with the amine from glycine, allowing the carboxylic acid functional group to couple with the complex (Figure 1.11).

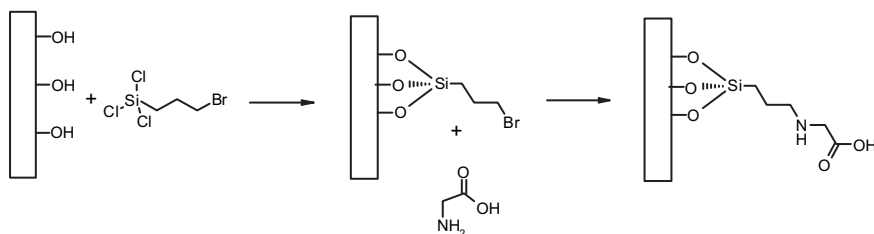


**Figure 1.11** Functionalization of the MCM-41 surface silanols with an alkyl bromide and its subsequent derivatization with glycine

The results of the catalytic experiments show that the material with this linker performs much better, in terms of TOF, leaching of the catalytic species, catalyst lifetime and conversion, than a similar material without the linker. Another example of attaching a linker to provide a reactive carboxylic acid functional group upon which to couple a metal complex is provided by the work of Hultman *et al.*<sup>[108,109]</sup> In this case, chiral dirhodium catalysts were immobilized through the coordination of the oxygen atoms of the carboxylic acid groups to the rhodium centres. The length of the linker was varied, with the three examples being an ethyl, an *n*-propyl and a (*para*-)phenyl group, i.e., obtaining five, six and seven atom spacers between the host wall and the active metal species. Unfortunately, the catalyst itself is large (13–19 Å) compared with the pore size of the MCM-41 used initially (approximately 19 Å). Therefore, fine-tuning of the mesoporous host, i.e. use of TUD-1 with much larger pore sizes, provided a more appropriate physical environment and an enhancement of the enantiomeric excess (*ee*) as compared with the homogeneous species could be determined. The catalytic results of these series of compounds indicate that improvements over the homogenous catalyst can result when immobilizing onto a solid support. In both these procedures, the silanols present on the external surface of the support were deactivated in order to (1) make sure that the complexes are attached only within the channels of the mesoporous material and (2) to avoid unwanted complex–complex interactions.

The most common type of functional group used to connect the support material to the catalytic species can broadly be defined as nitrogen-containing tethers. Besides amines,<sup>[106,110–112]</sup> amides,<sup>[113]</sup> pyridines<sup>[114,115]</sup> and bipyridyls<sup>[116]</sup> have been explored.<sup>[89]</sup> Chiral Mn(salen) complexes have been frequently the catalyst of choice to be immobilized on various materials.<sup>[90]</sup> The reason for this is the excellent reliability of this catalyst to facilitate the asymmetric epoxidation of alkenes. The most recent development of this type of catalyst (with respect to immobilization onto a solid mesoporous support) was the use of a phenoxy group, which coordinates with a Mn(salen) complex by displacing a chloride moiety with oxygen.<sup>[117]</sup> The inorganic host material is functionalized with (*para*-HO-Ph)Si(OEt)<sub>3</sub>, enabling coordination of the manganese ion by the phenoxy ligand. The active metal centre and the wall of the support are separated by six atoms. Catalytic results suggest a general improvement in the enantiomeric excess achieved

in the epoxidation of  $\alpha$ -methylstyrene and *cis*- $\beta$ -methylstyrene compared with the 'free' complex, however, yields were generally poorer. The first paper to illustrate the beneficial effect of confining a chiral catalyst inside a periodic mesoporous host regarding the regioselectivity and ee of the products was published by Johnson *et al.* in 1999.<sup>[110]</sup> The system used consisted of a palladium complex containing a MCM-41 surface-tethered, substituted ferrocene ligand. The catalytic results for the allylic amination of cinnamyl acetate showed conversion of approximately half of the starting material into the branched chiral product (the other 50% being converted into the straight-chained product), with up to 99% ee. In comparison, the homogeneous catalyst converted 79% of the starting material into only the straight-chained product. In this paper, the advantages of a well-defined, periodic mesoporous material (and its restrictive pores) in inducing chirality when compared with either a purely homogeneous catalyst, or a catalyst supported on a nonporous silica, are clearly illustrated.

A recent development of an amine tether was described by McKittrick *et al.*<sup>[106,118]</sup> In these publications, the linker effectively tethers both the Zr/Ti catalytic centre and simultaneously holds the cyclopentadienyl ligand of the metal complex in place. This feature leaves the zirconium or titanium fully exposed to the reactants. Depending on the method of synthesis, it is possible to tailor the anchoring of a metal complex by either one or two amine tethers. In the first case, the primary amine linker is allowed to react with both the ligand and metal, in the latter case, one amine coordinates with the metal centre whilst another amine group reacts with the ligand. It was mentioned earlier that microporous zeolite materials make poor hosts for supporting catalytic transition metal species mainly due to their limited pore size. Corma *et al.* reported, very early on in this field of research rhodium complexes anchored onto a modified Y-zeolite via an amine tether with outstanding results.<sup>[119]</sup> The 'supermicropores' (with a size range of 30–60 Å, i.e. mesopores) that are formed upon steam treatment of the zeolite USY host allow the introduction of such large entities, and this is, therefore, the first example of a tethered, albeit nonchiral, metal complex inside a mesoporous host. The catalytic test reactions showed no loss in hydrogenation activity, compared with the corresponding homogeneous catalyst, and no appreciable leaching of the complex after 10 cycles.

Moving onto other types of linkers, alkyl linkers have been developed by Sakthivel *et al.*<sup>[120]</sup> An alkyl halide is usually the reactive species, where the halide is displaced by either the metal centre itself or by the ligand of the complex. An interesting example of the use of phosphine tethers is in the heterogenization of Grubbs' type catalysts.<sup>[121]</sup> Here, the bound ruthenium complex allows the ROMP (ring opening metathesis polymerization) reaction to occur in aqueous conditions, a feature not possible with the homogeneous catalyst. Unfortunately, lower activities are observed, probably due to diffusion constraints. A notable use of a phosphine linker was reported by Shyu *et al.*,<sup>[122]</sup> who immobilized Wilkinson's catalyst [Rh(PPh<sub>3</sub>)<sub>3</sub>Cl] onto phosphinated MCM-41. The supported catalyst showed TOFs three times greater than the homogeneous catalyst, minimal leaching and maintained activity levels after 15 cycles.

### 1.3.3 NONCOVALENT IMMOBILIZATION APPROACHES

#### Noncovalently Bound Metal Complexes

Evidence of immobilization of a metal complex via hydrogen bonding interactions between the ligand and the silanol groups of the oxidic support has been reported by Bianchini *et al.*<sup>[123]</sup> Sulfonate groups on the end of a phosphine-based ligand formed strong non-covalent bonds with high surface area silica (Figure 1.12). These catalysts were shown to be promising in the hydrogenation of styrene and in the hydroformylation of 1-hexene. The activity in the hydroformylation reaction was even higher than in the corresponding homogeneous reaction, which is ascribed to the detrimental dimerization of the homogeneous Rh complex in solution. The high activity of the grafted complex is, therefore, ascribed to the presence of truly isolated Rh species. Leaching of the complex was not observed, as could be concluded from the fact that the catalytic results of the regenerated solid were unchanged, and that there was no evidence of catalysis in the filtrates taken from the first reactions. This method has not (yet) been further investigated for use on mesoporous materials. In 2000, the first example of this ion-exchange method as applied to mesoporous support materials was published by de Rege *et al.*<sup>[124]</sup> A triflate anion was used to immobilize a cationic rhodium complex onto MCM-41. The difference with the work of Bianchini and co-workers is that in their case the triflate moiety was part of the phosphine ligand, whereas in the MCM-41 based catalysts by de Rege *et al.* the strongly bound triflate anion (hydrogen bonding) was responsible for the anchoring of the cationic Rh complex. Other anions than triflate, such as the more lipophilic  $B[C_6H_3(CF_3)_2-3,5]_4$ , combined with the same Rh complex, were unable to cause the same effect. The supported complex displayed better catalytic activity (both in conversion and enantiomeric excess) than the unsupported complex. The newly heterogenized catalyst also proved to be recyclable and was stable to leaching in nonpolar solvents. Using exactly the same approach and anion, Raja *et al.* reported the immobilization of a range of chiral Rh phosphine complexes onto a set of inexpensive, commercially available silicas.<sup>[125]</sup> The ee values of the asymmetric hydrogenation of methyl benzoylformate were found to increase upon decreasing pore size of the inorganic host, which reflects the beneficial effect of a constrained environment on the enantioselective performance of a chiral catalyst. This method is, in fact, a combination of two immobilization techniques: the triflate ion is hydrogen bonded to the surface hydroxyl groups, and the cationic metal complex is anchored onto this modified surface via an ion-exchange step.

In this context, immobilization of metal complexes by means of ion exchange has been reported by Augustine *et al.*<sup>[126]</sup> in 1999. In their study, polytungstic acid was used as anchor to affix a metal-containing catalytic complex onto a support material. It is thought that hydroxyl groups of the support react with the heteropoly acid. The (cationic) metal complex is anchored to the modified support via a strong ionic interaction, which is illustrated by the fact that no leaching of the complex was observed. The method appeared to be applicable to a range of support materials such as Montmorillonite K, carbon, alumina and lanthana. It was shown to be an



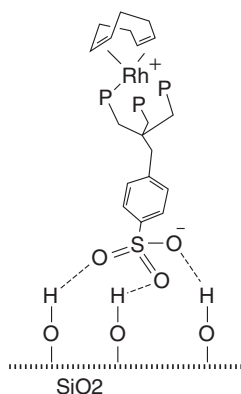


**Figure 1.12** Noncovalently bound Rh(I) complex for hydroformylation, immobilized onto the silica surface via hydrogen bonding with the triflate moiety. Reproduced from Bianchini *et al.*<sup>[123]</sup> by permission of American Chemical Society

effective means of anchoring a catalytic species without hampering its activity. Hölderich *et al.* reported the immobilization of rhodium diphosphine catalysts via ionic interactions with the aluminium-modified mesoporous materials Al-MCM-41 and Al-SBA-15.<sup>[127,128]</sup> The presence of aluminium in these materials generates acidic protons on the surface, which can be readily exchanged with a cationic metal complex. In this way, the metal complexes interact directly with the negatively charged surface, and hence no modification of the support with an anchoring group is required. Comparing the catalytic results of the two materials, it seems that immobilization onto Al-MCM-41 is more beneficial in terms of activity. However, there is a discrepancy in the respective methods of alumination of the materials. Al-MCM-41 was formed with aluminium as an integral part of the synthetic process, whereas aluminium was incorporated into a SBA-15 framework in a post-synthesis reaction step. The use of yet another mesoporous material, Al-TUD-1, was explored in the research reported by Simons *et al.*<sup>[129,130]</sup> The most notable part of these studies is the investigation into the effect of the catalyst in different solvents. The activity, enantioselectivity and the extent of Rh leaching all depend on the chosen solvent in asymmetric hydrogenation reactions using immobilized bidentate  $\{\text{Rh}^{\text{I}}(\text{cod})[(R,R)\text{-DuPHOS}]\}\text{BF}_4$  and  $\{\text{Rh}^{\text{I}}(\text{cod})[(S,S)\text{-DiPAMP}]\}\text{BF}_4$ .<sup>[130]</sup> In terms of ‘green’ chemistry, the most interesting result was in the use of water as the solvent in a hydrogenation reaction using Rh-MonoPhos on Al-TUD-1.<sup>[129]</sup> This catalyst was shown to achieve 95% ee (comparable with other solvents and the homogeneous catalyst) and 100% conversion levels, albeit with slightly longer reaction times. Even upon recycling of the catalyst, the results remained consistently good. The use of water as solvent allows the design of cascade reactions in which this immobilized ‘chemo-catalyst’ is coupled to a ‘bio-catalyst’, i.e. an enzymatic reaction system.<sup>[131]</sup>

Krijnen *et al.* reported on the noncovalent, nonionic immobilization of Ti-silsesquioxanes onto MCM-41, as an epoxidation catalyst.<sup>[132]</sup> An intriguing aspect

of this particular research is the unaltered state of the original catalyst upon immobilization onto the support. The active catalytic species seems to be adsorbed onto the silica framework based on entropic gain (i.e. one large molecule displaces many surface-adsorbed small solvent molecules) with evidence to show that the cyclopentadienyl ligand of the Ti-silsesquioxane complex is unadulterated. It has been suggested that the ancillary cyclohexyl ligands of the complex interact with the surface of the MCM-41 pores (hydrophobic interactions), allowing the cyclopentadienyl group connected to the Ti centre to sit freely in the channel. The adsorption of the complex occurs rapidly and particularly so on Al-MCM-41 materials.<sup>[132]</sup> However, functionalized Al-MCM-41 is prone to leaching and requires treatment with a silylating agent prior to catalysis to prevent this.<sup>[133]</sup> The significantly quicker adsorption onto aluminium-doped MCM-41 suggests that, in addition to entropic considerations, polarity influences adsorption characteristics of the host material. XPS analysis suggests that this rapid adsorption prevents a homogeneous distribution of the complex inside the host, instead higher concentrations are found in the outer regions of the channels. The explanation being that the large silsesquioxane complex already adsorbed on a surface prevents another complex passing through the channel to deeper regions of the material. With the slower adsorption onto the all-silica species, the complex is allowed to travel further into the channel before adsorption takes place. This lower loading of the actual catalyst in the Al-MCM-41 mesopores explains the difference in TOF with the all-silica MCM-41 material. In an investigation into a ‘tethered’ approach to immobilizing a Ti-silsesquioxane complex, Smet *et al.* reported on the development of a (3-glycidyoxypropyl)trimethoxysilane linker between MCM-41 and titanium(IV) silsesquioxane.<sup>[134]</sup> This approach however, offers no performance advantages over the pure-silica substrates described by Krijnen *et al.*

### Encapsulation of Metal Complexes

Encapsulation covers a wide selection of methods to activate otherwise sedate microporous and mesoporous host materials. This heading describes the trapping of an active catalytic species within the pores of an inorganic support system. Along with the relatively simple notion of grafting metal oxides and clusters within the pores, there is also a more synthetically challenging method, namely the ‘ship-in-a-bottle’ approach (Figure 1.13). This approach has most often been associated with microporous materials as the smaller pore dimensions in these solids render this method most appropriate for the incorporation of a metal complex. The theory is that various substrates are applied separately to the inorganic support and that these assemble themselves (to create the catalyst) within the cages or pores of the support. The first example of this type of immobilized metal complex was reported by Herron in 1986, who formed a Co–salen complex inside the cages of zeolite Y by adding an excess of salen ligand to a sample of zeolite Y that had been ion exchanged with  $\text{Co}^{2+}$  ions.<sup>[135]</sup> Since that time many examples of this encapsulation have been reported in the literature and the procedure is well described in a paper by Fukuoka *et al.*, where special attention is given to the synthesis of platinum



**Figure 1.13** The ‘ship-in-a-bottle’ concept: view of Mn(III)–salen inside the cavity of zeolite EMT. Reproduced from Ogunwumi and Bain<sup>[138]</sup> by permission of Royal Society of Chemistry

carbonyl clusters within both microporous (zeolite NaY) and mesoporous (FSM-16) materials.<sup>[136]</sup> The aim of this study was to synthesize nanometre-sized Pt particles inside these hosts. To this end, the support was impregnated with a Pt salt, which was in a subsequent reductive decarbonylation step converted into  $[\text{Pt}_3(\text{CO})_6]_n^{2-}$  inside NaY, and  $[\text{Pt}_{15}(\text{CO})_{30}]^{2-}$  inside FSM-16, respectively. The metal–carbonyl complexes were then converted to Pt nanoparticles with a size of less than 2 nm. Intrazeolite assembly of manganese–trimethyl triazacyclononane (tmtacn) complexes inside zeolite Y supercages has been shown to yield a highly selective epoxidation catalyst.<sup>[137]</sup> Similarly, Mn–salen complexes have been formed inside zeolite cavities and have been shown to be selective epoxidation catalysts.<sup>[138,139]</sup>

To avoid the limitations of the small apertures and cavities provided by zeolites, mesopores have been created inside zeolites X, Y and DAY.<sup>[140]</sup> By dealumination of the zeolite structure, mesoporous regions that are completely surrounded by micropores were obtained, and these intrazeolitic cavities were then used as the space in which to assemble metal complexes. The preparation of a cobalt–salen-5 complex provided a catalytic material that shows improvements in the conversion,

the selectivity and the diastereomeric excess over the homogeneous catalyst in the stereoselective epoxidation of limonene and pinene. Furthermore, the compounds are reusable and not prone to leaching.

### 1.3.4 SINGLE-SITE CATALYSTS INSPIRED BY NATURAL SYSTEMS

The general objective for all functionalized porous oxide materials described in the previous sections is that so-called 'single-site' catalytic species were the aim. This should ultimately result in highly selective catalysts as the local environment around each catalytic centre is very similar to that of neighbouring sites. In fact, this is very similar to catalysts in biological systems, which also feature very similar catalytic sites (protein-folding temporarily changing the precise environment at any given instant). The high selectivity of these biocatalytic/enzymatic systems is achieved by creating sites with well defined geometrical constraints, making them only accessible to certain substrate species. The approach to take ideas from nature in the design of new catalysts has been reviewed in detail.<sup>[141]</sup>

Mesoporous materials, as discussed in previous sections, contain pores of appropriate size to accommodate a broad range of enzymes, which often have dimensions of less than 100 Å in all three dimensions.<sup>[142]</sup> The interaction between the inorganic host and the enzyme is ionic in most cases, where the protonated form of the enzyme is attached to the negatively charged silica surface. In this way minimal or even no structural reorganization of the enzyme is required, resulting in comparable activities to the free enzyme species. Enzymes have also been grafted onto the surface of a foam-like silica, modified with aldehyde groups. Glucose oxidase was then coupled through its amine groups to the functional surface groups of the silica, although it appeared hard to control the degree of functionalization of the surface as such.<sup>[143]</sup>

The 'bio-inspired' molecular imprinting approach is based on the principle that the catalytic site should be shaped around a particular substrate, or alternatively, transition state species, in a similar manner as is the case in enzymes. When a template, which resembles the shape of the substrate, is used for the synthesis of the material, selectivity of the catalyst towards this particular substrate may be obtained after removal of the template. The catalytic reaction can only take place in this confined space, which resembles the way of action of enzymes. Most examples utilizing this technique involve polymerization of monomeric metal complexes containing a polymerizable group, such as styrene.<sup>[144]</sup> By copolymerizing with a cross-linking agent, e.g. ethylene glycol dimethacrylate, the final structure is expected to contain a high degree of cross-linking to make the structure rigid enough to retain its shape after removal of the template. Imprinted catalysts based on porous inorganic oxides are scarce. Corma and co-workers have reported on the synthesis and catalytic properties of ITQ-7, which contains 12-membered pores running in three dimensions. The template (or rather, SDA) used for its preparation was a quaternary ammonium species, prepared by a Diels–Alder reaction. When this catalyst, after removal of the template, was used in a Diels–Alder reaction

involving a transition state similar in shape to that of the template used, it was found to be more active than other zeolite species with similar morphology.<sup>[141]</sup>

Iwasawa and co-workers used a Rh–amine complex as a template to grow a silica network.<sup>[145]</sup> Firstly, a  $\text{Rh}(\eta^3\text{-C}_3\text{H}_5)/\text{SiO}_2$  (Aerosil 200) precursor was prepared, followed by a ligand exchange step where the  $\text{C}_3\text{H}_5$  ligand was exchanged for  $\alpha$ -methylbenzylamine. The actual imprinting step was performed by reaction of this precursor with TEOS. After removal of the  $\alpha$ -methylbenzylamine template, a catalyst with selectivity for  $\alpha$ -methylstyrene, which has a similar structure to the template, was obtained.

In the zeolitic system, a significant amount of lattice energy stabilizes this imprinted transition state motif – a situation that reflects the situation in enzymes where hydrogen bonding controls the protein folding. This is a significant advantage over such imprints in amorphous supports like organic polymers and amorphous oxide surfaces where such stabilizing forces are largely absent, and it should lead to better overall performance.

In the following chapters the various applications, limitations and opportunities of the catalysts described in this chapter will be discussed.

## REFERENCES

1. Coronado, E., Galan-Mascaros, J. R., Marti-Gastaldo, C., Palomares, E., Durrant, J. R., Vilar, R., Gratzel, M. and Nazeeruddin, M. K. Reversible colorimetric probes for mercury sensing. *J. Am. Chem. Soc.*, **2005**, *127*, 12351–12356.
2. Gratzel, M. Solar energy conversion by dye-sensitized photovoltaic cells, *Inorg. Chem.*, **2005**, *44*, 6841–6851.
3. Walcarius, A., Mandler, D., Cox, J. A., Collinson, M. and Lev, O. Exciting new directions in the intersection of functionalized sol–gel materials with electrochemistry, *J. Mater. Chem.*, **2005**, *15*, 3663–3689.
4. Attia, A., Zukalova, M., Rathousky, J., Zukal, A. and Kavan, L. Mesoporous electrode material from alumina-stabilized anatase  $\text{TiO}_2$  for lithium ion batteries, *J. Solid State Electrochem.*, **2005**, *9*, 138–145.
5. Coronado, E. and Palomares, E. Hybrid molecular materials for optoelectronic devices, *J. Mater. Chem.*, **2005**, *15*, 3593–3597.
6. van Bekkum, H., Jacobs, P. A., Flanigen, E. M. and Jansen, J. C. *Introduction to Zeolite Science and Practice*. Elsevier, Amsterdam, 2001.
7. Lok, B. M., Cannan, T. R. and Messina, C. A. The role of organic molecules in molecular sieve synthesis, *Zeolites*, **1983**, *3*, 282–291.
8. Maschmeyer, T., Raimondi, M. E. and Seddon, M. Mesoporous molecular sieves. In *The Encyclopedia of Materials: Science and Technology*, K. H. J. Buschow *et al.* (eds). Elsevier, Oxford, **2001**, Vol. 1, pp. 5342–5346.
9. Schuth, F. Engineered porous catalytic materials, *Annu. Rev. Mater. Res.*, **2005**, *35*, 209–238.
10. Zones, S. I., Hwang, S. J., Elomari, S., Ogino, I., Davis, M. E. and Burton, A. W. The fluoride-based route to all-silica molecular sieves; a strategy for synthesis of new materials based upon close-packing of guest-host products, *C. R. Chimie*, **2005**, *8*, 267–282.

11. Wagner, P., Nakagawa, Y., Lee, G. S., Davis, M. E., Elomari, S., Medrud, R. C. and Zones, S. I. Guest/host relationships in the synthesis of the novel cage-based zeolites SSZ-35, SSZ-36, and SSZ-39, *J. Am. Chem. Soc.*, **2000**, *122*, 263–273.
12. Cundy, C. S. and Cox, P. A. The hydrothermal synthesis of zeolites: precursors, intermediates and reaction mechanism, *Microporous Mesoporous Mater.*, **2005**, *82*, 1–78.
13. Burkett, S. L. and Davis, M. E. Mechanism of structure direction in the synthesis of Si-ZSM-5 – An investigation by intermolecular H-1-Si-29 CP MAS NMR, *J. Phys. Chem.*, **1994**, *98*, 4647–4653.
14. Burkett, S. L. and Davis, M. E. Mechanism of structure direction in the synthesis of pure-silica zeolites. 2. Hydrophobic hydration and structural specificity, *Chem. Mater.*, **1995**, *7*, 1453–1463.
15. de Moor, P., Beelen, T. P. M., Komanschek, B. U., Diat, O. and van Santen, R. A. In situ investigation of Si-TPA-MFI crystallization using (ultra-) small- and wide-angle X-ray scattering, *J. Phys. Chem. B*, **1997**, *101*, 11077–11086.
16. Barrer, R. M., Baynham, J. W., Bultitude, F. W. and Meier, W. M., *J. Chem. Soc.*, **1959**, 195–208.
17. Ravishankar, R., Kirschhock, C. E. A., Knops-Gerrits, P. P., Feijen, E. J. P., Grobet, P. J., Vanoppen, P., De Schryver, F. C., Mieke, G., Fuess, H., Schoeman, B. J., Jacobs, P. A. and Martens, J. A. Characterization of nanosized material extracted from clear suspensions for MFI zeolite synthesis, *J. Phys. Chem. B*, **1999**, *103*, 4960–4964.
18. Kirschhock, C. E. A., Ravishankar, R., Verspeurt, F., Grobet, P. J., Jacobs, P. A. and Martens, J. A. Identification of precursor species in the formation of MFI zeolite in the TPAOH-TEOS-H<sub>2</sub>O system, *J. Phys. Chem. B*, **1999**, *103*, 4965–4971.
19. Bu, X. H., Feng, P. Y. and Stucky, G. D. Isolation of germanate sheets with three-membered rings: a possible precursor to three-dimensional zeolite-type germanates, *Chem. Mater.*, **1999**, *11*, 3423–3424.
20. Anderson, M. W., Agger, J. R., Hanif, N. and Terasaki, O. Growth models in microporous materials, *Microporous Mesoporous Mater.*, **2001**, *48*, 1–9.
21. Bosnar, S., Antonic, T., Bronic, J. and Subotic, B. Mechanism and kinetics of the growth of zeolite microcrystals. Part 2: Influence of sodium ions concentration in the liquid phase on the growth kinetics of zeolite A microcrystals, *Microporous Mesoporous Mater.*, **2004**, *76*, 157–165.
22. Sankar, G., Thomas, J. M., Rey, F. and Greaves, G. N. Probing the onset of crystallization of a microporous catalyst by combined X-ray absorption spectroscopy and X-ray diffraction, *J. Chem. Soc., Chem. Comm.*, **1995**, 2549–2550.
23. Sankar, G. and Thomas, J. M. In situ combined X-ray absorption spectroscopic and X-ray diffractometric studies of solid catalysts, *Top. Catal.*, **1999**, *8*, 1–21.
24. Grandjean, D., Beale, A. M., Petukhov, A. V. and Weckhuysen, B. M. Unraveling the crystallization mechanism of CoAPO-5 molecular sieves under hydrothermal conditions, *J. Am. Chem. Soc.*, **2005**, *127*, 14454–14465.
25. Lewis, D. W., Catlow, C. R. A. and Thomas, J. M. Influence of organic templates on the structure and on the concentration of framework metal ions in microporous aluminophosphate catalysts, *Chem. Mater.*, **1996**, *8*, 1112–1118.
26. Lewis, D. W., Willock, D. J., Catlow, C. R. A., Thomas, J. M. and Hutchings, G. J. De novo design of structure-directing agents for the synthesis of microporous solids, *Nature*, **1996**, *382*, 604–606.
27. Blasco, T., Corma, A., Diaz-Cabanias, M. J., Rey, F., Vidal-Moya, J. A. and Zicovich-Wilson, C. M. Preferential location of Ge in the double four-membered ring units of ITQ-7 zeolite, *J. Phys. Chem. B*, **2002**, *106*, 2634–2642.

28. Corma, A. and Davis, M. E. Issues in the synthesis of crystalline molecular sieves: towards the crystallization of low framework-density structures, *Chem Phys Chem*, **2004**, *5*, 304–313.
29. Corma, A., Navarro, M. T., Rey, F., Rius, J. and Valencia, S. Pure polymorph C of zeolite beta synthesized by using framework isomorphous substitution as a structure-directing mechanism, *Angew. Chem. Int. Ed.*, **2001**, *40*, 2277–2280.
30. Beck, J. S., Vartuli, J. C., Roth, W. J., Leonowicz, M. E., Kresge, C. T., Schmitt, K. D., Chu, C. T. W., Olson, D. H., Sheppard, E. W., McCullen, S. B. Higgins, J. B. and Schlenker, J. L. A new family of mesoporous molecular-sieves prepared with liquid-crystal templates, *J. Am. Chem. Soc.*, **1992**, *114*, 10834–10843.
31. Kresge, C. T., Leonowicz, M. E., Roth, W. J., Vartuli, J. C. and Beck, J. S. Ordered mesoporous molecular-sieves synthesized by a liquid-crystal template mechanism, *Nature*, **1992**, *359*, 710–712.
32. Inagaki, S., Fukushima, Y. and Kuroda, K. Synthesis of highly ordered mesoporous materials from a layered polysilicate, *J. Chem. Soc., Chem. Commun.*, **1993**, 680–682.
33. Inagaki, S., Fukushima, Y. and Kuroda, K. Synthesis and characterization of highly ordered mesoporous material FSM-16, from a layered polysilicate, *Stud. Surf. Sci. Catal.*, **1994**, *84*, 125–132.
34. Behrens, P. Voids in variable chemical surroundings: Mesoporous metal oxides, *Angew. Chem. Int. Ed.*, **1996**, *35*, 515–518.
35. Vartuli, J. C., Schmitt, K. D., Kresge, C. T., Roth, W. J., Leonowicz, M. E., McCullen, S. B. Hellring, S. D., Beck, J. S., Schlenker, J. L., Olson, D. H. and Sheppard, E. W. Effect of surfactant silica molar ratios on the formation of mesoporous molecular-sieves— inorganic mimicry of surfactant liquid-crystal phases and mechanistic implications, *Chem. Mater.*, **1994**, *6*, 2317–2326.
36. Ulagappan, N. and Rao, C. N. R. Evidence for supramolecular organization of alkane and surfactant molecules in the process of forming mesoporous silica, *Chem. Commun.*, **1996**, 2759–2760.
37. Khushalani, D., Kuperman, A., Ozin, G. A., Tanaka, K., Garces, J., Olken, M. M. and Coombs, N. Metamorphic materials – restructuring siliceous mesoporous materials. *Adv. Mater.*, **1995**, *7*, 842.
38. Cheng, C. F., Zhou, W. Z., Park, D. H., Klinowski, J., Hargreaves, M. and Gladden, L. F. Controlling the channel diameter of the mesoporous molecular sieve MCM-41, *J. Chem. Soc., Faraday Trans.*, **1997**, *93*, 359–363.
39. Arafat, A., Jansen, J. C., Ebaid, A. R. and Vanbekkum, H. Microwave preparation of zeolite Y and ZSM-5, *Zeolites*, **1993**, *13*, 162–165.
40. Girnus, I., Jancke, K., Vetter, R., Richtermendau, J. and Caro, J. Large AlPO<sub>4</sub>-5 crystals by microwave-heating, *Zeolites*, **1995**, *15*, 33–39.
41. Lohse, U., Bertram, R., Jancke, K., Kurzawski, I., Parltitz, B., Löffler, E. and Schreier, E. Acidity of aluminophosphate structures. 2. Incorporation of cobalt into CHA and AFI by microwave synthesis, *J. Chem. Soc., Faraday Trans.*, **1995**, *91*, 1163–1172.
42. Wu, C. G. and Bein, T. Microwave synthesis of molecular sieve MCM-41, *Chem. Commun.*, **1996**, 925–926.
43. Vartuli, J. C., Kresge, C. T., Leonowicz, M. E., Chu, A. S., McCullen, S. B. Johnsen, I. D. and Sheppard, E. W. Synthesis of mesoporous materials – liquid-crystal templating versus intercalation of layered silicates, *Chem. Mater.*, **1994**, *6*, 2070–2077.
44. Zhao, X. S., Lu, G. Q. M. and Millar, G. J. Advances in mesoporous molecular sieve MCM-41, *Ind. Eng. Chem. Res.*, **1996**, *35*, 2075–2090.

45. Bagshaw, S. A., Prouzet, E. and Pinnavaia, T. J. Templating of mesoporous molecular sieves by nonionic polyethylene oxide surfactants, *Science*, **1995**, 269, 1242–1244.
46. Zhao, D. Y., Feng, J. L., Huo, Q. S., Melosh, N., Fredrickson, G. H., Chmelka, B. F. and Stucky, G. D. Triblock copolymer syntheses of mesoporous silica with periodic 50 to 300 Angstrom pores, *Science*, **1998**, 279, 548–552.
47. Wu, Y. Y., Cheng, G. S., Katsov, K., Sides, S. W., Wang, J. F., Tang, J., Fredrickson, G. H., Moskovits, M. and Stucky, G. D. Composite mesostructures by nano-confinement, *Nature Materials*, **2004**, 3, 816–822.
48. Shan, Z., Jansen, J. C. and Maschmeyer, T. WO 00/15551, 2000.
49. Jansen, J. C., Shan, Z., Marchese, L., Zhou, W., van der Puil, N. and Maschmeyer, T. A new templating method for three-dimensional mesopore networks, *Chem. Commun.*, **2001**, 713–714.
50. Davis, M. E. Ordered porous materials for emerging applications, *Nature*, **2002**, 417, 813–821.
51. Davis, M. E., Saldarriaga, C., Montes, C., Garces, J. and Crowder, C. VPI-5 – The 1st molecular-sieve with pores larger than 10 Angstroms, *Zeolites*, **1988**, 8, 362–366.
52. Freyhardt, C. C., Tsapatsis, M., Lobo, R. F., Balkus, K. J. and Davis, M. E. A high-silica zeolite with a 14-tetrahedral-atom pore opening, *Nature*, **1996**, 381, 295–298.
53. Lobo, R. F., Tsapatsis, M., Freyhardt, C. C., Khodabandeh, S., Wagner, P., Chen, C. Y., Balkus, K. J., Zones, S. I. and Davis, M. E. Characterization of the extra-large-pore zeolite UTD-1, *J. Am. Chem. Soc.*, **1997**, 119, 8474–8484.
54. Yoshikawa, M., Wagner, P., Lovallo, M., Tsuji, K., Takewaki, T., Chen, C. Y., Beck, L. W., Jones, C., Tsapatsis, M., Zones, S. I. and Davis, M. E. Synthesis, characterization, and structure solution of CIT-5, a new, high-silica, extra-large-pore molecular sieve, *J. Phys. Chem. B*, **1998**, 102, 7139–7147.
55. Paillaud, J. L., Harbuzaru, B., Patarin, J. and Bats, N. Extra-large-pore zeolites with two-dimensional channels formed by 14 and 12 rings, *Science*, **2004**, 304, 990–992.
56. Corma, A., Diaz-Cabanas, M. J., Rey, F., Nicolououlas, S. and Boulahya, K. ITQ-15: The first ultralarge pore zeolite with a bi-directional pore system formed by intersecting 14-and 12-ring channels, and its catalytic implications, *Chem. Commun.*, **2004**, 1356–1357.
57. Corma, A., Diaz-Cabanas, M., Martinez-Triguero, J., Rey, F. and Rius, J. A large-cavity zeolite with wide pore windows and potential as an oil refining catalyst, *Nature*, **2002**, 418, 514–517.
58. Strohmaier, K. G. and Vaughan, D. E. W. Structure of the first silicate molecular sieve with 18-ring pore openings, ECR-34, *J. Am. Chem. Soc.*, **2003**, 125, 16035–16039.
59. Zou, X. D., Conradsson, T., Klingstedt, M., Dadachov, M. S. and O’Keeffe, M. A mesoporous germanium oxide with crystalline pore walls and its chiral derivative, *Nature*, **2005**, 437, 716–719.
60. Ferey, G., Mellot-Draznieks, C., Serre, C., Millange, F., Dutour, J., Surble, S. and Margiolaki, I. A chromium terephthalate-based solid with unusually large pore volumes and surface area, *Science*, **2005**, 309, 2040–2042.
61. Brunner, G. O. and Meier, W. M. Framework density distribution of zeolite-type tetrahedral nets, *Nature*, **1989**, 337, 146–147.
62. Zwijnenburg, M. A., Bromley, S. T., Jansen, J. C. and Maschmeyer, T. Toward understanding extra-large-pore zeolite energetics and topology: a polyhedral approach, *Chem. Mater.*, **2004**, 16, 12–20.
63. Wyckoff, R. W. G. *Crystal Structures*. John Wiley & Sons, Inc. New York, **1969**.



64. Annen, M. J., Davis, M. E., Higgins, J. B. and Schlenker, J. L. VPI-7 — The 1st zincosilicate molecular-sieve containing 3-membered T-atom rings, *J. Chem. Soc., Chem. Commun.*, **1991**, 1175–1176.
65. Rohrig, C., Gies, H. and Marler, B. Rietveld refinement of the crystal-structure of the synthetic porous zincosilicate VPI-7, *Zeolites*, **1994**, *14*, 498–503.
66. Cheetham, A. K., Fjellvag, H., Gier, T. E., Kongshaug, K. O., Lillerud, K. P. and Stucky, G. D. Very open microporous materials: from concept to reality, *Stud. Surf. Sci. Catal.*, **2001**, 135.
67. Corma, A. From microporous to mesoporous molecular sieve materials and their use in catalysis, *Chem. Rev.*, **1997**, *97*, 2373–2419.
68. van Donk, S., Janssen, A. H., Bitter, J. H. and de Jong, K. P. Generation, characterization, and impact of mesopores in zeolite catalysts, *Catal. Rev. - Sci. Eng.*, **2003**, *45*, 297–319.
69. Perez-Pariente, J., Diaz, I. and Agundez, J. Organizing disordered matter: strategies for ordering the network of mesoporous materials, *C. R. Chimie*, **2005**, *8*, 569–578.
70. Marcilly, C. R. *Petrole et Techniques*, **1986**, 328, 12.
71. Ogura, M., Shinomiya, S. Y., Tateno, J., Nara, Y., Kikuchi, E. and Matsukata, H. Formation of uniform mesopores in ZSM-5 zeolite through treatment in alkaline solution, *Chem. Lett.*, **2001**, 882–883.
72. Ogura, M., Shinomiya, S. Y., Tateno, J., Nara, Y., Nomura, M., Kikuchi, E. and Matsukata, M. Alkali-treatment technique – New method for modification of structural and acid-catalytic properties of ZSM-5 zeolites, *Appl. Catal., A*, **2001**, *219*, 33–43.
73. Groen, J. C., Peffer, L. A. A., Moulijn, J. A. and Perez-Ramirez, J. Mechanism of hierarchical porosity development in MFI zeolites by desilication: the role of aluminium as a pore-directing agent, *Chem. Eur. J.*, **2005**, *11*, 4983–4994.
74. Groen, J. C., Bach, T., Ziese, U., Donk, A., de Jong, K. P., Moulijn, J. A. and Perez-Ramirez, J. Creation of hollow zeolite architectures by controlled desilication of Al-zoned ZSM-5 crystals, *J. Am. Chem. Soc.*, **2005**, *127*, 10792–10793.
75. Schmidt, I., Boisen, A., Gustavsson, E., Stahl, K., Pehrson, S., Dahl, S., Carlsson, A. and Jacobsen, C. J. H. Carbon nanotube templated growth of mesoporous zeolite single crystals, *Chem. Mater.*, **2001**, *13*, 4416–4418.
76. van de Water, L. G. A., van der Waal, J. C., Jansen, J. C., Cadoni, M., Marchese, L. and Maschmeyer, T. Ge-ZSM-5: the simultaneous incorporation of Ge and Al into ZSM-5 using a parallel synthesis approach, *J. Phys. Chem. B*, **2003**, *107*, 10423–10430.
77. van de Water, L. G. A., van der Waal, J. C., Jansen, J. C. and Maschmeyer, T. Improved catalytic activity upon Ge incorporation into ZSM-5 zeolites, *J. Catal.*, **2004**, *223*, 170–178.
78. Li, W. C., Lu, A. H., Palkovits, R., Schmidt, W., Spliethoff, B. and Schuth, F. Hierarchically structured monolithic silicalite-1 consisting of crystallized nanoparticles and its performance in the Beckmann rearrangement of cyclohexanone oxime, *J. Am. Chem. Soc.*, **2005**, *127*, 12595–12600.
79. Corma, A., Fornes, V., Pergher, S. B., Maesen, T. L. M. and Buglass, J. G. Delaminated zeolite precursors as selective acidic catalysts, *Nature*, **1998**, *396*, 353–356.
80. Kirschhock, C. E. A., Kremer, S. P. B., Vermant, J., G. Van Tendeloo, Jacobs, P. A. and Martens, J. A. Design and synthesis of hierarchical materials from ordered zeolitic building units, *Chem. Eur. J.*, **2005**, *11*, 4306–4313.
81. Kloetstra, K. R., van Bekkum, H. and Jansen, J. C. Mesoporous material containing framework tectosilicate by pore-wall recrystallization, *Chem. Commun.* **1997**, 2281–2282.
82. Zhang, Y. W., Okubo, T. and Ogura, M. Synthesis of mesoporous aluminosilicate with zeolitic characteristics using vapor phase transport, *Chem. Commun.* **2005**, 2719–2720.

83. Waller, P., Shan, Z. P., Marchese, L., Tartaglione, G., Zhou, W. Z., Jansen, J. C. and Maschmeyer, T. Zeolite nanocrystals inside mesoporous TUD-1: a high-performance catalytic composite, *Chem. Eur. J.*, **2004**, *10*, 4970–4976.
84. Hamdy-Saad, M. S. *Functionalized TUD-1: synthesis, Characterization and (Photo-) catalytic Performance*. Technische Universiteit Delft, The Netherlands, 2005.
85. Shan, Z., Gianotti, E., Jansen, J. C., Peters, J. A., Marchese, L. and Maschmeyer, T. One-step synthesis of a highly active, mesoporous, titanium-containing silica by using bifunctional templating, *Chem. Eur. J.*, **2001**, *7*, 1437–1443.
86. Moores, A., Goettmann, F., Sanchez, C. and Le Floch, P. Phosphinine stabilized gold nanoparticles; synthesis and immobilization on mesoporous materials, *Chem. Commun.* **2004**, 2842–2843.
87. Thomas, J. M., Raja, R. and Lewis, D. W. Single-site heterogeneous catalysts, *Angew. Chem. Int. Ed.*, **2005**, *44*, 6456–6482.
88. On, D. T., Desplandier-Giscard, D., Danumah, C. and Kaliaguine, S. Perspectives in catalytic applications of mesostructured materials, *Appl. Catal., A*, **2001**, *222*, 299–357.
89. De Vos, D. E., Dams, M., Sels, B. F. and Jacobs, P. A. Ordered mesoporous and microporous molecular sieves functionalized with transition metal complexes as catalysts for selective organic transformations, *Chem. Rev.*, **2002**, *102*, 3615–3640.
90. Song, C. E. and Lee, S. G. Supported chiral catalysts on inorganic materials, *Chem. Rev.*, **2002**, *102*, 3495–3524.
91. Li, C. Chiral synthesis on catalysts immobilized in microporous and mesoporous materials, *Catal. Rev. - Sci. Eng.*, **2004**, *46*, 419–492.
92. Horn, J., Michalek, F., Tzschucke, C. C. and Bannwarth, W. Non-covalently solid-phase bound catalysts for organic synthesis, *Top. Curr. Chem.*, **2004**, *242*, 43–75.
93. Maschmeyer, T., Rey, F., Sankar, G. and Thomas, J. M. Heterogeneous catalysts obtained by grafting metallocene complexes onto mesoporous silica, *Nature*, **1995**, *378*, 159–162.
94. Corma, A., Navarro, M. T. and Renz, M. Lewis acidic Sn(IV) centers – grafted onto MCM-41 – as catalytic sites for the Baeyer–Villiger oxidation with hydrogen peroxide, *J. Catal.*, **2003**, *219*, 242–246.
95. Shylesh, S. and Singh, A. P. Synthesis, characterization, and catalytic activity of vanadium-incorporated, -grafted, and -immobilized mesoporous MCM-41 in the oxidation, of aromatics, *J. Catal.*, **2004**, *228*, 333–346.
96. George, J., Shylesh, S. and Singh, A. P. Vanadium-containing ordered mesoporous silicas: Synthesis, characterization and catalytic activity in the hydroxylation of biphenyl, *Appl. Catal., A*, **2005**, *290*, 148–158.
97. Fernandes, A., Dexpert-Ghys, J., Gleizes, A., Galarneau, A. and Brunel, D. Grafting luminescent metal-organic species into mesoporous MCM-41 silica from europium(III) tetramethylheptanedionate, Eu(thd)(3), *Microporous Mesoporous Mater.*, **2005**, *83*, 35–46.
98. Pillinger, M., Nunes, C. D., Vaz, P. D., Valente, A. A., Goncalves, I. S., Ribeiro-Claro, P. J. A., Rocha, J., Carlos, L. D. and Kuhn, F. E. Immobilization of rhodium acetonitrile complexes in ordered mesoporous silica, *Phys. Chem. Chem. Phys.*, **2002**, *4*, 3098–3105.
99. Pillinger, M., Goncalves, I. S., Lopes, A. D., Ferreira, P., Rocha, J., Zhang, G. F., Schafer, M., Nuyken, O. and Kuhn, F. E. Mesoporous silica grafted with multiply bonded dimolybdenum cations: XAFS analysis and catalytic activity in cyclopentadiene polymerization, *Phys. Chem. Chem. Phys.*, **2002**, *4*, 696–702.
100. Zhou, W. Z., Thomas, J. M., Shephard, D. S., Johnson, B. F. G., Ozkaya, D., Maschmeyer, T., Bell, R. G. and Ge, Q. F. Ordering of ruthenium cluster carbonyls in mesoporous silica, *Science*, **1998**, *280*, 705–708.

101. Shephard, D. S., Maschmeyer, T., Johnson, B. F. G., Thomas, J. M., Sankar, G., Ozkaya, D., Zhou, W. Z., Oldroyd, R. D. and Bell, R. G. Bimetallic nanoparticle catalysts anchored inside mesoporous silica, *Angew. Chem. Int. Ed.*, **1997**, *36*, 2242–2245.
102. Shephard, D. S., Maschmeyer, T., Sankar, G., Thomas, J. M., Ozkaya, D., Johnson, B. F. G., Raja, R., Oldroyd, R. D. and Bell, R. G. Preparation, characterization and performance of encapsulated copper–ruthenium bimetallic catalysts derived from molecular cluster carbonyl precursors, *Chem. Eur. J.*, **1998**, *4*, 1214–1224.
103. Sakthivel, A., Zhao, J., Hanzlik, M. and Kuhn, F. E. Heterogenization of CpMo(CO)(3)Cl on mesoporous materials and its application as olefin epoxidation catalyst, *J. Chem. Soc., Dalton Trans.* **2004**, 3338–3341.
104. Sakthivel, A., Zhao, J. and Kuhn, F. E. Cyclopentadienyl molybdenum complexes grafted on zeolites – synthesis and catalytic application, *Catal. Lett.*, **2005**, *102*, 115–119.
105. Thomas, J. M., Maschmeyer, T., Johnson, B. F. G. and Shephard, D. S. Constrained chiral catalysts, *J. Mol. Catal., A*, **1999**, *141*, 139–144.
106. McKittrick, M. W., Yu, K. Q. and Jones, C. W. Effect of metallation protocol on the preparation and performance of silica-immobilized TiCGC-inspired ethylene polymerization catalysts, *J. Mol. Catal., A*, **2005**, *237*, 26–35.
107. Maschmeyer, T., Oldroyd, R. D., Sankar, G., Thomas, J. M., Shannon, I. J., Klepetko, J. A., Masters, A. F., Beattie, J. K. and Catlow, C. R. A. Designing a solid catalyst for the selective low-temperature oxidation of cyclohexane to cyclohexanone, *Angew. Chem. Int. Ed.*, **1997**, *36*, 1639–1642.
108. Hultman, H. M., de Lang, M., Nowotny, M., Arends, I., Hanefeld, U., Sheldon, R. A. and Maschmeyer, T. Chiral catalysts confined in porous hosts. 1. Synthesis, *J. Catal.*, **2003**, *217*, 264–274.
109. Hultman, H. M., de Lang, M., Arends, I., Hanefeld, U., Sheldon, R. A. and Maschmeyer, T. Chiral catalysts confined in porous hosts. 2. Catalysis, *J. Catal.*, **2003**, *217*, 275–283.
110. Johnson, B. F. G., Raynor, S. A., Shephard, D. S., Maschmeyer, T., Thomas, J. M., Sankar, G., Bromley, S., Oldroyd, R., Gladden, L. and Mantle, M. D. Superior performance of a chiral catalyst confined within mesoporous silica, *Chem. Commun.*, 1167–1168 (1999).
111. Thomas, J. M., Johnson, B. F. G., Raja, R., Sankar, G. and Midgley, P. A. High-performance nanocatalysts for single-step hydrogenations, *Acc. Chem. Res.*, **2003**, *36*, 20–30.
112. Choi, J. S., Kim, D. J., Chang, S. H. and Ahn, W. S. Catalytic applications of MCM-41 with different pore sizes in selected liquid phase reactions, *Appl. Catal., A*, **2003**, *254*, 225–237.
113. Abrantes, M., Gago, S., Valente, A. A., Pillinger, M., Goncalves, I. S., Santos, T. M., Rocha, J. and Romao, C. C. Incorporation of a (cyclopentadienyl)molybdenum oxo complex in MCM-41 and its use as a catalyst for olefin epoxidation, *Eur. J. Inorg. Chem.*, **2004**, 4914–4920.
114. Pruss, T., Macquarrie, D. J. and Clark, J. H. Cobalt-acetato complexes immobilised on PYP A-organomodified silica: a case study of different ways of immobilisation, *J. Mol. Catal., A*, **2004**, *211*, 209–217.
115. Gago, S., Zhang, Y. M., Santos, A. M., Kohler, K., Kuhn, F. E., Fernandes, J. A., Pillinger, M., Valente, A. A., Santos, T. M., Ribeiro-Claro, P. J. A. and Goncalves, I. S. Synthesis and characterization of a manganese(II) acetonitrile complex supported on functionalized MCM-41, *Microporous Mesoporous Mater.*, **2004**, *76*, 131–136.

116. Nunes, C. D., Pillinger, M., Valente, A. A., Goncalves, I. S., Rocha, J., Ferreira, P. and Kuhn, F. E. Synthesis and characterization of methyltrioxorhenium(VII) immobilized in bipyridyl-functionalized mesoporous silica, *Eur. J. Inorg. Chem.*, **2002**, 1100–1107.
117. Zhang, H. D., Xiang, S., Xiao, J. L. and Li, C. Heterogeneous enantioselective epoxidation catalyzed by Mn(salen) complexes grafted onto mesoporous materials by phenoxy group, *J. Mol. Catal., A*, **2005**, 238, 175–184.
118. Yu, K., McKittrick, M. W. and Jones, C. W. Role of amine structure and site isolation on the performance of aminosilica-immobilized zirconium CGC-inspired ethylene polymerization catalysts, *Organometallics*, **2004**, 23, 4089–4096.
119. Sanchez, F., Iglesias, M., Corma, A. and Delpino, C. New rhodium complexes anchored on silica and modified Y-zeolite as efficient catalysts for hydrogenation of olefins, *J. Mol. Catal.*, **1991**, 70, 369–379.
120. Sakthivel, A., Zhao, J., Hanzlik, M., Chiang, A. S. T., Herrmann, W. A. and Kuhn, F. E. Heterogenization of organometallic molybdenum complexes with siloxane functional groups and their catalytic application, *Adv. Synth. Catal.*, **2005**, 347, 473–483.
121. Melis, K., De Vos, D., Jacobs, P. and Verpoort, F. ROMP and RCM catalysed by (R3P)(2)Cl2Ru=CHPh immobilized on a mesoporous support, *J. Mol. Catal., A*, **2001**, 169, 47–56.
122. Shyu, S. G., Cheng, S. W. and Tzou, D. L. Immobilization of Rh(PPh3)(3)Cl on phosphinated MCM-41 for catalytic hydrogenation of olefins, *Chem. Commun.* **1999**, 2337–2338.
123. Bianchini, C., Burnaby, D. G., Evans, J., Frediani, P., Meli, A., Oberhauser, W., Psaro, R., Sordelli, L. and Vizza, F. Preparation, characterization, and performance of tripodal polyphosphine rhodium catalysts immobilized on silica via hydrogen bonding, *J. Am. Chem. Soc.*, **1999**, 121, 5961–5971.
124. de Rege, F. M., Morita, D. K., Ott, K. C., Tumas, W. and Broene, R. D. Non-covalent immobilization of homogeneous cationic chiral rhodium-phosphine catalysts on silica surfaces, *Chem. Commun.* **2000**, 1797–1798.
125. Raja, R., Thomas, J. M., Jones, M. D., Johnson, B. F. G. and Vaughan, D. E. W. Constraining asymmetric organometallic catalysts within mesoporous supports boosts their enantioselectivity, *J. Am. Chem. Soc.*, **2003**, 125, 14982–14983.
126. Augustine, R., Tanielyan, S., Anderson, S. and Yang, H. A new technique for anchoring homogeneous catalysts, *Chem. Commun.* **1999**, 1257–1258.
127. Wagner, H. H., Hausmann, H. and Hölderich, W. F. Immobilization of rhodium diphosphine complexes on mesoporous Al-MCM-41 materials: catalysts for enantioselective hydrogenation, *J. Catal.*, **2001**, 203, 150–156.
128. Crosman, A. and Hölderich, W. F. Selective hydrogenation over immobilized rhodium diphosphine complexes on aluminated SBA-15, *J. Catal.*, **2005**, 232, 43–50.
129. Simons, C., Hanefeld, U., Arends, I., Minnaard, A. J., Maschmeyer, T. and Sheldon, R. A. Efficient immobilization of Rh-MonoPhos on the aluminosilicate AITUD-1, *Chem. Commun.*, **2004**, 2830–2831.
130. Simons, C., Hanefeld, U., Arends, I., Sheldon, R. A. and Maschmeyer, T. Noncovalent anchoring of asymmetric hydrogenation catalysts on a new mesoporous aluminosilicate: application and solvent effects, *Chem. Eur. J.*, **2004**, 10, 5829–5835.
131. Simons, C., Hanefeld, U., Arends, I., Sheldon, R. A. and Maschmeyer, T. Towards genuine cascade reactions: asymmetric synthesis using combined chemo-enzymatic catalysts, *Top. Catal.*, in press.

132. Krijnen, S., Mojet, B. L., Abbenhuis, H. C. L., Van Hooff, J. H. C. and Van Santen, R. A. MCM-41 heterogenized titanium silsesquioxane epoxidation catalysts: a spectroscopic investigation of the adsorption characteristics, *Phys. Chem. Chem. Phys.*, **1999**, *1*, 361–365.
133. Krijnen, S., Abbenhuis, H. C. L., Hanssen, R., van Hooff, J. H. C. and van Santen, R. A. Solid-phase immobilization of a new epoxidation catalyst, *Angew. Chem. Int. Ed.*, **1998**, *37*, 356–358.
134. Smet, P., Riondato, J., Pauwels, T., Moens, L. and Verdonck, L. Preparation and characterization of a titanium(IV) silsesquioxane epoxidation catalyst anchored into mesoporous MCM-41, *Inorg. Chem. Commun.*, **2000**, *3*, 557–562.
135. Herron, N. A cobalt oxygen carrier in zeolite Y – a molecular ship in a bottle, *Inorg. Chem.*, **1986**, *25*, 4714–4717.
136. Fukuoka, A., Higashimoto, N., Sakamoto, Y., Sasaki, M., Sugimoto, N., Inagaki, S., Fukushima, Y. and Ichikawa, M. Ship-in-bottle synthesis and catalytic performances of platinum carbonyl clusters, nanowires, and nanoparticles in microporous and mesoporous materials, *Catal. Today*, **2001**, *66*, 23–31.
137. De Vos, D. E., Meinershagen, J. L. and Bein, T. Highly selective epoxidation catalysts derived from intrazeolite trimethyltriazacyclononane–manganese complexes, *Angew. Chem. Int. Ed.*, **1996**, *35*, 2211–2213.
138. Ogunwumi, S. B. and Bein, T. Intrazeolite assembly of a chiral manganese salen epoxidation catalyst, *Chem. Commun.* **1997**, 901–902.
139. Sabater, M. J., Corma, A., Domenech, A., Fornes, V. and Garcia, H. Chiral salen manganese complex encapsulated within zeolite Y: a heterogeneous enantioselective catalyst for the epoxidation of alkenes, *Chem. Commun.*, **1997**, 1285–1286.
140. Schuster, C. and Holderich, W. F. Modification of faujasites to generate novel hosts for ‘ship-in-a-bottle’ complexes, *Catal. Today*, **2000**, *60*, 193–207.
141. Corma, A. Attempts to fill the gap between enzymatic, homogeneous, and heterogeneous catalysis, *Catal. Rev. - Sci. Eng.*, **2004**, *46*, 369–417.
142. Hartmann, M. Ordered mesoporous materials for bioadsorption and biocatalysis, *Chem. Mater.*, **2005**, *17*, 4577–4593.
143. Zhang, X., Guan, R. F., Wu, D. Q. and Chan, K. Y. Enzyme immobilization on amino-functionalized mesostructured cellular foam surfaces, characterization and catalytic properties, *J. Mol. Catal., B*, **2005**, *33*, 43–50.
144. Polborn, K. and Severin, K. Molecular imprinting with an organometallic transition state analogue, *Chem. Commun.* **1999**, 2481–2482.
145. Tada, M., Sasaki, T. and Iwasawa, Y. Design of a novel molecular-imprinted Rh–amine complex on SiO<sub>2</sub> and its shape-selective catalysis for alpha-methylstyrene hydrogenation, *J. Phys. Chem. B*, **2004**, *108*, 2918–2930.

---

# 2 Problems and Pitfalls in the Applications of Zeolites and other Microporous and Mesoporous Solids to Catalytic Fine Chemical Synthesis

---

MICHEL GUISET<sup>a</sup> AND MATTEO GUIDOTTI<sup>b</sup>

<sup>a</sup>*Faculté des Sciences Fondamentales et Appliquées, Université de Poitiers, UMR CNRS 6503, 40 av. du Recteur Pineau, 86022 Poitiers Cedex, France*

<sup>b</sup>*CNR – Istituto di Scienze e Tecnologia Molecolari, via Venezian 21, 20133 Milano, Italy*

## CONTENTS

2.1	INTRODUCTION . . . . .	39
2.2	ZEOLITE CATALYSED ORGANIC REACTIONS . . . . .	42
2.2.1	Fundamental and practical differences with homogeneous reactions . . . .	42
2.2.2	Batch mode catalysis . . . . .	45
2.2.3	Continuous flow mode catalysis . . . . .	51
2.2.4	Competition for adsorption: influence on reaction rate, stability and selectivity . . . . .	53
2.2.5	Catalyst deactivation . . . . .	61
2.3	GENERAL CONCLUSIONS . . . . .	63
	REFERENCES . . . . .	64

## 2.1 INTRODUCTION

Since the early works on zeolite catalysed organic reactions (reviewed in 1968 by Venuto and Landis<sup>[1]</sup>), an incredibly large number of organic reactions was shown to be catalysed by microporous and mesoporous molecular sieves. Three main factors contribute to this broad applicability of zeolite catalysts:

- The rich variety of their active sites:<sup>[2,3]</sup> protonic acid sites of course, which play a major role in acid catalysed reactions, but also Lewis acid sites acting often in

conjunction with basic sites; redox sites incorporated either in the zeolite framework during hydrothermal synthesis and through post synthesis treatments (e.g. Ti of titanosilicates) or in the channels or cages (e.g. Pt clusters, metal complexes); in addition, redox and acid or basic sites can act in a concerted way for catalysing bifunctional processes.

- The molecular size pore system of zeolites in which the catalytic reactions occur. Therefore, zeolite catalysts can be considered as a succession of *nano* or *molecular reactors* (their channels, cages or channel intersections). The consequence is that the rate, selectivity and stability of all zeolite catalysed reactions are affected by the shape and size of their nanoreactors and of their apertures. This effect has two main origins: spatial constraints on the diffusion of reactant/product molecules or on the formation of intermediates or transition states (shape selective catalysis<sup>[4,5]</sup>), reactant confinement with a positive effect on the rate of the reactions, especially of the bimolecular ones.<sup>[6-8]</sup>
- Both the properties of the active sites (density, strength, etc.) and of the pore systems can be tailored by well-known methods.<sup>[3,9]</sup>

However, despite these remarkable properties, zeolites and related materials cannot be considered (as it is sometimes the case) as *magic* catalysts for the selective synthesis of Fine and Intermediate Chemicals. This is furthermore confirmed by the relatively small number of zeolite catalysed commercial processes, which were developed to substitute the very polluting catalytic systems (e.g.  $\text{AlCl}_3$ ) currently used in the synthesis of Fine Chemicals. This can be related to several reasons:<sup>[10]</sup>

- The relatively small size of units, hence the relatively low absolute amount of wastes, even for high values of the so-called E-factor (the ratio between the amount of waste and the amount of the desired compounds produced in the manufacture of chemicals).<sup>[11,12]</sup>
- The pressure of time, that leads Industry to prefer well established processes often stoichiometric or homogeneously catalysed, to heterogeneously catalysed processes.
- The completely independent historic evolution of organic synthesis and heterogeneous catalysis with, as a consequence, a large difficulty of communication and understanding between specialists of these fields. This difficulty of understanding is also at the origin of various problems met in academic laboratories (generally expert in only one of the fields) for the application of zeolite catalysts to the synthesis of Fine Chemicals.

There are indeed significant fundamental and practical differences between classical organic reactions (either stoichiometric or homogeneously catalysed ones) and those catalysed by solids and especially zeolites (Table 2.1). It is also the case when one compares the relatively simple transformations generally studied by the specialists in Heterogeneous Catalysis and the transformation of complex molecules involved in the synthesis of Fine Chemicals. The operating conditions are very different: high temperature, gas phase, fixed bed reactors on the one hand; low

**Table 2.1** Fundamental and practical differences between homogeneous and zeolite catalysed organic reactions

Parameter	Homogeneous	Zeolite catalysed	Possible consequences
Reaction scheme and mechanism	One phase process Only chemical steps In the same phase	Two phase process Physical steps in addition to chemical steps Chemical steps between species in the organic phase and on the zeolite (adsorption, desorption)	Mass and heat transfer limitations: external, internal Competition for adsorption within the zeolite micropores and on the active sites between reactant, solvent and product molecules Deactivation by poisoning or by pore blockage
Preparation of the reaction mixture	Drying of reactants, solvent and apparatus	Zeolite pretreatment (water elimination, etc.) in addition to the drying of reactants, solvent and apparatus	Very strict control of the residual water on the zeolite → modification of the active sites, hydrolysis of reactants, etc.
Reactor	Batch	Batch with efficient stirring  Fixed bed reactor with plug flow behaviour	External mass- and heat-transfer limitations, if too slow agitation. More precautions for sampling (no extraction of zeolite) Control of textural properties and reactor to avoid high pressure drops and external limitations
Product recovery	Easy for stoichiometric reactions Difficult for homogeneously catalysed reaction	Easy with fixed bed reactors Complicated with batch reactors by the separation of the zeolite from the organic phase	Difficult separation of fine zeolite particles

temperature and liquid phase because of the limited volatility and stability of bulky molecules and often batch reactors on the other. More precautions have to be taken for the safe handling and purification of the generally very toxic reactants, solvents and products of Fine Chemicals. The analytical methods are often more complex, as well.

Therefore the association in the same team of experts in organic chemistry and in catalysis on zeolites is ideal to develop zeolite catalysts for Fine Chemicals synthesis. The organic chemists bring the necessary knowledge about reaction mechanisms (with therefore the possible prediction of secondary products, etc.) and advanced methods in organic analysis and product purification; the specialists in catalysis on zeolites orient the choice of the zeolite catalysts and of activation procedures as well as the selection of the reactor and operating conditions. Moreover, the researchers should have a two-fold culture with, in addition to a



large experience in one field, the basic knowledge in the other, which will allow them to avoid the more frequent pitfalls.

## 2.2 ZEOLITE CATALYSED ORGANIC REACTIONS

### 2.2.1 FUNDAMENTAL AND PRACTICAL DIFFERENCES WITH HOMOGENEOUS REACTIONS

The use of solid catalysts, especially zeolites, introduces large differences in the reaction scheme and mechanisms as well as in the set-up of the desired transformation.

#### Fundamental Differences

In addition to the chemical steps, which are the only steps involved in stoichiometric or in homogeneous catalysis reactions, heterogeneous catalysis reactions involve also physical steps, i.e. transport (transfer) of organic molecules (and heat) from the reaction mixture to the active sites of the solid catalyst and vice versa.<sup>[13–15]</sup> Another difference deals with the chemical steps, which do not occur in the fluid phase, but for part of them involve both fluid and solid phases (chemisorption and desorption), the other part occurring at the surface of the catalyst.<sup>[13–15]</sup>

The various steps involved in a simple model reaction  $A + B \rightarrow C$  are indicated in Figure 2.1. All the steps can affect the reaction rate (i.e. can act as kinetically

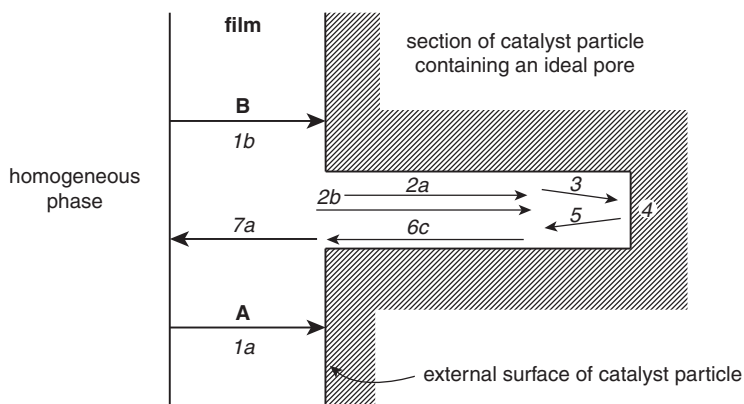


**Figure 2.1** Physical (1,2,6,7) and chemical (3–5) steps involved in the following heterogeneously catalysed model reaction:  $A + B \rightarrow C$ . For sake of simplification the surface reaction (4) is supposed to occur between chemisorbed A and nonadsorbed B molecules. 1, Diffusion of A (1a) and B (1b) molecules from the homogeneous phase to the external surface of catalyst particle. 2, Diffusion of A (2a) and B (2b) molecules along the pores. 3, Chemisorption of A on the active site. 4, Reaction between chemisorbed A and nonadsorbed B with formation of C chemisorbed on the active site. 5, Desorption of C from the active site. 6, Diffusion of C (6c) out of the pore. 7, Diffusion of C (7c) from the pore mouth to the homogenous phase

limiting steps). However, limitations in the mass transfer from the organic phase to the external surface of the catalyst particles, which have always a negative effect on the selectivity, can be generally avoided in both batch and fixed bed reactors. The absence of external limitations can be verified by using simple experimental tests, such as the measurement of the change in the reaction rate, as a function of the stirring rate of a batch reactor. In contrast, particularly with narrow-pore molecular sieves, as zeolites are, it is more difficult to operate in the absence of internal diffusion limitations. It should furthermore be remarked that these internal limitations can be responsible for desired reactant and/or product shape selectivity effects. However, these internal limitations of the reaction rate can be decreased by changing the operating conditions (in particular temperature) or by using, for example, zeolite catalysts with smaller crystallite size. A peculiarity of zeolite catalysts is the strong interaction between their framework and molecules adsorbed in their micropores. Zeolites can be considered as *solid solvents*.<sup>[7,16,17]</sup> This interaction is particularly pronounced between polar organic molecules and hydrophilic zeolites and could be responsible, in addition to steric effects, for limitations in desorption of polar product molecules from the zeolite micropores.

Heat transfer limitations could affect significantly the rate and selectivity of endothermic and especially of exothermic reactions.<sup>[13-15]</sup> Whereas the external thermal limitations could be minimized, this is much more difficult for the internal ones. Indeed the heat is produced or consumed inside the micropores and its transfer to the external surface is particularly slow because of the well-known insulator properties of zeolites.

The other complexity introduced by zeolite catalysts is related to the competition, which necessarily exists among the organic molecules (reactants, products, solvent) for interacting with the active sites. As an example, in the alkylation of phenol with cyclohexene over protonic zeolites,<sup>[18]</sup> whose mechanism involves the attack of phenol molecules by cyclohexenyl carbocations, there is not only the chemisorption of cyclohexene, but also that of phenol on protonic sites. Therefore the kinetic equation is more complex than that of homogeneously catalysed reactions: the reaction order with respect to phenol passes from one to zero with the increase in phenol concentration. Furthermore, like in homogeneous reactions, the reaction rate can be influenced by the solvation of reagents and activated complexes, but, in addition, the competition of the solvent with cyclohexene for the adsorption on the protonic sites can cause a significant decrease in the reaction rate. Likewise, the competition between the various organic molecules for entering the zeolite micropores, which is mainly governed by their polarity, may also affect significantly the rate and selectivity of the reaction.

The use of solid catalysts and especially zeolites in Fine Chemical synthesis introduces another complication with respect to homogeneous reactions. There is always a progressive decrease of the catalyst activity with increasing reaction time.<sup>[19]</sup> In some reactions, this deactivation can be due to irreversible chemical transformation of the zeolite catalyst, e.g. reactions with acid reactants causing dealumination and sometimes collapse of the framework. However, in most cases, deactivation results from poisoning of the active sites by the desired reaction

products (auto-inhibition) or by secondary products and from blockage of the access of the reactant molecules to the micropores by carbonaceous deposits ('coke'). Both types of deactivation can be limited by an adequate choice of the operating conditions (temperature, solvent). Both types of deactivation are reversible: poison molecules can be generally eliminated by solvent treatment under operating conditions, carbonaceous deposits by combustion under conditions that are often not very different from those of zeolite activation.

### Practical Differences

Homogeneous organic reactions (stoichiometric or homogeneously catalysed) are generally carried out in batch reactors and agitation may not be a crucial factor. Batch reactors can also be used for heterogeneously catalysed organic reactions, but, in this case, efficient stirring of the reaction mixture (organic phase plus catalyst) is indispensable to ensure the contact of the reactant(s) with the catalyst surface, hence to allow the catalytic reaction to proceed.

However, continuous reactors, generally fixed bed reactors, which are currently used in gas phase reactions in refining and the petrochemical industry, can also be used for liquid phase organic synthesis in the presence of zeolite catalysts. Better results in terms of catalyst stability are often obtained. However, efforts have still to be made to encourage Organic Chemists to substitute fixed bed reactors, whose set-up is relatively simple, to batch reactors, which are virtually the only devices used in academic organic chemistry.

Activation of solid catalysts under well-specified conditions is a key step for obtaining the desired catalytic performance. It is particularly the case with zeolites, which are hygroscopic solids and for which the efficiency can be significantly reduced by the presence of water (e.g. change in the characteristics of the protonic acid sites, loss of reactant by hydrolysis). Polar organic molecules (even present in low amounts in the atmosphere of the chemical laboratories) can also be rapidly and strongly adsorbed over zeolites causing a decrease of their catalytic efficiency. Pretreatment of the zeolite in the reactor is preferable. This *in situ* pretreatment is easier to carry out in fixed bed than in batch reactors.

The characteristics of the solid particles of catalyst (size, mechanical resistance, etc.) have to be adapted to the reactor. In many organic reactions catalysed by acid zeolites, the catalytic act is concentrated in the outer rim of the crystals and decreasing the zeolite particle size generates a significant gain in activity. However, the use of small particles in batch reactors causes serious drawbacks in the separation of the zeolite from the reaction mixture for the recovery of reaction products and the eventual reuse of the catalyst. Also, small particles cannot be used in fixed bed reactors because of excessive pressure drops.

### Conclusions

Large differences were shown to exist between zeolite catalysed and homogeneous organic reactions. These differences can generate problems and pitfalls in the

investigation of Fine Chemicals synthesis over zeolitic catalysts. The practical difficulties awaiting researchers, who are new to this area, will be presented for reactions carried out in batch and in fixed bed reactors, whereas the important phenomena of competition between reactant(s), solvent, product(s) for adsorption on the active sites and of zeolite deactivation will be shown on the well-documented example of the acetylation of aromatic substrates.

### 2.2.2 BATCH MODE CATALYSIS

In the production of Fine Chemicals, batch operation is the most popular because, in several cases, the quantity of product to be synthesized does not economically justify continuous operation. Moreover, many plants are successively used for the synthesis of different compounds (multipurpose or multiproduct plants). There are however some exceptions, in particular for heterogeneously catalysed processes. The investigation at the laboratory scale of heterogeneously catalysed organic reactions is also generally carried out in batch reactors. This is not surprising, since the set-up of batch reactors, in particular for liquid phase reactions, is reputed to be simpler than the set-up of continuous reactors. Furthermore, only batch reactors are used for stoichiometric and homogeneously catalysed organic reactions.

A standard batch reactor for studying zeolite catalysed organic reactions requires a small volume reaction with an efficient stirring system, a well-designed sampling device, a heating system and a good temperature control. Reactions are often carried out at atmospheric pressure, the (glass) reactor being thus equipped with a reflux condenser. This latter feature could cause problems in mass balance owing to the elimination of highly volatile products. Autoclaves (sealed batch glass, steel or PTFE-lined steel reactors) can also be used, the reactions being then carried out under autogenous or under 'forced' high pressures. The advantage of the autogenous systems is that reactions can be carried out at higher temperatures than at atmospheric pressure. With such devices, the stirring rate, textural properties and water content of the zeolite catalyst, the procedure of sampling and mass balance are critical to obtain valid and reproducible results.

#### **Stirring Rate**

The first role of agitation is to keep the catalyst particles uniformly suspended in the reaction medium. When gas and liquid reactants are simultaneously used, agitation plays an essential role in facilitating the gas to liquid mass transfer.<sup>[20]</sup> Moreover, an efficient stirring is needed to avoid external (i.e. from the organic phase to the external surface of the catalyst particles) mass and heat transfer limitations.<sup>[13-15]</sup>

A simple experimental method can be used to specify the minimum stirring rate to be chosen in order to avoid external mass transfer limitation (provided, however, there is no large temperature gradient between the bulk and surface of the catalyst). Indeed the reaction rate first increases with the stirring rate, then becomes constant, indicating that the rate is then limited by chemical steps. This type of experiment

should always be carried out before investigating a new reaction. However, generally two or three rate measurements are enough to verify the absence of external mass transfer limitations. Of course, the comparison of catalyst activities has no meaning when the reaction is limited by external mass transfer limitations. The same is true for the comparison of catalyst selectivities (generally lower in presence of external mass transfer limitations) and for the measurements of kinetic parameters: reaction order equal to one, activation energy equal to nearly zero for reactions limited by external mass transfer.<sup>[13,14]</sup>

### **Zeolite Particle Size**

In Fine Chemicals synthesis over zeolite catalysts, limitations in the diffusion of reactant(s), solvent and product(s) molecules along the narrow micropores are frequently observed. These limitations can have a positive effect on the selectivity (reactant and product shape selectivity), but have also a negative effect on the reaction rate. Indeed, despite the small size of the zeolite catalyst crystallites ( $\leq 1 \mu\text{m}$ ), only a small part of the zeolite crystal (the outer rim), hence of the potential active sites, can participate in the catalytic reaction. Decreasing the crystal size from micrometre to nanometre scale can generate a significant activity gain. However, this gain is generally limited by the agglomeration of the small crystals and moreover their separation from the reaction products becomes very tedious. Various solutions can be adopted to make this separation easier without significant loss of the benefit linked to the small crystal size. The most efficient method, which is also the most complicated, is to deposit, generally during the hydrothermal synthesis, the zeolite on the external surface of carriers or within their meso- and macropores.<sup>[21–26]</sup> Positive results were obtained with these structured zeolite catalysts, but significant advances are still necessary to generalize this solution for the synthesis of Fine Chemicals.

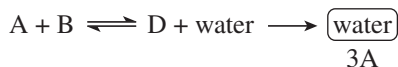
The simplest method is to pelletize the zeolite under low pressure then to crush the pellets into small particles (0.02–0.04 mm). This treatment causes no significant agglomeration of the small crystals and the organic molecules continue to enter easily the zeolite micropores through interparticular mesopores.

### **Activation of the Zeolite Catalyst**

Before their use, zeolite catalysts have always to undergo activation treatments. Part of these treatments depends on the nature of the active sites (e.g. metals supported over zeolites have to be reduced before reaction). However, the elimination of moisture from hygroscopic solids, as zeolites are, has always to be carried out.

The strong affinity of zeolites for water is well known and some of them (Na and K LTA also called 4A and 3A, NaX or 13X) are furthermore used for drying gases or liquid organic compounds both in industrial units and in academic laboratories. Zeolites can also be used as water scavenger to displace thermodynamic equilibrium

of water forming reactions (acetalization, esterification, enamine synthesis, etc.) towards the desired product (D):<sup>[27]</sup>



The amount of water, which is sorbed on zeolites, can be very significant, up to 25 wt% for Na and H-FAU samples with low Si/Al ratios. This amount depends on the partial pressure of water and on various characteristics of the zeolite, such as the pore system, which determines the micropore volume accessible to water, the framework Si/Al ratio, the nature of the cations and the crystallite size. Thus, a linear decrease was found in the amount of water adsorbed at low pressure (that is, strongly adsorbed) over various protonic high silica zeolite materials: MOR,<sup>[28]</sup> BEA<sup>[29]</sup> or MFI,<sup>[30]</sup> with a decrease in the framework Al content. This can be attributed to the decrease in the number of partially ionic, hydrophilic centres associated with the tetrahedrally coordinated Al atoms at the profit of nearly homopolar (hydrophobic)  $\equiv\text{Si-O-Si}\equiv$  bonds. A stoichiometry of four water molecules per H(Al) was found, suggesting the formation of  $\text{H}_9\text{O}_4^+$  species.

Water adsorption over H-MFI samples is particularly well documented.<sup>[31–33]</sup> In addition to the strong sorption on the hydrophilic centres, which occurs at low pressure, there is a weak adsorption of water on the nonpolar  $\equiv\text{Si-O-Si}\equiv$  groups of the MFI channels at higher pressure (1–2 Torr).<sup>[33]</sup> Furthermore, adsorption of water on framework defects can also be observed. A H-MFI sample with small crystal size (0.05  $\mu\text{m}$ ) was shown to sorb 20–25 % more water than a sample with similar Si/Al ratio and a larger crystal size (1–5  $\mu\text{m}$ ). This difference was attributed to water sorption on the terminal silanol groups on the external surface of H-MFI samples. The substitution of the protons of H-MFI by Cs was shown to cause a large decrease (about half) in the amount of water sorbed, which can be related to a stronger interaction of water with the small protons than with large Cs ions. Lastly, the extra-framework Al species created by steaming under severe conditions (24 h, 923 K, 1 bar steam) did not sorb water at room temperature.<sup>[33]</sup>

This short analysis of water adsorption over zeolites indicates that before pretreatment all the zeolite samples contain a certain amount of water depending on the storage and handling conditions as well as on the zeolite characteristics. Moreover, water adsorption at room temperature is so fast and occurs from so very low partial pressures that even exposure of the dry zeolite to the atmosphere for a short time results in the uptake of moisture.

Therefore two types of precautions have to be taken when using zeolite catalysts:

- (1) The first one deals with the determination of the actual amount of zeolite catalyst, i.e. of dry zeolite in the reactor. Indeed, the amount of dry zeolite can be lower, sometimes from 25 % than the amount of nonpretreated sample introduced in the reaction system. The only method for determining the actual

weight of a zeolite catalyst is by using water saturated samples, the water content of which was determined separately (e.g. by TG analysis).

- (2) The second one deals with the complete elimination of adsorbed water (and of other adsorbed polar molecules), which can have various detrimental effects on the reaction, such as modification of the characteristics of the active sites (e.g. decrease in the acid strength of protonic sites) or degradation of moisture sensitive reactants. *In situ* pretreatment, which is very easy to carry out with fixed bed reactors (generally treatment under dry air flow at high temperatures) is more difficult in batch reactors. In this latter case, a good reproducibility of the less severe pretreatment, which is generally chosen (often 523 K *in vacuo*), is not easy to be obtained. Moreover very polar organic molecules cannot be completely desorbed from zeolite micropores. Therefore zeolite catalysts are often pretreated in a specific apparatus with therefore a good reproducibility of pretreatment, but with problems related to moisture uptake during transportation from the pretreatment apparatus to the batch reactor.

### Mass Balance

What is generally essential is to determine with a good accuracy the yield in the desired product with respect to the limiting reactant (the one which is used in substoichiometric amounts). This yield can be determined using the classical approach of organic chemistry: extraction, purification by distillation, liquid phase column flash chromatography, etc. This laborious procedure can only be applied at the end of the reaction and cannot serve for following the increase in yield with reaction time. For this latter purpose, small volume samples have to be taken at different times and rapidly analysed, generally by GC. Only a small amount of the organic phase (<10 %) should be withdrawn during the entire sampling procedure. For reactions carried out at atmospheric pressure, a syringe inserted through a septum is generally used for sampling. For reactions run in autoclaves, sampling is made via a stopcock and a sampling tube dipped in the liquid phase and equipped with a filter to avoid extraction of zeolite catalyst from the reactor.

To obtain a good mass balance, it is advisable to dissolve a small amount of an inert compound in the reaction mixture so as to use it as an internal standard during chromatographic analysis. Of course, the internal standard has to be inert under the operation conditions. Moreover it should not exert a solvation effect and should not compete with the active molecules for adsorption within the zeolite micropores and on the active sites. Using a good internal standard is generally the only way to evidence immediately the elimination of very volatile products from atmospheric pressure reactors or the formation of heavy products not detectable by chromatographic analysis.

However, the use of an internal standard is far from being general. Very often, authors determine the yield in the desired products simply by comparing the relative amounts of this product and of the reactant(s) estimated by chromatographic

analysis. The conversion of the reactant and the selectivity for the desired product are obtained by comparing the relative amounts in the reaction mixture of the reactant and of the desired and secondary products. The average activity of the catalyst for the desired reaction is given by the following equation:

$$A = \frac{X_P Q}{mt} \quad (2.1)$$

where  $X_P$  is the yield in the desired product with respect to the limiting reactant,  $Q$  and  $m$  the amounts of the limiting reactant and of the zeolite catalyst which were introduced in the batch reactor and  $t$  the reaction time. The initial activity (obtained for low values of  $t$  and  $X_P$ ), which is kinetically representative, is generally used for comparing the fresh catalysts. For comparing the performance of the catalysts it is advisable to use the initial TOF values (TOF is the average activity of each of the potential active sites) rather than the values of the initial catalyst activity.

A rough estimation of the concentration of potential active sites is often possible from the composition of the catalyst. Thus the maximum value of the concentration of the protonic sites of zeolites, which are active in most of the acid catalysed reactions, can be estimated from the complete unit cell formula of the zeolite (with distinction between framework and extra-framework Al species). The actual concentration of these sites is often lower (two times or more).

Physicochemical methods, i.e. adsorption of probe molecules followed by varied analytical techniques (gravimetry, chromatography, calorimetry, spectroscopic techniques, etc.) are currently used for estimating more precisely the concentration of the potential active sites.<sup>[34–36]</sup> However, very few methods are well adapted for this purpose: most of the methods employed for the characterization of the acidity of solid catalysts lead to values of the total concentrations of the acid sites (Brønsted + Lewis) and to relative data on their strength, whereas few of them discriminate between Lewis and Brønsted acid sites. It is however the case for base adsorption (often pyridine) followed by IR spectroscopy, from which the concentrations of Brønsted and Lewis sites can be estimated from the absorbance of IR bands specific for adsorbed molecules on Brønsted or Lewis sites.

An additional difficulty in the determination of actual TOF values for zeolite catalysed reactions deals with the accessibility by reactant molecules to the narrow micropores in which most of the potential active sites are located. The didactic presentation in Khabtoui *et al.*<sup>[37]</sup> of the characterization of the protonic sites of FAU zeolites by pyridine adsorption followed by IR spectroscopy shows that the concentration of protonic sites located in the hexagonal prisms (not accessible to organic molecules) and in the supercages (accessible) can be estimated by this method. Base probe molecules with different sizes can also be used for estimating the concentrations of protonic sites located within the different types of micropores, which are presented by many zeolites (e.g. large channels and side pockets of mordenite<sup>[38]</sup>). The concentration of acid sites located on the external surface of the



zeolite crystals (at the pore mouth, in external cups such as with the MCM-22 zeolite, etc.) can also be estimated by adsorption of bulky base molecules, such as 2,6-di-*tert*-butylpyridine,<sup>[39]</sup> collidine,<sup>[40]</sup> and 2,4-dimethylquinoline.<sup>[41]</sup>

### **Stoichiometric or Catalytic Reactions?**

#### **Homogeneous or Heterogeneous Catalysis?**

An important point to check out is whether the reaction is truly catalytic, i.e. whether the total number of reactant molecules which can be transformed on each active site (the turnover number, TON) is greater than one. This is not always the case, generally owing to inhibition of the reaction by products (more details on auto-inhibition will be given in Section 2.2.4).

Leaching of catalytically active species from molecular sieve catalysts may sometimes occur and consequently the heterogeneously catalysed process becomes a homogeneously catalysed one. The problems linked to leaching and to the mode of catalysis were examined in depth in the case of the redox molecular sieves developed for catalytic oxidations with H<sub>2</sub>O<sub>2</sub> and organic peroxides.<sup>[42]</sup> The existence of leaching does not necessarily mean that the reaction occurs through homogeneous catalysis; indeed the leached species can be inactive in solution. However, experiments demonstrating that solid catalysts can be recovered and recycled without apparent loss of activity<sup>[43]</sup> or loss of active species are not enough to prove that the reaction is heterogeneously catalysed.<sup>[42,44]</sup> In fact, a very low amount (hence difficult to be detected) of highly active species in solution is sometimes enough to have a fast homogeneously catalysed process, as demonstrated for the allylic oxidation of  $\alpha$ -pinene with *tert*-butylhydroperoxide in the presence of molecular sieves.<sup>[42]</sup> A good proof of heterogeneity can be obtained by separating the reaction mixture from the catalyst (generally by filtration or centrifugation) before completion of the reaction and testing this mixture for activity.<sup>[42]</sup> However, it is also indispensable to take care in recovering the reaction mixture to avoid eventual re-adsorption or change in the nature of the solubilized species. The latter behaviour was shown to occur, for example, in the allylic oxidation of pinene when the filtration is carried out at room temperature [reduction of active Cr(VI) species into inactive Cr(III) species] and not at the reaction temperature (353 K).<sup>[42]</sup> Nevertheless, such a method could be not exhaustive, in some particular cases, since it may fail to detect active species which possess limited lifetime in solution, but which are continuously supplied by the solid catalyst. In this case, a more precise way of investigating metal leaching is the so-called 'three-phase test' in which the reactant is itself bound to an insoluble solid support.<sup>[45]</sup> Under such conditions, only soluble active metal species will be able to reach the heterogenized substrate and therefore the formation of a heterogenized reaction product is a quite conclusive proof for the existence of leaching of catalytically active species. It should be added that the extent of leaching depends on the reaction and on the operating conditions, which means that catalyst heterogeneity has to be proven for each reaction performed.<sup>[46,47]</sup>

### 2.2.3 CONTINUOUS FLOW MODE CATALYSIS

As indicated in the introduction of Section 2.2.2, continuous flow reactors (generally fixed bed reactors) are not frequently used in the investigation of the liquid phase zeolite catalysed synthesis of Fine Chemicals. However, fixed bed reactors present some significant advantages on batch reactors:

- The zeolite pretreatment can be carried out *in situ* under well-specified conditions with therefore a good reproducibility.
- The reaction products are simply (no step of separation from the zeolite catalyst) and totally (no elimination of the volatile products) recovered in the cooling trap allowing a good mass balance even without use of an internal standard.
- The continuous sweeping of the zeolite catalyst by the feed limits the negative effect of product inhibition.
- Information on catalyst deactivation can be easily obtained simply by following the change in conversion with time-on-stream.

Furthermore, the complexity in the set-up of liquid reactions in fixed bed reactors is largely overestimated, as shown by the simplicity of the scheme of a fixed bed reactor (Figure 2.2).

In a fixed bed reactor, the feed enters one end of the cylindrical tube containing the catalyst and the product stream leaves at the other end (Figure 2.2a). Such equipment is operated at steady state. To obtain the optimal performances (reaction rate and selectivity) a plug-flow behaviour of the reactor is desirable, i.e., no mixing in the axial direction (the direction of flow), complete mixing in the radial direction, and a uniform velocity across the reactor radius.<sup>[13–15]</sup> Therefore the conditions of concentration and temperature are constant in each point of the mass  $dm$  of catalyst, which is contained in the volume  $dV$ . In the study of Fine Chemical synthesis at the laboratory scale, the temperature is generally considered as constant in the whole fixed bed reactor, with also no change with time-on-stream (isothermal operation). The fixed bed reactor is generally considered as a plug-flow reactor when Equations (2.2) and (2.3) among the height  $H$ , the diameter  $D$  of the cylindrical bed of catalyst and the diameter  $d_p$  of the particles of catalyst are satisfied:<sup>[15]</sup>

$$\frac{H}{d_p} > \frac{8n}{0.5} \ln \left( \frac{1}{1-X} \right) \quad (2.2)$$

with  $n$  the reaction order and  $X$  the conversion of the reactant. Thus for  $n = 1$  and  $X = 0.8$ , the  $H/d_p$  ratio should be greater than 25. As this limit ratio increases with both reaction order and conversion, a higher value ( $> 50$ ) is generally chosen. Also,  $D/d_p$  should obey eqn. (2.3).

$$\frac{D}{d_p} > 10 \quad (2.3)$$

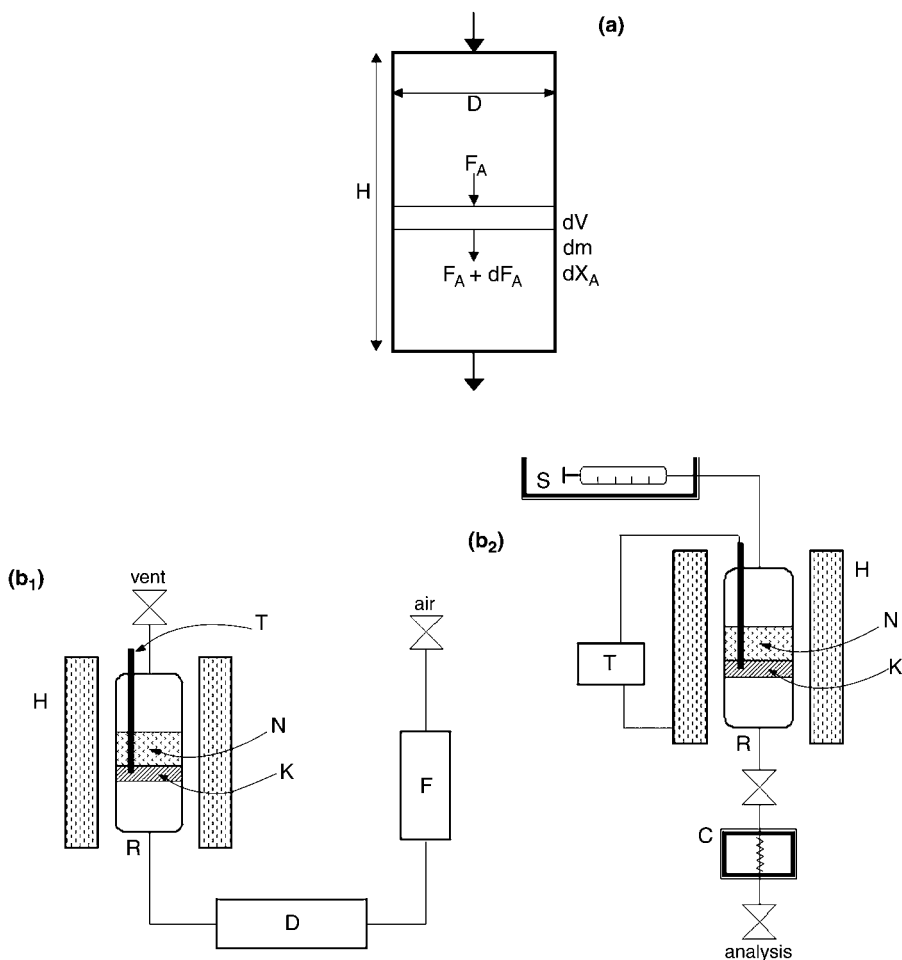


**Figure 2.2** Fixed bed reactor. (a) Scheme of a plug flow reactor. (b) Scheme of a flow type unit with a fixed bed reactor for studying a liquid-phase reaction on zeolite or mesoporous molecular sieve catalyst. (b<sub>1</sub>) Catalyst pretreatment: F, flowmeter; D, dessiccant; H, oven; R, pretreatment reactor; K, catalyst; N, inert material; T, thermocouple. (b<sub>2</sub>) Reaction: R, thermostated glass reactor; H, oven; S, syringe; C, cooling system; T, thermocouple and thermostat; K, catalyst; N, inert. Adapted from Richard *et al.*<sup>[84]</sup>

The size of the catalyst particles will be chosen so as to respect these conditions, but also to avoid a too high pressure drop. For this latter reason, zeolite powder cannot be used. Generally, the powder is pelletized, the resulting pellets being crushed and sieved to yield the desired particle size.

The mass balance for an isothermal transformation of a reactant A in a plug flow reactor operated at steady state can be established from Figure 2.2(a). This mass balance leads to the following relation between the contact time ( $\tau$  in h; taken as the reverse of the weight hourly space velocity, for instance, in grams of reactant

introduced in the reactor per gram of catalyst and per hour), the conversion of A ( $X_A$ ) and the reaction rate ( $r_A$ ; expressed in grams of A transformed per gram of catalyst and per hour):

$$\tau = \int_{X_E}^{X_S} \frac{dX_A}{r_A} \quad (2.4)$$

where  $X_E$  and  $X_S$  are the values of  $X_A$  at the inlet and the outlet of the reactor, respectively.

Additional information on the plug flow fixed bed reactors and on the heat and mass balance equations can be found in the *Handbook of Heterogeneous Catalysis*<sup>[15]</sup> and in the classical books devoted to chemical engineering kinetics.<sup>[13,14]</sup>

External mass transfer limitations, which cause a decrease in both the reaction rate and selectivity, have to be avoided. As in the batch reactor, there is a simple experimental test in order to verify the absence of these transport limitations in isothermal operations. The mass transfer coefficient increases with the fluid velocity in the catalyst bed. Therefore, when the flow rate and amount of catalyst are simultaneously changed while keeping their ratio constant (which is proportional to the contact time), identical conversion values should be found for flow rate high enough to avoid external mass transfer limitations.<sup>[15]</sup>

#### 2.2.4 COMPETITION FOR ADSORPTION: INFLUENCE ON REACTION RATE, STABILITY AND SELECTIVITY

Competition between reactant product and solvent molecules for adsorption within the zeolite micropores and on the internal active sites plays a significant role in the liquid phase transformation of functionalized compounds over zeolites.

The existence of this competition and its significance will be shown here utilising the example of liquid phase reactions involving either one type of reactant molecule (e.g. Fries rearrangement of phenyl acetate, PA) or two (e.g. acetylation of aryl ethers with acetic anhydride). These reactions were chosen because of the large amount of data dealing with their kinetic study, their sensitivity to the zeolite polarity, etc. The effect of the framework polarity will also be examined using the example of the extensively investigated liquid phase oxidations over titanium-containing molecular sieves.

##### Reactions Involving One Type of Reactant Only

The Fries rearrangement of PA over H-BEA zeolites, which is a simple reaction, was chosen to introduce the competition for adsorption on the zeolite catalysts and its role on the reaction rate. *Ortho*- and *para*-hydroxyacetophenones (o- and p-HAP), *para*-acetoxyacetophenone (p-AXAP) and phenol (P) are the main products: o-HAP, P and p-AXAP, which are directly formed (primary products),

result from the intramolecular rearrangement of PA; p-AXAP comes from PA autoacylation; p-HAP, which is not directly formed (secondary product), was shown to result from the acylation of P with PA.<sup>[48]</sup>

**Kinetic studies** A kinetic study of PA transformation was carried out in a batch reactor at 433 K in the presence of sulfolane (very polar) or dodecane (nonpolar) as solvent.<sup>[48]</sup> The initial reaction rates, the decrease in rate with time and the product distribution depend very much on the solvent polarity. The initial rates are lower in the polar sulfolane than in the nonpolar dodecane solvent. In the latter solvent, but not in sulfolane, there is a rapid decrease in the reaction rates, this decrease affecting preferentially the bimolecular formation of p-AXAP and p-HAP. As a consequence, these products are much more favoured with respect to o-HAP in sulfolane than in dodecane. The (p-AXAP + p-HAP)/o-HAP ratio is equal to 7 with sulfolane and 1 with dodecane.

Whatever the solvent, the greater the PA concentration, the greater the production of o-HAP, p-HAP and p-AXAP. However, the effect of PA concentration is always more significant in sulfolane: the apparent orders with respect to PA are close to 1 and 2 for o-HAP and p-AXAP formation in sulfolane and to 0.5 and 1.5 in dodecane.<sup>[48]</sup> Simple kinetic models were developed for o-HAP and p-AXAP formation, which account quantitatively for these observations.<sup>[48]</sup> The kinetic model for o-HAP formation is presented as an example in Figure 2.3. In addition to the three steps (*a*, *b*, *c*) involved in PA transformation into o-HAP (step *b* being generally considered as the kinetically limiting step), the adsorption of the solvent on the active sites was evaluated. The kinetic model for the bimolecular p-AXAP formation is also very simple, involving: (i) adsorption of PA; (ii) reaction of a nonadsorbed PA molecule over a chemisorbed one (Eley–Rideal scheme); and (iii) desorption.

As will be shown, the equation rates obtained for o-HAP formation in the case of strong (polar sulfolane) and weak (nonpolar dodecane) solvent adsorption (Figure 2.3) explain the inhibiting effect of sulfolane as well as the differences in reaction order with respect to PA in the polar (order 1) and nonpolar (order 0.5)

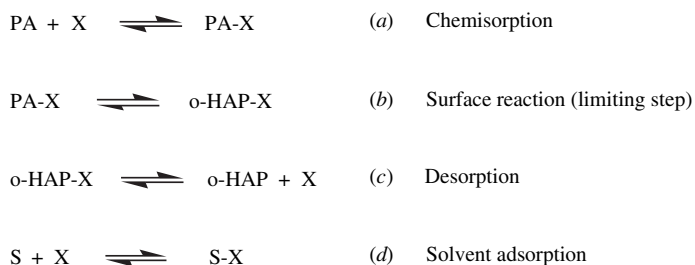


**Figure 2.3** Kinetic model for the rearrangement of phenyl acetate (PA) into *ortho*-hydroxyacetophenone (o-HAP) in presence of a solvent (S). X is the active protonic site of the zeolite

solvents. Indeed, the following general equation of the initial rate ( $r_o$ ) can be drawn from the kinetic model in Figure 2.3:

$$r_o = \frac{k_b K_a C_m C_{PA}}{1 + K_a C_{PA} + K_d C_S} \quad (2.5)$$

with  $k_b$  the rate constant of step  $b$ ,  $K_a$  and  $K_d$  the thermodynamic equilibrium constants of PA and S adsorption (steps  $a$  and  $d$ ),  $C_{PA}$  and  $C_S$  the concentrations of PA and S and  $C_m$  the total concentration in active sites of the catalyst. The adsorption of nonpolar solvents S such as dodecane can be neglected with respect to the adsorption of the PA reactant:  $K_d C_S \ll 1 + K_a C_{PA}$  and thus:

$$r_o = \frac{A C_{PA}}{1 + K_a C_{PA}} \text{ with } A = k_b K_a C_m \quad (2.6)$$

This means a reaction order with respect to PA between zero and 1. The value of 0.5 which is found indicates a relatively strong adsorption of PA ( $K_a C_{PA}$  non-negligible with respect to 1). On the other hand, the very polar sulfolane solvent is more strongly adsorbed than the PA reactant ( $K_d C_S \gg 1 + K_a C_{PA}$ ) and thus:

$$r_o = \frac{A C_{PA}}{K_d C_S} \quad (2.7)$$

that leads to a reaction order of 1 with respect to PA and an inhibiting effect of sulfolane.

The strong adsorption of sulfolane, which limits the contact time of reaction products with the protonic sites (hence the formation of deactivating bulky molecules, such as bisphenol derivatives) can also explain the slower decrease in the rates of the bimolecular transformations and thus the higher selectivity to p-HAP and p-AXAP.<sup>[48]</sup>

**Zeolite polarity and reaction rate** The competition between sulfolane, PA and product molecules for the adsorption on the active protonic sites is sufficient enough to explain the differences in reaction orders and catalyst stability and selectivity between PA transformation in sulfolane and in dodecane. However, the competition for the occupancy of the zeolite micropores plays a significant role as well. This was demonstrated by studying a related reaction: the transformation of an equimolar mixture of PA with phenol in sulfolane solvent on a series of H-BEA samples with different framework Si/Al ratios (from 15 to 90).<sup>[49]</sup> According to the largely accepted next nearest neighbour model,<sup>[50,51]</sup> the protonic sites of these zeolites should not differ by their acid strength, as furthermore confirmed by the

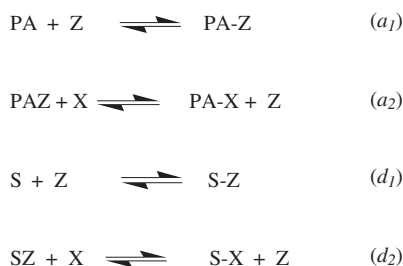


**Figure 2.4** Steps involved in the competition between solvent (S) and phenyl acetate (PA) for adsorption within the micropores of the zeolite (Z) during the rearrangement of PA into *ortho*-hydroxyacetophenone. X is the active protonic site of the zeolite

identical TOF of the protonic sites of all the BEA samples in *m*-xylene isomerization. In contrast, in the transformation of the P-PA mixture, the TOF value increases continuously with the Si/Al ratio.<sup>[49]</sup> As the acidic sites are identical in strength, this increase in TOF with the Si/Al ratio is most likely related to the decrease in the hydrophilicity properties of the zeolite framework. This latter feature would determine the distribution of organic compounds between the bulk solution and the zeolite micropores and hence the occupancy of the zeolite micropores by the different molecules.

The competition between solvent and PA for adsorption within the micropores can be introduced in the kinetic model in Figure 2.3, i.e. there are two successive steps involved in the adsorption of PA and S instead of only one. In Figure 2.4, these two supplementary steps are summarized.  $a_1$  corresponds to the adsorption of PA within the micropores (generally accepted as occurring following the Langmuir model),  $a_2$  to the chemisorption of PA molecules in the micropores on the active sites X,  $d_1$  to the adsorption of the solvent (S) within the micropores and  $d_2$  to the chemisorption of S molecules in the micropores on the active sites X. The substitution in the kinetic model of  $a$  and  $d$  steps by steps  $a_1$ ,  $a_2$  and  $d_1$ ,  $d_2$ , respectively, does not change the form of the kinetic equation for Fries rearrangement in dodecane or in sulfolane. Therefore, this modified kinetic model can also account for the measured reaction orders. The only changes in the kinetic equations reported in Figure 2.3 deal with the substitution of  $K_a$  and  $K_d$  by constants containing two terms corresponding to thermodynamic equilibrium for both adsorption within the zeolite micropores and chemisorption on the acidic sites.

### Reactions Involving Two Reactants

In these reactions, the competition for adsorption involves both reactant molecules and often solvent and product molecules, which makes the choice of optimal operating conditions (solvent, reactant concentrations, temperature) and catalysts much more difficult. The competition between product and reactants plays a major role because such molecules are often largely different in polarity and bulkiness, which was not the case in rearrangement reactions (see above).

**Kinetic studies** The acid catalysed acetylation of aryl ethers: anisole, veratrole, 2-methoxynaphthalene (2MN) with acetic anhydride (AA), for which the effect of operating conditions and of the zeolite polarity is well documented, was chosen as the main example. Kinetic studies of aryl ether acetylation were carried out over H-BEA in absence of solvent (anisole substrate) and over H-FAU (veratrole and 2MN), the reactants being diluted in a large amount of chlorobenzene. In the latter case, an Eley–Rideal model, in agreement with the acetylation mechanism, in which the kinetically limiting step is the reaction of the substrate in liquid phase with the adsorbed AA, has been proposed.<sup>[52,53]</sup> The zero-order with respect to veratrole and 2MN, which was found for high concentrations of these substrates, was related to their strong adsorption on the protonic sites. This strong adsorption has a negative effect on the concentration of chemisorbed AA molecules, hence on the acetylation rate. The competition between substrate and AA molecules for the occupancy of the zeolite micropores was not considered.

In contrast, the kinetic model proposed for anisole acetylation was essentially based on this competition for adsorption within the zeolite micropores.<sup>[54]</sup> Therefore a Langmuir–Hinshelwood model, in which the limiting step is the reaction between adsorbed anisole and AA molecules, was advanced to explain the kinetic results. Competition for adsorption within the micropores of the 4-methoxyacetophenone product with these molecules was also considered. Indeed, the addition of 4-methoxyacetophenone to the reactants was shown to cause a significant decrease in the rate of anisole acetylation suggesting an autoinhibited process owing to a strong adsorption of 4-methoxyacetophenone within the zeolite pores.<sup>[54,55]</sup> The relative values of the adsorption equilibrium constants  $K$  of anisole, AA and 4-methoxyacetophenone were estimated. The  $K$  value for 4-methoxyacetophenone adsorption within the zeolite micropores was found to be ca. 10 and 6 times greater than the  $K$  values for AA and anisole adsorption, respectively, which explains the large inhibiting effect of this acetylated reaction product. These  $K$  values were used to estimate the relative occupancy of the intracrystalline volume of the BEA zeolite by anisole, AA and 4-methoxyacetophenone (Figure 2.5) during the transformation of a 2:1 anisole–AA mixture.<sup>[54]</sup>

However, whereas this analysis of competition effects in anisole acetylation is very attractive, the following oversimplification which was made also has to be considered: indeed, the competitive adsorption of the very polar acetic acid product, which inhibits arene acetylation<sup>[52,53]</sup> and the adsorption equilibrium constants were related to adsorption within the zeolite micropores only, without taking into consideration chemisorption over the protonic active sites.

Autoinhibition of arene acetylation, i.e. the inhibition by the acetylated products and also by the very polar acetic acid product seems to be a general phenomenon. The effect is much more pronounced with hydrophobic substrate molecules such as methyl- and fluoro- substituted aromatics because of the larger difference in polarity between substrate and product molecules.<sup>[56,57]</sup> The occupancy of the zeolite micropores by these substrate molecules as well as their chemisorption on



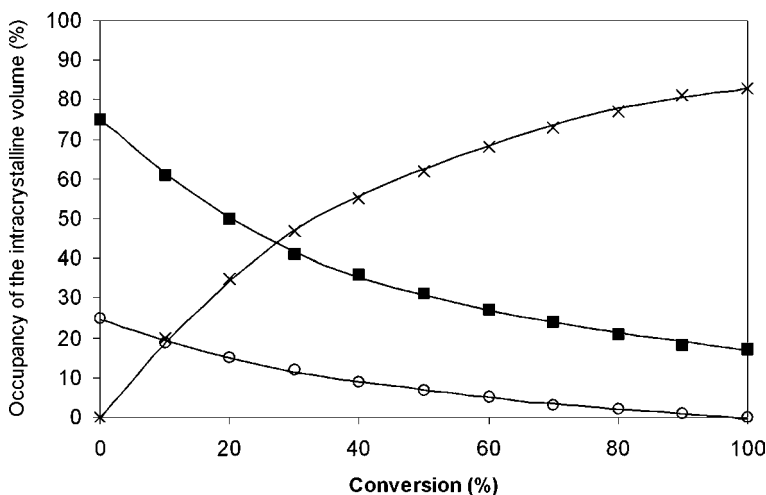


**Figure 2.5** Relative occupancy (%) of the intracrystalline volume of a H-BEA zeolite during the transformation of a 2:1 molar anisole – acetic anhydride mixture in a batch reactor, assuming no adsorption of acetic acid and full occupancy of the micropores. Anisole (■), acetic anhydride (○) and 4-methoxyacetophenone (×). Reprinted from *Journal of Catalysis*, Vol. 187, Derouane *et al.*, Zeolite catalysts as solid solvents in Fine Chemicals synthesis: 1. Catalyst deactivation in the Friedel–Crafts acetylation of anisole, pp. 209–218, copyright (1999), with permission from Elsevier

the protonic sites are very limited in the presence of more polar product species. This inhibition is responsible for a rapid decrease in reaction rate (apparent catalyst deactivation) with, as a consequence, a plateau in the yield in acetylated products after short times in batch reacting conditions. The greater the difference in polarity between product and reactant molecules, the shorter the time to obtain the plateau and the lower the final product yield.<sup>[57]</sup>

**Adsorption experiments** The method developed for the analysis of carbonaceous compounds formed and trapped within the zeolite micropores during catalytic reactions<sup>[58]</sup> can be adapted for determining the occupancy of micropores by reactant, solvent and product molecules. However, this method cannot be used with compounds sensitive to hydrolysis, such as AA, because of the step of dissolution of the zeolite in a hydrofluoric acid solution necessary for the complete recovery of the organic molecules located within the zeolite micropores.<sup>[58]</sup> This method was used to determine the composition of the organic compounds retained within the micropores of three different zeolites [H-BEA (zeolite Beta), H-FAU (zeolite Y), and H-MFI (zeolite ZSM-5)] after contact in a stirred batch reactor at 393 K for 4 min of a solution containing 20 mmol of 2-methoxynaphthalene (2-MN), 4 mmol of 1-acetyl-2-methoxynaphthalene (1-AMN) and 1 ml of solvent (sulfolane or nitrobenzene) with 500 mg of activated zeolite.<sup>[59–61]</sup> From the comparison of

the composition of the reaction mixture (RM) and of the organic compounds adsorbed within the micropores (AM) (Table 2.2), the following conclusions can be drawn:

- Whatever the solvent and the zeolite, large differences can be observed between the compositions of RM and AM mixtures and this behaviour confirms that organic molecules compete for adsorption within the zeolite micropores. Sulfolane, a very polar solvent, is more strongly adsorbed than 2-MN whereas the less polar nitrobenzene solvent is less strongly adsorbed (Table 2.2). This explains the lower rate of 2-MN acetylation with AA found with sulfolane as solvent.<sup>[59]</sup> AMN, the products of this acetylation, are more strongly adsorbed than 2-MN which suggests an autoinhibited process.
- With all zeolites, the bulky 1-AMN molecules enter the micropores (Table 2.2). This was quite unexpected in the case of H-MFI, whose pore opening has a smaller size than that of the molecules of 1-AMN. This can be explained by the high affinity of zeolites for polar molecules. Zeolites can be considered as solid solvents<sup>[7]</sup> and molecules can contract to enter pores which have a smaller size than their free molecular size, this contraction being similar to that observed upon mixing two liquids having a high affinity for each other.<sup>[7]</sup> It can be added that the adsorption of 1-AMN within the micropores of H-MFI is not reversible: 1-AMN produced within the micropores during 2-MN acetylation does not appear in the reaction mixture. Furthermore, the presence of adsorbed 1-AMN within the H-BEA micropores shows that the conversion of 2-MN into 1-AMN can take place within the micropores and not exclusively on the outer surface of the crystallites.
- Whatever the zeolite, 1-AMN is rapidly isomerized within the micropores into 2-acetyl-6-methoxynaphthalene (2-AMN). The 2-AMN/1-AMN ratios in the RM and AM mixtures are quite similar with H-FAU zeolite but smaller in RM than in AM with H-BEA and especially H-MFI (Table 2.2). This indicates limitations in the desorption of the 'linear' 2-AMN molecules from the micropores of the latter two zeolites. In the case of H-BEA, these unexpected limitations were

**Table 2.2** Composition (wt%) of the reaction mixture (RM) and of the organic compounds adsorbed within the zeolite micropores (AM) after contact of a 2-MN and 1-AMN mixture for 4 min at 393 K with the zeolite in nitrobenzene as solvent

	H-BEA (15) <sup>a</sup>		H-FAU (20) <sup>a</sup>		H-MFI (40) <sup>a</sup>	
	RM	AM	RM	AM	RM	AM
Solvent	18.4(15.4) <sup>b</sup>	2.8(75.2) <sup>b</sup>	17.7	10.1	16.7	0.1
2-MN	70.3(72.6)	70.0(17.7)	73.1	59.8	70.2	18.1
AMN	11.3 (12)	27.1 (7.1)	9.2	30.1	13.1	81.9
2-AMN/1-AMN	0.06(0.005)	0.15(0.08)	0.18	0.25	0	0.11

<sup>a</sup>Si/Al ratio values in parentheses.

<sup>b</sup>Data in parentheses refer to tests carried out in sulfolane as solvent.

shown to be related to the strongest interaction of 2-AMN with the zeolite micropores: minimum interaction energy of  $-261 \text{ kJ mol}^{-1}$  for 2-AMN compared with  $-115 \text{ kJ mol}^{-1}$  for 1-AMN.<sup>[62]</sup>

**Zeolite polarity and reaction rate** The relative occupancy of the micropores by reactants, solvent and products molecules depends on the polarity or hydrophobic/hydrophilic properties of the zeolites, which are mainly related to their Si/Al ratio. Unfortunately, no adsorption experiments were carried out to show directly this effect of the zeolite polarity. Nevertheless, such a behaviour is well-known and has been reported for other simpler molecules.<sup>[33,63,64]</sup> However, this effect is well demonstrated by the change in the activity of zeolites and of their active protonic sites (i.e. TOF) with their framework Si/Al ratio. Indeed, for various acid-catalysed reactions of Fine Chemical synthesis, the activity of the protonic sites (TOF) increases with the framework Si/Al ratio (i.e. with the hydrophobicity of the zeolite) because of changes in the competition for adsorption between reactant, solvent and product molecules within the zeolite micropores. This observation cannot be related to differences in the characteristics of the acid sites. In fact, the widely accepted next nearest neighbour model predicts a maximum acid strength value and therefore a constant TOF value for the protonic sites of zeolites with Si/Al ratios greater than 10. An increase in TOF with Si/Al was observed for many other acid catalysed reactions, e.g. acetylation of phenol with PA,<sup>[49]</sup> acetylation of 2-methoxynaphthalene,<sup>[65]</sup> acetylation of toluene with AA,<sup>[66]</sup> acetalization of phenylacetaldehyde and vanillin with glycerol.<sup>[67]</sup> Because of the decrease in the acid site concentration with increasing the Si/Al ratio of the zeolite framework a maximum in catalyst activity is generally found for a high value of the Si/Al ratio (from 30 to 90 depending on the reaction).

The effect of zeolite porosity on the reaction rate was also well demonstrated in liquid-phase oxidation over titanium-containing molecular sieves. Indeed, the remarkable activity in many oxidations with aqueous  $\text{H}_2\text{O}_2$  of titanium silicalite (TS-1) discovered by Enichem is claimed to be due to isolation of Ti(IV) active sites in the hydrophobic micropores of silicalite.<sup>[42,47,68,69]</sup> The hydrophobicity of this molecular sieve allows for the simultaneous adsorption within the micropores of both the hydrophobic substrate and the hydrophilic oxidant. The positive role of hydrophobicity in these oxidations, first demonstrated with titanium microporous glasses,<sup>[70]</sup> has been confirmed later with a series of titanium silicalites differing by their titanium content or their synthesis procedure.<sup>[71]</sup> The hydrophobicity index determined by the competitive adsorption of water and *n*-octane was shown to decrease linearly with the titanium content of the molecular sieve, hence with the content in polar Si-O-Ti bridges in the framework for Si/Al > 40.<sup>[71]</sup> This index can be correlated with the activity of the TS-1 samples in phenol hydroxylation with aqueous  $\text{H}_2\text{O}_2$ .<sup>[71]</sup> The specific activity of Ti sites of Ti/Al-MOR<sup>[72]</sup> and BEA<sup>[73]</sup> molecular sieves in arene hydroxylation and olefin epoxidation, respectively, was also found to increase significantly with the Si/Al ratio and hence with the hydrophobicity of the framework.

The hydrophobicity of TS-1 could also explain why the oxidation of hydrocarbons in aqueous  $\text{H}_2\text{O}_2$  is faster without added organic solvent (triphasic catalysis) than in organic solution (biphasic catalysis): e.g. benzene hydroxylation under triphasic conditions was up to 20 times faster than in acetonitrile or acetone (biphasic conditions).<sup>[74]</sup> Indeed, benzene competes more favourably with water than with organic solvents for adsorption within the micropores of hydrophobic TS-1, as furthermore confirmed through adsorption experiments.<sup>[47]</sup>

The specific activity of Ti-sites in oxidation with aqueous  $\text{H}_2\text{O}_2$  was shown to decrease from microporous to mesoporous molecular sieves such as MCM-41 and HMS. The surface hydrophilicity of the latter mesoporous silicates is likely one of the main reasons for the low activity of Ti sites.<sup>[47]</sup> Water molecules adsorbed on the surface silanol groups would limit the access of organophilic reagents to the Ti sites.<sup>[75]</sup> This can be limited, to a certain extent, by grafting hydrophobic groups on the surface silanols.<sup>[76]</sup>

## Conclusions

Competition between reactant, solvent and product molecules for adsorption within the zeolite micropores is demonstrated directly (adsorption experiments) and indirectly (effect of the framework Si/Al ratio on the activity, kinetic studies) to occur during Fine Chemical synthesis over molecular sieve catalysts. This competition, which is specific for molecular sieves (because of confinement effects within their micropores), adds up to the competition which exists over any catalyst for the chemisorption of reactant, solvent and product molecules on the active sites. Both types of competition could affect significantly the activity, stability and selectivity of the zeolite catalysts. Although the relative contributions of these two types of competition cannot be estimated, the large change in the activity of the acidic sites (TOF) with the zeolite polarity seems to indicate that the competition for adsorption within the zeolite micropores often plays the major role.

The negative effect that this latter competition has can be limited or even avoided by an adequate choice or tailoring of the molecular sieve hydrophilic/hydrophobic properties. The optimization of the operating conditions is also indispensable. Increasing the reaction temperature and the ratio between the concentrations of the less and more polar reactants, as well as a proper choice of the solvent polarity, are simple and complementary solutions to limit the negative effect of competition for adsorption between reactant and product molecules within the zeolite micropores.

### 2.2.5 CATALYST DEACTIVATION

There are different reasons leading to deactivation of zeolite and mesoporous molecular sieves during Fine Chemical synthesis:

- Inhibition (poisoning) of the active sites by impurities, feed components (reactants, solvent) and reaction products.

- Limitations or blockage of the access of reactant molecules to the active sites by carbonaceous deposits ('coke') and by species resulting from catalyst degradation (e.g. extra-framework species resulting from dealumination).
- Elimination of active sites by dealumination of the zeolite framework, leaching of active species, sintering of supported metals, etc.

In hydrocarbon conversion over zeolite catalysts, the formation and retention of heavy products (carbonaceous compounds often called 'coke') is the main cause of catalyst deactivation.<sup>[58,77–81]</sup> These carbonaceous compounds may poison or block the access of reactant molecules to the active sites. Moreover, their removal, carried out through oxidation treatment at high temperature, often causes a decrease in the number of accessible acid sites due to, e.g., zeolite dealumination or sintering of supported metals.

There are several differences between the deactivation of molecular sieve catalysts observed during the transformation of either hydrocarbons or richly functionalized compounds. They are due to different operating conditions: often high temperatures ( $>623$  K) and gas-phase reactions in the first case, generally low temperatures ( $<473$  K) and liquid-phase reactions in the second one. The greater polarity of functionalized compounds plays a key role as well. However, a thorough knowledge of the modes of coking and deactivation acquired with zeolite-catalysed hydrocarbon conversions<sup>[79]</sup> constitutes a solid basis for understanding the deactivation of molecular sieve catalysts used in Fine Chemical synthesis. Moreover, as shown in Section 2.2.4, the method developed for determining the chemical composition of carbonaceous hydrocarbon deposits ('coke')<sup>[58]</sup> can be adapted to the characterization of the compounds retained on the outer surface or within the pores during organic synthesis.

Carbonaceous compounds have the peculiarity of being nondesorbed products.<sup>[78,79]</sup> Therefore, their formation, besides reaction steps, requires the molecules to be retained either within the pores or on the outer surface of the molecular sieve.

In the case of gas-phase hydrocarbon reactions, 'coke' retention occurs for two main reasons:<sup>[77]</sup> (1) the condensation under liquid or even solid state of 'coke' molecules on the catalyst is generally observed at low temperature ( $<473$  K); 'coke' molecules are therefore not sufficiently mobile or volatile to be eliminated from the catalyst under operating conditions; and (2) the steric blockage (trapping) within the pores that often occurs at high temperatures ( $\geq 623$  K), when the size of the product molecules formed within the pores becomes intermediate between the size of the cages or channels and that of the pore apertures.

Both reasons can also play a role in the retention of carbonaceous compounds formed during the transformation of functionalized reactants. However, in both cases, there is an additional effect due to the polarity of these carbonaceous compounds, which is often high. These compounds are therefore strongly adsorbed, limiting the access of reactant molecules to the pores and to the active sites and causing consequently a decrease in the reaction rate. The more polar (hydrophilic) the zeolite, the more significant this effect (as shown in Section 2.2.4 for the arene

acetylation over acidic zeolites). Even the desired products can be strongly retained within the zeolite micropores, because of the coupled effect of their solvation by polar zeolites<sup>[7]</sup> and of steric limitations. These product molecules limit or block the access of reactant molecules to the micropores and hence limit or inhibit the reaction (auto-inhibition). Nevertheless, there are simple ways to reduce the retention of polar product molecules within the zeolite micropores and the following deactivation (see Section 2.2.4). Moreover, these products can be easily desorbed by treatment with an adequate solvent and the catalyst activity completely (or almost) recovered.

However, the long residence time of polar molecules within the pores of molecular sieves may lead to secondary reactions (rearrangement, condensation) yielding bulkier products (generally more polar), which are consequently more strongly retained and sometimes sterically blocked within the pores. Thus, the micropores of a H-BEA zeolite used for a long time for anisole acetylation with AA were shown to contain di- and tri-acetylated anisole resulting from secondary acetylation of the side chain of the desired *p*-methoxyacetophenone.<sup>[55]</sup> These types of compounds, in particular the diacetylated one, was also obtained in the acetylation of veratrole,<sup>[82]</sup> toluene<sup>[83]</sup> and benzofuran.<sup>[84]</sup> Other products resulting from further secondary reactions of the desired products (e.g. dimethoxydypnone, produced by aldolization of *p*-methoxyacetophenone followed by dehydration) or from the transformation of acetic acid via ketene could also be observed. In the acetylation of benzofuran, a large amount of products derived from substrate condensation were also formed and retained within the micropores of a H-FAU zeolite.<sup>[84]</sup>

The bulky and polar compounds trapped within the BEA micropores during anisole acetylation were shown to block the access of nitrogen (hence, obviously, also of the reactants) to these micropores<sup>[55]</sup> and this process is therefore responsible for deactivation. These compounds can only be eliminated from the zeolite by oxidation treatment under dry-air flow at high temperatures (at least 773 K), i.e. under the common pretreatment conditions. By means of this treatment the activity of a H-FAU zeolite for veratrole acetylation was totally recovered.<sup>[82]</sup>

## 2.3 GENERAL CONCLUSIONS

The most frequent problems and pitfalls met in the catalytic synthesis of Fine Chemicals over microporous and mesoporous molecular sieves have been presented and reviewed in this chapter.

Because of such drawbacks, despite the outstanding properties of these materials, their application to well-known stoichiometric or homogeneously catalysed organic transformations can sometimes be far from simple and that is why these catalysts, up to now, are involved in only a few commercial processes. At the origin of the development of these processes, there was always a close cooperation among experts in organic chemistry, synthesis and characterization of catalytic materials,

kinetics, reactor engineering, etc. Therefore, a multidisciplinary approach and a good synergy among researchers skilled in various domains and with a solid general interaction is one of the main conditions to succeed in the set-up of the desired synthetic route.

In addition, significant advances have been made in both basic and applied research which allow a smart and efficient solution to most of these problems. As an example, let us quote the development of the synthesis of novel catalytic materials with tailor-made and more suitable characteristics (stable nanocrystals, controlled hydrophobicity, better thermal and/or mechanical stability, etc.), the understanding of the complex phenomena involved in the catalytic transformation of polar molecules within zeolite micropores or the demonstration that fixed bed reactors, which have many advantages over conventional batch reactors, can be easily used, even for liquid-phase reactions and even for laboratory scale experiments.

Thanks to these positive aspects, it is evident that the time has come to update replace traditional stoichiometric and homogeneously catalysed Fine Chemical syntheses, which are often highly polluting and economically undesirable, with sustainable processes involving catalysis over zeolites and other molecular sieves.

## REFERENCES

1. Venuto, P. B. and Landis, P. S. *Adv. Catal.*, **1968**, *18*, 259–371.
2. Corma, A. *J. Catal.*, **2003**, *216*, 298–312.
3. Guisnet, M. and Gilson, J. P. In *Zeolites for Cleaner Technologies*, Guisnet, M. and Gilson, J. P. (eds), Catalytic Science Series 3. Imperial College Press, Singapore, **2002**, pp. 1–28.
4. Chen, N. Y., Garwood, W. E. and Dwyer, F. D. *Shape Selective Catalysis in Industrial Application*, Chemical Industries Vol. 36. Marcel Dekker Inc., New York and Basel, 1989.
5. Song, C., Garcés J. M. and Sugi, Y. *Shape Selective Catalysis*, American Chemical Society, Washington, DC, **2000**.
6. Derouane, E. G. In *Guidelines for Mastering the Properties of Molecular Sieves*, Barthomeuf, D., Derouane, E. G. and Hölderich, W. (eds), NATO ASI Series B: Physics. Plenum Press, New York, **1990**, pp. 225–239.
7. Derouane, E. G. *J. Mol. Catal. A: Chem.*, **1998**, *134*, 29–45.
8. Gates, B. C., Katzer, J. R. and Schuit, G. C. A. In *Chemistry of Catalytic Processes*. McGraw Hill Book Company, New York, **1979**, pp. 78–85.
9. Szostak, R. *Stud. Surf. Sci. Catal.*, **2001**, *137*, 261–297.
10. Sheldon, R. A. and van Bekkum, H. In *Fine Chemicals through Heterogeneous Catalysis*, Sheldon, R. A. and van Bekkum, H. (eds). Wiley-VCH, Weinheim, 2001, pp. 1–11.
11. Sheldon, R. A. *Chem. Ind. (London)*, **1992**, 903 and **1997**, 12.
12. Sheldon, R. A. *Chem. Tech.*, **1994**, 38–47.
13. Smith, J. M. *Chemical Engineering Kinetics*, McGraw-Hill Book Company, New York, **1970**.
14. Levenspiel, O. *Chemical Reaction Engineering*, John Wiley & Sons, Inc., New York, **1962**.

15. Ertl, G., Knözinger, H. and Weitkamp, J. *Handbook of Heterogeneous Catalysis*. Wiley-VCH, Weinheim, **1997**, Vol. 3, pp. 911–1558.
16. Rabo, J. A., Bezman, R. D. and Poutsma, M. L. *Proc. Symp. Zeolites*, **1978**, 39–52.
17. Barthomeuf, D. *Mater. Chem. Phys.*, **1987**, 17, 49–71.
18. Espeel, P. H. J., Vercruyse, K. A., Deberdemaker, M. and Jacobs, P.A. *Stud. Surf. Sci. Catal.*, **1994**, 84, 1457–1464.
19. Perot, G. and Guisnet, M. *J. Mol. Catal.*, **1990**, 61, 173–196.
20. van Diepen, A. E., Moulijn, J. A. In *Fine Chemicals through Heterogeneous Catalysis*, Sheldon, R. A. and van Bekkum, H. (eds). Wiley-VCH, Weinheim, **2001**, pp. 45–60.
21. van Bekkum, H., Geus, E. R. and Kouwenhoven, H. W. *Stud. Surf. Sci. Catal.*, **1994**, 85, 509–542.
22. Jansen, J. C., Koeqler, J. H., van Bekkum, H., Calis, H. P. A., van der Bleek, C. M., Kapteijn, F., Moulijn, J. A., Geus, E. R. and van der Puil, N. *Microporous Mesoporous Mater.*, **1998**, 21, 213–226.
23. Beers, A. E. W., Nighuis, T. A., Aalders, N., Kapteijn, F. and Moulijn, J.A. *Appl. Catal.*, A, **2003**, 243, 237–250.
24. Winé, G., Tessonnier, J. P., Pham-Huu, C. and Ledoux, M. J. *Chem. Commun.*, **2002** 2418–2419.
25. Madsen, C. and Jacobsen, C. J. H. *Chem. Commun.*, **1999**, 673–674.
26. Derouane, E. G., Schmidt, I., Lachas, H. and Christensen, C. J. H. *Catal. Lett.*, **2004**, 95, 13–19.
27. Hölderich, W. F. and van Bekkum, H. *Stud. Surf. Sci. Catal.*, **2001**, 137, 821–910.
28. Chen, N. Y. *Phys. J. Chem.*, **1976**, 80, 60–64.
29. Breiter, M. W., Farrington, G. C., Roth, W. L. and Duffy, J. L. *Mater. Res. Bull.*, **1977**, 12, 895–902.
30. Olson, D. H., Haag, W. O. and Lago, R. M. *J. Catal.*, **1980**, 60, 390–398.
31. Hunger, B., Heuchel, M., Matysik, S., Beck, K. and Einicke, W. D. *Thermochim. Acta*, **1995**, 269–270, 599–611.
32. Sano, T., Yamashita, N., Iwami, Y., Takoda, K. and Kawakami, Y. *Zeolites*, **1996**, 16, 258–264.
33. Olson, D. H., Haag, W. O. and Borghard, W. S. *Microporous Mesoporous Mater.*, **2000**, 35-36, 435–446.
34. Imelik, B. and Vedrine, J. C. (eds) *Catalyst Characterization, Physical Techniques for Solid Materials*. Plenum Press, New York, **1994**.
35. Ertl, G., Knözinger, H. and Weitkamp, J. (eds) *Handbook of Heterogeneous Catalysis*, Wiley-VCH, Weinheim, **1997**, Vol. 2, pp. 614–770.
36. Bellussi, G. (ed.) *Materials Design for Catalytic Application*. Tipografia Maraschi, Melegnano, **1996**, Part B, pp. 205–350.
37. Khabtou, S., Chevreau, T. and Lavalley, J. C. *Microporous Mater.*, **1994**, 3, 133–148.
38. Jentys, A. and Lercher, J. A. *Stud. Surf. Sci. Catal.*, **2001**, 137, 345–386.
39. Corma, A., Fornes, V., Forni, L., Marquez, F., Martinez-Triguero, J. and Moscotti, D. *J. Catal.*, **1998**, 179, 451–458.
40. Du, H. and Olson, D. H. *J. Phys. Chem. B*, **2002**, 106, 395–400.
41. Laforge, S., Martin, D. and Guisnet, M. *Microporous Mesoporous Mater*, **2004**, 67, 235–244.
42. Sheldon, R. A., Wallau, M., Arends, I. W. C. E. and Schuchardt, V. *Acc. Chem. Res.*, **1998**, 31, 485–493.
43. Lempers, H. E. B. and Sheldon, R. A. *Appl. Catal.*, A, **1996**, 143, 137–143.
44. Lempers, H. E. B. and Sheldon, R. A. *Stud. Surf. Sci. Catal.*, **1997**, 105, 1061–1068.



45. Rebek, J. and Gavina, F. *J. Am. Chem. Soc.*, **1974**, *96*, 7112–7114.
46. Reddy, J. S., Liu, P. and Sayari, A. *Appl. Catal., A*, **1996**, *148*, 7–21.
47. Clerici, M. G. In *Fine Chemicals through Heterogeneous Catalysis*, Sheldon, R. A. and van Bekkum, H. (eds), Wiley-VCH, Weinheim, **2001**, pp. 538–551.
48. Jayat, F., Sabater-Picot, M. J. and Guisnet, M. *Catal. Lett.*, **1996**, *41*, 181–187.
49. Jayat, F. PhD Thesis, University of Poitiers, **1996**.
50. Rabo, J. A. and Gajda, G. J. In *Guidelines for Mastering the Properties of Molecular Sieves*, Barthomeuf, D., Derouane E. G. and Hölderich, W. (eds), NATO ASI Series B: Physics. Plenum Press, New York and London, **1990**, Vol. 221, pp. 273–297.
51. Barthomeuf, D. *Mater. Chem. Phys.*, **1987**, *17*, 49–71.
52. Moreau, P., Finiels, A. and Meric, P. *J. Mol. Catal., A*, **2000**, *154*, 185–192.
53. Meric, P., Finiels, A. and Moreau, P. *J. Mol. Catal., A*, **2002**, *189*, 251–262.
54. Derouane, E. G., Dillon, C. J., Bethell, D. and Derouane-Abd Hamid, S. B. *J. Catal.*, **1999**, *187*, 209–218.
55. Rohan, D., Canaff, C., Fromentin, E. and Guisnet, M. *J. Catal.*, **1998**, *177*, 296–305.
56. Richard, F., Carreyre, H. and Perot, G. *J. Catal.*, **1996**, *159*, 427–437.
57. Guidotti, M., Canaff, C., Coustard, J. M., Magnoux, P. and Guisnet, M. *J. Catal.*, **2005**, *230*, 375–383.
58. Guisnet, M. and Magnoux, P. *Appl. Catal.*, **1989**, *54*, 1–27.
59. Fromentin, E., Coustard, J. M. and Guisnet, M. *J. Mol. Catal., A*, **2000**, *159*, 377–388.
60. Moreau, V., Fromentin, E., Magnoux, P. and Guisnet, M. *Stud. Surf. Sci. Catal.*, **2001**, *135*, 4113–4120.
61. Guisnet, M., Moreau, V. and Magnoux, P. *Bull. Polish Acad. Sci. Chem.*, **2002**, *50*, 203–218.
62. Martin, D. and Guisnet, M. unpublished results.
63. Derouane, E. G., Chang, C. D. *Microporous Mesoporous Mater.*, **2000**, *35–36*, 425–433.
64. Haag, W. O. *Stud. Surf. Sci. Catal.*, **1994**, *84*, 1375–1394.
65. Berreghis, A., Ayrault, P., Fromentin, E. and Guisnet, M. *Catal. Lett.*, **2000**, *68*, 121–127.
66. Derouane, E. G., Crehan, G., Dillon, C. J., Bethell, D., He, H. and Derouane-Abd Hamid, S. B. *J. Catal.*, **2000**, *194*, 410–423.
67. Climent, M. J., Corma, A. and Valles, A. *Appl. Catal., A*, **2004**, *263*, 155–161.
68. Bellussi, G. and Perego, C. In *Handbook of Heterogeneous Catalysis*, Ertl, G., Knözinger, H. and Weitkamp, J. (eds), VCH, Weinheim, **1997**, Vol. 5, pp. 2329–2334.
69. Bellussi, G. and Rigutto, M. S. *Stud. Surf. Sci. Catal.*, **2001**, *137*, 911–955.
70. Klein, S. and Maier, W. F. *Angew. Chem., Int. Ed. Engl.*, **1995**, *35*, 2230–2233.
71. Weitkamp, J., Ernst, S., Roland, E. and Thiele, G. F. *Stud. Surf. Sci. Catal.*, **1997**, *105*, 763–770.
72. Wu, P., Tomatsu, K. and Yashima, T. *Stud. Surf. Sci. Catal.*, **1997**, *105*, 663–670.
73. Corma, A., Cambor, M. A., Esteve, P., Martinez, A. and Perez-Pariente, J. *J. Catal.*, **1994**, *145*, 151–162.
74. Kumar, R. and Bhaumik, A. B. *Microporous Mesoporous Mater.*, **1998**, *21*, 497–504.
75. Khouw, C. B., Dartt, C. B., Laberger, J. A. and Davis, M. E. *J. Catal.*, **1994**, *149*, 195–203.
76. Corma, A., Domine, M., Gaona, J. A., Jorda, J. L., Navarro, M. T., Rey, F., Perez-Pariente, J., Tsuji, J., McCulloch, B. and Nemeth, L. *Chem. Commun.*, **1998**, 2211–2212.
77. Guisnet, M. and Magnoux, P. *Stud. Surf. Sci. Catal.*, **1994**, *88*, 53–68.
78. Guisnet, M. and Magnoux, P. *Catal.Today*, **1997**, *36*, 477–483.
79. Guisnet, M., Magnoux, P. and Martin, D. *Stud. Surf. Sci. Catal.*, **1997**, *111*, 1–19.
80. Guisnet, M. In *Handbook of Heterogeneous Catalysis*, Ertl, G. Knözinger, H. and Weitkamp, J. (eds), VCH, Weinheim, **1997**, Vol. 2, pp. 626–632.

81. Guisnet, M. and Magnoux, P. *Appl. Catal., A*, **2001**, *212*, 83–96.
82. Guignard, C., Pedron, V., Richard, F., Jacquot, R., Spagnol, M., Coustard, J. M. and Perot, G. *Appl. Catal., A*, **2002**, *234*, 79–90.
83. Botella, P., Corma, A., Lopez-Nieto, J. M., Valencia, S. and Jacquot, R. *J. Catal.*, **2000**, *195*, 161–168.
84. Richard, F., Carreyre, H. and Perot, G. *J. Catal.*, **1996**, *159*, 427–434.



---

# 3 Aromatic Acetylation

---

MICHEL GUISNET<sup>a</sup> AND MATTEO GUIDOTTI<sup>b</sup>

<sup>a</sup>*Faculté des Sciences Fondamentales et Appliquées, Université de Poitiers, UMR CNRS 6503, 40 av. du Recteur Pineau, 86022 Poitiers Cedex, France*

<sup>b</sup>*CNR – Istituto di Scienze e Tecnologia Molecolari, via Venezian 21, 20133 Milano, Italy*

## CONTENTS

3.1	AROMATIC ACETYLATION	69
3.1.1	Acetylation with Acetic Anhydride	70
3.1.2	Acetylation with Acetic Acid	82
3.2	PROCEDURES AND PROTOCOLS	89
3.2.1	Selective synthesis of acetophenones in batch reactors through acetylation with acetic anhydride	89
3.2.2	Selective synthesis of acetophenones in fixed bed reactors through acetylation with acetic anhydride	90
REFERENCES		91

### 3.1 AROMATIC ACETYLATION

Arylketones can be synthesized over zeolite catalysts by acylation of aromatic compounds with acetic acid, acetic anhydride (AA) or acetyl chloride.<sup>[1,2]</sup> The use of acetic acid or AA is attractive because of the absence of inorganic waste when using zeolites under their protonic (H) form. These protonic zeolites, which have essentially Brønsted sites, are much less active for acetylation of aromatics with acetyl chloride.<sup>[3,4]</sup> However, slightly better results can be obtained when the zeolites (or mesoporous molecular sieves) are exchanged with metals such as cobalt, zinc, iron, cerium, etc., which could act as precursors of Lewis acid chlorides.<sup>[3]</sup> The Fries rearrangement, which corresponds to an intramolecular transfer of an acetyl group in aromatic acetates (i.e. to an intramolecular acetylation), was also widely investigated over protonic zeolites.<sup>[5]</sup> Only the results obtained by acetylation with AA and acetic acid (including the Fries rearrangement) will be presented here. The mode of preparation over zeolite catalysts of some selected aryl ketones will be described in detail.

## 3.1.1 ACETYLATION WITH ACETIC ANHYDRIDE

In Tables 3.1–3.4 the main data on the electrophilic acetylation of aromatic substrates with AA catalysed by zeolites are listed. Essentially protonic large pore zeolites with FAU and BEA structures and the medium pore size MFI (ZSM-5) zeolite were used as catalysts. Most of the reactions were carried out in batch reactors and often in the presence of a solvent. The deactivating effect of the acetyl group inhibits multiple acylation reactions, hence generally monoacetylated products can be selectively synthesized. The strong influence of the substituents of the aromatic ring on the reactivity of the substrates, which is expected in electrophilic aromatic substitution and shown with Friedel–Crafts catalysts such as  $\text{AlCl}_3$ ,<sup>[1]</sup> is also found with zeolite catalysts. Moreover, with poorly activated substrates such as hydrocarbons, there is a quasi immediate decrease in the reaction rate (Figure 3.1). Hence only low yields in the corresponding acetylated products can be obtained even after long reaction times.<sup>[42]</sup> It is not the case with activated substrates such as aromatic ethers. Acidic zeolites therefore constitute a viable alternative to Friedel–Crafts catalysts for the acetylation of activated polar substrates. However, they could also be used for the acetylation of hydrocarbons by operating under more appropriate conditions, such as very high substrate/AA ratio (e.g. toluene acetylation in Table 3.3<sup>[41]</sup>.) Heterocyclic compounds (thiophene, furan, pyrrole, etc.) are also very reactive towards electrophilic substitution. So, their acetylated derivatives can be produced by acetylation over zeolite catalysts. However competition could exist between their acetylation and condensation reactions. In fact, within the HFAU zeolite micropores, benzofuran is rapidly transformed into bulky trimers, which cause a rapid deactivation of the zeolite.<sup>[50]</sup> Two examples of acetylation of polar substrates: anisole (and other phenyl ethers) and 2-methoxynaphthalene (2-MN) have been chosen to illustrate the possibilities of selective synthesis of acetylated aromatic compounds over protonic zeolites.

The liquid phase acetylation with AA of benzenic ethers, especially of anisole and veratrole [Reactions (3.1) and (3.2)], was investigated over various protonic zeolites with 12- (large pores) or 10- (medium pores) membered ring openings (Table 3.1).

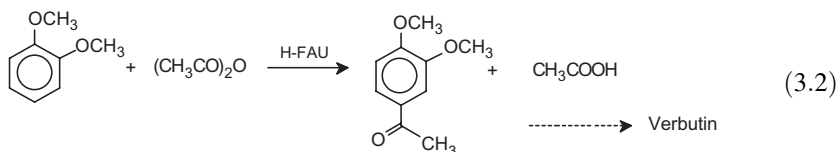
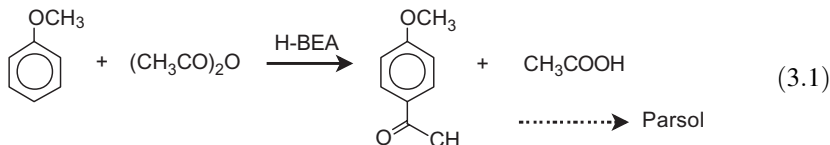


**Table 3.1** Liquid phase acetylation of anisole and derivatives (S) with acetic anhydride (AA) over zeolite catalysts. Batch reactors were employed except in References [6] and [9] (fixed bed reactor)

S	Solvent	Temperature (K)	S/AA	Catalysts	Maximum yield (%)	Ref.
A	No	363	2	HFAU, HBEA, HMOR, HMF1	92	[6]
A	No	363	5	HFAU, HBEA, HMOR, HMF1	70	[3]
1,2-DB	No	363	5		95	[3]
A	No	343	>100	HFAU, LaFAU	36	[7]
A	No	373	1	HBEA	98	[8]
AD	No	373	1	HBEA	52–77	[8]
A	No	363	5	HBEA	96	[9]
A	Toluene	388	1	HBEA, HFAU, HMF1	68	[10]
A	No	343	5	HBEA	85	[11]
A	No	363	2	HBEA	96	[12]
A	No	363	5	HBEA	90	[13]
DB	Chlorobenzene	403	1	HFAU, HBEA	95	[14]
1,2-DB	No	363	1	HFAU, HBEA	60	[15]
AD	No	393	0.8	HFAU, HBEA	>85	[16]
A	No	363	2	Nanosize HBEA	70	[17]
TA	No	353–453	0.3–3	HBEA, HFAU, HMOR, HMF1	32	[18]

A, anisole; DB, dimethoxybenzenes; TA, thioanisole; AD, other anisole derivatives.

**Table 3.2** Liquid phase acetylation in batch reactors of 2-methoxynaphthalene (S) with acetic anhydride (AA) over zeolites and mesoporous molecular sieves

Solvent	Temperature (K)	S/AA	Catalysts	Maximum <sup>a</sup> yield (%)	Ref.
No	373–453	2	HEU, HBEA, HMTW		[19]
Sulfolane	373		HFAU, HBEA		[20]
Chlorobenzene	373		HFAU, HBEA		[20]
Sulfolane	373		HBEA	84	[21]
Chlorobenzene	303–403	2	H-MCM-41	60	[22]
Nitrobenzene					
Carbon disulfide					
No	323	0.1	HFAU, HBEA, HMOR	0	[23]
Sulfolane	373	2	HBEA (modified)	49	[24]
Sulfolane	393	5	HBEA	100	[25]
Nitrobenzene					
1,2-Dichlorobenzene					
1-Methylnaphthalene					
Nitrobenzene	363–428	5	HBEA	~100	[26]
Nitrobenzene	393	5	HBEA (dealuminated)	100	[27]
1,2-Dichloroethane	373	1	HBEA	75	[28]
Sulfolane	373–423	1	HBEA, HFAU, HMOR	40	[29]
Nitrobenzene	400	2	HBEA	45	[30]
1,2-Dichlorobenzene					
Dichloromethane	393	0.5	HBEA, HFAU	63	[31]
Chlorobenzene	405	2	HBEA, Al-ITQ-7	84	[32]
Nitrobenzene	393	?	HFAU, HBEA, HMF1	Isom <sup>b</sup>	[33]
Chlorobenzene	353	1	HFAU	~50	[34]
Nitrobenzene	393	5	HBEA	100	[35]
Nitrobenzene	403	0.5	HBEA, MBEA (M=In,Zn, Al,Fe,La)	58	[36]
Chlorobenzene	405	2	HBEA	80	[37]
Chlorobenzene	353–453	1	HBEA	36	[38]
Chlorobenzene	405	0.5	HBEA	71	[39]

<sup>a</sup>All the acetylmethoxynaphthalenes were considered.

<sup>b</sup>2-Methoxynaphthalene and 1-acetyl-2-methoxynaphthalene as reactants.

Whatever the zeolite, 4-methoxyacetophenone and 3,4-dimethoxyacetophenone are largely predominant (>95%), which indicates that this selective formation is not due to shape selectivity effects, but is a characteristic of the reaction. In contrast, the selectivity of 2-MN acetylation (Figure 3.2) depends very much on the

**Table 3.3** Liquid and gas phase acetylation of aromatic hydrocarbons (S) with acetic anhydride (AA) over zeolites

S	Solvent	Temperature (K)	S/AA	Catalyst	Maximum yield (%)	Ref.
<i>Liquid phase acetylation (batch reactor)</i>						
Isobutylbenzene	No	413	10	HBEA	80	[40]
Isobutylbenzene	1,2-Dichloroethane	373	1	HBEA	17	[28]
Toluene	No	388	1–20	HFAU,HBEA, HMOR,HMFI	20	[13]
Toluene	No	423	20	HBEA	80	[41]
Toluene	Nitrobenzene	373	5	HBEA	11	[42]
Toluene	Nitrobenzene, <i>o</i> -Dichlorobenzene	408	0.5	RE-BEA	66	[46]
<i>m</i> -Xylene	No	403	5	HBEA	20	[10]
<i>m</i> -Xylene	No	383	10	HBEA	40	[36]
<i>m</i> -Xylene	Nitrobenzene	373	5	HBEA	16	[42]
Naphthalene	Decaline	408	1–4	HFAU,HBEA,HMOR	35	[43]
Naphthalene	Decaline	408	2 <sup>a</sup>	HFAU,HBEA,HMOR	43	[44]
2-Methylnaphthalene	Nitrobenzene	373	5	HBEA	5	[42]
Biphenyl	1,2-Dichloroethane	356	1	HBEA	7	[45]
	1,2-Dichlorobenzene	418	1		8.5	
<i>Gas phase acetylation (fixed bed reactor)</i>						
Benzene	No	423	2	HMFI, CeHMFI	82	[47]

<sup>a</sup>Stepwise addition of AA.



**Table 3.4** Liquid and gas phase acetylation of heteroarenes (s) with acetic anhydride (AA) over zeolite catalysts

S	Solvent	T (K)	S/AA	Catalyst	Yield (%)	Selectivity (%)	Ref.
<i>Liquid phase synthesis of acetyl derivatives<sup>a</sup></i>							
Benzofuran	Chlorobenzene	333	0.08	HFAU	60	>95 (2ac)	[48]
Benzofuran	Chlorobenzene	333	0.5	HFAU	32	>95 (2ac)	[49]
Benzofuran	No	333	0.08	HFAU (16)	40	90 (2ac)	[50]
2-Methylbenzofuran	No	333	0.08	HFAU (16)	96	96 (3ac 2Me)	[50]
Benzofuran	No	333	0.075	HFAU (16)	65	60 (2ac)	[51]
2-Methylbenzofuran	No	333	0.066	HFAU (16)	96	96 (3ac 2Me)	[51]
<i>Gas phase synthesis of 2-acetyl derivatives<sup>b</sup></i>							
Thiophene	—	523	3	BMFI	32	98	[52]
Furan	—	473	2	CsBMFI	23	99	[52]
Pyrrrole	—	423	2	CsBMFI	41	98	[52]
Furan	—	423	1	HMFI (30)	67.5	72	[53]
Pyrrrole	—	523	1	HMFI (280)	75.5	97.5	[53]
Imidazole	—	673	1	BMFI	32 <sup>c</sup>	56 <sup>c</sup>	[54]

<sup>a</sup>Batch reactor except in Reference [51] (fixed bed reactor).

<sup>b</sup>Fixed bed reactor.

<sup>c</sup>4-Acetylimidazole.

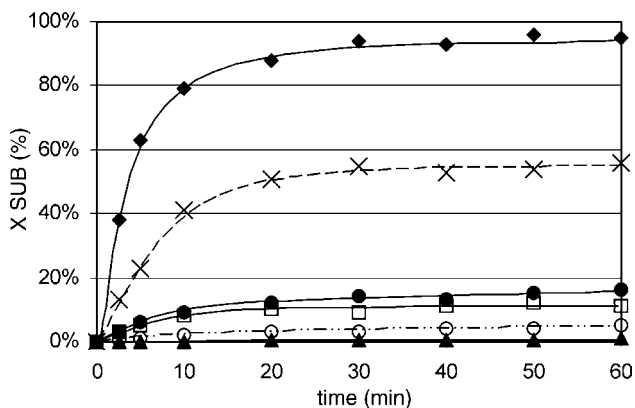


**Figure 3.1** Acetylation at 373 K with acetic anhydride of a series of aromatic compounds over HBEA-15 zeolite. Conversion ( $X_{\text{SUB}}$ ) of anisole ( $\blacklozenge$ ), 2-methoxynaphthalene ( $\times$ ), *m*-xylene ( $\bullet$ ), toluene ( $\square$ ), 2-methylnaphthalene ( $\circ$ ) and fluorobenzene ( $\blacktriangle$ ) versus time. Reprinted from *Journal of Catalysis*, Vol. 230, Guidotti *et al.* Acetylation of aromatic compounds with H-BEA zeolite: the influence of the substituents on the reactivity and on the catalyst stability, pp. 375–383, Copyright (2005), with permission from Elsevier

zeolite or mesoporous molecular sieve employed as catalyst. Acetylation at the C-6 position (Figure 3.2) is of particular interest, 2-acetyl-6-methoxynaphthalene (2-AMN) being a precursor of the anti-inflammatory (*S*)-Naproxen. Because of the bulkiness of 2-MN and 2-AMN molecules, 2-MN acetylation was essentially

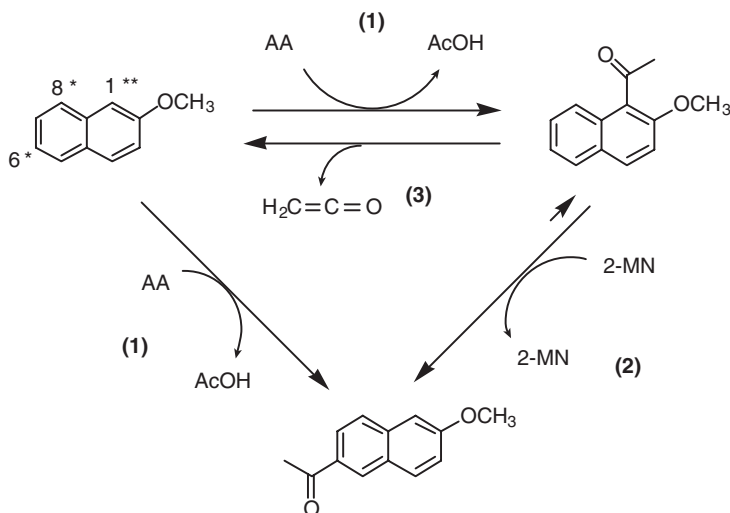


**Figure 3.2** Reaction scheme of the acylation of 2-methoxynaphthalene (2-MN) with acetic anhydride (AA) over zeolites. Most activated and activated positions for the electrophilic substitution are indicated by \*\* and \*, respectively

investigated over large pore zeolites: HFAU, HMOR, HMTW, HBEA, HITQ-7 and over mesoporous MCM-41 molecular sieves (Table 3.2). Furthermore, because of the high melting point of substrate and products (e.g. 2-MN, 70 °C; 2-AMN, 108 °C), 2-MN acetylation was generally carried out in the presence of solvents.

Industrial processes were developed for the production of 4-methoxyacetophenone (HBEA catalyst) and of 3,4-dimethoxyacetophenone (HFAU catalyst), which are, respectively, precursors of Parsol, a solar protector and of Verbutin, a synergist for insecticides.<sup>[4]</sup> It is not the case for the synthesis of 2-AMN despite the significant advances made in the selective acetylation of 2-MN over zeolite catalysts.

Most of the academic studies of aryl ether acetylation are carried out in a batch reactor often in the presence of solvents, whereas in the industrial units the reactions are operated in fixed bed reactors and in the absence of solvent.

**Reaction mechanism** It is generally admitted that, over zeolites, acetylation of arenes with AA is catalysed by protonic acid sites. Comparison of the activity of a series of dealuminated HBEA samples allows one to exclude any direct participation of Lewis acid sites in 2-MN acetylation with AA. Indeed, two HBEA samples with similar protonic acidities but with very different concentrations of Lewis acid sites (170 and 16  $\mu\text{mol g}^{-1}$ ) have practically the same acylating activity.<sup>[27]</sup> The role of Brønsted sites is also clearly expressed in Spagnol *et al.*<sup>[31]</sup>

The acetylation mechanism which is currently accepted involves three successive steps, e.g. for anisole acetylation (Figure 3.3):

- Chemisorption of acetic anhydride on the zeolite protonic sites with formation of acylium ions and of acetic acid (Step 1).

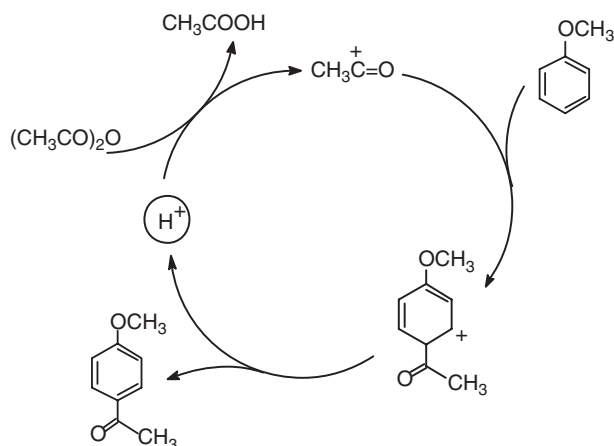


**Figure 3.3** Mechanism of anisole acetylation over protonic sites

- Attack of anisole molecules by acylium ions with formation of cyclohexadienylium cations (Step 2).
- Desorption of acetoanisole from the protonic sites (Step 3).

In the absence of diffusion limitations, Step 2 is the kinetically limiting step.

Whereas the acetylation of phenyl ethers over zeolite catalysts leads to the desired products, acetylation of 2-MN occurs generally at the very activated C-1 position with formation of 1-acetyl-2-methoxynaphthalene (1-AMN). A selectivity for 1-AMN close to 100% can be obtained over silicoaluminate MCM-41 mesoporous molecular sieves<sup>[22]</sup> and FAU zeolites,<sup>[33,34]</sup> whereas with other large pore zeolites with smaller pore size (BEA, MTW, ITQ-7), 2-AMN (and a small amount of 1-acetyl-7-methoxynaphthalene, 3-AMN) also appears as a primary product. Average pore size zeolites, such as MFI, are much less active than large pore zeolites. These differences were related to shape selectivity effects and a great deal of research work was carried out over BEA zeolites in order to specify the origin of this shape selectivity: the difference is either in the location for the formation of the bulkier (1-AMN) and 'linear' (2-AMN) isomers (only on the outer surface for 1-AMN, preferentially within the micropores for 2-AMN)<sup>[19,21,24,28,38]</sup> or more simply in the rates of desorption from the zeolite micropores.<sup>[26,32,33,35]</sup>

In addition to 2-MN acetylation, secondary reactions of 1-AMN, isomerization into 2-AMN, and deacetylation, which both increase the selectivity to the desired product 2-AMN were demonstrated to occur on BEA zeolites.<sup>[26]</sup> This is shown in Figure 3.4 on a HBEA-15 (framework Si/Al ratio of 15). After 45 min of reaction, AA is completely consumed, AMN and acetic acid being the only reaction products (yield in AMN with respect to AA close to 100%). Afterward there is a slow decrease in this yield indicating a deacetylation process, and a faster increase in the 2- and 3-AMN

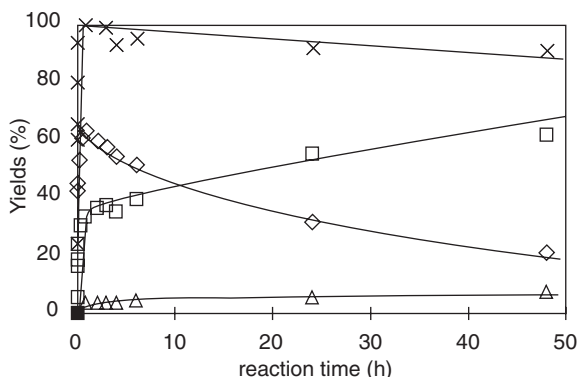
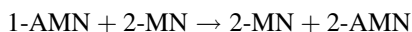


**Figure 3.4** Acetylation at 393 K of 2-methoxynaphthalene with acetic anhydride over HBEA-15 zeolite. Total yield in acetyl-methoxynaphthalene (x) and yields in 1-acetyl-2-methoxynaphthalene (◇), 2-acetyl-6-methoxynaphthalene (□) and 1-acetyl-7-methoxynaphthalene (△). Reprinted from *Journal of Molecular Catalysis A: Chemical*, Vol. 159, Fromentin *et al.*, Acetylation of 2-methoxynaphthalene with acetic anhydride over a HBFA zeolite, pp. 377–388, Copyright (2000), with permission from Elsevier

yields at the expense of 1-AMN (isomerization).<sup>[25]</sup> Initially (extrapolation at time zero), the AMN distribution is largely in favour of 1-AMN (75 %) and at long reaction times in favour of 2-AMN (69 % after 50 h). Furthermore, deacylation was shown to occur essentially from 1-AMN.<sup>[19,25]</sup> The various reactions occurring during the acetylation of 2-MN with AA on a BEA zeolite are presented in Figure 3.2.

Deacylation of 1-AMN involves, most likely, the reverse steps of acetylation. The resulting acylium ions can react with 2-MN with formation of the 2-AMN isomer. However, the isomerization of 1-AMN into 2-AMN does not occur essentially through this deacylation–acylation mechanism, but through the following intermolecular transacylation process reaction:



Indeed, isomerization of 1-AMN into 2-AMN was found to be much faster in the presence of 2-MN than in its absence. Furthermore, this intermolecular mechanism was confirmed by investigating the transformation of a mixture of 1-AMN with a deuterated methoxy group (OCD<sub>3</sub>) and of nondeuterated 2-MN.<sup>26</sup>

The location of 2-MN acetylation reactions over HBEA zeolites was widely debated. Some authors claim that the bulkier isomer 1-AMN can only be formed at the generally large external surface of BEA zeolite, the ‘linear’ isomer 2-AMN both within the micropores and on the external surface,<sup>[19,21,24,28,38]</sup> other authors state that both isomers are essentially formed within the micropores.<sup>[26,32,33,35]</sup> Both proposals can explain the increase in the selectivity to the bulky isomer (1-AMN) with decrease in the crystallite size.<sup>[28,32]</sup> Indeed the smaller this size, the greater the external surface, hence the higher the rate of reactions on this surface, but also the shorter the micropore length and, consequently, the smaller the differences in the rates of desorption of the bulky and ‘linear’ isomers. Both proposals can also explain the decrease in the selectivity for 1-AMN with the passivation or the poisoning of the external surface by bulky base molecules.<sup>[28]</sup> Additional arguments in favour of the formation of both isomers within the micropores are provided by:

- (i) Molecular modelling:<sup>[55]</sup> 1-AMN molecules can easily lodge within the micropores of HBEA (minimum interaction energy of  $-114.5 \text{ kJ mol}^{-1}$ ), hence can be formed on the inner acid sites.
- (ii) Adsorption of a mixture of 2-MN, 1-AMN and solvent on zeolites under the conditions of acetylation,<sup>[33,35]</sup> which demonstrates that 1-AMN can enter the micropores of HBEA and even those of HMFI, whose pore aperture is smaller than the molecular size of 1-AMN. The confinement model developed by Derouane<sup>[56]</sup> account for this unexpected latter observation.
- (iii) Experiments with ITQ-7, a tridirectional zeolite with channels smaller than those of BEA: the higher selectivities for 2-AMN can only be related to the lower diffusion coefficient of 1-AMN in ITQ-7 than in BEA.<sup>[32]</sup>

Therefore, it can be concluded that 1- and 2-AMN can be formed within the zeolite micropores of large and even medium pore zeolites, their distribution

depending on the physicochemical characteristics of the zeolite and on the operating conditions. When the rate of 1-AMN isomerization into 2-AMN is lower than the rate of desorption of 1-AMN from the zeolite, 1-AMN isomer can be selectively formed (e.g. with HFAU and MCM-41). In the reverse case (e.g. with HBEA), a large part of 1-AMN molecules formed within the micropores will be transformed into 2-AMN molecules, which because of their smaller size desorb more easily from the zeolite. Therefore, although 2-MN is selectively acetylated into 1-AMN within the BEA zeolite micropores, 2-AMN could appear in large amounts as a primary product.

**Optimal operating conditions and catalysts** Acetylation of phenyl ethers was generally carried out in the absence of solvents, which makes easier the recovery of the acetylated product from the reaction mixture. On the other hand, because of the high melting point of substrate and acetylated products, solvents were always used in the acetylation of 2-methoxynaphthalene. Flow reactors (e.g. fixed bed tubular reactors), in which the detrimental effect of competitive adsorption of substrate and products on the acetylation yield is lower than in the batch reactors, should be preferred. However although the set up of fixed bed reactors for liquid phase reactions is relatively simple, their substitution to the batch reactors, which are the only system used in academic organic chemistry, remains essentially limited to commercial units.

Anisole and veratrole acetylation with AA were carried out over three large pore zeolites: HFAU, HBEA and HMOR and one average pore size zeolite HMF1.<sup>[3]</sup> With both substrates, the initial rates as well as the maximum yield were found lower over the monodimensional MOR zeolite and with MFI, which was explained by diffusion limitations. Anisole acetylation was shown to be quicker and the maximum yield higher over HBEA than over HFAU, whereas the reverse was found with veratrole acetylation.<sup>[3,4]</sup> Such behaviour could be explained from the relative sizes of the acetylation intermediates and of the micropores (transition shape selectivity).<sup>[3]</sup> Whereas HFAU and HBEA zeolites with similar Si/Al ratios have practically the same activity for 2-MN acetylation, HMF1 is practically inactive. Furthermore, HBEA is more active than HFAU for 1-AMN isomerization.

The initial rate of 2-MN acetylation depends on the framework Si/Al ratio of the zeolite catalyst.<sup>[27]</sup> For a series of dealuminated BEA samples (by treatment with hydrochloric acid or with ammonium hexafluorosilicate), the acetylation rate passes through a maximum for a number of framework Al atoms per unit cell ( $N_{Al}$ ) between 1.5 and 2.0 (Si/Al ratio between 30 and 40). The activity of the protonic sites (i.e. the TOF) increases significantly with Si/Al: from  $420 \text{ h}^{-1}$  for Si/Al = 15 to  $2650 \text{ h}^{-1}$  for Si/Al = 90. It should be noted that similar TOF values could be expected from the next nearest neighbour (NNN) model. Indeed all the framework Al atoms of the zeolite (hence all the corresponding protonic acid sites) are isolated for Si/Al ratio > 10.5. Therefore the acid strength of the protonic sites is then maximal as well as their activity.<sup>[57,58]</sup> This was furthermore found for *m*-xylene isomerization over the same series of BEA zeolites.<sup>[27]</sup> This increase in TOF for

2-MN acetylation is most likely related to the high polarity and bulkiness of the products with limitations in the reaction rate by product desorption. Dealumination would have a positive effect on the acetylation rate because of the decrease in the zeolite hydrophilicity and of the increase in the rate of diffusion of the bulky products owing to elimination of extra-framework Al species. Curiously, in anisole acetylation, the Si/Al ratio of the HBEA zeolite had practically no effect on the reaction rate. However it is worth noting that most of the tested samples had Si/Al ratios between 11 and 30. Like for 2-MN acetylation,<sup>[28,32]</sup> the performance of HBEA zeolites in anisole acetylation depends on their crystallite size.<sup>[17]</sup> This was shown by comparing the activities of samples with large size (0.1–0.4  $\mu\text{m}$ ) and of a nanosize sample (0.01–0.02  $\mu\text{m}$ ) prepared within the pores of a carbon black matrix. The superior performance of the nanosize sample was ascribed to a decrease in diffusional constraints limiting the desorption of the bulky and polar *p*-methoxyacetophenone product from the BEA micropores.

The solvents used to solubilize 2-MN reactant and AMN products were shown to have a large effect on the reaction rate and selectivity.<sup>[25]</sup> Thus, the rate of acetylation was maximum in 1,2-dichloromethane, higher than in 1-methylnaphthalene, which is less polar, and in nitrobenzene and sulfolane, which are more polar. The polarity referred to here relates to the polarity parameter ET proposed by Dimroth and Reichardt.<sup>[59,60]</sup> This change in acetylation rate can be explained by two opposite effects of the solvent polarity:<sup>[25]</sup>

- (i) The solvation of acylium intermediates: the more polar the solvent, the more significant the solvation, hence the faster the acylation.
- (ii) The competition between solvent and reactant molecules for entering the zeolite micropores and for adsorbing on the acidic sites: the more polar the solvent, the less significant the amount of acylium ions and of 2-MN molecules within the zeolite micropores, hence the slower the acylation.

Most likely, this competition between solvent and the other organic molecules is responsible for the decrease in the initial selectivity for 2-AMN and in deacylation with the increase of solvent polarity: there is a decrease in the residence time of 1-AMN molecules within the zeolite pores with consequently less secondary reactions. However at long reaction times, the highest yield in 2-AMN is obtained with nitrobenzene, a solvent of intermediate polarity, and not with the less polar solvents. It is probably because competition with solvent plays a role in both the residence times of 1-AMN and 2-AMN.<sup>25</sup>

Even though it is generally admitted that both the reaction temperature and the substrate/AA ratio have a positive effect on the production of acetylated phenyl ethers,<sup>[3]</sup> there are no papers describing the effect of temperature and in only one study is the effect of the anisole/AA ratio in fixed bed reactor experiments described.<sup>[9]</sup> At 363 K, for a contact time  $\tau \geq 0.05$  h ( $\tau$  is taken as the inverse of the weight hour space velocity for anisole), anisole is almost completely acetylated initially [time on stream (TOS) of 10 min] when anisole/AA is 5, whereas less than 50 % of anisole is transformed with an equimolar ratio. Moreover with higher ratio

values, there is only a limited decrease with time in anisole conversion, whereas with the equimolar ratio the anisole conversion decreases significantly becoming lower than 5 % after a reaction time of 20 h.<sup>[9]</sup>

In 2-MN acetylation, the reaction temperature was shown to have a large effect on the initial distribution of acetylated products (AMN) as well as on the significance of the secondary deacylation and isomerization reactions. The higher the temperature, the higher the initial selectivity to 2-AMN: 8 % at 363 K to 46 % at 443 K.<sup>[25]</sup> This increase can be related for a large part to a more pronounced effect of the limitations in the desorption of 1-AMN. The significance of deacylation and isomerization increases with temperature: 10 % of deacylation at 363–393 K in 24 h and 24 % at 443 K in 4 h, 19 % of isomerization at 363 K in 24 h, 71 % at 443 K in 10 min.<sup>[25]</sup> At this latter temperature, 1-AMN can be completely converted after 4 h with a yield in isomers greater than 75 %, a maximum value of this yield of 83 % being obtained after a 30 min reaction.<sup>[25]</sup> In agreement with the intermolecular mechanism of 1-AMN isomerization, operating with a high concentration of reactants and with a 2-MN/AA ratio greater than 1 is necessary to observe the secondary isomerization of the acetylation product, hence to obtain a high yield in the desired 2-AMN product.

**Industrial processes** Rhodia is operating two industrial processes for the acetylation of anisole into 4-methoxyacetophenone and of veratrole into 3,4-dimethoxyacetophenone over zeolitic catalysts using HBEA in the first case and HFAU in the second.<sup>[4,62]</sup> Table 3.5 shows the dramatic improvement brought by the replacement of the old technology for anisole acetylation ( $\text{AlCl}_3$ , acetyl chloride as acetylating agent, batch reactor) by the new technology (HBEA zeolite catalyst, AA as acetylating agent, fixed bed reactor). This new process represents a major breakthrough in the 4-methoxyacetophenone synthesis and it is not only environmentally friendly, but also economically more sustainable than the older one.<sup>[62]</sup>

**Table 3.5** Acetylation of anisole. Characteristics of the old and new technologies

Old process	New process
$\text{AlCl}_3 >$ stoichiometric amount	Zeolite catalyst
1,2-Dichloroethane as solvent	No solvent
Batch reactor	Continuous reactor
Hydrolysis at the end of reaction	No water
Destruction of the catalyst	Periodic catalyst regeneration
Separation of organic/aqueous phases	Distillation of organic phase
Treatment and discharge of aqueous phase	
Distillation of organic phase	
Recycling of the solvent	
Yield/anisole: 85–95 %	Yield/anisole: 95%
	Higher purity of the final product

Adapted from Methivier<sup>[4]</sup> and Marion *et al.*<sup>[61]</sup>

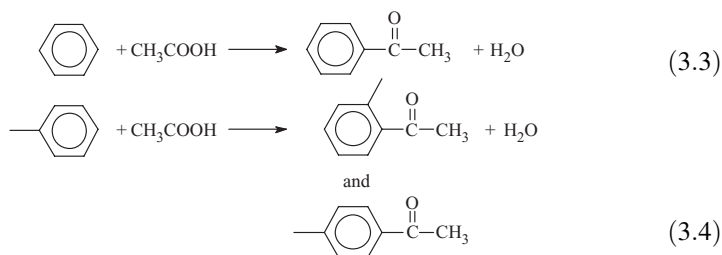


- This process is much simpler than the conventional one (two steps instead of eight).
- There is a dramatic reduction of water consumption and of aqueous effluents: 35 kg per ton of 4-methoxyacetophenone instead of 4500 kg per ton with the old process.
- The aqueous effluents contain 99 wt % water, 0.8 % acetic acid and less than 0.2 % of other organics, whereas those of the AlCl<sub>3</sub> unit contained more organic compounds (0.7 % solvent, 0.8 % acetic acid and 0.8 % of other organics) and a large amount of inorganic compounds (5 wt% Al<sup>3+</sup> and 24 % Cl).

### 3.1.2 ACETYLATION WITH ACETIC ACID

The reactivity of acetic acid is much weaker than that of AA and the aromatic ring can generally be acetylated with acetic acid over zeolite catalysts only at high temperatures (gas phase reactions).<sup>[62,63]</sup> This acetylation appears also at low temperatures (liquid phase reactions), but only with hydroxyarene substrates as a secondary transformation of aryl acetates rapidly formed through O acylation. This section will be split into two parts: gas phase acetylation of aromatic substrates without hydroxyl substituents and transformation of aryl acetates, the so-called Fries rearrangement.

**Gas phase acetylation** Acetylation of benzene and toluene with acetic acid was shown to be catalysed at 523–548 K over HMFI zeolites contained in a fixed bed reactor (Reactions (3.3) and (3.4)).<sup>[62,63]</sup> A 2/1 molar substrate/AcOH was chosen.



During the first 2 h of reaction, a decrease in AcOH conversion (from 48 to 43 %) for benzene acetylation at 523 K with an increase in selectivity to the monoacetylated product (from 80 to 90 %) can be observed. The only problem involves the low catalyst activity: 1.5 mmol h<sup>-1</sup> g<sup>-1</sup> of acetophenone, which corresponds to a TOF value of 2.2 h<sup>-1</sup>. This means that less than 0.2 g of this acetylated arene can be produced per hour and per gram of catalyst under the operating conditions (i.e. 10 times less than in the liquid phase acetylation of anisole with AA). The kinetic study of the reaction shows an increase in the selectivity with the substrate/acetic acid ratio, but no increase in yield, an increase in acetic acid conversion with the reaction temperature with a significant decrease in selectivity due to a greater formation of diacetylated products.<sup>[62,63]</sup> HFAU and RE-FAU zeolites do

not catalyse this reaction, probably because of the strength of their protonic sites is too low.<sup>[63]</sup> As could be expected, toluene is more reactive than benzene, acetylation occurring at practically the same rate in *ortho* and *para* positions.

**Fries rearrangement and phenol acetylation** The Fries rearrangement is the acid catalysed transformation of aryl esters into hydroxyarylketones. Both this rearrangement and the two-step transformation (esterification, Fries rearrangement) in one-pot operation of phenols with carboxylic acid or anhydrides will be examined hereafter. Most studies in which acid zeolites were used as catalysts (Tables 3.6 and 3.7) deal with the synthesis of *o*- and *p*-hydroxyacetophenones (*o*- and *p*-HAP) either by the Fries rearrangement of phenyl acetate [Reaction (3.5)]:

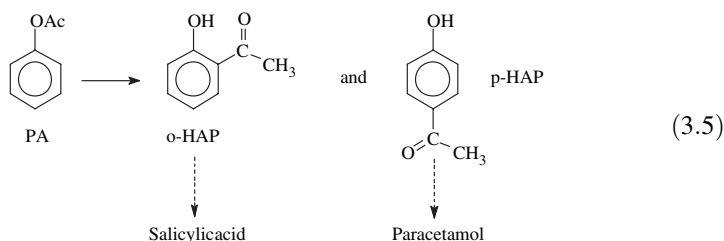


**Table 3.6** Gas phase Fries rearrangement of phenyl acetate and phenol acetylation over zeolite and mesoporous molecular sieves. All the reactions were carried out in fixed bed reactors

Reactant(s)	Temperature (K)	Catalysts	Maximum yield (%)	<i>o/p</i> ratio	Ref.
PA	673	HFAU-HMFI	3–4	12.5	[65]
PA	673	HFAU-HMFI	11	20	[66]
PA	453–693	HMFI	30	— <sup>a</sup>	[67]
PA	673	HFAU-HMFI	3.5	9	[68]
P + AcOH(1-1) <sup>b</sup>	673	HFAU-HMFI	3.5	9	[68]
P + AcOH(1-1)	553	HMFI	17	27	[69]
P + AcOH(1-1)	533	Passivated HMFI	— <sup>a</sup>	>30	[70]
P + AcOH(1-8)	553	HMFI	29	35	[71]
P + A-A(1-1)	523	HMFI	43	66	[72]
PA	523–693	HMFI	36	— <sup>a</sup>	[73]
P + AcOH	523–673	HMFI	9	16	[74]
PA	673	HFAU	— <sup>a</sup>	— <sup>a</sup>	[75]
P + AcOH(1-1)	673	HFAU	— <sup>a</sup>	— <sup>a</sup>	[75]
PA	423–673	NCL-1	14	0.5–1	[76]
PA	573	CeBEA	52	— <sup>a</sup>	[77]
PA	538	HMFI	63	35	[78]
P + AcOH	553	HFAU-HMFI, MCM-41	12	300	[79]
P + A-A (1-1)	623	Al-MCM-41	8	19	[80]

<sup>a</sup>Not indicated.

<sup>b</sup>In parentheses molar ratio between reactants

AA, acetic anhydride; AcOH, acetic acid; P, phenol, PA, phenyl acetate.

**Table 3.7** Liquid phase Fries rearrangement of phenyl acetate (PA) over zeolite catalysts

Reactor	Solvent	Temperature (K)	Catalysts	Maximum <sup>a</sup> yield (%)	<i>o/p</i> ratio	Ref.
Batch	No	443	HNu2	20.5	0.4	[81]
Batch	Sulfolane	453	HMF1	41	0.4	[67]
Batch	No	453	HMF1	62	1.25	[67]
Batch	No	453	HBEA, HFAU, HMF1	65	0.65	[6]
Fixed bed	No	453	HBEA	21	n.i. <sup>c</sup>	[6]
Batch	No	453	HMF1 (passivated)	74	0.5	[73]
Fixed bed	No	453	HMF1 (passivated)	51	0.6	[73]
Batch	Sulfolane	433	HBEA	7	0.4	[82]
Batch	Dodecane	433	HBEA	10	4	[82]
Batch <sup>b</sup>	Sulfolane	433	HBEA	27	0.15	[83]
Batch <sup>b</sup>	Dodecane	433	HBEA	14	1	[83]
Batch	No	473	HBEA	22	1.1	[10]
Batch	Sulfolane	493	HBEA	31	0.45	[10]
Batch	Decane	443	HBEA	11	4.2	[10]
Batch	Cumene	423	HBEA-HFAU	6–9	0.8	[84]
Batch	Phenol	423	HBEA-HFAU	30	0.3	[84]

<sup>a</sup>Hydroxyacetophenones and *p*-acetoxyacetophenones.

<sup>b</sup>In the presence of phenol (P) (P/PA = 1).

<sup>c</sup>Note indicated.

or by the successive esterification of phenol with acetic acid or AA and then Fries rearrangement.<sup>[5]</sup> The *para* isomer is a key intermediate in the Hoechst–Celanese process for the manufacture of paracetamol (*p*-acetaminophenol). The *ortho* isomer can be used for the synthesis of salicylic acid. Zeolite catalysed synthesis of hydroxyacetophenones was carried out in gas phase (always in fixed bed reactors) and in liquid phase (partly in batch, partly in fixed bed reactors). *o*-HAP can be selectively produced through gas phase reaction, *p*-HAP through liquid phase reaction.<sup>[5]</sup>

**Gas phase reactions** Most of the studies which were carried out over zeolite catalysts were devoted to the establishment of the reaction scheme. Few of them dealt with the choice of the optimal catalysts and operating conditions, probably because of the relatively fast deactivation of the catalysts.

*Reaction scheme* The Fries rearrangement of phenyl acetate (PA) was first mentioned as occurring over zeolites in the review paper published in 1968 by Venuto and Landis.<sup>[64]</sup> This rearrangement was afterwards investigated at 673 K over HFAU and HMF1 zeolites.<sup>[65]</sup> The reaction was not selective: the expected *o*- and *p*-hydroxyacetophenones (*o*- and *p*-HAP) were minor components and phenol the main component. With both zeolites, *o*-HAP was highly favoured over the *para* isomer.

The scheme proposed for the reaction over HFAU was that PA dissociates in phenol (P) and ketene and that *o*-HAP, which was highly favoured over the *para* isomer, results partly from an intramolecular rearrangement of PA, partly from acyl group transfer from PA to P whereas *p*-HAP results from this latter reaction only. In these experiments, the zeolite deactivation was very fast, as a result of coke deposition and zeolite dehydroxylation. Catalyst stability can be considerably improved by operating at lower temperatures and especially by substituting equimolar mixtures of PA and water or P and acetic acid for PA. Much higher HAP yields were obtained by using the P – acetic acid mixture as reactants.<sup>[68]</sup>

The scheme (Figure 3.5) of the transformation of this P – acetic acid mixture over HMF1 at 553 K was established from the effect of conversion (or of contact time) on product distribution.<sup>[69]</sup> At short contact times (i.e. at low conversions), PA was practically the only reaction product. However, there was also formation of a very small amount of *o*-HAP (Figure 3.6). This means that O acetylation is much faster than C acetylation (ca. 20 times) and that the latter reaction leads to the *ortho* isomer only. Because of the high rate of O acetylation, thermodynamic equilibrium between P, acetic acid and PA was established at relatively short contact times. At high conversions, the formation of *o*-HAP involved the participation of PA as demonstrated by the decrease in PA yield and the apparent secondary mode of *o*-HAP formation (Figure 3.6). This mode of *o*-HAP formation from PA is mainly intermolecular involving the acetylation of P by PA. The intramolecular transformation of PA into *o*-HAP is much slower as shown by comparing the transformations of pure PA and of an equimolar mixture of PA and P.<sup>[69]</sup> The formation of small amounts of *p*-HAP would result mainly from the hydrolysis of

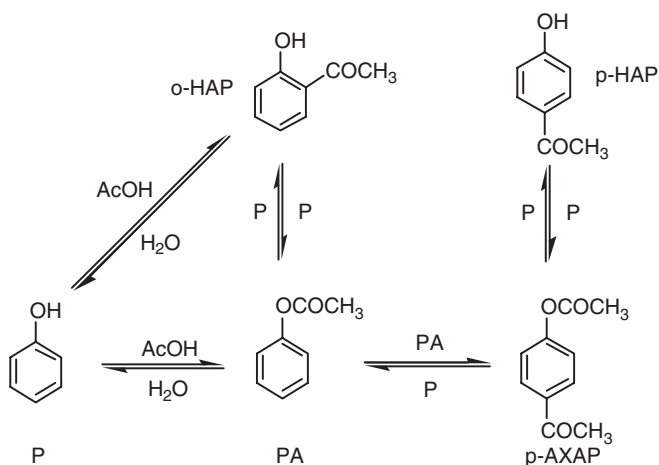


**Figure 3.5** Reaction scheme of the gas phase phenol acylation with acetic acid (AcOH) over HMF1 at 553 K. Reprinted with permission from *Industrial & Engineering Chemistry Research*, Vol. 34, Guisnet *et al.*, Kinetic modelling of phenol acylation with acetic acid on HZSM5, pp. 1624–1629, Copyright (1995), American Chemical Society

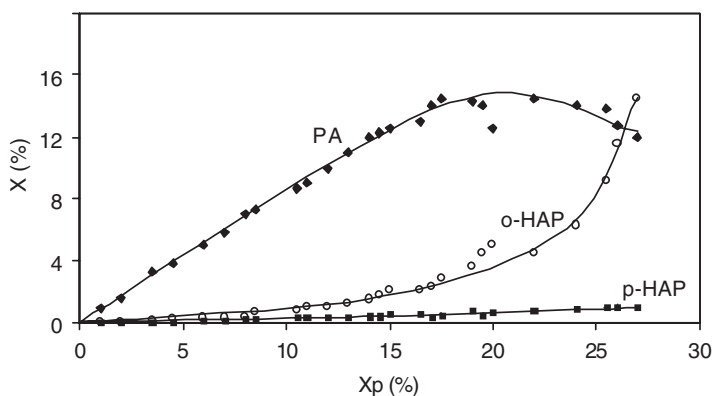
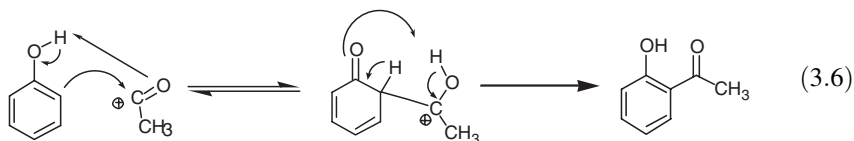


**Figure 3.6** Yields,  $X$  (%) of phenyl acetate, PA ( $\blacklozenge$ ), *o*-hydroxyacetophenone, o-HAP ( $\circ$ ) and *p*-hydroxyacetophenone, p-HAP ( $\blacksquare$ ) as a function of the conversion of phenol,  $X_p$  (%), in an equimolar mixture with acetic acid over HMF1 at 553 K. Reprinted from *Journal of Molecular Catalysis*, Vol. 93, Neves *et al.*, Acylation of phenol with acetic acid over a HZSM-5 zeolite, reaction scheme, pp. 169–179, Copyright (1994), with permission from Elsevier

*p*-acetoxyacetophenone (*p*-AXAP), which is selectively formed (no *o*-AXAP is observed) by autoacylation of PA. The high *ortho*-selectivity of P acylation was related to the pronounced stability of the transition state [Reaction (3.6)] whereas the *para*-selectivity of PA autoacylation was attributed to steric hindrance of the approach of the acetyl group in the *ortho* position of PA.<sup>69</sup>



Kinetic modelling confirms the reaction scheme of P acylation (Figure 3.5) and moreover shows that high *o*-HAP yield and selectivity can be obtained by reacting over HMF1 mixtures of AcOH and P with a high AcOH/P ratio: e.g. *o*-HAP yield of ca. 90% with a molar AcOH/P ratio of 50.<sup>[71]</sup> This large increase in *o*-HAP yields with the AcOH/P ratio was confirmed experimentally: the *o*-HAP yield passes from 16% for a ratio of 1 to 29% for a ratio of 4.<sup>[71]</sup>

*Optimal operating conditions and catalysts* Only the effect of temperature was investigated. Generally, the higher the temperature, the higher the conversion of PA, but the faster the deactivation and the lower the selectivity for HAP (see, for example, in Table 3.8 with a HBEA sample<sup>[77]</sup>). The same can be observed for the transformation of a 1:1 molar P–acetic acid mixture over HMF1,<sup>[73,74]</sup> but the deactivation was much slower than for PA transformation.<sup>[74]</sup> A zero reaction order

**Table 3.8** Influence of the reaction temperature on the gas phase Fries rearrangement of phenyl acetate over a HBEA zeolite. Values of conversion obtained after 1 and 10 h reaction ( $X_1$ ,  $X_{10}$ ) and of selectivity and yield to hydroxyacetophenones after 1 h reaction

Temperature (K)	$X_1$ (%)	$X_{10}/X_1$	(Selectivity) <sub>1</sub> (%)	(Yield) <sub>1</sub> (%)
573	55	0.29	55	30
623	80	0.24	42	34
673	90	0.21	10	9

Data from Wang and Zou.<sup>[77]</sup>

with respect to P was found, which suggests a strong adsorption of this very polar reactant.<sup>[74]</sup> Furthermore, as previously indicated, the o-HAP yield increases with the acetic acid/P ratio.<sup>[73,74]</sup> AA can be substituted for acetic acid in the acylation of P with better yield and selectivity for HAP under similar conditions.<sup>[72]</sup>

In the Fries rearrangement of PA, high yield and selectivity for o-HAP can be obtained with large pore zeolites such as HFAU, HBEA and average pore zeolites such as HMFJ. HBEA zeolite modified by ion exchange with cerium<sup>[77]</sup> and especially a commercial HMFJ made of primary crystallites and agglomerates joined by finely dispersed alumina<sup>[78]</sup> were claimed to be particularly stable and selective for the formation of o-HAP.

**Liquid phase reactions** As in the gas phase, o- and p-HAP, p-AXAP and P are the main products of PA transformation (Figure 3.7). o-HAP, P and p-AXAP are primary products whereas p-HAP is not formed directly (Figure 3.8).

The direct formation of o-HAP from PA suggests an intramolecular rearrangement, whereas the secondary mode of p-HAP formation requires the participation of one primary product in addition to PA. p-AXAP and P result from PA autoacylation. However the production of P is greater than expected from this reaction, which indicates either dissociation of PA into P and ketene or its hydrolysis with aqueous impurities or zeolite hydroxyl groups. The secondary formation of p-HAP can be explained as acylation of P with PA or as a dissociation or hydrolysis of p-AXAP. To discriminate between these two possibilities, the effect of adding P to the PA reactant was determined.<sup>[82]</sup> p-HAP appears as a primary product (Figure 3.8b), which shows that p-HAP can result from the acylation of P with PA. Furthermore, the transformation of p-AXAP into p-HAP can be considered as negligible in comparison with the acylation of P with PA because of very large positive effect of P and no apparent consumption of the p-AXAP product. This is quite different to what was proposed for the formation of p-HAP during the gas phase transformation of the P – acetic acid mixture (Figure 3.5), which can be related to the absence of water in the liquid phase Fries rearrangement of PA (Figure 3.7).

*Optimal operating conditions and catalysts* The effect of temperature on PA transformation was investigated in a fixed bed reactor with HMFJ zeolites as catalysts.<sup>[73]</sup> An increase in temperature from 453 to 523 K causes a significant increase in PA conversion (e.g. from 28 to 71 %), with practically no change in the

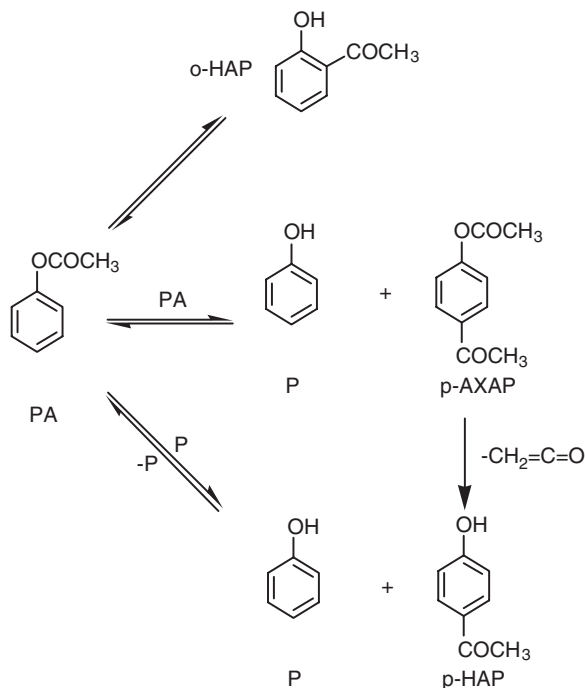


**Figure 3.7** Reaction scheme of the liquid phase transformation of phenyl acetate over protonic zeolite

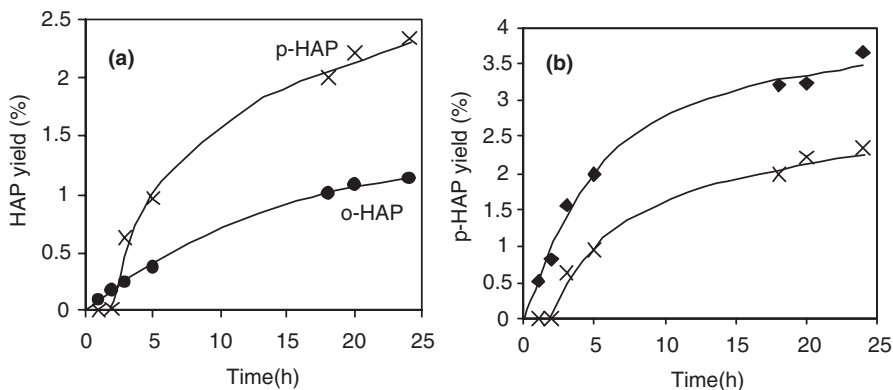


**Figure 3.8** Liquid phase transformation of phenyl acetate (2.2 mol l<sup>-1</sup> in sulfolane solvent) at 433 K. (a) Yield in *o*-hydroxyacetophenone, *o*-HAP (●) and *p*-hydroxyacetophenone, *p*-HAP (X) versus reaction time. (b) Effect of the addition of phenol (P) on the *p*-HAP yield. [P] = 0 mol l<sup>-1</sup> (X) and [P] = 0.6 mol l<sup>-1</sup> (◆). Reprinted from *Catalysis Letters*, Vol. 41, Jayat *et al.*, Solvent effects in liquid phase Fries rearrangement of phenyl acetate using a HBEA zeolite, pp. 181–187, copyright (1996), Kluwer Academic Publishers, with kind permission of Springer Science and Business Media

selectivity for HAP (from 86 to 87%), but a decrease in the *para* to *ortho* ratio (from 1.1 to 0.5).

A kinetic study of PA transformation was carried out in a batch reactor over a HBEA zeolite<sup>[82]</sup> in the presence of nonpolar (dodecane) and very polar (sulfolane) solvents. The solvent polarity has a negative effect on the initial reaction rate, but a positive effect on the catalyst stability and selectivity for p-HAP (Table 3.7).

Advantage can be drawn from the positive effect of phenol on PA transformation into p-HAP to improve the yield and selectivity of p-HAP production.<sup>[82–84]</sup> Thus, with a HBEA zeolite the yield and selectivity for p-HAP passes from ca. 5 and 28% respectively with cumene solvent to 24 and 60% with phenol as a ‘solvent’.<sup>[84]</sup> Again sulfolane was shown to have a very positive effect on the selectivity for p-HAP and limits the catalyst deactivation. To explain these observations as well as the effect of P and PA concentrations on the reaction rates, it was proposed that sulfolane plays two independent roles in phenol acylation: solvation of acylium ion intermediates and competition with P and PA for adsorption on the acid sites.<sup>[83]</sup>

The transformation of either PA pure (in the absence of solvent) or in equimolar mixture with P (with sulfolane as solvent) was investigated over various zeolite catalysts, mainly HFAU, HBEA and HMFI. For PA transformation, HMFI leads to the best results in terms of stability and selectivity for HAP, with moreover a higher selectivity for the *para* isomer.<sup>[6]</sup> In contrast, for the transformation of the P–PA mixture,<sup>[85]</sup> the higher PA conversion, selectivity for HAP and especially for the *para* isomer were obtained with HBEA. The difference between these results can be related to the greater significance of the bimolecular transformations during the P–PA transformation. For the transformation of the P–PA mixture over a series of HBEA samples dealuminated by acid treatment, there is, like in 2-MN acetylation, a maximum in activity for a Si/Al ratio between 30 and 40 and an increase in the TOF values with Si/Al.<sup>[85]</sup> Therefore, the origin of this effect is probably the same, that is, an increase in TOF with the zeolite hydrophobicity. The deactivation of the outer surface of MFI and TON samples by treatment with triphenylchlorosilane was shown to increase their activity and their selectivity to the *para* isomer. These observations were related to a better accessibility of the inner surface owing to a lower rate of formation of polymeric deposits on the outer surface.<sup>[73]</sup>

## 3.2 PROCEDURES AND PROTOCOLS

### 3.2.1 SELECTIVE SYNTHESIS OF ACETOPHENONES IN BATCH REACTORS THROUGH ACETYLATION WITH ACETIC ANHYDRIDE

#### Materials and Equipment

- Three-neck round-bottom flask equipped with thermometer
- Reflux condenser
- Magnetic stirring (750 rpm) hotplate equipped with a temperature controller
- Oil bath
- Dry nitrogen/vacuum manifold



- Rotary evaporator
- Substrate and AA previously dried on 3A molecular sieves
- Zeolite catalyst previously activated under dry air for 8 h at 773 K

**Procedure** (e.g. preparation of ca. 5 g of 4-methoxyacetophenone)

Anisole (5.1 g; 0.047 mol) and AA (4.7 g; 0.047 mol) are introduced in the flask and heated at the reaction temperature (393 K). Then, the activated HBEA-15 zeolite (2.5 g; from Zeolyst International) is added, preferably under inert atmosphere, to the reactant mixture under stirring. The progress of the acetylation can be controlled by GC-FID analysis on a capillary CP-Sil-8 CB column. In general, after a reaction time of 3 h, acetylation is complete. The zeolite is filtered off and washed with dichloromethane ( $5 \times 10$  ml). The filtrate and the washings are combined and mixed with a saturated solution of  $\text{NaHCO}_3$ . The organic phase is dried over  $\text{MgSO}_4$  and evaporated on a rotary evaporator. The residue is distilled under reduced pressure to give colourless crystals of 4-methoxyacetophenone (m.p. 38–39 °C). 4-methoxyacetophenone can also be isolated by liquid phase column flash chromatography. Expected isolated yield = 75 % (5.3 g).

### Remarks

- Molar anisole/AA ratios bigger than 1 (preferably  $\geq 2$ ) can be used in order to get higher reaction rate and selectivity for 4-methoxyacetophenone, with the drawback that large amounts of anisole are to be removed from the final mixture.
- The HBEA catalyst can be reused after regeneration simply by heating in air for 8 h at 773 K (i.e. under the conditions of catalyst activation).

### Adaptation of the Procedure to the Selective Synthesis of other Acetophenones

With activated substrates the operating conditions for acetylation will be very similar to those of anisole acetylation. It is worth noting however that, for the acetylation of bulky substrates (e.g. veratrole), zeolites with larger pores than HBEA are to be preferred (generally HFAU). Lastly, with poorly activated substrates, higher temperatures, longer reaction times and very high substrate/AA ratios have to be chosen. As an example, for toluene acetylation, a temperature of 423 K, a toluene/AA ratio of 20 and the replacement of a stainless steel autoclave for the glass reactor are recommended.

## 3.2.2 SELECTIVE SYNTHESIS OF ACETOPHENONES IN FIXED BED REACTORS THROUGH ACETYLATION WITH ACETIC ANHYDRIDE

### Materials and Equipment

- Thermostated glass tubular reactor with fritted glass septum
- Syringe pump

- Collecting trap
- Substrate and AA previously dried on 3A molecular sieves
- Zeolite catalyst, pelletized and crushed so as to obtain particles with 0.2–0.4 mm diameter, then activated under dry air for 8 h at 773 K

**Procedure** (e.g. preparation of ca. 100 g of 4-methoxyacetophenone)

HBEA-15 zeolite (2.0 g; from Zeolyst International) are introduced in the reactor (internal diameter = 15 mm, which corresponds to a 40 mm high zeolite bed) between two layers of an inert solid powder with a rough granulometry. The upper inert layer (minimum 20 mm high) allows a preheating and a homogeneous flow of the reagents. The reactant mixture (anisole/AA ratio = 5) is introduced with a syringe pump at a flow rate of  $20 \text{ ml h}^{-1}$  ( $0.158 \text{ mol h}^{-1}$  anisole and  $0.032 \text{ mol h}^{-1}$  AA). The product mixture is collected in a trap. After 30 h at 373 K (the progress of the reaction is verified by periodical analysis), the anisole conversion becomes lower than 90 % and the introduction of the reactant mixture has to be stopped for catalyst regeneration. The methodology used for the recovery of 4-methoxyacetophenone from the raw product mixture is described above. Expected isolated yield after a time on stream of 30 h = 75 % (107 g).

### **Adaptation of the Procedure to the Selective Synthesis of Acetylated Heteroarenes**

Some acetylated heteroarenes, such as 3-acetyl-2-methylbenzofuran, can be synthesized in flow reactors. However, because of a fast oligomerization of the substrate, the reaction should be carried out at low temperatures and with a large excess of AA (e.g. 333 K and substrate/AA ratio = 0.067 for 2-methylbenzofuran acetylation).

### **REFERENCES**

1. Kouwenhoven, H. W. and van Bekkum, H. Acylation of aromatics. In *Handbook of Heterogeneous Catalysis*, G. Ertl, H. Knözinger and J. Weitkamp (eds). Wiley-VCH, Weinheim, **1997**, Vol. 5, pp. 2358–2364.
2. Bezouhanova, C. P. *Appl. Catal.*, **2002**, 229, 127–133.
3. Spagnol, M., Gilbert, L. and Alby, D. In *The roots of organic development*, Desmurs, J. R. and Ratton, S. (eds). Elsevier, Amsterdam, **1996**, Vol. 8, pp. 29–38.
4. Methivier, P., Friedel–Crafts acylation. In *Fine Chemicals through Heterogeneous Catalysis*, Sheldon, R. A., and van Bekkum, H. (eds). Wiley-VCH, Weinheim, **2001**, pp. 161–172.
5. Guisnet M. and Perot, G. The Fries rearrangement. In *Fine Chemicals through Heterogeneous Catalysis*, Sheldon, R. A. and van Bekkum, H. (eds), Wiley-VCH, Weinheim, **2001**, pp. 211–216.
6. Harvey, G., Vogt, A., Kouwenhoven, H. W. and Prins, R. In *Proceedings of the 9th International Zeolite Conference, Montreal 1992*, R. van Ballmoos *et al.* (eds). Butterworth-Heissmann, Boston, **1993**, pp. 363–370.

7. Gaare, K. Akporiaye, D. *J. Mol. Catal., A*, **1996**, *109*, 177–187.
8. Smith, K., Zhenhua, Z., Hodgson P. K. G. *J. Mol. Catal., A*, **1998**, *134*, 121–128.
9. Rohan, D., Canaff, C., Fromentin, E. and Guisnet, M. *J. Catal.*, **1998**, *177*, 296–305.
10. Freese, U., Heinrich, F. and Roessner, F. *Catal. Today*, **1999**, *49*, 237–244.
11. Heinichen, H. K. and Hölderich, W. F. In *Proceedings of the 12th International Zeolite Conference*, M. Treacy *et al.* (eds). Materials Research Society, Warrendale, **1999**, pp. 1085–1092.
12. Derouane, E. G., Dillon, C. J., Bethell, D. and Derouane-Abd Hamid, S. B. *J. Catal.*, **1999**, *187*, 209–218.
13. Derouane, E. G., Crehan, G., Dillon, C. J., Bethell, D., He, H. and Derouane-Abd Hamid, S. B. *J. Catal.*, **2000**, *194*, 410–423.
14. Moreau, P., Finiels, A. and Meric, P. *J. Mol. Catal., A*, **2000**, *154*, 185–192.
15. Guignard, C., Pèdrón, V., Richard, F., Jacquot, R., Spagnol, M., Coustard, J. M. and Pérot, G. *Appl. Catal.*, **2002**, *234*, 79–90.
16. Smith, K., El-Hiti, G. A., Jayne, A. J. and Butters, M. *Org. Biomol. Chem.*, **2003**, *1*, 1560–1564.
17. Derouane, E. G., Schmidt, I., Lackas, H. and Christensen, C. J. H. *Catal. Lett.*, **2004**, *95*, 13–17.
18. Savant, D. P. and Halligudi, S. B. *Catal. Commun.*, **2004**, *5*, 659–663.
19. Harvey, G. and Mäder, G. *Collect. Czech Chem. Commun.*, **1997**, *57*, 862–866.
20. van Bekkum, H., Hoefnagel, A. J., Gunnewegh, M. A., Vogt, A. H. G. and Kouvenhoven, H. W. *Stud. Surf. Sci. Catal.*, **1994**, *83*, 379–389.
21. Harvey, G., Binder, G. and Prins, R. *Stud. Surf. Sci. Catal.*, **1995**, *94*, 397–404.
22. Neuber, M. and Leupold, E. I. *Eur. Pat. Appl.*, **1991**, EP 459.495 B1.
23. Yadav, G. Y. and Krishnan, M. S. *Chem. Eng. Sci.*, **1999**, *54*, 4189–4197.
24. Heinichen, H. K. and Hölderich, W. F. *J. Catal.*, **1999**, *185*, 408–414.
25. Fromentin, E., Coustard, J. M. and Guisnet, M. *J. Mol. Catal., A*, **2000**, *159*, 377–388.
26. Fromentin, E., Coustard, J. M. and Guisnet, M. *J. Catal.*, **2000**, *190*, 433–438.
27. Berreghis, A., Ayrault, P., Fromentin, E. and Guisnet, M. *Catal. Lett.*, **2000**, *68*, 121–127.
28. Andy, P., Garcia-Martinez, J., Lee, G., Gonzalez, H., Jones, C. W. and Davis, M. E. *J. Catal.*, **2000**, *192*, 215–223.
29. Das, D. and Cheng, S. *Appl. Catal., A*, **2000**, *201*, 159–168.
30. Casagrande, M., Storaro, L., Lenarda, M. and Ganzerla, R. *Appl. Catal., A*, **2000**, *201*, 263–270.
31. Kim, S. D., Lee, K. H., Lee, J. S., Kim, Y. G. and Yoon, K. E. *J. Mol. Catal., A*, **2000**, *158*, 33–45.
32. Botella, P., Corma, A. and Sastre, G. *J. Catal.*, **2001**, *197*, 81–89.
33. Moreau, V., Fromentin, E., Magnoux, P. and Guisnet, M. *Stud. Surf. Sci. Catal.*, **2001**, *135*, 4113–4120.
34. Meric, P., Finiels, A. and Moreau, P. *J. Mol. Catal., A*, **2002**, *189*, 251–262.
35. Guisnet, M., Moreau, V. and Magnoux, P. *Bull. Polish Acad. Sci. Chem.*, **2002**, *50*, 203–218.
36. Kantarli, I. C., Artok, L., Bulut, H., Yilmaz, S. and Ulku, S. *Stud. Surf. Sci. Catal.*, **2002**, *142*, 799–806.
37. Botella, P., Corma, A., Rey, F. and Valencia, S. *Stud. Surf. Sci. Catal.*, **2002**, *142*, 651–658.
38. Moreau, P., Finiels, A., Meric, P. and Fajula, F. *Catal. Lett.*, **2003**, *85*, 199–203.
39. Hwang, K. Y. and Rhu H. K. *React. Kinet. Catal. Lett.*, **2003**, *79*, 189–196.
40. Vogt A. and Pfenninger, A. *Eur. Pat. Appl.*, **1996**, EP 0701.987 A1 to Uetikon AG.

41. Botella, P., Corma, A., Lopez-Nieto, J. M., Valencia, S. and Jacquot, R. *J. Catal.*, **2000**, *195*, 161–168.
42. Guidotti, M., Canaff, C., Coustard, J. M., Magnoux, P. and Guisnet, M. *J. Catal.*, **2005**, *230*, 375–383.
43. Cejka, J., Prokesova, P., Cerveny, L. and Mikulcova, K. *Stud. Surf. Sci. Catal.*, **2002**, *142*, 627–634.
44. Cerveny, L., Mikulcova, K. and Cejka, J. *Appl. Catal.*, **A**, **2002**, *223*, 65–72.
45. Escola, J. M. and Davis, M. E. *Appl. Catal.*, **A**, **2001**, *214*, 111–120.
46. Shaemol, V. N., Tyagi, B. and Jasra, R. V. *J. Mol. Catal.*, **A**, **2004**, *215*, 201–208.
47. Reddy, P. R., Subrahmanyam, M. and Kumari, V. D. *Catal. Lett.*, **1995**, *61*, 207–211.
48. Richard, F., Drouillard, J., Carreyre, H., Lemberston, J. L. and Perot, G. *Stud. Surf. Sci. Catal.*, **1993**, *78*, 601–606.
49. Richard, F., Carreyre, H. and Perot, G. *J. Mol. Catal.*, **A**, **1995**, *103*, 51–61.
50. Richard, F., Carreyre, H. and Perot, G. *J. Mol. Catal.*, **A**, **1995**, *101*, L167–L169.
51. Richard, F., Carreyre, H. and Perot, G. *J. Catal.*, **1996**, *159*, 427–434.
52. Scharzmann, M., Hölderich, W. F. and Lermer, H. *German Pat.*, **1987**, DE 3618.964 to BASF AG.
53. Reddy, P. R., Subrahmanyam, M. and Kulkarni, S. J. *Catal. Lett.*, **1998**, *54*, 95–100.
54. Dockner, T., Hölderich, W. F., Koehler, H. and Lermer, H. *Pat.*, **1989**, DE 3724.035 to BASF AG.
55. Martin D. and Guisnet, M. unpublished results.
56. Derouane, E. G. *J. Mol. Catal.*, **A**, **1998**, *134*, 29–45.
57. Rabo, J. A. and Gajda, G. J. In *Guidelines for Mastering the Properties of Molecular Sieves*, D. Barthomeuf *et al.* (eds), NATO ASI Series B: Physics. Plenum Press, New York and London, **1990**, Vol. 221, pp. 273–297.
58. Barthomeuf, D. *Mater. Chem. Phys.*, **1987**, *17*, 49–71.
59. Dimroth, K., Reichardt, C., Siepmann, T. and Bohlmann, F. *Liebigs Ann. Chem.*, **1963**, *661*, 1–24.
60. Reichardt, C. *Solvents and Solvent Effects in Organic Chemistry*. VCH, Weinheim, **1988**.
61. Marion, P., Jacquot, R., Ratton, S. and Guisnet, M. In *Zeolites for Cleaner Technologies*, Guisnet M. and Gilson J. P. (eds), Catalytic Science Series 3. Imperial College Press, Singapore, **2002**, pp. 281–299.
62. Pandey, A. K. and Singh, A. P. *Catal. Lett.*, **1997**, *44*, 129–133.
63. Singh, A. P. and Pandey, A. K. *J. Mol. Catal.*, **A**, **1997**, *123*, 141–147.
64. Venuto, P. B. and Landis, P. S. *Adv. Catal.*, **1968**, *18*, 259–371.
65. Pouilloux, Y., Gnep, N. S., Magnoux, P. and Perot, G. *J. Mol. Catal.*, **A**, **1987**, *40*, 231–233.
66. Pouilloux, Y., Bodibo, J. P., Neves, I., Gubelmann, M., Perot, G. and Guisnet, M. *Stud. Surf. Sci. Catal.*, **1991**, *59*, 513–522.
67. Vogt, A. H. G. and Kouwenhoven, H. W. *Coll. Czech. Chem. Commun.*, **1992**, *57*, 853–861.
68. Neves, I., Ribeiro, F. R., Bodibo, J. P., Pouilloux, Y., Gubelmann, M., Magnoux, P., Guisnet, M. and Perot, G. In *Proceedings of the 9th International Zeolite Conference*, R. van Ballmoos *et al.* (eds). Butterworth-Heissmann, Boston, **1993**, pp. 543–550.
69. Neves, I., Jayat, F., Magnoux, P., Perot, G., Ribeiro, F. R., Gubelmann, M. and Guisnet, M. *J. Mol. Catal.*, **A**, **1994**, *93*, 169–179.
70. Neves, I., Jayat, F., Magnoux, P., Perot, G., Ribeiro, F. R., Gubelmann, M. and Guisnet, M. *J. Chem. Soc., Chem. Commun.* **1994**, 717–718.

71. Guisnet, M., Lukyanov, D. B., Jayat, F., Magnoux, P. and Neves, I. *Ind. Eng. Chem. Res.*, **1995**, *34*, 1624–1629.
72. Rao Subba, Y. V., Kulkarni, S. J., Subrahmanyam, M. and Rama Rao, A. V. *Appl. Catal., A*, **1995**, *133*, L1–L6.
73. Vogt, A., Kouwenhoven, H. W. and Prins, R. *Appl. Catal., A*, **1995**, *123*, 37–49.
74. Neves, I., Jayat, F., Lukyanov, D. B., Magnoux, P., Perot, G., Ribeiro, F. R., Gubelmann, M. and Guisnet, M. In *Catalysis of Organic Reactions*, Scaros, M. G. and Prunier M. L. (eds). Marcel Dekker Inc., New York, **1995**, pp. 515–519.
75. Neves, I., Magnoux, P. and Guisnet, M. *Bull. Soc. Chim. Fr.*, **1995**, *132*, 156–165.
76. Sasidharan, M. and Kumar, R. *Stud. Surf. Sci. Catal.*, **1997**, *105*, 1197–1201.
77. Wang, H. and Zou, Y. *Catal. Lett.*, **2003**, *86*, 163–167.
78. Borzatta, V., Busca, G., Poluzzi, E., Rossetti, V., Trombetta, M. and Vaccari, A. *Appl. Catal., A*, **2004**, *257*, 85–95.
79. Padro, C. L. and Apesteguia, C. R. *J. Catal.*, **2004**, *226*, 308–320.
80. Bhattacharyya, K. G., Talukdar, A. K., Dao, P. and Sisavanker, S. *Catal. Commun.*, **2001**, *2*, 105–111.
81. Cundy, C. S., Higgins, R., Kibby, S. A. M., Lowe, B. M. and Paton, R. M. *Tetrahedron Lett.*, **1999**, *30*, 2281–2284.
82. Jayat, F., Sabater Picot, M. J. and Guisnet, M. *Catal. Lett.*, **1996**, *41*, 181–187.
83. Jayat, F., Sabater Picot, M. J., Rohan, D. and Guisnet, M. *Stud. Surf. Sci. Catal*, **1997**, *108*, 91–98.
84. Heidekum, A., Harmer, M. A. and Hölderich, W. F. *J. Catal.*, **1998**, *176*, 260–263.
85. Jayat, F. PhD Thesis, University of Poitiers, **1996**.

---

# 4 Aromatic Benzoylation

---

PATRICK GENESTE AND ANNIE FINIELS

*Laboratoire des Matériaux Catalytiques et Catalyse en Chimie Organique, UMR 5618 CNRS-ENSCM-UMI, Institut C. Gerhardt FR 1878, 8 rue de l'Ecole Normale, 34296 Montpellier Cedex 05, France*

## CONTENTS

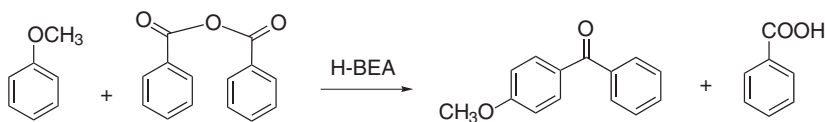
4.1	AROMATIC BENZOYLATION	95
4.1.1	Effect of the zeolite	96
4.1.2	Effect of the acylating agent	97
4.1.3	Effect of the solvent	97
4.1.4	Benzoylation of phenol and the Fries rearrangement	97
4.1.5	Kinetic law	99
4.1.6	Substituent effect	100
4.1.7	Experimental	101
4.2	ACYLATION OF ANISOLE OVER MESOPOROUS ALUMINOSILICATES	102
	REFERENCES	103

## 4.1 AROMATIC BENZOYLATION

The Friedel–Crafts acylation of aromatics is the main route for the formation of aromatic ketones, intermediates widely used for the production of pharmaceuticals, fragrances, flavours insecticides and other products.

Our pioneering work in 1986<sup>[1]</sup> has shown that acid zeolites are efficient catalysts in the Friedel–Crafts acylation of toluene and xylene with carboxylic acids and constitutes a breakthrough in environmentally friendly fine chemistry replacing the conventional  $\text{AlCl}_3$  method by a heterogeneous catalysts. Since this initial study, a tremendous amount of work has been performed in this area<sup>[2]</sup> and particularly, in recent years, the acetylation reaction, which is a field of research with large potential for the production of fine chemicals, has been intensively investigated.

In literature in this field, a large number of zeolite catalysts (FAU, MOR, ZSM-5, BEA, etc.) have been described as active catalysts in the acylation of aromatics.<sup>[2]</sup> One of the solid acid catalysts that gives very high activities and selectivities is the



**Scheme 4.1** Benzoylation reaction of anisole with benzoic anhydride.

large pore, three-dimensional H-BEA zeolite, which possesses particular acid and textural properties.

The preceding chapter emphasizes the acetylation reaction which is the major reaction studied since 1998. Few articles concern the acylation reaction using aliphatic acids or their derivatives (propionic,<sup>[3-5]</sup> isobutyric<sup>[6]</sup> or octanoic acid<sup>[7]</sup>). In this section, attention will be given to benzoylation of aromatic compounds.

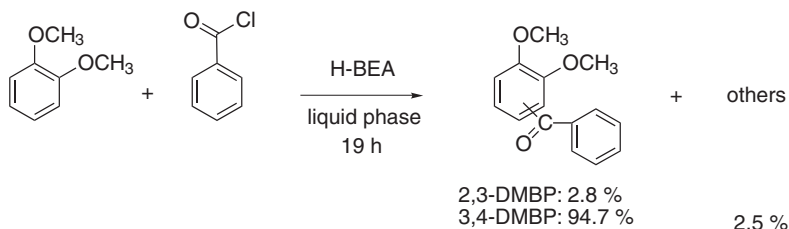
Benzoylation constitutes an important class among acylation reactions, due to the commercial importance of benzophenone and its substituted analogues, especially as additives in the perfumery industry.<sup>[8]</sup>

In the years since 1998, some papers have reported the benzoylation of substituted benzene derivatives, such as toluene,<sup>[9-11]</sup> ethyl benzene,<sup>[11]</sup> xylene,<sup>[9,11,12]</sup> anisole,<sup>[9,13]</sup> dimethoxybenzene,<sup>[14]</sup> biphenyl,<sup>[15]</sup> phenol<sup>[16]</sup> and chlorobenzene<sup>[17]</sup> in the presence of zeolites and, in most cases, particularly H-BEA zeolite.

The formation of 4-methoxybenzophenone by the benzoylation of anisole with benzoic anhydride is shown in Scheme 4.1.

#### 4.1.1 EFFECT OF THE ZEOLITE

Jacob *et al.*<sup>[12]</sup> found that *o*-xylene can be benzoylated selectively to 3,4-dimethylbenzophenone using zeolites as catalysts and benzoyl chloride as benzoylating agent. As shown in Scheme 4.2, zeolite H-BEA exhibits higher activity and selectivity for 3,4-dimethylbenzophenone (3,4-DMBP) than that of the other zeolite catalysts (H-ZSM-5, H-Y and H-MOR), due on the one hand to its stronger acid sites compared with the other zeolite catalysts and on the other hand to smaller pore openings ( $7.6 \times 6.4 \text{ \AA}$  and  $5.5 \times 5.5 \text{ \AA}$ ) than H-Y ( $7.4 \times 7.4 \text{ \AA}$ ) zeolite, leading to a shape selectivity. In another article on benzoylation of toluene and naphthalene,<sup>[10]</sup>



**Scheme 4.2** Benzoylation of *o*-xylene to 3,4-dimethylbenzophenone with benzoyl chloride over H-BEA zeolite.

molecular mechanics were used to calculate the individual strain, dimensions of reactant and product molecules, then the dimensions of zeolite cages were compared. So, the superiority of zeolite BEA is demonstrated by the structural fitting of the reactant and product molecules inside the zeolite pore.

#### 4.1.2 EFFECT OF THE ACYLATING AGENT

Carboxylic acids, acid chlorides and acid anhydrides can be used as acylating acids. In the benzylation of 1,2-dimethoxybenzene,<sup>[14]</sup> the reactivity of benzoic anhydride is higher than that of the corresponding chloride. This difference of behaviour can be attributed to a stronger adsorption of benzoic anhydride because of its molecular weight being about twice that of benzoyl chloride, as suggested by Derouane.<sup>[18]</sup> Benzoic anhydride should thus be adsorbed more strongly and behave as a better acylation agent.

The same effect is found for toluene acylation over BEA zeolite with derivatives of isobutyric acid: isobutyric anhydride presents a higher initial activity compared with isobutyric chloride.<sup>[6]</sup>

Consequently, adsorption phenomena of the acylating agent on the zeolitic catalyst plays a major role in determining the course of the reaction.

#### 4.1.3 EFFECT OF THE SOLVENT

Different solvents have been used, such as chlorobenzene<sup>[3,14]</sup> or dichloroethane,<sup>[9]</sup> but very often the arene plays the dual role of substrate and solvent.<sup>[9,11,15-17]</sup>

In recent years, ionic liquids have attracted intense interest as a possible replacement for traditional solvents for organic reactions, particularly in the area of green chemistry, due to their advantageous properties (negligible vapour pressure as well as high thermal and chemical stability).

It is worth noting that a paper recently published concerning the Friedel–Crafts benzylation of anisole using zeolites in ionic liquids<sup>[13]</sup> reports higher rates of reaction using ionic liquids compared with organic solvents: an anisole conversion of 40 % with a protonic ultrastable FAU (H-USY) as zeolite in an ionic liquid (1-ethyl-3-methylimidazolium *bis*-trifluoromethanesulfonimide) against 22 % with the same zeolite in 1,2-dichloroethane. The reaction is thought to proceed via a homogeneous mechanism, catalysed by the *bis*-trifluoromethane sulfonimide generated *in situ* by the exchange of the cation from the ionic liquid with the acid proton on the zeolite.

#### 4.1.4 BENZOYLATION OF PHENOL AND THE FRIES REARRANGEMENT<sup>[16]</sup>

Among all the benzylation reactions of substituted benzene derivatives, the phenol reaction is interesting to consider and to develop due to the fact that it may occur



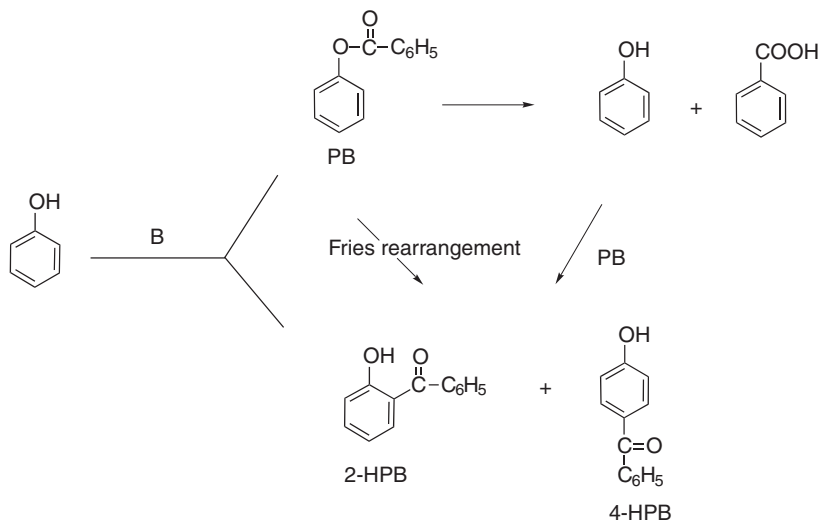
**Table 4.1** Benzoylation of phenol with benzoic anhydride over various zeolites and  $\text{AlCl}_3$ 

Catalyst	$\text{SiO}_2/\text{Al}_2\text{O}_3$	Conversion BA (wt%)			Product (yields wt%)		
		PB	2-HPB	4-HPB	others	<i>p/o</i>	
H-BEA	26.0	95.9	61.2	11.4	23.3	—	2.1
H-Y	4.1	97.6	55.0	25.7	16.9	—	0.6
H-MOR	22.0	87.7	87.0	0.7	—	—	—
H-ZSM-5	41.0	86.1	86.1	—	—	—	—
$\text{AlCl}_3$	—	91.4	70.8	5.4	3.3	11.9	0.6

through different reaction pathways and the aryl esters Fries rearrangement often plays an important role in the production of hydroxyarylketones by acylation of phenol. The catalytic activities of different catalysts such as H-BEA, H-Y, H-MOR, H-ZSM-5 and conventional catalyst  $\text{AlCl}_3$ , in the benzoylation of phenol at  $220^\circ\text{C}$  are summarized in Table 4.1.

Zeolites H-BEA and H-Y were found to be the most active catalysts, however all catalysts readily form the phenyl benzoate (Table 4.1). In the conditions of the reaction, the formation of phenyl benzoate (PB) occurs rapidly via O-acylation of phenol. Direct C-alkylation of phenol with benzoic anhydride (B) and Fries rearrangement of phenyl benzoate results in the formation of 2- and 4-hydroxybenzophenones (2-HPB and 4-HPB) (Scheme 4.3).

For phenylbenzoate, the relatively more constrained H-BEA zeolite shows a much higher selectivity and an improved 4-HPB/2-HPB ratio ( $p/o = 2.1$ ). Such a

**Scheme 4.3** Reaction of phenol with benzoic anhydride: O- and C-acylation and Fries rearrangement.

result is attributed to the three-dimensional pore system with straight channels of  $7.6 \times 6.4 \text{ \AA}$  and a tortuous channel of  $5.5 \times 5.5 \text{ \AA}$  of H-BEA.

#### 4.1.5 KINETIC LAW

For a bimolecular heterogeneous reaction, either a Langmuir–Hinshelwood or an Eley–Rideal type kinetic mechanism is generally considered. In a Langmuir–Hinshelwood process, the two reactants are adsorbed on the catalyst, whereas in an Eley–Rideal mechanism, an adsorbed agent reacts with the substrate in the liquid phase. In the acylation reaction, it is well-established that the first step is a protonation of the acylating agent by the zeolite Brönsted acid sites and formation of the acylium cation, which reacts with the aromatic substrate in the second step. The question to be answered is whether the substrate is adsorbed or not. The adsorption of the aromatic substrate at a protonic site generates a species with a significant degree of positive charge and the attack of such a species on a positively charged carbocation would not be expected. Consequently, a Langmuir–Hinshelwood mechanism in the strict sense could be ruled out at first glance.

In order to circumvent this problem, Derouane *et al.* for acetylation reaction of anisole and toluene,<sup>[19,20]</sup> consider that the adsorption terms of the aromatic system represents only a physisorption process rather than also including chemisorption. This could be interpreted as the reaction not occurring between the two adsorbed species.

On the other hand, a pure Eley–Rideal mechanism, in which the aromatic compound in the liquid phase reacts with the adsorbed acylating agent was first proposed by Venuto *et al.*<sup>[21,22]</sup> and more recently by others.<sup>[23]</sup> However, for acylation reactions of polar substrates (anisole, veratrole), chemisorption of the latter must be taken into account in the kinetic law. A modification, the ‘modified Eley–Rideal’ mechanism, has been proposed:<sup>[14,24–26]</sup> an adsorbed molecule of acylating agent should react with a nonadsorbed aromatic substrate, within the porous volume of the catalyst. However, the substrate is also competitively adsorbed on the active sites of the zeolite, acting somehow as a poison of the acid sites. That is what we checked through different kinetic studies of various aromatic electrophilic substitution reactions.<sup>[24–26]</sup>

For example, in the acylation of veratrole with benzoic anhydride,<sup>[14]</sup> following this mechanism, we assume that the veratrole chemisorption reduces the number of acid sites available for benzoic anhydride, but that the reaction does not proceed between the two adsorbed species. Such an assumption leads to the corresponding initial rate equation as follows:

$$r_0 = \frac{k w \lambda_B [B]_0 [V]_0}{1 + \lambda_B [B]_0 + \lambda_V [V]_0} \quad (4.1)$$

where  $k$  is the reaction rate constant,  $w$  is the catalyst mass,  $\lambda_B$  and  $\lambda_V$  are the adsorption coefficients of benzoic anhydride and veratrole and  $[B]_0$  and  $[V]_0$  their initial concentrations, respectively.

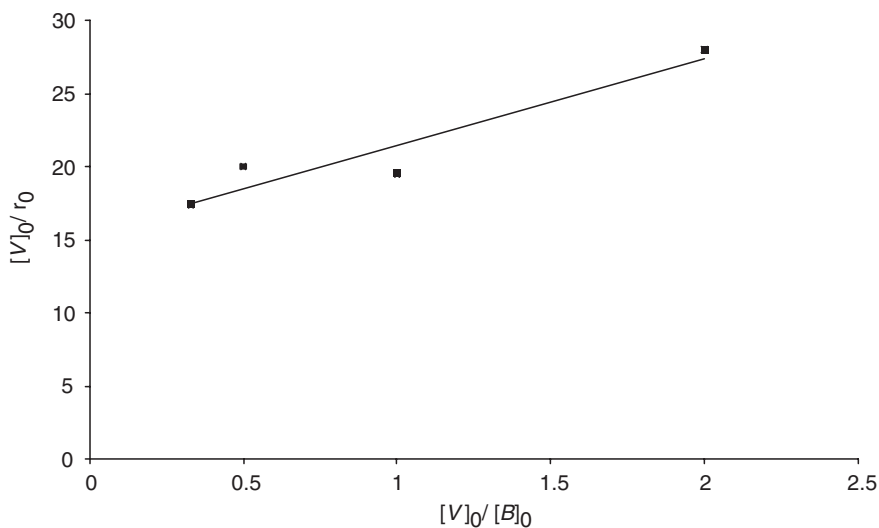


**Figure 4.1** Plot of  $[V]_0/r_0$  against  $[V]_0/[B]_0$

As the reaction operates in the liquid phase,  $\lambda_B[B]_0 + \lambda_V[V]_0$  is far higher than 1 so that Equation (4.1) can be expressed as:

$$r_0 = \frac{k_w \lambda_B [B]_0 [V]_0}{\lambda_B [B]_0 + \lambda_V [V]_0} \quad (4.2)$$

By linearizing Equation (4.2), the following equation is obtained:

$$\frac{1}{r_0} = \frac{1}{k_w} \frac{1}{[V]_0} + \frac{1}{k_w} \frac{\lambda_V}{\lambda_B} \frac{1}{[B]_0}$$

The plot of  $[V]_0/r_0$  against  $[V]_0/[B]_0$  yields a slope of  $\lambda_V/(k_w \lambda_B)$  and an intercept of  $1/(k_w)$  from which the adsorption coefficient ratio  $\lambda_V/\lambda_B$  could be established (Figure 4.1).

A ratio  $\lambda_V/\lambda_B$  of 0.5 is found. This value indicates that veratrole is less strongly adsorbed on the catalytic sites than benzoic anhydride which is twice as large. This result shows that, for two polar reactants, the competitive adsorption is in favour of the larger molecule in the intracrystalline microporous volume.

#### 4.1.6 SUBSTITUENT EFFECT

##### On the Acylating Agent

The reaction of veratrole with a series of substituted benzoyl chlorides has been studied.<sup>[14]</sup> The effect of the substituent on the initial rate is not particularly

**Table 4.2** Benzoylation of different aromatic compounds with benzoyl chloride over In<sub>2</sub>O<sub>3</sub>/H-BEA catalyst

Aromatic compound	Time required for half reaction, $t_{1/2}$ (min)	$\sigma$
Benzene	120	0
Toluene	46.5	-0.16
<i>p</i> -Xylene	30	-0.21
Anisole	16.7	-0.28

From Choudhary *et al.*<sup>[9]</sup>

significant, as only a factor of 3 is observed between OCH<sub>3</sub> and Cl at the *p*-position (initial rate  $4.7 \times 10^{-3}$  and  $8.9 \times 10^{-3}$  mol L<sup>-1</sup> min<sup>-1</sup>, respectively). The Hammett  $\rho$ - $\sigma^+$  relationship shows a linear correlation with a weak positive slope of 0.5 which indicates a weak variation of the positive charge between the benzoyl cation and the transition state. Such results, already observed in the case of the thiophene benzoylation over large pore zeolites,<sup>[27]</sup> leads to the conclusion that the electrophilicity of the acylating agent does not play a relevant role. In contrast, the presence of electron-donating substituents on the aromatic substrate leads to a significant increase of the reaction rate as reported in the following paragraph.

### On the Aromatic Substrate

Benzoylation of benzene and other aromatic compounds by benzoyl chloride over H-BEA zeolite modified by indium oxides has been investigated.<sup>[9]</sup> We report in Table 4.2 the time required for half reaction ( $t_{1/2}$ ) for a series of aromatic substrates used in the above reaction. The benzoylation reaction rate (via  $t_{1/2}$  value) depends strongly on the substituent group present in the aromatic substrate and increases due to the presence of the electron-donating group, depending upon its electron-donating ability. The activity order is as follows: benzene  $\ll$  toluene  $<$  *p*-xylene  $<$  anisole.

In Figure 4.2,  $\log t_{1/2}$  is plotted against Hammett substituent constant  $\sigma$  values giving a straight line correlation, and a large negative value of  $\rho$  ( $-3$ ). Such a result is consistent with that already observed for acylation of aromatic compounds on CeY zeolite<sup>[28]</sup> and for the conventional acid catalysed Friedel-Crafts acylation. These electronic effects are analogous to those reported in the case of classical electrophilic aromatic substitutions.

#### 4.1.7 EXPERIMENTAL

The liquid phase benzoylation reactions over HBEA zeolite catalyst were operated under nitrogen to minimize the hydrolysis of acylating agent in a magnetically stirred glass reactor equipped with a condenser and a dropping funnel.

The typical reaction with benzoic anhydride as acylating agent was carried out as follows: a solution of 20 mmol of aromatic substrate in 50 ml dry chlorobenzene were introduced in the flask and magnetically stirred under nitrogen atmosphere.

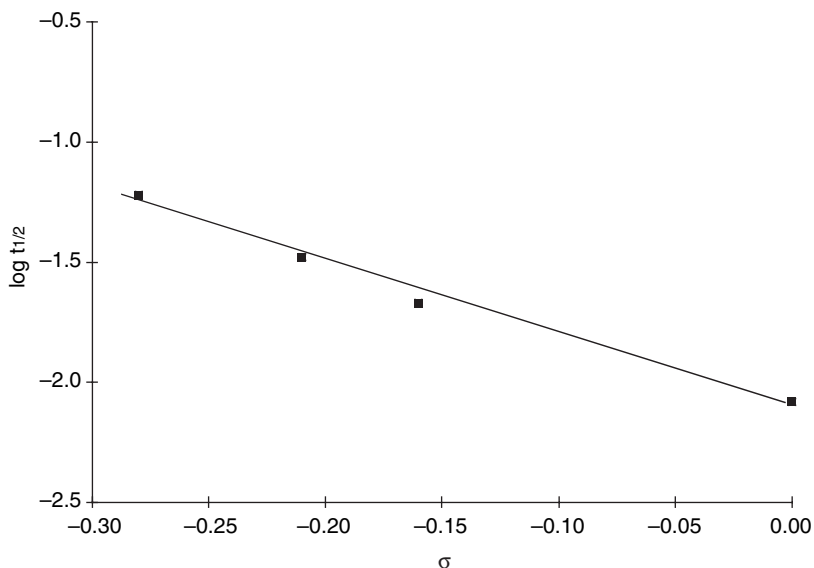


**Figure 4.2** Hammett relationship ( $\log t_{1/2}$  versus  $\sigma$ ) in the benzylation reaction of benzene and substituted aromatic compounds with benzoyl chloride over H-BEA zeolite modified by indium oxides

The freshly activated catalyst (0.5 g activated at 500 °C for 6 h in a flow of dry air) was added and the reaction mixture was allowed to heat to reflux of chlorobenzene. Then, 10 mmol of benzoic anhydride were added slowly through the addition funnel, and the mixture was stirred. Samples were periodically collected and analysed by GC, on a HP-1 type capillary column (25 m  $\times$  0.2 mm, 0.33  $\mu$ m film thickness).

## 4.2 ACYLATION OF ANISOLE OVER MESOPOROUS ALUMINOSILICATES

Mesoporous aluminosilicates have attracted much recent attention because of their potential use as versatile catalysts and catalyst supports, especially for large molecules, but their acidity is always much weaker than that of zeolites. They must be modified to enhance their acidity. Mesoporous Si-MCM-41 supported metal chloride catalysts<sup>[29]</sup> have shown high activity in the acylation of benzene by benzoyl chloride even in the presence of moisture in the reaction mixture. The time required for 54 % conversion of benzoyl chloride at 80 °C was 2.2 h in the presence of InCl<sub>3</sub>/Si-MCM-41, against 18 h with H-BEA.

A recent article reported the use of strongly acidic mesoporous aluminosilicates prepared from zeolite seeds in the acylation of anisole with octanoyl chloride.<sup>[30]</sup> The mesoporosity improving the transport of the reactants and the presence of strong acid sites lead to high conversion (>90 %) and high selectivity (100 %).

## REFERENCES

1. Chiche, B., Finiels, A., Gauthier, C., Geneste, P., Graille, J. and Pioch, D. Friedel–Crafts acylation of toluene and *p*-xylene with carboxylic acids catalyzed by zeolites. *J. Org. Chem.*, **1986**, *51*, 2128–2130.
2. Bezouhanova, C. P. Synthesis of aromatic ketones in the presence of zeolite catalysts, *Appl. Catal., A*, **2002**, *229*, 127–133.
3. Jaimol, T., Moreau, P., Finiels, A., Ramaswamy, A. V. and Singh, A. P. Selective propionylation of veratrole to 3,4-dimethoxypropiophenone using zeolite H-beta catalysts, *Appl. Catal., A*, **2001**, *214*, 1–10.
4. Chaube, V. D., Moreau, P., Finiels, A., Ramaswamy, A. V. and Singh, A. P. Propionylation of phenol to 4-hydroxypropiophenone over zeolite H-beta, *J. Mol. Catal., A*, **2001**, *174*, 255–264.
5. Kantam, M. L., Sri Ranganath, K. V., Sateesh, M., Kumar, K. B. S. and Choudary, B. M. Friedel–Crafts acylation of aromatics and heteroaromatics by beta zeolite, *J. Mol. Catal., A*, **2004**, *225*, 15–20.
6. Klisáková, J., Cervený, L. and Cejka, J. On the role of zeolite structure and acidity in toluene acylation with isobutyric acid derivatives, *Appl. Catal., A*, **2004**, *272*, 79–86.
7. Beers, A. E. W., van Bokhoven, J. A., de Lathouder, K. M., Kapteijn, F. and Moulijn, J. A. Optimization of zeolite Beta by steaming and acid leaching for the acylation of anisole with octanoic acid: a structure-activity relation, *J. Catal.*, **2003**, *218*, 239–248.
8. Windholz, M. *An Encyclopedia of Chemical Drugs and Biochemicals*, 10th edition. Merck & Co., Rahway, **1983**.
9. Choudhary, V. R., Jana, S. K., Patil, N. S., Bhargava, S.K. Friedel–Crafts type benzylation and benzylation of aromatic compounds over H $\beta$  zeolite modified by oxides or chlorides of gallium and indium. *Microporous Mesoporous Mater.*, **2003**, *57*, 21–35.
10. Chatterjee, A., Bhattacharya, D., Iwasaki, T. and Ebina, T. A computer simulation study on acylation reaction of aromatic hydrocarbons over acidic zeolites, *J. Catal.*, **1999**, *185*, 23–32.
11. Laidlaw, P., Bethell, D., Brown, S. M. and Hutchings, G. J. Benzoylation of substituted arenes using Zn- and Fe- exchanged zeolites as catalysts, *J. Mol. Catal., A*, **2001**, *174*, 187–191.
12. Jacob, B., Sugunan, S. and Singh, A. P. Selective benzoylation of *o*-xylene to 3,4-dimethylbenzophenone using various zeolite catalysts, *J. Mol. Catal., A*, **1999**, *139*, 43–53.
13. Hardacre, C., Katdare, S. P., Milroy, D., Nancarrow, P., Rooney D. W. and Thompson, J. M. A catalytic and mechanistic study of the Friedel–Crafts benzoylation of anisole using zeolites in ionic liquids, *J. Catal.*, **2004**, *227*, 44–52.
14. Raja, T., Singh, A. P., Ramaswamy, A. V., Finiels, A. and Moreau, P. Benzoylation of 1,2-dimethoxybenzene with benzoic anhydride and substituted benzoyl chlorides over large pore zeolites, *Appl. Catal., A*, **2001**, *211*, 31–39.
15. Chidambaram, M., Venkatesan, C., Moreau, P., Finiels, A., Ramaswamy, A. V. and Singh, A. P. Selective benzoylation of biphenyl to 4-phenylbenzophenone over zeolite H-beta, *Appl. Catal., A*, **2002**, *224*, 129–140.
16. Chaube, V. D., Moreau, P., Finiels, A., Ramaswamy, A. V., and Singh, A. P., A novel single step selective synthesis of 4-hydroxybenzophenone (4-HBP) using zeolite H-beta. *Catal. Lett.*, **2002**, *79*, 1–4.
17. Venkatesan, C., Jaimol, T., Moreau, P., Finiels, A., Ramaswamy, A. V. and Singh, A. P. Liquid phase selective benzoylation of chlorobenzene to 4, 4'-dichlorobenzophenone over zeolite H-beta, *Catal. Lett.*, **2001**, *75*, 119–123.

18. Derouane, E. G. Zeolites as solid solvents, *J. Mol. Catal., A*, **1998**, *134*, 29–45.
19. Derouane, E. G., Dillon, C. J., Bethell, D., Derouane Abd-Hamid, S. B. Zeolite catalysts as solid solvents in fine chemicals synthesis-1. Catalyst deactivation in the Friedel–Crafts acetylation of anisole, *J. Catal.*, **1999**, *187*, 209–218.
20. Derouane, E. G., Crehan, G., Dillon, C. J., Bethell, D., He, H., Derouane Abd-Hamid, S. B. Zeolite catalysts as solid solvents in fine chemicals synthesis-2. Competitive adsorption of the reactants and products in the Friedel–Crafts acetylations of anisole and toluene, *J. Catal.*, **2000**, *194*, 410–423.
21. Venuto, P. B., Landis, P. S. Organic reactions catalyzed by crystalline aluminosilicates. III. Condensation reactions of carbonyl compounds, *J. Catal.*, **1966**, *6*, 237–244.
22. Venuto, P. B., Hamilton, L. A., Landis, P. S. Organic reactions catalyzed by crystalline aluminosilicates- II. Alkylation reactions: mechanistic and aging considerations, *J. Catal.*, **1996**, *5*, 484–493.
23. Yadav, G. D., Krishnan, M. S. Solid acid catalysed acylation of 2-methoxy-naphthalene: role of intraparticle diffusional resistance, *Chem. Eng. Sci.*, **1999**, *54*, 4189–4197.
24. Moreau, P., Finiels, A., Méric, P. Acetylation of dimethoxybenzenes with acetic anhydride in the presence of acidic zeolites, *J. Mol. Catal., A*, **2000**, *154*, 185–192.
25. Barthel, N., Finiels, A., Moreau, C., Jacquot, R., Spagnol, M. Kinetic study and reaction mechanism of the hydroxyalkylation of aromatic compounds over H-BEA zeolites, *J. Mol. Catal., A*, **2001**, *169*, 163–169.
26. Méric, P., Finiels, A., Moreau, P. Kinetics of 2-methoxynaphthlene acetylation with acetic anhydride over dealuminated HY zeolites, *J. Mol. Catal., A*, **2002**, *189*, 251–262.
27. Finiels, A., Calmettes, A., Geneste, P. and Moreau, P. Kinetic study of the acylation of thiophene with acyl chlorides in liquid phase over HY zeolites, *Stud. Surf. Sci. Catal.*, **1993**, *78*, 595–600.
28. Chiche, B., Finiels, A., Gauthier, C., Geneste, P. The effect of structure on reactivity in zeolite catalyzed acylation of aromatic compounds: a  $\rho$ – $\sigma^+$  relationship, *Appl. Catal.*, **1987**, *30*, 365–369.
29. Choudhary, V. R., Jana, S. K., Patil, N. S. Acylation of benzene over clay and mesoporous Si-MCM-41 supported  $\text{InCl}_3$ ,  $\text{GaCl}_3$  and  $\text{ZnCl}_2$  catalysts, *Catal. Lett.*, **2001**, *76*, 235–239.
30. Shih, P.-C., Wang, J.-H., Mou, C.-Y. Strongly acidic mesoporous aluminosilicates prepared from zeolite seeds: acylation of anisole with octanoyl chloride, *Catal. Today*, **2004**, *93–95*, 365–370.

---

# 5 Nitration of Aromatic Compounds

---

AVELINO CORMA AND SARA IBORRA

*Instituto de Tecnología Química, UPV, Av. Naranjos s/n, E-46022 Valencia, Spain*

## CONTENTS

5.1 INTRODUCTION . . . . .	105
5.2 REACTION MECHANISM . . . . .	106
5.3 NITRATION OF AROMATIC COMPOUNDS USING ZEOLITES AS CATALYSTS . . . . .	107
5.3.1 Nitration in liquid phase . . . . .	107
5.3.2 Vapour phase nitration . . . . .	116
5.4 CONCLUSIONS . . . . .	118
REFERENCES . . . . .	118

## 5.1 INTRODUCTION

Aromatic nitro compounds are versatile chemical intermediates for the synthesis of drugs, pesticides, dyes, polymers and explosives. Nitration of aromatic substrates is one of the most widely studied chemical reactions, and excellent and extensive reviews concerning aromatic nitration in homogeneous media have been reported by Olah *et al.*,<sup>[1,2]</sup> Ingold<sup>[3]</sup> and Schofield *et al.*<sup>[4,5]</sup> More recently, Malysheva *et al.*<sup>[6]</sup> have surveyed the use of zeolites as catalysts in the nitration of aromatics by nitrogen oxides, whereas recent research on the application of heterogeneous catalysts in the nitration of aromatic compounds has been summarized by Kogelbauer *et al.*<sup>[7]</sup> in a general review.

The conventional nitration process,<sup>[2,5]</sup> that involves a mixture of nitric and sulfuric acids (mixed acids method) has remained unchallenged, in the commercial area, for the last 150 years owing to the very favourable economics. However, the method is notoriously unselective for nitration of substituted aromatic compounds and the disposal of waste products and spent acids is a serious environmental issue. For instance, nitration of toluene for production of mononitrotoluenes (MNTs) is conducted using a nitrating mixture usually composed of 52–56 % (w/w) H<sub>2</sub>SO<sub>4</sub>, 28–32 % (w/w) HNO<sub>3</sub> and 12–20 % (w/w) H<sub>2</sub>O. The reaction performed at temperatures between 25 and 40°C, yields ca. 96 % MNTs, which are composed of a mixture of ca. 60 % (w/w) *o*-nitrotoluene, ca. 37 % (w/w) *p*-nitrotoluene and

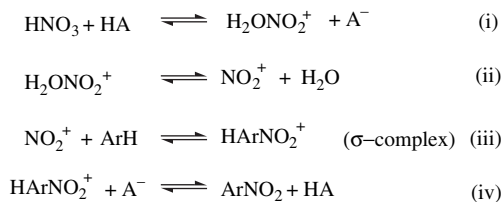


less than 3 % (w/w) *m*-nitrotoluene. Since *p*-nitrotoluene is in greater demand than the *ortho*-isomer, there is a strong incentive to find *para*-selective catalysts. Furthermore, the regeneration of the used acid requires expensive and energy intensive recovery, purification, and reconcentration steps.<sup>[8]</sup> Thus, the use of solid acids appears as an attractive alternative because of the easy removal and recycling of the catalyst, and potential introduction of regioselectivity. Consequently, in recent years a substantial research effort has been devoted to the development of new nitration methods using solid acid catalysts.<sup>[7]</sup> For example, lanthanide triflates,<sup>[9]</sup> Nafion-H and other polysulfonic acid resins,<sup>[10]</sup> claycop [copper(II) nitrate supported on K-10 montmorillonite],<sup>[11]</sup> supported acids on SiO<sub>2</sub><sup>[12,13]</sup> and acid zeolites<sup>[14,15]</sup> have been used with different success as acid catalysts for nitration of aromatics. Among them, zeolites appear as the most promising catalysts because of their thermal stability, their success in shape-selective reactions<sup>[16]</sup> and regenerability. In this chapter, we will discuss recent research on the application of zeolites as solid acid catalysts for the nitration of aromatic substrates.

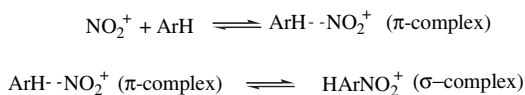
## 5.2 REACTION MECHANISM

The accepted reaction mechanism for the electrophilic aromatic nitration was postulated by Ingold in 1969<sup>[3]</sup> and involves several steps (Scheme 5.1). Firstly, the nitric acid is protonated by a stronger acid (sulfuric). The protonated nitric acid gives water and the nitronium ion (NO<sub>2</sub><sup>+</sup>) which is the electrophilic active species for nitration of aromatics. Nitric acid heterolysis is considered to be accelerated by the polarity of the solvent, and solvation of nitronium ion in different media affects its reactivity and the selectivity of the reaction. Combination of nitronium ion and an aromatic molecule form an intermediate named the Wheland complex or  $\sigma$ -complex. The loss of a proton from the  $\sigma$ -complex gives the aromatic nitrocompound (Scheme 5.1).

For highly reactive aromatics, an additional kinetic step with the formation of a first intermediate ( $\pi$ -complex) between Steps (ii) and (iii), must be considered in the above mechanism (Scheme 5.2). Reaction energy diagrams show that in activated aromatics, the reactivity is controlled by the transition state with the highest activation barrier ( $\pi$ -transition estate), while the position selectivity depends on



Scheme 5.1



Scheme 5.2

the subsequent  $\sigma$ -transition state. For low activated aromatics the  $\sigma$ -transition state, which possesses the highest barrier, determines both reaction rate and selectivity.<sup>[2]</sup>

### 5.3 NITRATION OF AROMATIC COMPOUNDS USING ZEOLITES AS CATALYSTS

The use of nitric acid as nitrating agent for the large-scale industrial nitration of aromatics is still the most preferred method owing to economic considerations. All the systems based on acid heterogeneous catalysts reported up to now are less active than the nitric–sulfuric method. This is mainly because the use of nitric acid as the nitrating agent normally deactivates the solid acid due to poisoning of the acid sites by water.<sup>[17,18]</sup> In order to maintain the activity of the solid acid, the water must be removed from the reaction system. This can be achieved by three methods: (1) by working in vapour phase; (2) removing the water by distillation from the liquid reaction mixture; (3) removing the water by chemical trapping with acetic anhydride. Besides the above methods, which involve the use of nitric acid, other nitration procedures have been reported in recent years. They involve the use of nitrating organic agents, such as acyl or alkyl nitrates, and the use of nitrogen dioxide or dinitrogen pentoxide. In this section, the use of these nitrating systems in the presence of zeolites as catalysts for the formation of nitroaromatics is discussed.

#### 5.3.1 NITRATION IN LIQUID PHASE

##### Alkyl and Acyl Nitrates as Nitrating Agents

Nitration of monosubstituted aromatics, toluene in particular, has been extensively studied using zeolites in order to direct the reaction towards the formation of the desired *para*-isomer. Toluene has been nitrated *para*-selectively with benzoyl nitrate over zeolite catalysts.<sup>[14,15]</sup> For example, when mordenite is used as a catalyst, MNTs are formed in almost quantitative yields, giving 67% of the *para*-isomer in 10 min, but tetrachloromethane is required as solvent. However, the main problems associated with the use of benzoyl nitrate are: handling difficulties due to its sensitivity toward decomposition, and the tendency toward detonation upon contact with rough surfaces. Nagy *et al.*<sup>[19–21]</sup> reported the nitration of benzene, chlorobenzene, toluene and *o*-xylene with benzoyl nitrate in the presence of an amorphous aluminosilicate, as well as with zeolites HY and ZSM-11, in hexane as a

solvent. ZSM-11 zeolite gives higher selectivity to *para*-isomers (75 %) than amorphous aluminosilicates and HY zeolite (55 and 64 %, respectively). However, when the external acid sites of the zeolite were selectively poisoned by treatment with tributylamine, the selectivity of ZSM-11 was considerably improved (98 %), whereas the selectivity for HY remains unchanged. These results suggest that the superior *para*-selectivity exhibited by ZSM-11 is due to shape-selectivity effects. The same authors studied the effect of the nature of nitrating agents. An increase in *para*-selectivity was observed when increasing the size of the substituent in acyl nitrates.<sup>[20]</sup> The authors suggested that the reaction transition state involves the whole nitrating agent as a molecule, and the electrophilic agents involved in the reaction are the protonated forms of acylnitrated, rather than the nitronium cation bound to the zeolite framework structure. Unfortunately, the authors do not discuss isolated yields, the formation of by-products, or the effect of the deactivation of the external active sites on the overall yield.

Mononitration of alkylbenzenes was studied using acyl nitrates and trimethylsilyl nitrate supported on clay minerals. High *para*-selectivity was obtained with the supported reagents. Thus, nitration of toluene with acetyl nitrate impregnated on chrysotile gave 78 % *p*-nitrotoluene, and 19 % *o*-nitrotoluene.<sup>[22]</sup> Toluene has also been successfully nitrated with propyl nitrate in the presence of ZSM-5 zeolite as catalyst.<sup>[23]</sup> The authors studied the influence of varying the zeolite framework Si/Al ratio on the catalytic activity by working at 116 °C with toluene, which also acts as solvent, and with large zeolite/alkyl nitrate ratios. ZSM-5 zeolite with a Si/Al = 1000 produced MNTs in 54 % yield, with a product distribution of *o*:*m*:*p* of 5:0:95. However ZSM-5 zeolites with lower Si/Al ratio (<100) were less selective (<79 %). Catalyst deactivation and shape selectivity effects in toluene nitration using propyl nitrate, has been studied over solid acid catalysts such as HZSM-5, HMordenite, HBeta, HL zeolites, MCM-41 and sulfated zirconia.<sup>[24]</sup> The reactions were performed in batch conditions as well as in vapour phase (in this case using NO<sub>2</sub> as nitrating agent) at 66–100 °C. The results showed that the size of the pores of the zeolite has an important effect on the regioselectivity of the reaction. The highest selectivity for *p*-nitrotoluene was observed with HZSM-5 followed by HMordenite, HL and MCM-41. All catalysts exhibited significant deactivation, as well as a decrease in *para*-selectivity, with reaction time. For HZSM-5 the *para*-selectivity found at 94 °C and after 5 h on stream was 75 % at 18 % conversion. In general, it was found that in the low temperature range, the catalysts become deactivated by pore plugging due to the aromatic molecules, while at higher temperatures the catalyst deactivates by coke formation.

### Nitration by Using Nitric Acid and Acetic Anhydride as Water Trapping Reagent

Laszlo and co-workers<sup>[11,25–27]</sup> developed a reagent known as claycop, which is Cu(NO<sub>3</sub>)<sub>2</sub> supported on acidic montmorillonite clay, that selectively nitrates toluene using nitric acid, and acetic anhydride as water trapping reagent (Menke conditions). The reaction conditions required to obtain high selectivity of the *para*-isomer

were: high dilution of toluene in tetrachloromethane as solvent and 120 h reaction time. Quantitative yields of MNT were achieved with a *o:m:p* distribution of 23:1:76. The authors suggest that the clay surface induces electronic stability favouring the *para*-position. This system has also been used for the dinitration of toluene leading to a mixture of 2,4- and 2,6- dinitro isomes in a ratio of 9:1.<sup>[28]</sup> Several disadvantages, such as the requirement of high dilution, an excess of acetic anhydride, the stoichiometric use of copper nitrate and the difficulty in the reutilization of catalyst, makes the system inadequate for industrial applications.

Using Menke's conditions, Smith *et al.*<sup>[29,30]</sup> have described a method for the nitration of benzene, alkylbenzenes and halogenobenzenes using zeolites with different topologies (HBeta, HY, HZSM-5 and HMordenite) as catalysts and a stoichiometric amount of nitric acid and acetic anhydride. The reactions were carried out without solvent at temperatures between  $-50^{\circ}\text{C}$  and  $20^{\circ}\text{C}$ . For the nitration of toluene, tridirectional zeolites HBeta and HY were the most active catalysts achieving  $>99\%$  conversion in 5 min reaction time. However, HY exhibited selectivity to the *p*-nitrotoluene very similar to the homogeneous phase, while with HBeta, selectivities to *p*-nitrotoluene higher than 70% could be achieved. HBeta zeolite exhibited excellent *para*-selectivity for the nitration of the different monosubstituted aromatics (Table 5.1). The catalyst can be recycled and the only by-product, acetic acid, can be separated by vacuum distillation.

Trifluoroacetyl nitrate is more reactive than acetyl nitrate, and it has been successfully used for the nitration of deactivated aromatics such as nitrobenzene and bromobenzene<sup>[31]</sup> using fuming nitric acid and trifluoroacetic anhydride in equimolar proportion at  $45-55^{\circ}\text{C}$ . The reaction between trifluoroacetic anhydride and nitric acid gives the nitrating agent trifluoroacetyl nitrate according to Scheme 5.3.

Recently Smith *et al.*<sup>[32]</sup> have also reported the novel nitration systems comprising nitric acid, trifluoroacetic anhydride and zeolite HBeta, with or without acetic anhydride for the nitration of deactivated aromatic compounds such as

**Table 5.1** Nitration of PhR with  $\text{HNO}_3$ /acetic anhydride using HBeta as catalyst<sup>a[30]</sup>

R	Time (min)	Yield (%)	<i>ortho</i>	<i>meta</i>	<i>para</i>
F	30	>99	6	0	94
Cl	30	>99	7	0	93
Br	5	>99	13	0	87
H	30	>99			
Me	30	>99	18	3	79
Et	10	>99	15	3	82
iPr	30	>99	9	3	88
tBu	30	92	8	Trace	92
Ph <sup>b</sup>	30	70	Trace	0	>99

<sup>a</sup>Reaction conditions:  $\text{HNO}_3$  (2.5 g of 90%, 35 mmol),  $\text{Ac}_2\text{O}$  (5.0 ml, 53 mmol), PhR (35 mmol) HBeta (Si/Al = 13, 1 g), ambient temperature for the indicated time followed by distillation under reduced pressure.

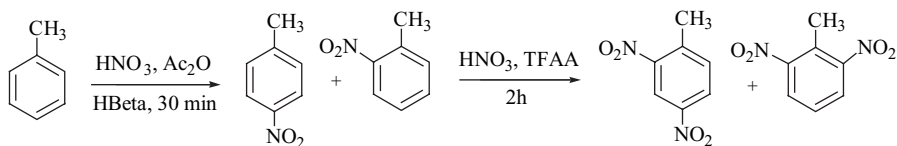
<sup>b</sup>Only 0.38 g of HBeta used. Reprinted with permission from The Journal of Organic Chemistry, Vol. 63, Smith *et al.*, pp. 8448–8454. Copyright 1998 American Chemistry Society



Scheme 5.3

nitrobenzene, benzonitrile, benzoic acid, 2-nitrotoluene (2-NT) and halogenobenzenes. Classically, the dinitration of *o*-nitrotoluene with mixed acids produces 2,4- and 2,6-dinitrotoluenes in a ratio 2:1. The 2,4-isomer is the most desirable commercially because it is the starting material for the production of toluene diisocyanate (TDI) and toluenediamine, both of which are used in the manufacture of polyurethanes. Smith *et al.*<sup>[32]</sup> found that the trifluoroacetyl nitrate mixture (Scheme 5.3) was active for the nitration of *o*-nitrotoluene at room temperature without using zeolite as catalyst, giving 2,4-dinitrotoluene and 2,6-trinitrotoluene in a ratio of 2:1. However, the presence of HBeta zeolite improves the regioselectivity towards the 2,4-isomer, achieving a 2,4- to 2,6- ratio of 3:1. Moreover, they found that adding acetic anhydride to the mixture, prior to addition of the substrate, the regioselectivity towards the 2,4-isomer was further improved. The increase in the regioselectivity was attributed to the dilution effect of the acetic anhydride which improves the diffusion of the substrate into the pore system, and the fact that HBeta zeolite has a stronger influence over both the reaction rate and selectivity. Optimization of catalyst amount and reaction temperature ( $-10^\circ\text{C}$ ) allowed a 98% yield of dinitrotoluenes with a 2,4- to 2,6- ratio of 17:1 after 2 h reaction time to be achieved. The system incorporating acetic anhydride can also be successfully used for the nitration of deactivated aromatics as well as for the direct dinitration of toluene. In this case, 92% yield of dinitrotoluenes with a 2,4- to 2,6- ratio of 25:1, was obtained, which is clearly superior to those achieved using the conventional method (mixed acids) which gives a 2,4- to 2,6- ratio of 4:1. Furthermore, greater selectivity (96% yield and 70:1 regioselectivity) can be achieved by performing the dinitration of toluene in one flask but in two stages with trifluoroacetic anhydride added only in the second stage (Scheme 5.4). From this system, pure 2,4-dinitrotoluene could be isolated in 90% yield simply by filtering the zeolite, concentrating the mother liquor, and performing recrystallization from acetone.

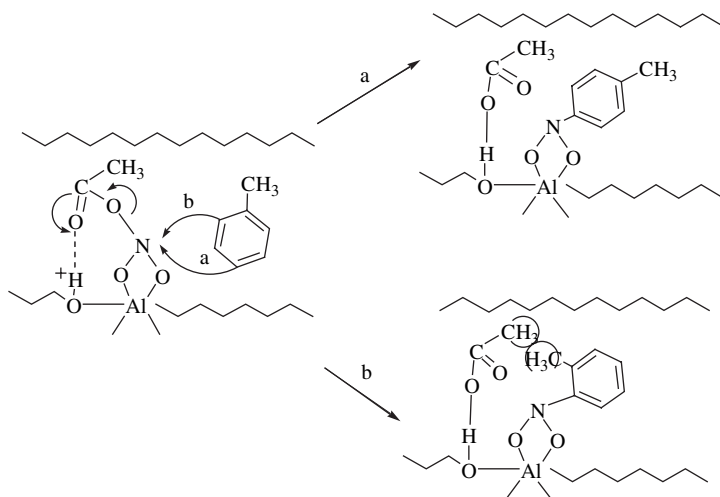
Vassena *et al.*<sup>[33,34]</sup> studied the nitration of toluene and nitrotoluene using different solid acid catalysts (Deloxan, HBeta, ZSM-5 and Mordenite) and nitric acid in acetic anhydride. Increased *para*-selectivity was also observed with zeolite HBeta both for the nitration of toluene and nitrotoluene.



Scheme 5.4

As has been shown, zeolite Beta is a highly *para*-selective catalyst for the nitration of a broad range of substituted aromatics. Thus, the nitration of toluene with nitric acid and acetic anhydride with zeolites has been studied by means of multi-nuclear solid state NMR spectroscopy<sup>[35–37]</sup> in order to explain the enhanced *para*-selectivity observed for zeolite HBeta. The reversible transformation of the framework aluminium from tetrahedral into an octahedral coordination was observed by <sup>27</sup>Al NMR upon interaction of the zeolite with nitric acid, acetyl nitrate and acetic acid. The ability of the zeolite Beta to accommodate such a coordination state transformation is consistent with the high degree of lattice flexibility and makes HBeta unique for this type of reaction. It was proposed that toluene reacts with the preadsorbed reactive nitrating species, i.e. the surface-bonded acetyl nitrate, and forms the sterically least-hindered Wheland intermediate (Scheme 5.5). These studies suggest that the high *para*-selectivity of zeolite Beta might be linked to steric hindrance of the *ortho*-position, induced by adsorption, rather than to classical transition-state selectivity.<sup>[37]</sup> The model also explains the higher reactivity of 2-NT compared with 4-NT towards further nitration, the high 2,4-dinitrotoluene selectivity observed, as well as the absence of *para*-selectivity in the case of Si-Beta where the nitrating agent cannot coordinate to the zeolite framework.<sup>[38]</sup> <sup>15</sup>N NMR studies showed that the portion of surface-bound acetyl nitrate present on Beta zeolite was larger than on other structures having different void space or shape, like ZSM-5 or Mordenite, and explain why a high *para*-selectivity is found exclusively with zeolite Beta.<sup>[38]</sup>

Recently, the same authors reported the nitration of toluene and 2-NT using the nitric acid–acetic anhydride system, and using different batches of zeolite Beta.<sup>[39]</sup> The results showed that the number of Brønsted acid sites and diffusion rates of the products out of the pores play a major role in determining the performance. Lewis



**Scheme 5.5** Reproduced from *Phy. Chem. Chem. Phy.*, vol. 3, Haouas *et al.*, p. 5067, 2001 by permission of PCCP Owner Societies.

acidity appears not to play an important role in the nitration reactions, whereas Brønsted acid sites are required to catalyse the heterogeneous nitration, which has to compete with the fast nitration of toluene in homogeneous phase. However a high number of Brønsted acid sites decreases the *para*-selectivity for the nitration of toluene and the activity in the nitration of 2-NT. Diffusion limitations play an important role, particularly in the nitration of 2-NT, and the reaction rate is determined by the diffusion of the dinitrocompounds out of the zeolite pores.

### Nitrogen Oxides as Nitrating Agents

Pioneering work performed by Suzuki *et al.* using dinitrogen tetroxide and ozone,<sup>[40]</sup> or dinitrogen tetroxide with oxygen and a catalyst<sup>[41]</sup> for the nitration of aromatics, showed to be an alternative approach towards clean nitration. However, the isomeric composition of the nitration products obtained is similar in most cases to those of classical nitration based on nitric and sulfuric acids.

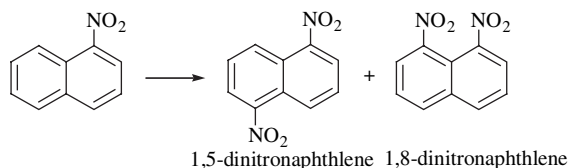
Smith *et al.*<sup>[42]</sup> have recently reported that halobenzenes can be nitrated with nitrogen dioxide and oxygen in the presence of zeolites. The effect of the pore size, channel structure, and zeolite framework Si/Al ratio were studied. Reactions were carried out using a molar excess of liquid N<sub>2</sub>O<sub>4</sub>, dichloromethane as a solvent, at 0 °C using Beta, Y, Mordenite and ZSM-5 zeolites as catalysts. Moreover the effect of the type of extra-framework cation was studied by using Na<sup>+</sup>, K<sup>+</sup> and NH<sub>4</sub><sup>+</sup> exchanged Beta zeolite, and Na<sup>+</sup> exchanged Y. The results showed that all zeolites were active catalysts for the nitration of chlorobenzene giving higher yields than in absence of any catalyst. Tridirectional zeolites (Beta and Y) in the acid form or alkali cation exchanged, were the most active and selective catalysts. HBeta and NaBeta produced quantitative conversions with high selectivity to *p*-nitrochlorobenzene (85 %) within 50 h reaction time. High *para*-selectivity was also observed for fluorobenzene, bromobenzene and iodobenzene (93 %, 77 % and 67 %, respectively). However, nitration of toluene resulted in low selectivity (45 %). The same authors reported that is possible to carry out the nitration of halobenzenes to give high yields, with modest *para*-selectivity (although better than for traditional methods), in the presence of HBeta zeolite in a free solvent system, with stoichiometric amounts of dinitrogen tetroxide, using air instead of oxygen at room temperature and modest pressure (200 psi). A speculative reaction mechanism is proposed.<sup>[43,44]</sup>

Peng *et al.*<sup>[45]</sup> reported the nitration of toluene with liquid nitrogen dioxide and oxygen in the presence of a variety of zeolites, and using toluene as reactant and solvent. The reactions were performed at room temperature over 22 h. In the absence of catalyst the reaction was highly unselective giving a mixture of MNTs, dinitrotoluenes, phenylnitromethane and benzaldehyde. In the presence of zeolites, HZSM-5 and HBeta, the selectivity to the *p*-nitrotoluene was enhanced. In contrast with the results reported by Smith *et al.*,<sup>[14]</sup> HZSM-5 zeolite exhibited better selectivity than Beta zeolite (57 % and 46 %, respectively), which can be attributed to the absence of mediation of the chlorinated solvent molecules, as well as to the higher Si/Al of the HZSM-5 sample (Si/Al=1000). It was found that zeolites

modified with metal ions (Fe, Zn, Cu, Bi and Na) do not accelerate the reaction, while HZSM-5 treated with methanesulfonic acid considerably facilitated nuclear nitration. However, the distribution of *o*:-*m*:-*p*- isomers approached those of conventional nitration (51:3:44). Recently, the same authors reported the nitration of moderately deactivated  $\alpha$ -arenes, such as 1-nitronaphthalene, naphthonitriles and methylated benzonitriles using nitrogen dioxide and molecular oxygen in the presence of zeolites at room temperature.<sup>[46]</sup> The presence of zeolites considerably improves the regioselectivity as compared with conventional nitration based on the mixed acids method. As an example, the nitration of 1-nitronaphthalene using the conventional mixed acid method gives a mixture of dinitro compounds, where the ratio of 1,5- to 1,8-isomers is 0.45:1<sup>[47]</sup> (Scheme 5.6). The former isomer has industrial relevance as a precursor for high performance polyurethane resins and consequently is in a greater market demand than the 1,8-isomer. However, when the nitration of 1-nitronaphthalene is carried out using liquid NO<sub>2</sub> and O<sub>2</sub> at -10 °C, in dichloromethane as a solvent, in the presence of zeolites, the 1,5-isomer becomes highly favoured, especially in the presence of zeolite HBeta giving a 1,5- to 1,8-isomer ratio of 2.6:1.

The nonacid method for aromatic nitration using the NO<sub>2</sub>/O<sub>3</sub> system as nitrating agent (Kyodai nitration) has shown an excellent conversion of a variety of aromatic substrates to the corresponding nitro derivatives under mild conditions.<sup>[48-50]</sup> Perg and Suzuki<sup>[51]</sup> performed the Kyodai nitration of toluene and chlorobenzene in the presence of several solid catalysts, such as HZSM-5 and HBeta zeolites and montmorillonite K10. The reactions were carried out at -10 °C with liquid NO<sub>2</sub> and using dichloromethane as solvent. For the nitration of toluene, the presence of the catalyst does not influence the selectivity to the *para*-isomer giving results very similar to those of traditional nitration based on mixed acids (*o*:*p* ratio 1.3-1.4:1) or those of the Koydai nitration performed in the absence of solid catalyst (*o*:*p* ratio 1.5:1). However for the double nitration of toluene and chlorobenzene the system resulted highly selective towards to the formation of the 2,4-dinitro isomers, particularly with HBeta zeolite. Thus, using optimized amount of catalyst and solvent (acetonitrile), ratios of 2,4- to 2,6-isomers of 28:1 and 30:1 were obtained for the dinitration of toluene and chlorobenzene, respectively.

Recently, Claridge *et al.*<sup>[52,53]</sup> reported for the first time the use of dinitrogen pentoxide and zeolites as new nitrating system. The reaction of 2-NT with N<sub>2</sub>O<sub>5</sub> in dichloromethane at 0 °C was carried out in the presence of HZSM-5,



**Scheme 5.6**



HMordenite, HFaujasite-780, HFaujasite 720 and Na-Faujasite zeolites. Among the different catalysts, HFaujasite-720 was the most active and selective catalyst towards 2,4-dinitrotoluene, achieving a yield of dinitrotoluenes of 92 % with a ratio of 2,4- to 2,6- isomers of 4.3:1 in 3 min reaction time. Using this zeolite, 1-chloro-2-nitrobenzene and pyrazole were also nitrated regioselectively to obtain 1-chloro-2,4-dinitrobenzene in a 1-chloro-2,4-dinitro:1-chloro-2,6-dinitro ratio of 30:1, and 1,4-dinitropyrazole in 80 % yield, respectively. The authors proposed a nitration mechanism in which the protons in the zeolite are replaced by nitronium ions derived from  $N_2O_5$  in a fast pre-equilibrium process. This produces active sites for transfer of nitronium ion from faujasite to aromatic in the rate-controlling step.

### Nitric Acid as Nitrating Agent

As described above, nitrations conducted with nitric acid without removal of water are totally inhibited after some time on stream owing to a poisoning effect of the water present in the reaction mixture or formed during the reaction. Nitration of aromatics have been carried out with good success using nitric acid as the nitrating agent in the presence of clays and zeolites combined with the simultaneous distillation of the water produced. Choudary *et al.*<sup>[54–56]</sup> have performed the nitration of different aromatic compounds using 60 % nitric acid under reflux, and removing continuously the liberated water by means of a Dean–Stark trap. Different solid acid materials such as metal exchanged clays, HBeta, HY, HMordenite, TS-1 and HZSM-5 were tested as catalysts.  $Fe^{3+}$  montmorillonite catalyst was found to be highly active. For the nitration of benzene, mononitrobenzene was obtained selectively without formation of any di- or poly nitrobenzenes.<sup>[56]</sup> For the nitration of toluene, metal exchanged clays induce some shift in *para*-selectivity. However, zeolite HBeta (Si/Al=11) was found to be the best catalyst for the nitration of aromatic hydrocarbons to nitroaromatics in terms of yield and *para*-selectivity. Thus, during the nitration of toluene, yields of mononitro compounds of 96 % were obtained with a selectivity of 67 % toward the *para*-isomer (38 % selectivity is obtained using the classical mixed acid method). For cumene, chlorobenzene and anisole selectivities of 81, 90 and 75 %, respectively, were reported.<sup>[54]</sup> Moreover, zeolite HBeta catalyst showed consistent activity and selectivity even after five cycles.

Vassena *et al.*<sup>[18]</sup> reported the production of dinitrotoluenes from an equimolar mixture of 2-NT and 4-NT and nitric acid (65 wt%) by working under reduced pressure at 130 °C using a Dean–Stark trap. Zeolites (HBeta and Mordenite), Nafion, Deloxan and preshaped silicas impregnated with sulfuric acid were used as catalysts. Supported liquid acids exhibited the highest activity for the formation of dinitrotoluene giving 46 % yield after 3 h reaction time. However, they were not stable and a loss of the impregnated acid was observed. HBeta zeolite was less active than supported liquid acids, achieving a 20.1 % yield of dinitroluene, but gave an exceptionally high 2,4-dinitrotoluene selectivity (up to 94 %). Selectivities between 74 and 79 % were achieved with all other solids.

Nitroxyls are especially important because 4-amino-*o*-xylene (xyloidine), formed from 4-nitro-*o*-xylene (4-*o*-NX) upon reduction, is used as a starting material for the production of riboflavin. Nitration of *o*-xylene by the conventional mixed acid method gives a mixture of 4-*o*-NX 31–55 % and 3-*o*-NX 45–69 %.

Recently Milczak *et al.*<sup>[57]</sup> have reported the nitration of *o*-xylene using 100 % nitric acid over silica supported metal oxide solid acid catalysts with high yields (up to 90 %) but low selectivity to 4-*o*-NX (40–57 %). Choudary *et al.*<sup>[58,59]</sup> performed the nitration of *o*-xylene and other aromatic hydrocarbons by azeotropic removal of water over modified clay catalysts achieving low yields of 4-*o*-NX and a selectivity of 52 %. Better results were obtained when HBeta zeolite was used as catalyst, performing the reaction in dichloromethane at reflux temperature.<sup>[60]</sup> Conversions of 40 % and maximum selectivity 68 % of 4-*o*-NX were obtained. Similar conversions and higher selectivities for 4-*o*-NX (65–75 %) were reported by Rao *et al.*<sup>[61]</sup> using a nanocrystalline HBeta sample and working at 90 °C in the absence of solvent.

Nitrophenols are important intermediates for the manufacture of drugs and pharmaceuticals. *o*-Nitrophenol is an important starting material used in multiple step synthesis of valuable compounds. In the nitration of phenol using a mixture of nitric and sulfuric acid, the *o*:*p* nitration ratio changes from 2.4 to 0.9 over the 56–83 % H<sub>2</sub>SO<sub>4</sub> range.<sup>[62]</sup> However, polynitration is the main problem associated with the nitration of arenes with strongly activating groups, and this is a serious handicap for selective nitration.

Nitration of phenol has been performed using 100 % nitric acid over silica supported metal oxide solid acid catalysts<sup>[57]</sup> and acetyl nitrate preadsorbed on silica gel.<sup>[63]</sup> Recently Dagade *et al.*<sup>[64]</sup> have reported the nitration of phenol using diluted nitric acid (30 %) at room temperature using zeolites as acid catalysts (HZSM-5, HY, HBeta and La-HBeta). The effect of various solvents on the nitration of phenol was also studied. The results showed that the most active and selective catalyst was HBeta zeolite. Thus, using this zeolite and tetrachloromethane as a solvent, 93 % yield of nitrophenol with an *o*:*p* ratio of 8.70 was obtained within 2 h reaction time. This result was attributed to the preferred orientation of phenol inside the zeolite pores increasing the accessibility of the *ortho*-position to the nitronium ion, leading to selective formation of *o*-nitrophenol.

Phenol has also been nitrated regioselectively using fuming nitric acid inside the cages of alkali metal cation exchanged faujasite zeolites.<sup>[65,66]</sup> Thus, it was found that while nitration in the presence of CsY at 0–5 °C leads to phenol 100 % of phenol conversion with predominant formation of *p*-nitrophenol (*o*:*p* ratio 0.2:1), the solid state nitration (the phenol is adsorbed on the catalyst and fuming nitric acid is added) gives predominantly *o*-nitrophenol with a NaY zeolite. The relative yield of the nitrophenols and other by-products such as 2,4-nitrophenol depends on the loading level of the substrate inside the supercage. Exclusive *o*-isomer formation was observed when the loading level of phenol corresponded to eight molecules per supercage.

### 5.3.2 VAPOUR PHASE NITRATION

The nitration of aromatics in the vapour phase has two main advantages namely: the continuous removal/desorption of water; and the possibility to use a fixed bed reactor, which allows a continuous nitration process.

Nitration of benzene and toluene in the vapour phase using nitrogen dioxide and silica gel as acid catalysts was reported already in 1936 by McKee and Wilhelm.<sup>[67]</sup> More recently, zeolites have been used in the vapour phase nitration of aromatic compounds using dinitrogen tetroxide.<sup>[68–70]</sup> Germain *et al.*<sup>[68]</sup> studied the mechanism of the vapour phase mononitration of aromatics over silica-alumina and HBeta zeolite. The kinetic results did not agree with the classical electrophilic aromatic substitution<sup>[71]</sup> nor with the mechanism proposed by Malysheva *et al.*,<sup>[6]</sup> who suggested the formation of aromatic radicals that can recombine easily with the nitrogen dioxide radical to form nitroaromatics. Germain *et al.* proposed a one-electron transfer mechanism through the formation of an aromatic radical cation intermediate at the surface of the catalysts and the subsequent recombination of this radical cation with a nitrogen dioxide radical from the gas phase. HBeta zeolite proved to be an effective catalyst for nitration of various aromatic compounds, although a complete catalyst deactivation was observed after 30 min on stream at 140 °C when working with toluene. The addition of water in the feed inhibits the reaction when using the hydrophilic silica-alumina as a catalyst. However, over the HBeta zeolite an improvement of the efficiency of the catalyst was observed. This was attributed to a steam-cleaning effect of the strongly adsorbed products such as dinitroarenes. The same authors studied the vapour phase nitration of fluorobenzene with N<sub>2</sub>O<sub>4</sub> over zeolites with different structures (BEA, FAU, MOR, MFI) and aluminium contents.<sup>[69]</sup> It was found that the catalyst activity is determined by the acidity of the active sites. In all cases, *p*-nitrofluorobenzene was the predominant isomer (between 87 and 91 %), but no relation between the *para*-selectivity and the pore size of the catalyst was observed. HBeta zeolite showed the highest activity and stability, which was explained by its small particle size and adequate pore structure for this aromatic substitution.

Smith *et al.*<sup>[24]</sup> have investigated deactivation and shape-selectivity effects in toluene nitration in the vapour phase with NO<sub>2</sub> as nitrating agent using zeolites, MCM-41 and sulfated zirconia as catalysts. Almost all the catalysts exhibited deactivation over a period of about 5 h on stream, due mainly to coke formation.

Nitration of *o*-xylene with NO<sub>2</sub> has been performed in the gas phase over several zeolites (HBeta, HY, HZSM-5 and HMordenite), as well as on sulfuric acid supported on silica and sulfated zirconia at temperatures between 50 and 130 °C.<sup>[72]</sup> HBeta was found the most active and selective catalyst for the production of 4-*o*-NX giving ratios of 4-*o*-NX: 3-*o*-NX as high as 6:1, whereas no dinitro-*o*-xylene compounds were detected.

Bertea *et al.*<sup>[73–75]</sup> reported the vapour phase nitration of benzene with aqueous nitric acid (65 %) at 170 °C over post-synthetic dealuminated Y, ZSM-5 and Mordenite zeolites by high temperature and acid treatment. This treatment reduces the framework as well as the nonframework aluminium content, which results in

highly active and stable catalysts. Especially for the modified Mordenite, they reported a yield of nitrobenzene of 80 % with selectivities between 80 and 100 % and high space time yield ( $0.6 \text{ kg nitrobenzene kg}^{-1} \text{ catalyst h}^{-1}$ ).

Vapour phase nitration of benzene has been performed by Kuznetsova *et al.*<sup>[76]</sup> using 56 % nitric acid over HZSM-5 at 140–170 °C. Increase in the  $\text{HNO}_3$ /benzene ratio of the starting mixture was shown to increase the nitrobenzene yield achieving a yield of ca. 90 % for a feed ratio of 3.8. However, a fast deactivation of the catalysts due to strongly adsorbed species was observed. Benzene has also been nitrated with nitric acid (70 %) over acidic catalysts such as montmorillonite ion-exchanged with multivalent metal cation and metal oxides containing  $\text{TiO}_2$  or  $\text{ZrO}_2$  at temperatures between 140 and 160 °C.<sup>[77]</sup> Yields of nitrobenzene between 80 and 90 % were achieved, the most active catalyst being  $\text{Al}^{3+}$  montmorillonite. With this catalyst, no decay of the initial conversion of nitric acid (92.4 %) was observed even after 480 h on stream giving a space–time yield of  $0.64 \text{ kg nitrobenzene kg}^{-1} \text{ catalyst h}^{-1}$ .

Vassena *et al.*<sup>[18,34,78]</sup> reported the nitration of toluene in the vapour phase with 65 % nitric acid using HBeta, HMordenite, HZSM-5, HZSM-12, Deloxan and preshaped silica impregnated with sulfuric acid as acid catalysts, with the reaction temperature between 120 and 160 °C. Silica impregnated with sulfuric acid was the most active catalyst but a continuous loss of sulfuric acid with time on stream was observed. Zeolite HBeta exhibited a *p:o* ratio of nitrotoluenes higher than 1.1 during the first hours on stream. However, activity and selectivity to 4-NT decreased with time on stream (about 10 h) due to pore filling/blockage by strongly adsorbed products and by-products. HMordenite gave the same *p:o* ratio of nitrotoluenes than in absence of catalyst, whereas HZSM-5, HZSM-12 and Deloxan catalysts gave *p:o* ratios of nitrotoluenes close to 0.9 during the first hours on stream. The formation of dinitrotoluene was negligible with all solid acids tested. Dealumination of HBeta zeolite decreased the catalyst activity and the *para*-selectivity suggesting that catalytic activity was related to the concentration of acid sites. The enhanced *para*-selectivity appears to be originated by acid sites located inside the micropores of the catalyst and is most probably linked to steric hindrance induced by adsorption on the solid surface rather than to diffusion shape selectivity since 2-NT and 4-NT can easily diffuse through the pore system of Beta zeolite.

Regio-selective nitration of toluene to *p*-nitrotoluene has been reported using dilute  $\text{HNO}_3$  (20 %) over HBeta zeolite at 120 °C.<sup>[79]</sup> Maximum conversions of 55 % with 70 % selectivity to *p*-nitrotoluene and catalyst life of 75 h were obtained. The rate of deactivation of the catalyst increases with the concentration of the nitric acid, temperature and weight hourly space velocity (WHSV). Catalyst deactivation is mainly due to the partial blockage of the pores during the course of the reaction and the deposition of oxidation products, such as 4-nitrobenzoic acid, on the catalyst surface. However, although the catalyst deactivates, the selectivity for *p*-nitrotoluene is maintained. The molecular modelling study indicates that the *para*-selectivity is due to the faster diffusion of *para*-isomer in the pores of the catalyst.

Regioselective vapour phase nitration of *o*-xylene to 4-*o*-NX with dilute nitric acid (30 %) using HBeta catalyst at 150 °C has been reported.<sup>[80,81]</sup> Under these

reaction conditions a maximum conversion of 65 % with 60 % selectivity for 4-*o*-NX and a 4-*o*-NX:3-*o*-NX isomer ratio of 3:1 was obtained. Deactivation of the catalyst is observed after 78 h indicating the high stability of Beta zeolite. The authors found that deactivation is mainly due to the formation of oxidation products such as *o*-toluic acid, *o*-tolualdehyde and  $\alpha$ -methylphenyl nitromethane, which remain strongly adsorbed on the catalyst surface.

## 5.4 CONCLUSIONS

There is a strong incentive for the development of a continuous fixed bed catalytic process for regioselective nitration of aromatics. Solid acid catalysts are able to carry out the reaction, but, for most of them, selectivities are similar to those obtained using nitric acid plus sulfuric in homogeneous phase.

Fe<sup>3+</sup> and Al<sup>3+</sup> exchanged montmorillonites and zeolites appear to be suitable catalysts. Among those, Beta zeolites gives high activity and selectivity when using acid nitric as nitrating agent and acetic anhydride for trapping the water. In this case ratios of 2,4- to 2,6-dinitrotoluene isomers as high as 70:1 have been achieved. It appears that the shape selectivity observed in Beta for the *para*-isomer is better related to steric hindrance of the *ortho*-position induced by adsorption, rather than to diffusion shape selectivity. Such a specific adsorption could explain why very high *para*-selectivity is only found with Beta.

Nitrogen oxides and oxygen in combination with Beta zeolites give also high conversion but do not show a selectivity improvement with respect to the classical Kyodai nitration process. However, for the double nitration of toluene, Beta is very selective towards the 2,4-dinitro isomer.

Nitric acid can also be used as nitrating agent. In this case, water should be removed when working in the liquid phase. When working in the vapour phase, water is desorbed allowing the solid acid catalyst to run for long periods of time. Zeolites such as HZSM-5, HMordenite, HBeta and Al<sup>3+</sup> montmorillonite give good activity and regioselectivities with times of continuous operation as long as 480 h.

The problem associated with zeolites as nitration catalysts will be a reversible deactivation by coke deposition, and an irreversible deactivation by framework Al removal (acid leaching). Optimization of zeolite activity, selectivity and life will be controlled by density of acid sites, crystalline size and hydrophobic/hydrophilic surface properties.

## REFERENCES

1. Olah, G. A., Kuhn, S. J. *Friedel-Crafts and Related Reactions*, G. A. Olah (ed.). Wiley-Interscience, New York, **1964**.
2. Olah, G. A., Malhotra, R. and Narang, S. C. *Nitration. Methods and Mechanisms*, H. Feuer (ed.). VCH Publishers, New York, **1989**.

3. Ingold, C. K., *Structure and Mechanism in Organic Chemistry*. Cornell University Press, Ithaca, New York, **1969**.
4. Hoggett, J. G., Moodie, R. B., Penton, J. R. and Schofield, K. *Nitration and Aromatic Reactivity*. Cambridge University Press, London, **1971**.
5. Schofield, K. *Aromatic Nitration*. Cambridge University Press, Cambridge, **1980**.
6. Malysheva, L. V., Paukshtis, E. A. and Ione, K. G. Nitration of aromatics by nitrogen oxides on zeolite catalysts: comparison of reaction in the gas phase and solutions, *Catal. Rev. - Sci. Eng.*, **1995**, *37*, 179–226.
7. Kogelbauer, A. and Kouwenhoven, H. W. In *Nitration of Aromatic Compounds*, R. A. Sheldon and H. Van Bekkum (eds). Wiley-VCH, Weinheim, **2001**, pp. 123–132.
8. Evans, C. M., Practical considerations in concentration and recovery of nitration-spent acids. *ACS Symp. Ser.*, **1996**, *623*, 250–268.
9. Waller, F. J., Barrett, A. G. M., Braddock, D. C. and Ramprasad, D. Lanthanide(III) triflates as recyclable catalysts for atom economic aromatic nitration, *Chem. Commun.*, **1997**, 613–614.
10. Olah, G. A., Malhotra, R. and Narang, S. C. Aromatic-substitution. 43. Perfluorinated resinsulfonic acid-catalyzed nitration of aromatics. *J. Org. Chem.*, **1978**, *43*, 4628–4630.
11. Laszlo, P. Catalysis of organic reactions by inorganic solids. *Acc. Chem. Res.*, **1986**, *19*, 121–127.
12. Tapia, R., Torres, G. and Valderrama, J. A. Nitric acid on silica-gel – a useful nitrating reagent for activated aromatic compounds. *Synth. Commun.*, **1986**, *16*, 681–687.
13. Riego, J. M., Sedin, Z., Zaldivar, J. M., Marziano, N. C. and Tortato, C. Sulfuric acid on silica-gel: an inexpensive catalyst for aromatic nitration, *Tetrahedron Lett.*, **1996**, *37*, 513–516.
14. Smith, K., Fry, K., Butters, M. and Nay, B. Para-selective mononitration of alkylbenzenes under mild conditions by use of benzoyl nitrate in the presence of a zeolite catalyst, *Tetrahedron Lett.*, **1989**, *30*, 5333–5336.
15. Smith, K. Controlled organic synthesis with the aid of microporous solids, *Bull. Soc. Chim. Fr.*, **1989**, 272–278.
16. Corma, A. and Garcia, H. Organic reactions catalyzed over solid acids, *Catal. Today*, **1997**, *38*, 257–308.
17. Kogelbauer, A., Vassena, D., Prins, R. and Armor, J.N. Solid acids as substitutes for sulfuric acid in the liquid phase nitration of toluene to nitrotoluene and dinitrotoluene, *Catal. Today*, **2000**, *55*, 151–160.
18. Vassena, D., Kogelbauer, A. and Prins, R. Potential routes for the nitration of toluene and nitrotoluene with solid acids, *Catal. Today*, **2000**, *60*, 275–287.
19. Nagy, S. M., Yarovoi, K. A., Shakirov, M. M., Shubin, V. G., Vostrikova, L. A. and Ione, K. G. Nitration of aromatic compounds with benzoyl nitrate on zeolites, *J. Mol. Catal.*, **1991**, *64*, L31–L34.
20. Nagy, S. M., Yarovoy, K. A., Vostrikova, L. A., Ione, K. G. and Shubin, V. G. On the nature of zeolite catalyst effect on the selectivity of toluene nitration by acyl nitrates, *Stud. Surf. Sci. Catal.*, **1993**, *75*, 1669–1672.
21. Nagy, S. M., Yarovoy, K. A. Shubin, V. G. and Vostrikova, L. A. Selectivity of nitration reactions of aromatic compounds on zeolites H-Y and H-ZSM-11, *J. Phys. Org. Chem.*, **1994**, *7*, 385–393.
22. Rodrigues, J. A. R., Oliveira, A. P. and Moran, P. J. S. Regioselectivity of the mononitration of alkylbenzenes by immobilized acyl nitrates, *Synth. Commun.*, **1999**, *29*, 2169–2174.

23. Kwok, T. J., Jayasuriya, K., Damavarapu, R. and Brodman, B. W. Application of H-ZSM-5 zeolite for regioselective mononitration of toluene, *J. Org. Chem.*, **1994**, *59*, 4939–4942.
24. Smith, J. M., Liu, H. and Resasco, D. E. Deactivation and shape selectivity effects in toluene nitration over zeolite catalysts, *Stud. Surf. Sci. Catal.*, **1997**, *111*, 199–206.
25. Cornelis, A., Delaude, L., Gerstmans, A. and Laszlo, P. A procedure for quantitative regioselective nitration of aromatic-hydrocarbons in the laboratory, *Tetrahedron Lett.*, **1988**, *29*, 5909–5912.
26. Cornelis, A., Delaude, L., Gerstmans, A. and Laszlo, P. A procedure for quantitative regioselective nitration of aromatic-hydrocarbons in the laboratory, *Tetrahedron Lett.*, **1988**, *29*, 5657–5660.
27. Delaude, L., Laszlo, P. and Smith, K. Heightened selectivity in aromatic nitrations and chlorinations by the use of solid supports and catalysts, *Acc. Chem. Res.*, **1993**, *26*, 607–613.
28. Gigante, B., Prazeres, A. O. and Marcelocurto, M. J. Mild and selective nitration by claycop, *J. Org. Chem.*, **1995**, *60*, 3445–3447.
29. Smith, K., Musson, A. and G. A. DeBoos, Superior methodology for the nitration of simple aromatic compounds, *Chem. Commun.*, **1996**, 469–470.
30. Smith, K., Musson, A. and DeBoos, G. A. A novel method for the nitration of simple aromatic compounds, *J. Org. Chem.*, **1998**, *63*, 8448–8454.
31. Bourne, E. J., Stacey, M., Tatlow, J. C. and Tedder, J. M. Studies of trifluoroacetic acid. 5. Trifluoroacetic anhydride as a condensing agent in reactions of nitrous and nitric acids, *J. Chem. Soc.*, **1952**, 1695–1696.
32. Smith, K., Gibbins, T., Millar, R. W. and Claridge, R. P. A novel method for the nitration of deactivated aromatic compounds, *Perkin 1*, **2000**, 2753–2758.
33. Vassena, D., Kogelbauer, A. and Prins, R. Selective nitration of toluene with acetyl nitrate and zeolites, *Stud. Surf. Sci. Catal.*, **1999**, *125*, 501–506.
34. Vassena, D., Kogelbauer, A. and Prins, R. The highly selective conversion of toluene into 4-nitrotoluene and 2,4-dinitrotoluene using zeolite H-beta, *Stud. Surf. Sci. Catal.*, **2000**, *130A*, 515–520.
35. Haouas, M., Kogelbauer, A. and Prins, R. The effect of flexible lattice aluminum in zeolites during the nitration of aromatics, *Stud. Surf. Sci. Catal.*, **2001**, *135*, 2113–2120.
36. Haouas, M., Kogelbauer, A. and Prins, R. The effect of flexible lattice aluminum in zeolite beta during the nitration of toluene with nitric acid and acetic anhydride. *Catal. Lett.*, **2000**, *70*, 61–65.
37. Haouas, M., Bernasconi, S., Kogelbauer, A. and Prins, R. An NMR study of the nitration of toluene over zeolites by HNO<sub>3</sub>-Ac<sub>2</sub>O, *Phys. Chem. Chem. Phys.*, **2001**, *3*, 5067–5075.
38. Bernasconi, S., Pirngruber, G. D., Kogelbauer, A. and Prins, R. Factors determining the suitability of zeolite BEA as para-selective nitration catalyst. *J. Catal.*, **2003**, *219*, 231–241.
39. Bernasconi, S., Pirngruber, G. D. and Prins, R. Influence of the properties of zeolite BEA on its performance in the nitration of toluene and nitrotoluene, *J. Catal.*, **2004**, *224*, 297–303.
40. Suzuki, H. and Mori, T. Ozone-mediated nitration of chlorobenzene and bromobenzene and some methyl derivatives with nitrogen dioxide – High *ortho*-Directing trends of the chlorine and bromine substituents, *J. Chem. Soc., Perkin Trans. 2*, 479–484, **1994**.

41. Suzuki, H., Yonezawa, S., Nonoyama, N. and Mori, T. Iron(III)-catalysed nitration of non-activated and moderately activated arenes with nitrogen dioxide molecular oxygen under neutral conditions, *J. Chem. Soc., Perkin Trans. 1*, **1996**, 2385–2389.
42. Smith, K., Almeer, S. and Black, S. J. para-Selective nitration of halogenobenzenes using a nitrogen dioxide-oxygen-zeolite system, *Chem. Commun.*, **2000**, 1571–1572.
43. Smith, K., Almeer, S. and Peters, C. Regioselective mononitration of aromatic compounds by zeolite/dinitrogen tetroxide/air in a solvent-free system, *Chem. Commun.*, **2001**, 2748–2749.
44. Smith, K., Almeer, S., Black, S. J. and Peters, C. Development of a system for clean and regioselective mononitration of aromatic compounds involving a microporous solid, dinitrogen tetroxide and air. *J. Mater. Chem.*, **2002**, *12*, 3285–3289.
45. Peng, X., Suzuki, H. and Lu, C. Zeolite-assisted nitration of neat toluene and chlorobenzene with a nitrogen dioxide/molecular oxygen system. Remarkable enhancement of para-selectivity, *Tetrahedron Lett.*, **2001**, *42*, 4357–4359.
46. Peng, X., Fukui, N., Mizuta, M. and Suzuki, H. Nitration of moderately deactivated arenes with nitrogen dioxide and molecular oxygen under neutral conditions. Zeolite-induced enhancement of regioselectivity and reversal of isomer ratios, *Org. Biomol. Chem.*, **2003**, *1*, 2326–2335.
47. E. R. Ward and Hawkins, J. G. The nitration of Beta-nitronaphthalene, *J. Chem. Soc.*, **1954**, 2975–2975.
48. Mori T. and Suzuki, H. Ozone-mediated nitration of aromatic compounds with lower oxides of nitrogen (the Kyodai nitration). *Synlett*, **1995**, 383–392.
49. Suzuki, H., Tatsumi, A., Ishibashi, T. and Mori, T. Ozone-mediated reaction of anilides and phenyl esters with nitrogen dioxide – Enhanced *ortho*-reactivity and mechanistic implications. *J. Chem. Soc., Perkin Trans. 1*, **1995**, 339–343.
50. Suzuki, H. and Mori, T. Unusual isomer distribution of dinitrobenzenes and nitrophenols formed as side products during the ozone-mediated nitration of benzene with nitrogen dioxide – further evidence for the alternative mechanism of electrophilic nitration of arenes. *J. Chem. Soc., Perkin Trans. 2*, **1995**, 41–44.
51. Peng, X. and Suzuki, H. Regioselective double Kyodai nitration of toluene and chlorobenzene over zeolites. High preference for the 2,4-dinitro isomer at the second nitration stage, *Org. Lett.*, **2001**, *3*, 3431–3434.
52. Claridge, R. P., Llewellyn, Lancaster, N. Millar, R. W., Moodie, R. B. and Sandall, J. P. B. Zeolite catalysis of aromatic nitrations with dinitrogen pentoxide, *J. Chem. Soc., Perkin Trans. 2*, **1999**, 1815–1818.
53. Claridge, R. P., Lancaster, N. L., Millar, R. W., Moodie, R. B. and Sandall, J. P. B. Faujasite catalysis of aromatic nitrations with dinitrogen pentoxide. The effect of aluminum content on catalytic activity and regioselectivity. The nitration of pyrazole, *J. Chem. Soc., Perkin Trans. 2*, **2001**, 197–200.
54. Choudary, B. M., Sateesh, M., Lakshmi, Kantam, M. Koteswara Rao, K. Ram Prasad, K. V. Raghavan, K. V. and Sarma, J. A. R. P. Selective nitration of aromatic compounds by solid acid catalysts, *Chem. Commun.*, **2000** 25–26.
55. Choudary, B. M., Kantam, M. L. and Ramprasad, K. V. US Patent 6620981, **2002**.
56. Kantam, M. L., Sateesh, M., Choudary, B. M., Raghavan, K. V. K. K., Rao, EP0949240, 1999.
57. Milczak, T., Jacniacki, J., Zawadzki, J., Malesa, M. and Skupinski, W. Nitration of aromatic compounds on solid catalysts, *Synth. Commun.*, **2001**, *31*, 173–187.



58. Choudary, B. M., Sateesh, M., Kantam, M. L., Rao, K. K., Prasad, K. V. R., Raghavan, K. V. US Patent 6034287, **1998**.
59. Choudary, B. M., Kantam, M. L., Sateesh, M., Rao, K. K., Raghavan, K. V., US Patent 6376726, **1998**.
60. Choudary, B. M., Kantam, M. L., Kumar, N. S., Prasad, K. V. R., Raghavan, K. V. EP Patent 1323705, **2001**.
61. Rao, K. K., Rao, B. P. C., Choudary, B. M., Mannepalli, L. K., Kondapuram, V. R. WO Patent 2004050555, **2002**.
62. Coombes, R. G., Golding, J. G. and Hadjigeorgiou, P. Electrophilic aromatic substitution. Part 23. The nitration of phenol and the cresols in aqueous sulfuric acid, *J. Chem. Soc., Perkin Trans.* **1979**, 2, 1451–1459.
63. Rodrigues, J. A. R., de Oliveira, A. P., Moran, P. J. S. and Custodio, R. Regioselectivity of the nitration of phenol by acetyl nitrate adsorbed on silica gel, *Tetrahedron*, **1999**, 55, 6733–6738.
64. Dagade, S. P., Kadam, V. S. and Dongare, M. K. Regioselective nitration of phenol over solid acid catalysts, *Catal. Commun.*, **2002**, 3, 67–70.
65. Esakkidurai, T. and Pitchumani, K. Zeolite-mediated regioselective nitration of phenol in solid state, *J. Mol. Catal: Chemical A*, **2002**, 185, 305–309.
66. Esakkidurai, T., Kumarraja, M. and Pitchumani, K. Regioselective nitration of aromatic substrates in zeolite cages, *Proc. Indian Acad. Sci., Chem. Sci.*, **2003**, 115, 113–121.
67. McKee, R. H. and Wilhelm, R. H. Catalytic Vapour phase nitration of benzene, *J. Ind. Eng. Chem.*, **1936**, 28, 662–667.
68. Germain, A., Akouz, T. and Figueras, F. Vapour-phase aromatic nitration with dinitrogen tetroxide over solid acids: kinetics and mechanism, *J. Catal.*, **1994**, 147, 163–170.
69. Germain, A., Akouz, T. and Figueras, F. Vapour-phase nitration of fluorobenzene with N<sub>2</sub>O<sub>4</sub> over aluminosilicates. Effects of structure and acidity of the catalyst, *Appl. Catal., A*, **1996**, 136, 57–68.
70. Schumacher, I., EP Patent 53031, **1981**.
71. Salakhutdinov, N. V., Ione, K. G., Kobzar, E. A. and Malysheva, L. V. Gas-phase nitration of aromatic compounds by nitrogen dioxide on zeolites, *Zh.I Org. Khim.*, **1993**, 29, 546–558.
72. Landau, M. V., Kogan, S. B., Tavor, D., Herskowitz, M. and Koresh, J. E. Selectivity in heterogeneous catalytic processes, *Catal. Today*, **1997**, 36, 497–510.
73. Berteau, L. E., Kouwenhoven, H. W. and Prins, R. Vapor-phase nitration of benzene over modified mordenite catalysts, *Appl. Catal., A*, **1995**, 129, 229–250.
74. Berteau, L. E., Kouwenhoven, H. W. and Prins, R. Vapour-phase nitration of benzene over zeolitic catalysts, *Stud. Surf. Sci. Catal.*, **1994**, 84, 1973–1980.
75. Berteau, L. E., Kouwenhoven, H. W. and Prins, R. Catalytic vapour-phase nitration of benzene over modified Y zeolites: influence of catalyst treatment, *Stud. Surf. Sci. Catal.*, **1993**, 78, 607–614.
76. Kuznetsova, T. G., Ione, K. G. and Malysheva, L. V. Gas phase nitration of benzene by nitric acid on ZSM-5 zeolite, *React. Kinet. Catal. Lett.*, **1998**, 63, 61–66.
77. Sato, H., Hirose, K., Nagai, K., Yoshioka, H. and Nagaoka, Y. Vapour phase nitration of benzene over solid acid catalysts II. Nitration with nitric acid (1); montmorillonite and mixed metal oxide catalysts, *Appl. Catal., A*, **1998**, 175, 201–207.
78. Vassena, D., Malossa, D., Kogelbauer, A. and Prins, R. In *Zeolites as Catalysts for the Selective p-Nitration of Toluene*, M. M. J. Treacy, B. K. Marcus, M. E. Bisher, J. B. Higgins (eds). Materials Research Society, Warrendale, PA, **1999**, pp. 1471–1476.

79. Dagade, S. P., Waghmode, S. B., Kadam, V. S. and Dongare, M. K. Vapour phase nitration of toluene using dilute nitric acid and molecular modeling studies over beta zeolite, *Appl. Catal., A*, **2002**, 226, 49–61.
80. Dongare, M. K., Patil, P. T. and Malshe, K. M., US 2004192977, **2003**.
81. Patil, P. T., Malshe, K. M., Dagade, S. P. and Dongare, M. K. Regioselective nitration of *o*-xylene to 4-nitro-*o*-xylene using nitric acid over solid acid catalysts. *Catal. Commun.*, **2003**, 4, 429–434.



---

# 6 Oligomerization of Alkenes

---

AVELINO CORMA AND SARA IBORRA

*Instituto de Tecnología Química, UPV, Av. Naranjos s/n, E-46022 Valencia, Spain*

## CONTENTS

6.1 INTRODUCTION . . . . .	125
6.2 REACTION MECHANISMS . . . . .	126
6.3 ACID ZEOLITES AS CATALYSTS FOR OLIGOMERIZATION OF ALKENES . . . . .	127
6.3.1 Medium pore zeolites: influence of crystal size and acid site density . . . . .	127
6.3.2 Use of large pore zeolites . . . . .	130
6.3.3 Catalytic membranes for olefin oligomerization . . . . .	131
6.4 MESOPOROUS ALUMINOSILICATES AS OLIGOMERIZATION CATALYSTS . . . . .	131
6.5 NICKEL SUPPORTED ALUMINOSILICATES AS CATALYSTS . . . . .	132
REFERENCES . . . . .	136

## 6.1 INTRODUCTION

The oligomerization of alkenes to a variety of higher weight homologues is an important and extensively studied area of petroleum chemistry because it represents a route to the production of motor fuels, lubricants, plasticizers, pharmaceuticals, dyes, resins, detergents and additives. Oligomerization generally refers to the production of molecules formed by only a relatively few monomers units ( $2 > n > 100$ ,  $n$  being the number of reacting molecules), while polymerization implies the production of high molecular weight compounds ( $n > 100$ ). The oligomerization of alkenes is a catalysed reaction which involves two main classes of heterogeneous catalysts: acid catalysts (especially zeolites) and supported nickel catalysts.

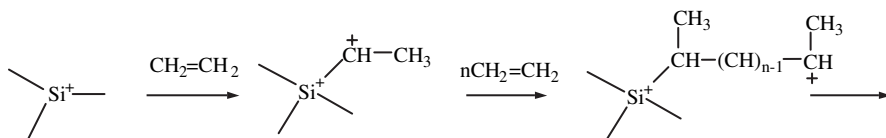
The technology for light alkene oligomerization via acid catalysis goes back to the 1930s with the commercialization of a process developed by Universal Oil Products (UOP) to convert propene/butene mixtures over supported phosphoric acid into gasoline-range iso-olefins ( $C_6$ – $C_{10}$ ).<sup>[1–5]</sup> The main disadvantages of UOP's catalyst are: short catalyst life, lack of any possibility to tailor the catalyst properties to product demand, problems for catalyst discharging from the reactor and environmental issues related to disposal. Owing to these problems, other solid acid

catalysts, such as zeolites, were investigated. Development in zeolite catalysis resulted in the MOGD process (Mobil Olefin to gasoline and distillate), which converts light olefins to gasoline and diesel fuel using a ZSM-5 zeolite as catalyst.<sup>[6-8]</sup> Today, oligomerization of light alkenes represents an important route for production of high-octane liquid fuels. Extensive reviews concerning the oligomerization of olefins in homogeneous media have been reported.<sup>[9,10]</sup> Homogeneous and heterogeneous catalysis have been reviewed by O'Connor *et al.*<sup>[11-13]</sup>, more recently Sanati *et al.*<sup>[14]</sup> have reviewed the use of heterogeneous catalyst for the oligomerization of alkenes. In this chapter, we will discuss recent research on the application of acid zeolites, mesoporous aluminosilicates and Ni supported aluminosilicates as catalysts in olefin oligomerization.

## 6.2 REACTION MECHANISMS

Acid-catalysed alkene oligomerization can be rationalized by means of carbocation chemistry. The reaction occurs in several steps: (1) protonation of an alkene and formation of an alkylcarbenium ion; (2) addition of a second alkene to the alkylcarbenium ion (propagation); and (3) deprotonation.<sup>[9]</sup> When the rate constants for the propagation and deprotonation have similar values oligomers are formed, while when the rate constant for propagation is higher than the rate of deprotonation, polyolefins will be formed. The oligomerization reactions are often accompanied by other reactions, such as skeletal and double bond isomerization, disproportionation via the carbenium ion intermediate, methyl and hydrogen transfer, cyclization, cracking and aromatization giving in addition to oligomers, aromatics, coke and saturated hydrocarbons.<sup>[13,15-18]</sup> The extent to which such accompanying reactions take place depends on both the nature of the catalyst and the reaction conditions.

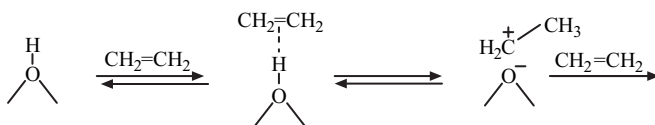
Reaction mechanisms have been proposed for oligomerization of olefins that involve a cationic mechanism initiated by Lewis or Brønsted acid sites.<sup>[19]</sup> In the first case, a cationic intermediate is formed and the products obtained are mainly branched oligomers (Scheme 6.1).



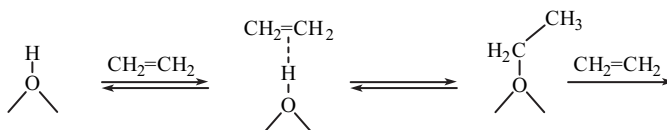
**Scheme 6.1**

In the case of Brønsted acidity, two reaction mechanisms have been suggested: the formation of carbenium ion intermediate species (Scheme 6.2), which lead to the formation of branched oligomers<sup>[20]</sup> and the formation of a surface alkoxy structure intermediate, which leads to the formation of linear oligomers<sup>[19]</sup> (Scheme 6.3). In this case, the formation of alkoxy species has been recently

proved by an *in situ* EXAFS study of the Al K edge for ethene adsorbed on a zeolite.<sup>[21]</sup>

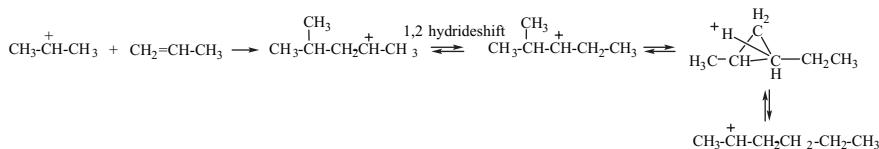


**Scheme 6.2**



**Scheme 6.3**

A fourth mechanism has been suggested by several researchers in order to explain the formation of near-linear polyethylene type oligomers produced on modified<sup>[22]</sup> and unmodified<sup>[23]</sup> ZSM-5 zeolite from olefins such as propene, isobutene and 1-decene. They propose a mechanism which proceeds by losing methyl branches via protonated cyclopropyl intermediates as presented in Scheme 6.4.



**Scheme 6.4**

## 6.3 ACID ZEOLITES AS CATALYSTS FOR OLIGOMERIZATION OF ALKENES

### 6.3.1 MEDIUM PORE ZEOLITES: INFLUENCE OF CRYSTAL SIZE AND ACID SITE DENSITY

An advantage of zeolite-based olefin oligomerization routes is that only minimal olefin feed purification is required. Compared with the commonly employed supported phosphoric acid catalyst, zeolites also have the advantage of being stable over a wide range of temperature and, thus, being regenerable. However, the main drawback of zeolites is their high deactivation rate. Deactivation is due to coke deposition, which forms either during subsequent oligomerization and hydrocarbon dehydrogenation reactions, or from catalytic cracking of long chain species.<sup>[24]</sup>

The oligomerization of light olefins such as ethylene for the production of synthetic fuels using zeolites as catalysts has been extensively studied.<sup>[25–28]</sup> In general, it has been found that the rate of oligomerization of ethylene over ZSM-5 zeolite is slower compared with other olefins and higher reaction temperatures are necessary. The catalytic performance of this reaction is related to the nature and number of acid sites of the zeolite.

Kustov *et al.*<sup>[19]</sup> found that linear oligomers are mainly formed using zeolites with high Si/Al ratios possessing strong Brønsted acid sites and it was assumed that the ethoxy groups were the intermediates species in ethylene oligomerization. IR spectroscopic studies<sup>[19]</sup> showed that the degree of product branching was not restricted by the size of the cavities and channels in the zeolites, in contrast to the findings of Miller.<sup>[17]</sup> The oligomerization of ethylene in large (150 μm) crystals of HZSM-5 has been studied by <sup>13</sup>C NMR, FTIR microscopy and Raman microscopy.<sup>[29]</sup> The authors conclude that the degree of branching and average chain length depends on the density of Brønsted acid sites in the crystal. At the outer edges of the crystals there is a high density of Brønsted acid sites, which produces short chain highly branched oligomers, whereas in the interior of the crystals long chain linear oligomer is formed. The dependence of chain branching on acid site density may explain differences in the literature as to the extent of chain branching during formation of ethene oligomers in ZSM-5 zeolite.

The role of Brønsted acid sites in the oligomerization of ethylene over HZSM-5 has been studied.<sup>[30,31]</sup> Amin and Anggoro<sup>[31]</sup> concluded that dealumination of HZSM-5 led to higher ethylene conversion, but the gasoline selectivity was reduced compared with a nondealuminated HZSM-5 (Si/Al = 15) zeolite sample.

The catalytic properties of the external and internal surface sites in zeolites for olefin oligomerization have been extensively studied.<sup>[28,32–34]</sup> It has been found that for zeolites having an internal/external surface area ratio higher than 300, the contribution of external active sites to the reaction is practically negligible, while for small zeolite crystallites (<100) the external active sites become important for reactions which are highly limited by diffusion. In addition, shape selectivity decreases when increasing external surface area, and more C<sub>9</sub>+ aromatic hydrocarbons are formed. Also, coke formation is less favoured on the external than on the internal surface; small zeolite crystals give longer catalyst lifetime.

Propene oligomerization leads to different products using the same catalyst but varying the reaction conditions. Thus, at moderate temperature and relatively high pressure the reaction conditions favour the formation of products with boiling point of at least 438 K. However, at elevated temperatures and moderate total pressure (from atmospheric to about 5.5 MPa) the gasoline range (C<sub>5</sub>–C<sub>10</sub>) is formed.<sup>[14]</sup>

Martens *et al.*<sup>[35]</sup> showed that HZSM-22 synthesized in a pure form with controlled crystal size is a promising catalyst for the oligomerization of propene to C<sub>6</sub>–C<sub>12</sub> olefins. It was found that the reaction occurs at or near the outer surface and the products formed are mainly dimers. In addition, an increase of the linearity of the oligomers as compared with HZSM-5 or solid phosphoric acid was found. It was tentatively proposed that active sites located at the pore mouths are responsible for this shape selective effect.

Among all the zeolitic systems, HZSM-5 zeolite has been the catalyst most extensively studied for the oligomerization of light alkenes, and in fact it is the most utilized zeolite, since it is the catalyst for the MOGD process.<sup>[8]</sup> It is widely accepted that Brønsted acid sites inside the channels of HZSM-5 are responsible for the production of linear oligomers, while acid sites existing on the outer surface produced more branched products. Thus, by decreasing the external acidity of HZSM-5 zeolite an increase of more linear products (with higher viscosity index and higher cetane number) can be obtained.<sup>[22,36,37]</sup> Deactivation of surface acidity of HZSM-5 has been achieved by treatment of the catalyst surface with bulky amines such as 4-methylquinoline<sup>[37]</sup> and 2,6-di-*tert*-butyl pyridine<sup>[22]</sup> and in both cases relatively linear oligomers have been obtained from propene and other alkenes. Also, the medium pore zeolite HZSM-23 has been used as a catalyst, following previous surface deactivation with 2,4,6-collidine, for oligomerization of propene<sup>[36]</sup> and C<sub>2</sub>-C<sub>6</sub> olefins<sup>[38,39]</sup> yielding C<sub>12</sub>+ olefins useful as alkylating agents for the preparation of surfactants. The surface acidity of HZSM-23, HZSM-22 and HZSM-35 was reduced with oxalic acid, and when the catalysts were used in the oligomerization of propene they yielded almost linear oligomers.<sup>[40]</sup>

HZSM-5 zeolite has a strong activity for hydrogen transfer, that produces the partial hydrogenation of olefins to the corresponding alkanes (while forming aromatics with cyclic products), resulting in a decrease of the selectivity to gasoline range hydrocarbons. In order to modify strong acid sites in HZSM-5 and to introduce new catalytic function, isomorphous substitution of various kinds of transition metal elements by aluminium has been studied. It has been found that HFe-silicalite<sup>[41-44]</sup> and HCo-silicalite<sup>[41,44]</sup> could convert light olefins completely into high octane-number gasoline with high space-time yield. For instance 95 % propylene can be converted mainly into branched olefins with a smaller fraction of aromatics with a space-time yield of 8.09 kg L<sup>-1</sup>h<sup>-1</sup>.

Zeolites have been intensively studied in butene oligomerization. For instance, the oligomerization of mixed butenes, diluted with butanes over ZSM-22 zeolite with high Si/Al ratio gives oligomers with a reduced degree of branching.<sup>[45]</sup> Chen and Bridger<sup>[22]</sup> reported that HZSM-5, surface deactivated with 2,6-di-*tert*-butyl pyridine produces synthetic oils with a high viscosity index. The formation of linear oligomers was explained by the formation of a protonated cyclopropyl intermediate as explained before.

C<sub>6</sub>-C<sub>12</sub> alkenes are important intermediates used in industry to synthesize plasticizer and surfactant alcohol derivatives through hydroformylation. The oligomerization of 2-butene as well as binary mixtures of alkenes has recently been studied over HZSM-57 zeolite by Martens *et al.*<sup>[46]</sup> in order to produce this type of olefin. They compared the activity and selectivity of HZSM-57 with other medium pore zeolites of different topologies (HZSM-48, HBeta, HFerrierite, HSAPO-11, HZSM-11, HZSM-22, HMCM-22 and HZSM-5). It was found that HZSM-57 catalyst gave a butene conversion of 89 % at 353 K, while with the other zeolites higher temperatures of 383-483 K were necessary to achieve similar conversions. Moreover, HZSM-57 combined high activity with high selectivity for C<sub>8</sub> alkenes,



while C<sub>12</sub> alkenes were formed in minor amounts. The other catalysts tested were substantially less selective for C<sub>8</sub>. The oligomerization behaviour of HZSM-57 was rationalized by molecular modelling and repulsion energy calculations. In addition, the authors found, by working with binary alkene mixtures, that on using HZSM-57 zeolite as catalyst the molecular weight of the oligomers can be tailored by mixing the appropriate short alkenes.

### 6.3.2 USE OF LARGE PORE ZEOLITES

Occelli *et al.*<sup>[18]</sup> have studied the activity of different zeolites for high pressure propene oligomerization (HZSM-5, HBoralite, HOfretite, HY, HMordenite and HOmega). Working at weight hourly space velocity (WHSV) of 1 h<sup>-1</sup> and 4.8 MPa, they found that HY zeolite was active at 313 K. The activity of HOmega and HOfretite increases with increasing reaction temperature (from 473 to 623 K and from 423 to 523 K, respectively). HZSM-5 showed poor activity below 573 K, while HBoralite, under similar reaction conditions, achieved total conversion. Finally, HMordenite gave low conversion of propene below 523 K which was attributed to deactivation by strong adsorption of reactants and/or products at low temperature. In addition, it was found that the degree of chain branching (calculated from <sup>1</sup>H and <sup>13</sup>C NMR spectra) depends on the pore size of the zeolite and decreases following the order: Omega > HY > Mordenite > ZSM-5 > Ofretite > Boralite.<sup>[18,47]</sup>

Oligomerization of butene over HMordenite has been carried out at 5 MPa and 523 K. The reaction gave mainly dimers and trimers with a minor fraction of tetramers and pentamers.<sup>[13]</sup> In contrast, oligomerization of butene over solid phosphoric acid catalyst gave mainly dimers.

Oligomerization of 1-butene adsorbed over HBeta, HMCM-22 and HMordenite has been followed by *in situ* FTIR spectroscopy.<sup>[48]</sup> The authors found that 1-butene oligomerizes instantaneously at 300 K. Mechanistic details were provided by *in situ* IR measurements. At low temperatures, 1-butene forms a transient H-bonded precursor with the acid sites of the zeolites prior to oligomerization. The strength of the H-bonded precursor seems to be very similar in the three zeolite structures, which suggests that the Brønsted acid sites have similar acidities in the three samples. The concentration of these adducts soon reaches a maximum when the temperature is raised, and decreases to zero as the oligomerization reaction proceeds. It was also observed that adducts accumulate fastest over HBeta zeolite indicating that there is a diffusion-limited oligomerization in the case of HMCM-22 and HMordenite. Furthermore, it was found that the accessibility of monomers is not rate-limiting for the oligomerization reaction in the HBeta zeolite, and that the oligomerization reaction is not diffusion-limited at temperatures up to 300 K. The lengths of the oligomeric chains turned out to be dependent on zeolite topology. Thus, the chain grows most extensively in the three-dimensional HBeta zeolite.

### 6.3.3 CATALYTIC MEMBRANES FOR OLEFIN OLIGOMERIZATION

Materials based on composite materials made with porous inorganic membranes and catalytic active components confined within the porous system of the membrane are being developed. With a membrane it becomes possible to combine selective diffusion and catalytic reaction effects. Recently Torres *et al.*<sup>[49]</sup> have reported the synthesis of Beta zeolite films on a ceramic membrane support ( $\gamma$ -Al<sub>2</sub>O<sub>3</sub>) and their use as catalysts for the oligomerization of isobutene. The membrane was used as a thin catalytic layer and the reactants were forced to permeate through. The authors found that the membrane does not provide any separation function, but it can be used as an efficient contact medium for controlling short residence times. This advantage allows the selectivity towards C<sub>8</sub> alkenes to be enhanced, while limiting the fraction of products in the C<sub>12</sub>–C<sub>16</sub> olefins range. The authors obtained yields for C<sub>8</sub> alkenes close to 60% above 370 K. In addition, the Beta zeolite membrane reactor showed no deactivation and was shown to be chemically and thermally stable for reuse.

## 6.4 MESOPOROUS ALUMINOSILICATES AS OLIGOMERIZATION CATALYSTS

The textural and acidic characteristics of mesoporous acid catalyst have opened new perspectives for the synthesis and conversion of large molecules unable to enter the micropores of zeolites. These materials have shown excellent activities and selectivities into gasoline and middle distillates in the oligomerization of light olefins. Bellusi *et al.*<sup>[50]</sup> described the use of a mesoporous silica alumina of large surface area and narrow pore diameter distribution as a catalyst in the oligomerization of propylene. The product obtained contains a gasoline fraction (boiling point between 353 and 448 K) of high octane number and a higher molecular weight hydrocarbon fraction (boiling point between 448 and 633 K) and does not contain aromatics. The reaction temperature was much lower (between 393 and 473 K) than that required for zeolite catalyst (above 523 K).

A catalyst based on the mesoporous molecular sieve MCM-41 aluminosilicate has been used for the oligomerization of propene and butenes<sup>[51–53]</sup> at low temperatures (between 353 and 473 K). The catalyst shows higher activity and selectivity for the formation of trimers and tetramers as compared with HZSM-5 and HZSM-23.

Kim and Inui<sup>[54]</sup> have reported the synthesis of MCM-41 with incorporation of various metal components such as Al, Ga or Fe with different Si/metal ratio. These catalysts were used for the oligomerization of propene, and it was found that the order of activity was: Al-MCM-41 > Fe-MCM-41 > Ga-MCM-41 with the optimum Si/metal ratio being equal to 200. The propene conversion increases with the temperature from 423 up to 523 K. The catalytic activity of mesoporous silicates was lower than zeolitic catalysts, such as MFI metallosilicates. However,

mesoporous silicates were able to produce a considerable amount of oligomers (in the gasoline range) from propene even at the lower temperature range, which was due to the limited geometrical restrictions existing within the pore size of these materials.

A thermodynamic and kinetic study of the oligomerization of propylene over mesoporous silica alumina has been reported by Peratello *et al.*<sup>[55]</sup> Considering that the rate determining step is the reaction between an adsorbed molecule of propylene over a surface site and another molecule coming from the gaseous phase, it was found that the reaction rate of oligomerization catalysed by the mesoporous silica alumina can be described by a Langmuir–Hinshelwood–Hougen–Watson kinetic model. Considering the activation energy value ( $18 \text{ kJ mol}^{-1}$ ) along with catalytic results, it was suggested that the propylene oligomerization is limited by mass transfer inside the mesopores of the catalyst.

Chiche *et al.*<sup>[56]</sup> have studied the oligomerization of butene over a series of zeolite (HBeta and HZSM-5), amorphous silica alumina and mesoporous MTS-type aluminosilicates with different pores. The authors found that MTS catalyst converts selectively butenes into a mixture of branched dimers at 423 K and 1.5–2 MPa. Under the same reaction conditions, acid zeolites and amorphous silica alumina are practically inactive due to rapid deactivation caused by the accumulation of hydrocarbon residue on the catalyst surface blocking pores and active sites. The catalytic behaviour observed for the MTS catalyst was attributed to the low density of sites on their surface along with the absence of diffusional limitations due to an open porosity. This would result in a low concentration of reactive species on the surface with short residence times, and favour deprotonation and desorption of the octyl cations, thus preventing secondary reaction of the olefinic products.

Diesel fuel obtained by oligomerization of light olefins has the advantage of the absence of sulfur and aromatics. Catani *et al.*<sup>[57]</sup> have recently reported the use of mesoporous aluminosilicates (MCM-41) as efficient catalysts for the synthesis of clean diesel fuels. MCM-41 samples with different Si/Al ratios were investigated in the oligomerization of ethene,  $\text{C}_4$  and  $\text{C}_5$  olefins. While almost no conversion occurred with ethylene, very good catalytic performances in terms of activity and selectivity to diesel range were obtained with  $\text{C}_4$  and  $\text{C}_5$  olefins. An optimum for catalytic performance was found for a sample with Si/Al ratio of 20. Moreover, catalytic activity was also favoured by increasing pressure, temperature and contact time. It was found that the presence of small amounts of metal (Ni, Rh or Pt) inside the mesoporous structure did not significantly modify the catalytic activity. In addition, the authors propose a new algorithm to calculate the cetane number.

## 6.5 NICKEL SUPPORTED ALUMINOSILICATES AS CATALYSTS

Propylene and other olefins of higher molecular weight can be easily oligomerized over a wide range of zeolitic and nonzeolitic acid catalysts.<sup>[11,14]</sup> However, in the case of ethylene only low conversions can be obtained over acidic catalysts. Transition metal catalysts, on the other hand, and particularly those based on Ni

are active for both ethylene dimerization and oligomerization.<sup>[9,10,58]</sup> In homogeneous catalysis, the oligomerization of olefins using Ni-complex catalysts has already been achieved in several processes with industrial application, such as Dimersol (IFP)<sup>[59–61]</sup> for conversion of propenes and butenes into hexenes, heptenes and octenes and SHOP (Shell)<sup>[62]</sup> where ethylene is converted to highly linear oligomers (C<sub>4</sub>–C<sub>20</sub>). On the other hand, heterogeneous Ni catalysts can be prepared by techniques such as ion-exchange, impregnation, coprecipitation and even from decomposition of organometallics pre-deposited on the support. These supports include silica alumina, silica, layered and mesoporous aluminosilicates and zeolites.

Ni-modified zeolites have extensively been used for the oligomerization of ethene.<sup>[27,63–67]</sup> Ethylene is relatively unreactive at low temperatures over HZSM-5 and temperatures higher than 523 K are necessary in order to enhance the activity. However, it was found that Ni-exchanged ZSM-5 can be used to oligomerize ethylene at 373 K.<sup>[68]</sup> In general it is accepted that isolated Ni<sup>+</sup> species are the active metal sites involved in the oligomerization reaction.<sup>[64,69,70]</sup> It has been reported that the ethylene oligomerization activity of the Ni-exchanged silica alumina is proportional to the acid strength of the surface.<sup>[65,71]</sup> Ng and Creaser<sup>[65]</sup> suggested that the Ni<sup>+</sup>-H<sup>+</sup> couple is involved in the oligomerization mechanism of ethylene. More recently, Davydov *et al.*<sup>[69]</sup> showed that the presence of acid sites plays an essential role promoting the Ni<sup>2+</sup>/Ni<sup>+</sup> redox cycle and stabilizing the Ni<sup>+</sup> ion active sites involved in the ethylene oligomerization.

Miller<sup>[72]</sup> has described a process for the production of hydrocarbons in the lube base stock range. The process involves the use of a Ni-ZSM5 zeolite as catalyst for dimerization of C<sub>5</sub>–C<sub>11</sub> olefins into a first product containing C<sub>10</sub>–C<sub>22</sub> olefins. This first product is subjected to an additional dimerization step, using the same or similar catalyst giving a second product that includes hydrocarbons in the lube base stock range.

Ethylene oligomerization over Ni and Pd zeolites has been reported by Lapidus and Krylova.<sup>[73]</sup> It was found that NiCaX exhibited high selectivity for ethylene dimerization at 508 K. The highest activity and selectivity were achieved with a sample with a Ni content of 2.5 wt%, *trans*-2-butene being the major product. PdCaX also shows excellent selectivity to *trans*-2-butene, giving 65 % selectivity for a total yield of the C<sub>4</sub> fraction of 78 %.

Unfortunately most of these catalysts based on zeolites suffered a severe deactivation during the oligomerization reactions mainly due to the blocking of micropores with heavy compounds.<sup>[27,65,66]</sup> It was found that the formation of heavy products is due to further transformation of primary oligomers on strong acid sites. Therefore one of the approaches to overcome these problems has been the use of catalysts with larger pores and tunable acidity, under mild oligomerization conditions. It has been reported that catalyst based on Ni(II) ion-exchanged silica alumina<sup>[71,74,75]</sup> are very stable and possessed high initial activity for the oligomerization of ethylene. These catalysts required no pre-reduction as is necessary, for example, for the Ni/SiO<sub>2</sub> type systems<sup>[76]</sup> and are able to perform the oligomerization of ethylene to C<sub>4</sub>–C<sub>20</sub> products at low temperature and high pressure.<sup>[77]</sup>

Working in a fixed bed flow reactor, at 393 K, 3.5 MPa and WHSV of  $2 \text{ h}^{-1}$  the conversion of ethylene typically reaches 97–99 % with a selectivity to product with an even number of carbon atoms of 97 %. In addition, it was found that these type of catalysts were very stable when in use showing no detectable loss of activity after 108 days on stream under the reaction conditions employed. More recently, Heydenrych *et al.*<sup>[78]</sup> have performed the oligomerization of ethylene in a slurry reactor using Ni(II)-exchanged silica alumina, in order to determine the intrinsic kinetics of oligomerization, the product spectrum, and the stability of the catalyst under the slurry system. The authors found that the rate of consumption of ethylene is dependent on the rate of ethylene dimerization and on the rate of reaction between ethene and product oligomers. Thus, the rate of ethylene oligomerization (at 393 K and 3.5 MPa) obtained with a Ni silica alumina (1.56 wt% of Ni) was  $11.5 \text{ g g}^{-1} \text{ catalyst h}^{-1}$ . Very little deactivation of the catalyst was observed after 900 h of time on stream, with conversions being maintained at over 90 % and giving oligomers up to  $\text{C}_{16}$ . These catalysts can also be successfully used for the oligomerization of propene and butene.<sup>[79]</sup>

Sakaguchi *et al.*<sup>[80]</sup> have reported that combined use of Ni-silica alumina and  $\text{BPO}_4$  is more effective promoting the oligomerization of ethylene than Ni silica alumina alone. An increased  $\text{C}_6$  fraction and an equilibrium mixture of *n*-butene was formed as  $\text{C}_4$  products using the catalyst combination, whereas on Ni-silica alumina alone 1-butene was mainly obtained.

The selective formation of 1-alkenes, such as 1-hexene, is important because they are valuable chemical feedstocks (e.g. for use as co monomers in alkene polymerization processes). Recently Nicolaides *et al.*<sup>[81]</sup> have studied the possibility of controlling the formation of 1-alkene products in the oligomerization of ethene using Ni-silica alumina catalysts. The aim was to reduce the relatively high rate of double bond isomerization which leads to the formation of internal alkene compounds. The effect of the Si/Al ratio, time on stream, the incorporation of additional Ni ions and the introduction of  $\text{K}^+$  ions into Ni silica alumina were studied. From this study, the authors conclude that the highest selectivity to 1-hexene can be obtained for catalysts having Si/Al ratios between 50 and 200, with some additional Ni present over and above that incorporated by ion exchange (1.5 wt%), and the incorporation of a small amount of  $\text{K}^+$  ions. In addition, some improvements in overall 1-hexene yield resulted from the use of catalysts which have been in use for some time. This was in agreement with the results reported by Belltrame *et al.*<sup>[82]</sup> using Ni-ZSM-5 zeolite.

Hartmann *et al.*<sup>[83]</sup> have reported that Ni-MCM-41 and Ni- $\text{AlMCM-41}$  are active as catalysts for ethylene dimerization. More recently Hulea and Fajula<sup>[84]</sup> have studied the oligomerization of ethylene in a slurry batch reactor over a series of Ni- $\text{AlMCM-41}$  catalysts with a carefully controlled concentration of  $\text{Ni}^{2+}$  and acidic sites, in order to understand their influence on the catalytic performance. They found that the presence of a uniform pore-size distribution in the ordered mesoporous material is very favourable for the oligomerization process, being the rate of oligomerization ( $20.5\text{--}63.2 \text{ g g}^{-1} \text{ catalyst h}^{-1}$ ) much higher than those reported by Heydenrych *et al.*<sup>[78]</sup> with Ni-exchanged amorphous silica alumina under similar reaction

conditions. The reaction was highly selective, yielding almost exclusively olefins with an even number of C<sub>4</sub>–C<sub>12</sub> carbon atoms. It was shown that Ni<sup>2+</sup> and acid sites are required for the activation of ethylene oligomerization. However it was observed that the amount of oligomers strongly increases when the acidic site concentration decreases from 0.72 mmol NH<sub>3</sub> g<sup>-1</sup> catalyst (for MCM41; Si/Al = 10) to 0.3 mmol NH<sub>3</sub> g<sup>-1</sup> catalyst (for MCM-41; Si/Al = 80). This behaviour was attributed to the lower deactivation rate of the sample with lower concentration of acid sites. Moreover, it was shown that catalytic activity and product distribution strongly depend on the reaction conditions.

Finally, Ni complexes supported on silica, silica alumina, zeolites and polymeric materials have been reported to be active for ethylene dimerization.<sup>[63,85–90]</sup> In most cases, Ni complexes exhibit high activity and selectivity for the formation of linear 1-olefins. For instance, a comparative study of the activity and selectivity of Ni(MeCN)<sub>6</sub>(BF<sub>4</sub>)<sub>2</sub> associated with AlEt<sub>2</sub>Cl or AlEt<sub>3</sub> as cocatalyst for the ethylene oligomerization in homogenous phase, under biphasic conditions (dissolved in an ionic liquid) and heterogenized in zeolites has been reported.<sup>[91]</sup> It was found that in homogeneous phase and mild reaction conditions the Ni(MeCN)<sub>6</sub>(BF<sub>4</sub>)<sub>2</sub> showed high activity and 97 % selectivity to C<sub>4</sub> with 30 % selectivity to 1-butene was obtained. When the catalyst is dissolved in an ionic liquid (1-methyl-3-butylimidazolium chloroaluminate), ethylene dimerization occurs with 83 % selectivity to 1-butene, whereas when the Ni(MeCN)<sub>6</sub>(BF<sub>4</sub>)<sub>2</sub> was immobilized in zeolite NaX the selectivity to 1-butene was 78 %.

Recently, Angelescu *et al.*<sup>[92]</sup> have studied the activity and selectivity for dimerization of ethylene of various catalysts based on Ni(4,4-bipyridine)Cl<sub>2</sub> complex coactivated with AlCl(C<sub>2</sub>H<sub>5</sub>)<sub>2</sub> and supported on different molecular sieves such as zeolites (Y, L, Mordenite), mesoporous MCM-41 and on amorphous silica alumina. They found that this type of catalyst is active and selective for ethylene dimerization to *n*-butenes under mild reaction conditions (298 K and 12 atm). The complex supported on zeolites and MCM-41 favours the formation of higher amounts of *n*-butenes than the complex supported on silica alumina, which is more favourable for the formation of oligomers. It was also found that the concentration in 1-butene and *cis*-2-butene in the *n*-butene fraction obtained with the complex supported on zeolites and MCM-41, is higher compared with the corresponding values at thermodynamic equilibrium.

Overall, it can be concluded that zeolites, and more specifically MFI, are adequate catalysts for oligomerization of short chain olefins to produce gasoline and even diesel range fuels. Selectivity and catalyst life is strongly dependent on parameters such as crystallite size, Si/Al ratio, and poisoning of external surface sites. The introduction of some metals (Ni) can be helpful.

It has to be remarked that amorphous Ni-silica aluminas with a narrower distribution of pore diameter, and lower density of acid sites, can offer new opportunities for the production of diesel and lubes from short chain olefins. In this sense, MCM-41 materials could be of interest.

With all the catalysts described above, the most important issues are still selectivity and catalyst life.

## REFERENCES

1. Ipatieff, V. N. and Egloff, G. Polymer gasoline has higher blending value than pure iso-octane. *Oil Gas J.*, **33**, **1935**, 31–32.
2. Ipatieff, V. N., Corson, B. B. and Egloff, G. Polymerization, a new source of gasoline, *J. Ind. Eng. Chem.*, **1935**, **27**, 1077–1081.
3. Ipatieff, V. N. and Pines, H. Polymerization of ethylene under high pressure in the presence of phosphoric acid, *J. Ind. Eng. Chem.*, **1935**, **27**, 1364–1369.
4. Ipatieff, V. N. Catalytic polymerization of gaseous olefins by liquid phosphoric acid. I. Propylene, *J. Ind. Eng. Chem.*, **1935**, **27**, 1067–1069.
5. Ipatieff, V. N. and Corson, B. B. Catalytic polymerization of gaseous olefins by liquid phosphoric acid, *J. Ind. Eng. Chem.*, **1935**, **27**, 1069–1071.
6. Owen, H., Marsh, S. K. and Wright, B. S. US 4456779, 1984.
7. Tabak, S. A. US 4433185, 1984.
8. Blauwhoff, P. M. M., Gosselink, J. W., Kieffer, E. P., Sie, S. T. and Stork, W. H. J. Zeolites as catalysts in industrial processes. In *Catalysis and Zeolites. Fundamentals and Applications*, J. Weitkamp and L. Puppe (eds). Springer-Verlag, Berlin, 1999, pp. 509–512.
9. Skupinska, J. Oligomerization of  $\alpha$ -olefins to higher oligomers, *Chem. Rev.*, **1991**, **91**, 613–648.
10. Al-Jarallah, A. M., Anabtawi, J. A., Siddiqui, M. A. B., Aitani, A. M. and Al-Sa'doun, A. W. Ethylene dimerization and oligomerization to butene-1 and linear  $\alpha$ -olefins: a review of catalytic systems and processes. *Catal. Today*, **1992**, **14**, 1–121.
11. O'Connor, C. T. and Kojima, M. Alkene oligomerization. *Catal. Today*, **1990**, **6**, 329–349.
12. O'Connor, C. T., Van Steen, E. and Dry, M. E. New catalytic applications of zeolites for petrochemicals, *Stud. Surf. Sci. Catal.*, **1996**, **102**, 323–362.
13. O'Connor, C. T. Oligomerization. In *Handbook of Heterogeneous Catalysis*, G. Ertl, H., Knözinger and J. Weitkamp, (eds). VCH, Weinheim, **1997**, pp. 2380–2386.
14. Sanati, M., Hornell, C. and Jaras, S. G. The oligomerization of alkenes by heterogeneous catalysts, *Catalysis*, **1999**, **14**, 236–287.
15. Garwood, W. E. Conversion of C<sub>2</sub>–C<sub>10</sub> to higher olefins over synthetic zeolite, *ACS Symp. Ser.*, **1983**, **218**, 383–396.
16. Lukyanov, D. B., Gnep, N. S. and Guisnet, M. R. Kinetic modeling of ethene and propene aromatization over HZSM-5 and GHZSM-5, *Ind. Eng. Chem. Res.*, **1994**, **33**, 223–234.
17. Miller, S. J. Olefin oligomerization over high silica zeolites. *Stud. Surf. Sci. Catal.*, **1987**, **38**, 187–197.
18. Occelli, M. L., Hsu, J. T. and Galya, L. G. Propylene oligomerization over molecular sieves. Part I. Zeolite effects on reactivity and liquid products selectivities. *J. Mol. Catal.*, **1985**, **32**, 377–390.
19. Kustov, L. M., Borovkov, V. Y. and Kazanskii, V. B. Study of ethylene oligomerization on Brønsted and Lewis acidic sites of zeolites using diffuse reflectance IR spectroscopy. *Stud. Surf. Sci. Catal.*, **1984**, **18**, 241–247.
20. Kofke, T. J. G. and Gorte, R. J. A temperature-programmed desorption study of olefin oligomerization in H-ZSM-5. *J. Catal.*, **1989**, **115**, 233–243.
21. van Bokhoven, J. A., Van der Eerden, A. M. J. and Prins, R. Local structure of the zeolitic catalytically active site during reaction. *J. Am. Chem. Soc.*, **2004**, **126**, 4506–4507.
22. Chen, C. S. H. and Bridger, R. F. Shape-selective oligomerization of alkenes to near-linear hydrocarbons by zeolite catalysis, *J. Catal.*, **1996**, **161**, 687–693.

23. Van den Berg, J. P., Wolthuisen, J. P., Clague, A. D. H., Hays, G. R., Huis, R. and Van Hooff, J. H. C. Low-temperature oligomerization of small olefins on zeolite H-ZSM-5. An investigation with high-resolution solid-state carbon-13 NMR, *J. Catal.*, **1983**, *80*, 130–138.
24. Quann, R. J., Green, L. A., Tabak, S. A. and Krambeck, F. J. Chemistry of olefin oligomerization over Zsm-5 catalyst, *Ind. Eng. Chem. Res.*, **1988**, *27*, 565–670.
25. Derouane, E. G., Lefebvre, C. and Nagy, J. B. Channel network effects in ethylene oligomerization and aromatization using HZSM-5, HZSM-11 and HZSM-48 catalysts. An in situ carbon-13 NMR study, *J. Mol. Catal.*, **1986**, *38*, 387–391.
26. Costa, C., Lopes, J. M., Lemos, F. and Ramoa Ribeiro, F. Activity–acidity relationship in zeolite Y. Part 1. Transformation of light olefins, *J. Mol. Catal., A*, **1999**, *144*, 207–220.
27. Heveling, J., Van der Beek, A. and De Pender, M. Oligomerization of ethene over nickel-exchanged zeolite Y into a diesel-range product, *Appl. Catal.*, **1988**, *42*, 325–336.
28. Yamamura, M., Chaki, K., Wakatsuki, T., Okado, H. and Fujimoto, K. Synthesis of ZSM-5 zeolite with small crystal size and its catalytic performance for ethylene oligomerization, *Zeolites*, **1994**, *14*, 643–649.
29. Jackson, K. J. and Howe, R. F. Studies of zeolite single crystals: ethene oligomerization in HZSM-5. *Stud. Surf. Sci. Catal.*, **1994**, *83*, 187–194.
30. Shete, B. S., Belapurkar, A. D. and Gupta, N. M. On role of Bronsted acid sites in reactions of ethylene over ZSM-5 and HZSM-5 zeolites. *Stud. Surf. Sci. Catal.*, **1998**, *113*, 721–727.
31. Amin, N. A. S. and Anggoro, D. D. Dealuminated ZSM-5 zeolite catalyst for ethylene oligomerization to liquid fuels, *J. Natural Gas Chem.*, **2002**, *11*, 79–86.
32. Farcasiu, D., Hutchison, J. and Luowei, L. Analysis of factors that influence shape selectivity in the craking of long-chain alkanes on zeolites catalysts, *J. Catal.*, **1990**, *122*, 34–43.
33. Fraenkel, D. Role of external surface sites in shape-selective catalysis over zeolites, *Ind. Eng. Chem. Res.*, **1990**, *29*, 1814–1821.
34. Schwartz, S., Kojima, M. and O'Connor, C. T. Effect of silicon-to-aluminum ratio and synthesis time on high-pressure oligomerization over ZSM-5, *Appl. Catal.*, **1989**, *56*, 263–280.
35. Martens, L. R., Verduijn, J. P. and Mathys, G. M. The development of an environmental friendly catalytic system for the conversion of olefins, *Catal. Today*, **1997**, *36*, 451–460.
36. Page, N. M., Young, L. B. and Blain, D. A. US Patent 4870038, 1989.
37. Wilshier, K. G., Smart, P., Western, R., Mole, T. and Behrsing, T. Oligomerization of propene over H-Zsm-5 zeolite, *Appl. Catal.*, **1987**, *31*, 339–359.
38. Beadle, S. W. Oligomerization process and catalyst system for preparing an oligomeric olefinic hydrocarbon mixture from propylene and butenes. WO Patent 2003082779, **2003**.
39. Duncan, C. B. Process and surface-deactivated ZSM-23 zeolite catalysts for a C2–6 olefin oligomerization process. WO 2003082781, **2003**.
40. Apelian, M. R., Boulton, J. R. and Fung, A. S. US 5284989, **1994**.
41. Inui, T., Tarumoto, J., Okazumi, F. and Matsuda, H. Highly selective synthesis of high-octane gasoline from light olefins on novel metallosilicates. *Chem. Express*, **1986**, *1*, 49–52.
42. Inui, T., Okazumi, F., Tarumoto, J., Yamase, O., Matsuda, H., Nagata, H., Daito, N. and Miyamoto, J. Highly selective synthesis of high octane-number gasoline from light olefins on iron-silicates. *Jpn. Petrol. Inst.*, **1987**, *30*, 249–256.
43. Inui, T. and Kim, J. B. High quality gasoline synthesis by selective oligomerization of light olefins and successive hydrogenation. *Stud. Surf. Sci. Catal.*, **1996**, *100*, 489–498.



44. Inui, T. Selective conversion of light olefins to high octane-number gasoline on novel Fe-silicate catalysts. *React. Kinet. Catal. Lett.*, **1987**, *35*, 227–236.
45. Verrelst, W. H., Martens, L. R. M., Verduijn, J. P. Olefin oligomerization and zeolite catalysts therefor, WO Patent 9624567, **1996**.
46. Martens, J. A., Ravishankar, R., Mishin, I. E. and Jacobs, P. A. Tailored alkene oligomerization with H-ZSM-57 zeolite, *Angew. Chem., Int. Ed. Engl.*, **2000**, *39*, 4376–4379.
47. Galya, L. G., Occelli, M. L. and Hsu, J. T. Propylene oligomerization over molecular sieves. Part II. Proton NMR and carbon-13 NMR characterization of reaction products., *J. Mol. Catal.*, **1985**, *32*, 391–403.
48. Bjorgen, M., Lillerud, K. P., Olsbye, U., Bordiga, S. and Zecchina, A. 1-Butene oligomerization in Bronsted acidic zeolites: mechanistic insights from low-temperature *in situ* FTIR spectroscopy. *J. Phys. Chem. B*, **2004**, *108*, 7862–7870.
49. Torres, M., Lopez, L., Dominguez, J. M., Mantilla, A., Ferrat, G., Gutierrez, M. and Maubert, M. Olefins catalytic oligomerization on new composites of beta-zeolite films supported on a-Al<sub>2</sub>O<sub>3</sub> membranes. *Chem. Eng. J.*, **2003**, *92*, 1–6.
50. Bellusi, G., Cavani, F., Arrigoni, V. and Ghezzi, R. Process for oligomerizing light olefins. EP Patent 0463673, **1992**.
51. Le, Q. N. Multistage olefin upgrading process using synthetic mesoporous crystalline material. US Patent 5134241, **1991**.
52. Bhole, N. A. Catalytic oligomerization process using synthetic mesoporous crystalline material. US Patent 5134243, **1991**.
53. Le, Q. N. Catalytic olefin upgrading process using synthetic mesoporous crystalline material. US Patent 5134242, **1991**.
54. Kim, J. B. and Inui, T. Synthesis of metal-incorporated mesoporous crystalline silicates for oligomerization of propene, *Catal. Lett.*, **1996**, *36*, 255–261.
55. Peratello, S., Molinari, M., Bellussi, G. and Perego, C. Olefins oligomerization: thermodynamics and kinetics over a mesoporous silica-alumina. *Catal. Today*, **1999**, *52*, 271–277.
56. Chiche, B., Sauvage, E., Di Renzo, F., Ivanova, I. I. and Fajula, F. Butene oligomerization over mesoporous MTS-type aluminosilicates. *J. Mol. Catal. A*, **1998**, *134*, 145–157.
57. Catani, R., Mandreoli, M., Rossini, S. and Vaccari, A. Mesoporous catalysts for the synthesis of clean diesel fuels by oligomerization of olefins. *Catal. Today*, **2002**, *75*, 125–131.
58. Keim, W. Nickel – an element with wide application in industrial homogeneous catalysis. *Angew. Chem., Int. Ed. Engl.*, **1990**, *29*, 235–244.
59. Kroschwitz, J. and Howe-Grant, M. (eds) *Kirk–Othmer Encyclopaedia of Chemical Technology*. John Wiley & Sons, Inc., New York, **1996**.
60. Chauvin, Y., Gaillard, J., Leonard, J., Bonnifay, P. and Andrews, K. W. Another use for Dimersol. *Hydroc. Proc.*, **1982**, *61*, 110–112.
61. Commereuc, D., Chauvin, Y., Gaillard, J., Leonard, J. and Andrews, K. W. Dimerize ethylene to 1-butene. *Hydroc. Proc.*, **1984**, *63*, 118–120.
62. Moulijn, J. A., van Leeuwen, P. W. N. M. and van Santen, R. A. *Catalysis: an Integrated Approach to Homogeneous, Heterogeneous and Industrial Catalysis*. Elsevier Science, Amsterdam, **1993**.
63. Bonneviot, L., Olivier, D. and Che, M. Dimerization of olefins with nickel surface complexes in X-type zeolite or on silica, *J. Mol. Catal.*, **1983**, *21*, 415–430.
64. Elev, I. V., Shelimov, B. N. and Kazansky, V. B. The role of Ni<sup>+</sup> ions in the activity of nicay zeolite catalysts for ethylene dimerization. *J. Catal.*, **1984**, *89*, 470–477.

65. Ng, F. T. T. and Creaser, D. C. Ethylene dimerization over modified nickel exchanged Y-zeolite. *Appl. Catal.*, **1994**, *119*, 327–339.
66. Nkosi, B., Ng, F. T. T. and Rempel, G. L. The oligomerization of butenes with partially alkali exchanged NiNaY zeolite catalysts. *Appl. Catal. A*, **1997**, *158*, 225–241.
67. Yashima, T., Ushida, Y., Ebisawa, M. and Hara, N. Polymerization of ethylene over transition-metal exchanged Y-zeolites. *J. Catal.*, **1975**, *36*, 320–326.
68. Garwood, W. E. Catalytic process for oligomerizing ethene, US Patent 4717782, 1986.
69. Davydov, A. A., Kantcheva, M. and Chepotko, M. L. FTIR spectroscopic study on nickel(II)-exchanged sulfated alumina: nature of the active sites in the catalytic oligomerization of ethene. *Catal. Lett.*, **2002**, *83*, 97–108.
70. Cai, FX. Studies of a new alkene oligomerization catalyst derived from nickel sulfate. *Catal. Today*, **1999**, *51*, 153–160.
71. Espinoza, R. L., Snel, R., Korf, C. J. and Nicolaidis, C. P. Catalytic oligomerization of ethene over nickel-exchanged amorphous silica-aluminas; effect of the acid strength of the support. *Appl. Catal.*, **1987**, *29*, 295–303.
72. Miller, S. J. Two-stage dimerization of C5–11-alkene fractions for production of base-stocks for lubricating oils. WO 2002055633, **2001**.
73. Lapidus, A. and Krylova, A. Ethylene oligomerization over Ni- and Pd-zeolites, *DGMK Tagungsber.*, **2001**, *2001–4*, 245–251.
74. Espinoza, R. L., Korf, C. J., Nicolaidis, C. P. and Snel, R. Catalytic oligomerization of ethene over nickel-exchanged amorphous silica-alumina; effect of the reaction conditions and modeling of the reaction. *Appl. Catal.*, **1987**, *29*, 175–184.
75. Zhang, Q., Kantcheva, M. and Dalla Lana, L. G. Oligomerization of ethylene in a slurry reactor using a nickel/sulfated alumina catalyst, *Ind. Eng. Chem. Res.*, **1997**, *36*, 3433–3438.
76. Cai, F. X., Lepetit, C., Kermarec, M. and Olivier, D. Dimerization of ethylene into 1-butene over supported tailor-made nickel-catalysts. *J. Mol. Catal.*, **1987**, *43*, 93–116.
77. Heveling, J., Nicolaidis, C. P. and Scurrrell, M. S. Catalysts and conditions for the highly efficient, selective and stable heterogeneous oligomerization of ethylene. *Appl. Catal., A* **1998**, *173*, 1–9.
78. Heydenrych, M. D., Nicolaidis, C. P. and Scurrrell, M. S. Oligomerization of ethene in a slurry reactor using a nickel(II)-exchanged silica-alumina catalyst. *J. Catal.*, **2001**, *197*, 49–57.
79. Nicolaidis, C. P. and Scurrrell, M. S. Supported reagents and catalysts in chemistry. *Spec. Publ. - R. Soc. Chem.*, **2001**, *266*, 226.
80. Sakaguchi, T., Mita, S., Matsui, E., Takahashi, M., Okazaki, N. and Tada, A. Oligomerization of ethene over several catalyst beds consisting of both Ni/SiO<sub>2</sub>.Al<sub>2</sub>O<sub>3</sub> and BPO<sub>4</sub>, *Phosphorus Res. Bull.*, **2002**, *14*, 129–134.
81. Nicolaidis, C. P., Scurrrell, M. S. and Semano, P. M. Nickel silica-alumina catalysts for ethene oligomerization – control of the selectivity to 1-alkene products. *Appl. Catal., A*, **2003**, *245*, 43–53.
82. Beltrame, P., Forni, L., Talamini, A. and Zuretti, G. Dimerization of 1-butene over nickel zeolitic catalysts – a search for linear dimers. *Appl. Catal.*, **1994**, *110*, 39–48.
83. Hartmann, M., Poppl, A. and Kevan, L. Ethylene dimerization and butene isomerization in nickel-containing MCM-41 and AlMCM-41 mesoporous molecular sieves: an electron spin resonance and gas chromatography study. *J. Phys. Chem.*, **1996**, *100*, 9906–9910.
84. Hulea, V. and Fajula, F. Ni-exchanged AlMCM-41 – an efficient bifunctional catalyst for ethylene oligomerization, *J. Catal.*, **2004**, *225*, 213–222.

85. Nesterov, G. A., Fink, G. and Zakharov, V. A. Ethylene oligomerization by supported nickel-complexes. *Makromol. Chem., Rapid Commun.*, **1989**, *10*, 669–673.
86. Nesterov, G. A., Zakharov, V. A., Fink, G. and Fenzl, W. Supported nickel catalysts for ethylene oligomerization. *J. Mol. Catal.*, **1991**, *69*, 129–136.
87. Nesterov, G. A., Zakharov, V. A., Fink, G. and Fenzl, W. Heterogenization of a homogeneous nickel chelate ethylene oligomerization catalyst. *J. Mol. Catal.*, **1991**, *66*, 367–372.
88. Carlu, J. C. and Caze, C. Dimerization of ethylene catalyzed by a nickel-catalyst supported on porous polymers. *React. Polym.*, **1990**, *13*, 153–160.
89. Ceder, R., Muller, G., Saleh, J. and Vidal, J. Catalytic dimerization of ethylene to 1-butene by square-planar nickel-complexes. *J. Mol. Catal.*, **1991**, *68*, 23–31.
90. Sohn, J. R., Kim, H. W. and Kim, J. T. New syntheses of solid catalysts for ethylene dimerization. *J. Mol. Catal.*, **1987**, *41*, 375–378.
91. Oberson de Souza, M. and de Souza, R. F. Ethylene oligomerization with  $\text{Ni}(\text{MeCN})_6(\text{BF}_4)_2$  in homogeneous phase, immobilized in ionic liquids or heterogenized in zeolite. *Current Top. Catal.*, **3**, **2002**, 267–273.
92. Angelescu, E., Che, M., Andruh, M., Zavoianu, R., Costentin, G., Mirica, C. and Dumitru Pavel, O. Ethylene selective dimerization on polymer complex catalyst of  $\text{Ni}(4,4'$ -bipyridine) $\text{Cl}_2$  coactivated with  $\text{AlCl}(\text{C}_2\text{H}_5)_2$ . *J. Mol. Catal., A*, **219**, **2004**, 13–19.

---

# 7 Microporous and Mesoporous Catalysts for the Transformation of Carbohydrates

---

CLAUDE MOREAU

*Laboratoire de Matériaux Catalytiques et Catalyse en Chimie Organique, UMR 5618 CNRS-ENSCM-UMI, Ecole Nationale Supérieure de Chimie de Montpellier, 8 rue de l'Ecole Normale, 34296 Montpellier Cedex 5, France*

## CONTENTS

7.1 INTRODUCTION . . . . .	141
7.2 HYDROLYSIS OF SUCROSE IN THE PRESENCE OF H-FORM ZEOLITES . . . . .	142
7.3 HYDROLYSIS OF FRUCTOSE AND GLUCOSE PRECURSORS. . . . .	143
7.4 ISOMERIZATION OF GLUCOSE INTO FRUCTOSE . . . . .	144
7.5 DEHYDRATION OF FRUCTOSE AND FRUCTOSE-PRECURSORS . . . . .	145
7.6 DEHYDRATION OF XYLOSE . . . . .	146
7.7 SYNTHESIS OF ALKYL-D-GLUCOSIDES. . . . .	147
7.7.1 Synthesis of butyl-D-glucosides . . . . .	147
7.7.2 Synthesis of long-chain alkyl-D-glucosides . . . . .	150
7.8 SYNTHESIS OF ALKYL-D-FRUCTOSIDES . . . . .	151
7.9 HYDROGENATION OF GLUCOSE . . . . .	151
7.10 OXIDATION OF GLUCOSE . . . . .	153
7.11 CONCLUSIONS . . . . .	154
REFERENCES. . . . .	154

## 7.1 INTRODUCTION

Since the last review by Venuto in 1968,<sup>[1]</sup> there has been a continuous interest in the application of microporous and mesoporous materials as catalysts in the synthesis of bulk and fine chemicals.<sup>[2-4]</sup> Indeed, their acidic and basic properties can be combined with their structural properties in order to take advantage of their adsorption and shape selectivity properties, the latter being an advantageous feature of zeolites compared with other heterogeneous catalysts. Another important aspect

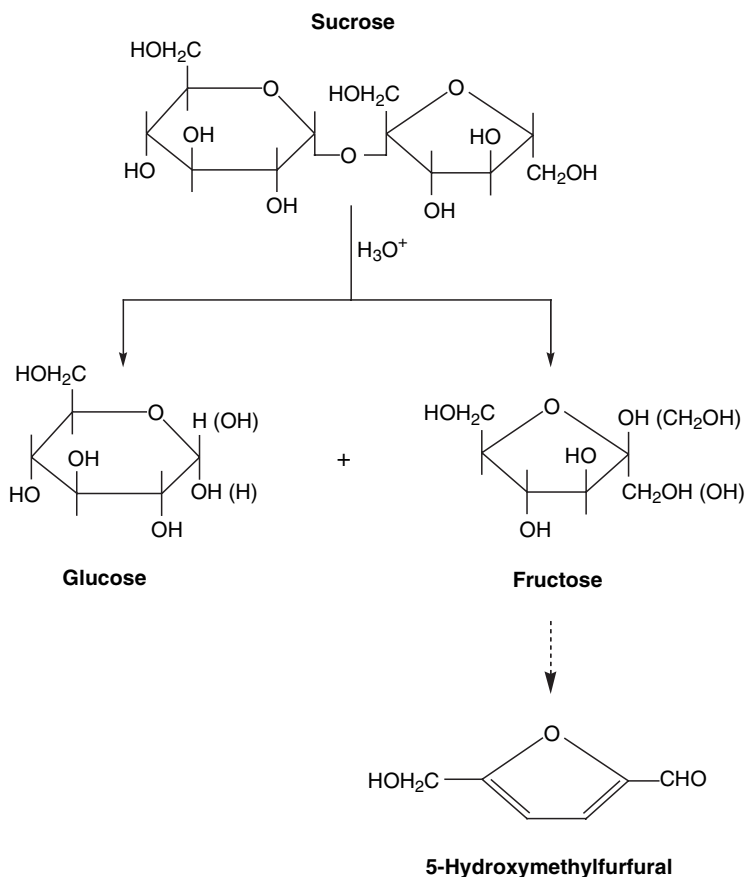
is that zeolites and related materials can also contribute to the development of environmentally friendly processes.

However, if the literature is relatively abundant concerning 'classical' organic chemistry in the presence of such catalytic materials, this is not the case in the chemistry of carbohydrates, where enzymes are often the preferred and most appropriate catalysts.

This chapter will summarize what has been done in the transformation of mono-, di- and polysaccharides using heterogeneous microporous and mesoporous catalysts.

## 7.2 HYDROLYSIS OF SUCROSE IN THE PRESENCE OF H-FORM ZEOLITES

Sucrose is widely used in the food industry as such or as precursor of invert sugar through its partial or total hydrolysis (Scheme 7.1). Enzymes are the catalysts most



**Scheme 7.1** Simplified reaction scheme for hydrolysis of sucrose. Reprinted from Agro-Food-Industry Hi-Tech, 2002, Moreau, pp. 17–26, with permission from Teknoscienze.

often used on the industrial scale.<sup>[5]</sup> However, their use is restricted to the food industry as far as the products formed, glucose and fructose, inhibit the hydrolysis reaction,<sup>[6]</sup> with a conversion of sucrose which does not exceed 95%. Strong H<sup>+</sup> ion-exchange resins are also used and allow a complete conversion of sucrose in the temperature range compatible with their stability, but with a relatively high level of impurities.<sup>[7,8]</sup>

By contrast, acidic zeolites allow the formation of invert sugar under mild operating conditions, for high concentrations in the starting sucrose, and with an efficient control of the degree of coloured materials due to their adsorbent properties.

For example, we have shown that the microporous H-Y zeolite with a Si/Al ratio of 15 had the better balance between activity, selectivity and by-product amounts at temperatures ranging from 75 to 95°C, aqueous sucrose solution up to 800 g L<sup>-1</sup> and catalyst weight from 1 to 6 wt%, in batch or flow mode.<sup>[9,10]</sup> Thanks to their intrinsic properties, the formation of by-products, 5-hydroxymethylfurfural in particular, is less important with microporous zeolites than with macroporous resins, thus ensuring a better control of the formation of coloured impurities nonacceptable in the food industry.

### 7.3 HYDROLYSIS OF FRUCTOSE AND GLUCOSE PRECURSORS

Hydrolysis of inulin has already been performed in the presence of a zeolite, namely the zeolite LZ-M-8.<sup>[11]</sup> This catalyst has been found to be extremely selective towards hydrolysis compared with fructose decomposition, thus illustrating the superiority of the zeolite over sulfuric acid or ion-exchange resins as catalysts. As an example, a 96% yield in fructose was obtained after 15 min at 130°C starting from 2 ml of a 0.257 mol L<sup>-1</sup> inulin solution and 0.25 g of zeolite.

In the presence of a H-Y zeolite with a Si/Al ratio of 15, we have performed the hydrolysis of other fructose and glucose precursors under operating conditions quite close to those used for sucrose hydrolysis. It was found that aqueous solutions of inulin, maltose, cellobiose and starch (50–120 g L<sup>-1</sup>) were hydrolysed into the corresponding monosaccharides within 30–150 min at temperatures between 90°C and 150°C in the presence of 0.5–2.5 g of catalyst in 50 ml of starting solution, with yields of monosaccharides from 92 to 98%.<sup>[12]</sup>

From this work, an important feature to be noted was the influence of stereoelectronic effects toward cleavage of  $\beta$ -1,4 (cellobiose) and  $\alpha$ -1,4 linkage (maltose).<sup>[13]</sup> In the presence of zeolites, there is insufficient space inside the channels for conformational changes both in ground and transition states. In such a way, maltose is hydrolysed faster than cellobiose compared with homogeneous or macroporous ion-exchange resin catalysis.<sup>[7]</sup>

In the presence of MCM-41, acidic Mordenites and Beta zeolites with different Si/Al ratios, it has been shown by Abbadi *et al.*<sup>[14]</sup> that maltose (1g in 50 ml of water, batch reactor, 0.5g of catalyst) was also selectively hydrolysed into glucose at 130°C. For other polysaccharides, such as amylose and starch, the conversion and

the selectivity reached during hydrolysis were comparable to those obtained with maltose.<sup>[15]</sup> It was also shown that the hydrolysis reaction may be partly homogeneously catalysed as far as leaching of catalytically active species from heterogeneous catalysts was observed. Again, it was shown that activity and selectivity are affected by temperature and pressure effects. For example, in maltose hydrolysis, when a nitrogen pressure higher than 20 bar is applied, the selectivity to produce glucose tends to drop.

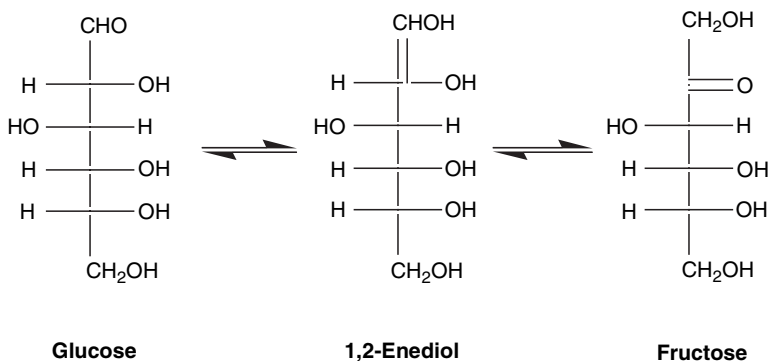
However, for hydrolysis of inulin over a H-Beta zeolite at 100 °C (1 g of inulin in 50 ml of water, batch reactor, 0.25 g of catalyst), a large effect of the nitrogen pressure was observed. Hydrolysis goes to completion within 5 h at 1 bar N<sub>2</sub> and within 20 min at 100 bar N<sub>2</sub>, without any effect on the selectivity of the reaction.

Thus, as for hydrolysis of sucrose, conventional microporous and mesoporous catalysts in their protonic form can advantageously replace enzymes or ion-exchange resins in hydrolytic processes involving other di- or polysaccharides by combining shape selectivity and adsorbent properties. No product inhibition is observed, and higher reaction temperatures can be used. Whatever the food or nonfood applications are for fructose and glucose, it is clear that significant improvements are obtained by using heterogeneous processes.

#### 7.4 ISOMERIZATION OF GLUCOSE INTO FRUCTOSE

Nowadays, there is a renewed interest for the preparation of fructose, for its food applications as a diet sugar<sup>[16]</sup> as well as for its nonfood applications as a starting material for the synthesis of furanic precursors of nonpetroleum derived polymeric materials.<sup>[17–19]</sup>

We have shown that the isomerization of glucose into fructose (Scheme 7.2) was easily achieved in the presence of cation-exchanged zeolites and hydrotalcites, in water as the solvent, at higher temperatures and higher glucose concentrations than in the case of ion-exchange resins and enzymes as catalysts.<sup>[20]</sup>



**Scheme 7.2** Simplified reaction scheme for isomerization of glucose. Reprinted from Agro-Food-Industry Hi-Tech, Jan–Feb 2002, Moreau, pp. 17–26, with permission from Teknoscienze.

**Table 7.1** Glucose conversion, selectivity to fructose, percentage of cation leaching and pseudo first-order rate constants for the disappearance of glucose (5 g of glucose in 50 ml of water, 95 °C, 1 g of catalyst)

Catalyst	Glucose conversion (%)	Fructose selectivity (%)	Cation leaching (%)	Glucose disappearance rate ( $\times 10^4 \text{ s}^{-1}$ )
LiX (19% Li)	19	85	16	0.64
NaX (100% Na)	20	86	16	0.70
KX (51% K)	23	80	20	0.86
CsX (43% Cs)	25	77	23	0.94

Under the operating conditions used (aqueous solution of glucose up to 200 g L<sup>-1</sup> catalyst up to 20 wt % and 95 °C), NaX and KX catalysts were found to give the best balance between activity and selectivity. A high selectivity in fructose ( $\geq 85\%$ ) is obtained with NaX and KX catalysts (Table 7.1), but at a low glucose conversion ( $\leq 20\%$ ). Unfortunately, a leaching effect is observed, about 15%, even for the most selective X zeolites. This leaching effect disappears after the second run, the conversion of glucose is then close to 8–10% without loss in the selectivity to fructose.

However, no leaching effect was observed with hydrotalcites in their hydroxide or mixed carbonate–hydroxide form.<sup>[21]</sup> Modifications of their basic properties lead to an increase in the selectivity to fructose to nearly 100%, but once again at a glucose conversion lower than 20%.

Cation-exchanged KX and CaY zeolites are also known to be used for the separation of glucose and fructose on the basis of the selective adsorption properties of that kind of material.<sup>[22–25]</sup> Some experiments have then been performed in the presence of Ca- and Ba-exchanged A, X and Y zeolites. Unfortunately, the CaY zeolite claimed for the separation of glucose and fructose was not as efficient as expected for a two-stage process involving isomerization followed by separation on the same type of material.

## 7.5 DEHYDRATION OF FRUCTOSE AND FRUCTOSE-PRECURSORS

As already mentioned, there has been renewed interest for using carbohydrates as a source of chemicals since the 1980s with the development of the chemistry of furanic compounds, particularly for the preparation of nonpetroleum derived polymeric materials, such as polyesters, polyamides and polyurethanes.<sup>[17,19]</sup>

Two basic nonpetroleum chemicals readily accessible from renewable resources, furfural arising from the acid-catalysed dehydration of pentoses, and 5-hydroxymethylfurfural arising from the acid-catalysed dehydration of hexoses, are suitable starting materials for the preparation of further monomers required for polymer applications. Whereas the former is industrially available (200 000 tons year<sup>-1</sup>), the latter is only produced on a pilot plant scale.<sup>[26]</sup>



**Table 7.2** Conversion and selectivity to 5-hydroxymethylfurfural (HMF) for dehydration of fructose and precursors over H-Mordenite (Si/Al = 11) at 165 °C in water/methyl isobutyl ketone (1:5 by volume)

Starting material	Fructose conversion <sup>a</sup> (%)	Selectivity to HMF (%)
Fructose	76	91
Sucrose	57	98
Fructose + sucrose (1:1)	67	99
Jerusalem artichoke	66	87
Inulin	44	88

<sup>a</sup>Conversion based on the fructose content of the starting material at 60 min reaction time.

Although several methods have been reported in recent literature concerning the preparation of 5-hydroxymethylfurfural by dehydration of fructose, we have shown that microporous catalyts in their protonic form, for instance, Mordenites, Beta, Y-faujasites and ZSM-5 zeolites constituted a convenient alternative route to the catalysts used up to now, namely mineral acids, oxides or ion-exchange resins.<sup>[27,28]</sup>

Dehydration of fructose was performed in the presence of dealuminated H-form zeolites in a batch reactor starting from an aqueous solution of fructose up to 200 g L<sup>-1</sup> and methyl isobutyl ketone (1/5 by volume), and a catalyst weight up to 6%. All catalysts were found to be active, but only the H-Mordenite, with a Si/Al ratio of 11 and with a low mesoporous volume (0.056 cm<sup>3</sup> g<sup>-1</sup>), was found to have the better balance between activity, selectivity and by-product amounts at 165 °C. After 30 min of reaction, the conversion of fructose is 54% and the selectivity to 5-hydroxymethylfurfural is 92%. The selectivity remains unchanged (91%) after 1 h of reaction for a fructose conversion of 76%. Compared with other catalytic systems, the bidimensional structure of the Mordenite with only one large channel allows the accessibility of fructose to the catalytic sites and the rapid diffusion of 5-hydroxymethylfurfural once formed, thus avoiding its rearrangement into higher molecular weight compounds.

Starting from raw fructose-containing precursors such as sucrose, Jerusalem artichoke and inulin hydrolysates, high selectivities to 5-hydroxymethylfurfural were obtained for relatively high fructose conversion after 60 min of reaction time at 165 °C (Table 7.2). Under the operating conditions used, glucose does not react significantly in the presence of the H-Mordenite (Si/Al = 11), thus only acting as a sleeping partner in the dehydration step. Unreacted glucose can be easily separated from the reaction medium in a liquid–liquid extractor working in a countercurrent mode.<sup>[29,30]</sup>

## 7.6 DEHYDRATION OF XYLOSE

As previously stated, furfural is obtained through dehydration of pentoses, xylose in particular, or hemicelluloses, at high temperatures (200–250 °C), and in the presence of mineral acids as catalysts, mainly sulfuric acid.<sup>[31]</sup> Under these

conditions, the selectivity in furfural does not exceed 70%, except in the case of its continuous extraction with supercritical CO<sub>2</sub> where the selectivity reaches 80%.<sup>[32]</sup>

In the presence of the H-Mordenite with a Si/Al ratio of 11 as catalyst, a close parallelism is observed with the results obtained for the dehydration of fructose, except that toluene is the co-solvent instead of methyl isobutyl ketone. The transformation of xylose into furfural is easily achieved at 170 °C with a selectivity as high as 90 to 95% as far as the conversion is kept at a low extent, 30 to 40%.<sup>[33]</sup> At those high temperatures, ion-exchange resins cannot compete with zeolites.

## 7.7 SYNTHESIS OF ALKYL-D-GLUCOSIDES

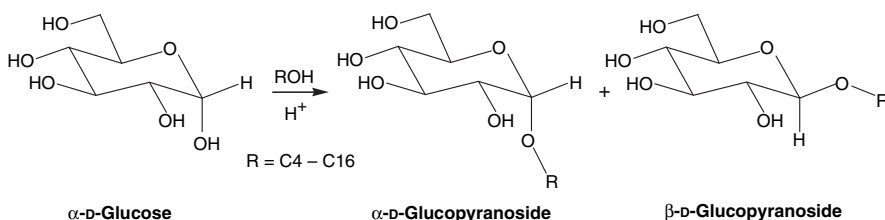
Alkylglucosides are a new class of nonionic surfactants which find applications in cosmetics, food emulsifiers and detergency<sup>[34,35]</sup> because of their nontoxic and biodegradable properties.<sup>[36]</sup> Although the first synthesis of alkylglucosides (Scheme 7.3) was described over 100 years ago by Fischer,<sup>[37]</sup> this reaction is continually under investigation. Protection and deprotection steps are generally required in order to obtain alkylglucosides with a high selectivity.

Alkylglucosides have already been directly synthesized using heterogeneous catalysts as, for example, macroporous sulfonated resins but with a relatively important amount of oligosaccharides.<sup>[38,39]</sup> However, it was recently shown that acid zeolites were capable of performing the direct Fischer synthesis by avoiding the formation of oligomer species.<sup>[18,40,41]</sup>

### 7.7.1 SYNTHESIS OF BUTYL-D-GLUCOSIDES

In a preliminary work by Corma *et al.*,<sup>[42]</sup> it was shown that large-pore tridirectional zeolites H-Beta and H-Y were capable of achieving the glycosylation reaction between D-glucose and *n*-butanol with reasonable activity providing that the *n*-butanol/D-glucose molar ratio is higher than 20 (Table 7.3). The conversion is lower over small-pore H-Mordenite and HZSM-5 catalysts, for which catalysts the reaction may occur on the external surface.

From their results, the authors have proposed a consecutive reaction scheme with glucofuranosides as primary products and glucopyranosides as secondary products.



**Scheme 7.3** Simplified reaction scheme for glycosylation of alcohols. Reprinted from Agro-Food-Industry Hi-Tech, 2002, Moreau, pp.17–26, with permission from Teknoscienze.

**Table 7.3** Product distribution in the presence of different zeolites with nearly similar Brønsted acidity

Zeolite	Si/Al	Glucofuranosides yield <sup>a</sup> (%)	Glucopyranosides yield <sup>a</sup> (%)
HY-100	4.5	51	21
HY-2	15.0	23	65
HZSM-5	26.5	48	9
H-Beta	13.0	33	65
H-Mordenite	14.0	37	14

<sup>a</sup>Data from Corma *et al.*<sup>[42]</sup> Yields after 4 h of reaction at 383 K, *n*-butanol/*D*-glucose molar ratio = 40, 1.5 wt % catalyst.

A more complete study was then carried out in the same research group over H-Beta zeolites.<sup>[43]</sup> In particular, the influence of the crystal size and of the hydrophobic versus hydrophilic properties of the catalysts on the initial reaction rate and product distribution was examined.

For a given structure, the reaction rate is maximum for samples with a crystallite size  $\leq 0.35 \mu\text{m}$  and for a glucose conversion of 60%. The ratio glucofuranosides/glucopyranosides is practically the same for crystal size of 0.05–0.35  $\mu\text{m}$  and increases when increasing crystal sizes up to 0.90  $\mu\text{m}$  (Table 7.4). In the absence of shape selectivity effects, a decrease in the influence of the diffusion through the micropores is obtained for a given structure by decreasing the crystallite size. It was then concluded that the formation of glucopyranosides is more affected by diffusion than glucofuranosides.

Another important feature from this work is concerned with the influence of the hydrophobic versus hydrophilic properties of the catalysts on the catalytic activity. The optimum activity is reached at lower Si/Al ratios when the catalyst is more hydrophobic, thus resulting from the balance between the number of active sites and the adsorption properties of the catalysts.

Again in the same research group,<sup>[44]</sup> it has been shown that over Al-containing MCM-41 mesoporous materials with acidity always lower than that of zeolites, the glycosylation of *D*-glucose and *n*-butanol proceeded at reaction rates not very far

**Table 7.4** Influence of the crystal size on the initial reaction rate and on product distribution at 60 % glucose conversion

Zeolite H-Beta	Crystal size ( $\mu\text{m}$ )	Initial reaction rate ( $\times 10^4 \text{ mol min}^{-1} \text{ g}^{-1}$ )	Glucofuranosides yield <sup>a</sup> (%)	Glucopyranosides yield <sup>a</sup> (%)
H-Beta-1	0.05	4.9	50	10
H-Beta-2	0.35	5.2	48	12
H-Beta-3	0.60	3.7	55	5
H-Beta-4	0.90	1.8	57	3

<sup>a</sup>Data from Cambor *et al.*<sup>[43]</sup> Yields after 4 h of reaction at 383 K, *n*-butanol/*D*-glucose molar ratio = 40, 3 wt % catalyst.

**Table 7.5** Influence of Si/Al ratio on the initial reaction rate at constant pore 5 nm diameter

Si/Al	Initial reaction rate ( $\times 10^4 \text{ mol min}^{-1} \text{ g}^{-1}$ )	Glucufuranosides yield (%)	Glucopyranosides yield (%)
14	2.7	55	42
26	3.13	61	33
50	3.68	39	59

Data from Climent *et al.*<sup>[44]</sup>

from those observed with zeolites for similar operating conditions. A nearly complete glucose conversion is obtained after 4 h of reaction.

Two important features were particularly relevant. The first one is that, at a constant pore diameter of 5 nm, the activity increases on increasing the Si/Al ratio, and with increasing hydrophobicity of the catalysts, as already reported for beta zeolites as catalysts (Table 7.5).

The second one is that the activity increases with increasing pore diameter whereas the ratio glucufuranosides/glucopyranosides decreases (Table 7.6), once again in accordance with a lower diffusion of the glucopyranosides compared with the glucufuranosides.

In our research group the glycosylation reaction between D-glucose and *n*-butanol was investigated over a dealuminated H-Y zeolite with a Si/Al ratio of 15.<sup>[45, 46]</sup> In this way, butyl-D-glucufuranosides and glucopyranosides are readily synthesized, at temperatures from 90 to 110 °C, with 6 wt% of catalyst and with a butanol/glucose ratio from 5 to 40.

From the systematic study of the glycosylation reaction, a kinetic scheme involving both consecutive and competitive steps has been proposed (Figure 7.1). Butyl-D-glucufuranosides and butyl-D-glucopyranosides are primary products, butyl-D-glucufuranosides being then quantitatively converted into their pyranoside form.

Another important feature between H-Y and H-Beta zeolites is the difference observed for the  $\beta/\alpha$  ratio of butyl-D-glucopyranosides versus D-glucose conversion (Figure 7.2). The  $\beta/\alpha$  ratio of pyranosides is higher for H-Y (Si/Al = 15) than for H-Beta (Si/Al = 12.5) up to a glucose conversion of 80%. At complete glucose conversion, the thermodynamic  $\beta/\alpha$  ratio of 0.5 is obtained.

As for hydrolysis of disaccharides maltose and cellobiose, the  $\beta/\alpha$  anomeric ratios are in agreement in terms of stereoelectronic effects which are, according to the

**Table 7.6** Influence of pore diameter on the initial reaction rate at constant Si/Al ratio

Pore diameter (nm)	Initial reaction rate ( $\times 10^4 \text{ mol min}^{-1} \text{ g}^{-1}$ )	Glucufuranosides yield (%)	Glucopyranosides yield (%)
5.3	3.68	39	59
4.5	2.30	58	36
2.5	1.38	55	25

Data from Climent *et al.*<sup>[44]</sup>

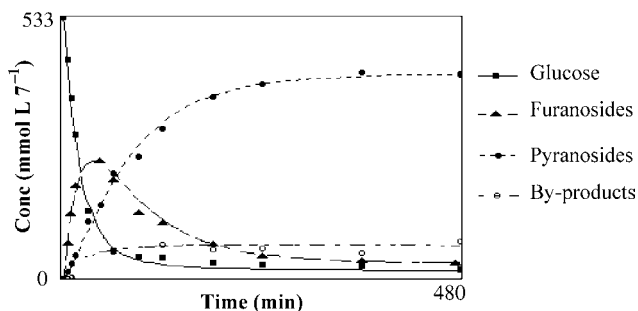


**Figure 7.1** AnaCin modelling plot for glycosylation of D-glucose (4.8 g) with *n*-butanol (50 ml) in the presence of freshly calcined H-Y zeolite with a Si/Al ratio of 15 (6 wt %) at 383 K and 1000 rpm agitation speed. Reprinted from *J. Catal.*, Vol. 185, Chapat *et al.*, pp. 445–453, Copyright 1999, with permission from Elsevier

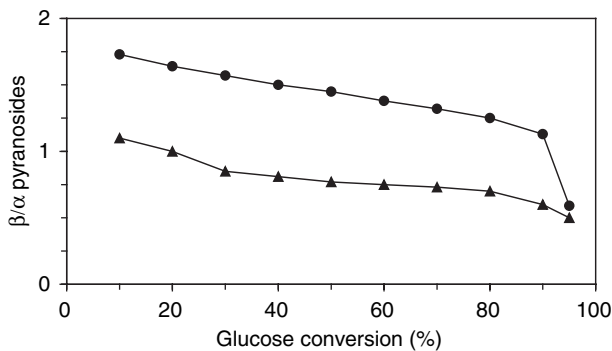


**Figure 7.2** Plot of the  $\beta/\alpha$  ratio of butyl-D-glucopyranosides versus D-glucose conversion in the presence of different catalysts [ $\bullet$ , H-Y (Si/Al = 15);  $\blacktriangle$ , H-Beta (Si/Al = 12.5)] for glycosylation of glucose (4.8 g) with *n*-butanol (50 ml) at 383 K and 1000 rpm agitation speed. Reprinted from *J. Catal.*, Vol. 185, Chapat *et al.*, pp. 445–453, Copyright 1999, with permission from Elsevier

principle of microreversibility, of the same nature as those reported for the reverse reaction, i.e. hydrolysis of alkyl-D-glucopyranosides.<sup>[47]</sup>

### 7.7.2 SYNTHESIS OF LONG-CHAIN ALKYL-D-GLUCOSIDES

In addition, it should also be noted that this reaction works with long alkyl chain fatty alcohols, *n*-octanol, *n*-dodecanol and hexadecanol with high yields in the corresponding alkyl-D-glucopyranosides. For example, it was shown by Corma *et al.* that over a H-Beta zeolite with a Si/Al ratio of 13, octyl-D-glucosides were obtained in 90% yield after 6 h at 120 °C. Dodecyl-D-glucosides were obtained in a similar yield after 8 h.<sup>[48]</sup> In parallel, we have shown that, with *n*-hexadecanol, a yield of 60% in hexadecyl-D-glucosides was obtained after 6 h of reaction time over a H-Y zeolite with a Si/Al ratio of 15 at 110 °C, but with incomplete glucose conversion.<sup>[46]</sup>

It then appears that the direct synthesis of alkyl-D-glucosides starting from glucose and fatty alcohols is easily achieved in the presence of acid large-pore zeolites as catalysts. The amount of oligomers is significantly reduced compared with the homogeneous catalysed reaction, thus allowing a nearly quantitative yield of alkyl-D-glucosides under mild operating conditions. The selectivity to the  $\beta$ -anomer is higher for H-Y compared with H-Beta zeolite. The kinetic reaction scheme proposed with HY zeolites involves both consecutive and competitive steps and accounts for the higher  $\beta/\alpha$  ratio observed with Y-zeolites as due to the result of stereoelectronic effects associated with the shape selective properties of the catalysts in the transition states. The factors of reactivity invoked in the direct glycosylation reaction are of the same nature as those involved in the reverse reaction, i.e. hydrolysis of alkyl-D-glucopyranosides, thus allowing one to consider for the first time, the principle of microreversibility for reactions catalysed by solids, and, finally, such a process could be easily transposed to the synthesis of long chain alkyl-D-glucosides.

## 7.8 SYNTHESIS OF ALKYL-D-FRUCTOSIDES

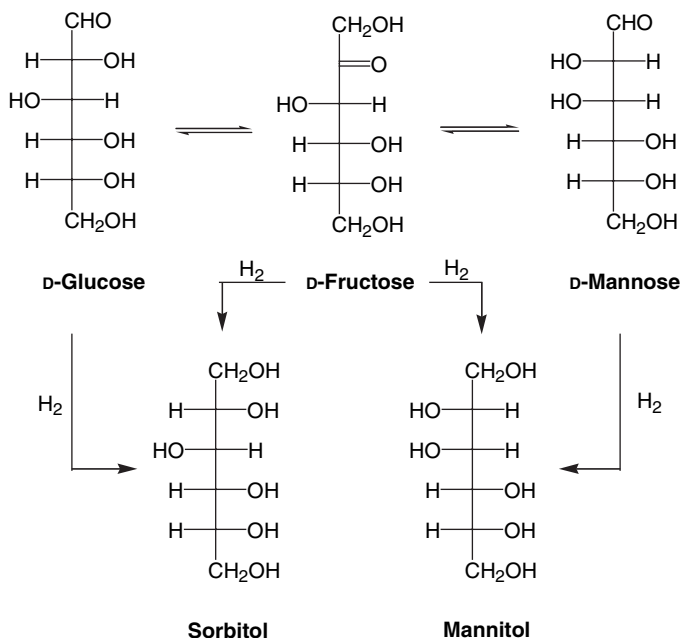
In fructose alkylation, van der Heiden *et al.* have shown that MCM-41 was the catalyst of choice. With short alkyl chain alcohols, quantitative conversions were obtained.<sup>[49]</sup> In the case of alkyl-fructosides, 5 h of reaction time at reflux of the competent alcohol were required. Only the two kinetically favoured fructofuranosides were formed. With butanol, the reaction took place at a slightly higher temperature and required a longer reaction time, thus allowing the formation of the  $\beta$ -D-fructopyranoside isomer besides the two fructofuranosides.

With long alkyl chain alcohols, the conversion of fructose with 1-octanol to octylfructosides was only 60%, but with 1-decanol and 1-dodecanol the conversion dropped to 40% due to competing of fructose ring opening. However, in 1,2-dimethoxyethane as solvent, a yield in dodecyl-D-fructosides of 60% was obtained after 1.5 h at 83 °C.

Fructose-containing disaccharides, such as leucrose, isomaltulose and lactulose, can also be alkylated over H-MCM-41 without any cleavage of the glycosidic bond between the two sugar units.<sup>[50]</sup> MCM-41 can be used as catalyst, yields in alkyl leucosides, isomaltulosides and lactulosides are obtained in 24 h at reflux of short alkyl chain (C<sub>2</sub>-C<sub>4</sub>) alcohols with yields of 80–99%.

## 7.9 HYDROGENATION OF GLUCOSE

As recently reviewed by Abbadi and van Bekkum,<sup>[51]</sup> the most important carbohydrate hydrogenation reaction is the transformation of glucose into sorbitol (Scheme 7.4). The world production of sorbitol is around 650 000 tons year<sup>-1</sup>.<sup>[52]</sup> Sorbitol is used in many fields, pharmaceuticals, foods, cosmetics, chemical industry, and is the starting material for the preparation of vitamin C.



**Scheme 7.4** Hydrogenation routes to sorbitol and mannitol.

In general, metal-based (Ni, Pt, Ru) catalysts are used for hydrogenation of glucose. For example, a new process has been recently developed in a 1.5 m<sup>3</sup> gas–liquid–solid three-phase Airlift Loop Reactor over Raney nickel catalysts.<sup>[53]</sup> As compared with a Stirred Tank Reactor process, some improvements have been obtained, namely, shorter reaction time, higher yield in sorbitol and less than 1% yield of mannitol.

When supported, inert carriers such as carbon,  $\gamma$ -alumina or silica are generally used. However, due to their acid–base properties, zeolitic materials as supports are capable of introducing a second functionality to the catalytic system. For example, after 16 h of reaction time in water as the solvent, at 60 °C and 7 MPa of hydrogen, D-mannitol can be produced by the simultaneous action of a Ru/Na-Y zeolite and glucose isomerase.<sup>[54]</sup> Glucose is partially isomerized into fructose over the Na-Y support and mannitol results from the hydrogenation of fructose in the ketose form, thus leading to a mixture of sorbitol and mannitol (Scheme 7.4). A similar behaviour was also observed in the absence of glucose isomerase.<sup>[55]</sup> Depending on the acid–base properties of the zeolite as support, Sosa *et al.* have shown that glucose might be preferentially isomerized into mannose or fructose, and that mannitol was always present as hydrogenation product. For example, hydrogenation of an aqueous mixture of glucose and mannose leads to the preferential formation of mannitol. The formation of mannitol is not affected by the alkaline or alkaline earth nature of the compensating cation.<sup>[55]</sup>

However, when acidic zeolites are used as supports in the hydrogenation of aqueous solutions of disaccharides, such as sucrose, and polysaccharides, such as starch, a cooperative hydrolysis effect is observed.<sup>[56]</sup> The simultaneous hydrolysis of sucrose and hydrogenation of the two liberated monosaccharides, i.e. glucose and fructose, leads to a mixture of glucitol and mannitol in the expected ratio 3:1. For starch, consisting only of glucose units, sorbitol is the major product obtained after simultaneous hydrolysis and hydrogenation.

## 7.10 OXIDATION OF GLUCOSE

As for hydrogenation, heterogeneous catalytic oxidation of carbohydrates was essentially performed in the presence of carbon-supported metal catalysts, namely Pt, Pd or Bi-doped Pd.<sup>[57]</sup> Oxidation of glucose into gluconic acid, the worldwide production of which is around 60000 tons year<sup>-1</sup>,<sup>[52]</sup> is used in the food and pharmaceutical industry, and is produced today by enzymatic oxidation of D-glucose with a selectivity in gluconic acid close to 100%.

Ti-containing zeolites have recently appeared as selective oxidation catalysts, in particular the TS-1 catalyst.<sup>[58]</sup> TS-1 has a MFI structure with small pore dimensions so that its used is not suitable for the oxidation of carbohydrates. Several attempts have been made to incorporate Ti in MCM-41 materials in order to perform oxidation of carbohydrates.<sup>[59,60]</sup>

In the a approach by Mombarg *et al.*,<sup>[59]</sup> oxidation of disaccharides, such as trehalose and sucrose (25 mmol), was performed in 25 ml of water at 70 °C, with 100 mg of Ti-MCM-41 (7.2 μmol of Ti) and 25 g of 35 wt% H<sub>2</sub>O<sub>2</sub>, at pH = 4. After 20 h of reaction, a deep oxidation is observed leading to C<sub>1</sub>–C<sub>4</sub> mono- and dicarboxylic acids, formic acid, glycolic acid, tartronic acid and tartaric acid. The absence of selectivity is then a major drawback compared with other oxidation processes, but another drawback was identified with Ti leaching from the molecular sieve framework.

More recently, a novel method for incorporating Ti into zeolites framework was developed by Martinez Velarde *et al.*<sup>[60]</sup> to avoid Ti leaching. Indeed, in the oxidation of glucose in the presence of Ti-containing ZSM-5, Mordenite, Y-faujasite, L and MCM-41 catalysts (70 °C, reactant/catalyst mass ratio of 28.4, 30% aqueous H<sub>2</sub>O<sub>2</sub>, H<sub>2</sub>O<sub>2</sub>/substrate ratio of 1.3), no leaching of Ti was reported. Once again, several oxidation products have been identified after 3 h of reaction time; gluconic acid as the main product, and glucuronic, tartaric, glyceric and glycolic acids as overoxidation products. The highest selectivity in gluconic acid is reached for Ti-Y catalysts (27.9%) for a glucose conversion of 23.2%. Neither the conversion of glucose nor the selectivity to gluconic acid of the oxidation of glucose seems to be determined by the pore size or the Ti species of the catalysts used. Several other parameters, such as SiO<sub>2</sub>/Al<sub>2</sub>O<sub>3</sub> ratio, hydrophobicity of the materials, the Si/Ti ratio, acidity, size of counterions, microporous and mesoporosity, and ratio of the outer/inner surface ratio of the materials seem to have an influence on the investigated oxidation of glucose.



The situation was not so simple since similar results, conversion and selectivity, were obtained when comparing Ti-Y with the TiO<sub>2</sub>-P25 catalyst from Degussa. Again, Ti-free materials were also found to be active. ZSM-5, Mordenite and L zeolites were shown to have nearly comparable glucose conversions (around 30%) and gluconic acid selectivity (around 20%), whereas Y and MCM-41 zeolites were found to be less active, but more selective, particularly in the case of Y (27%). Although the activity of the Ti-free Y catalyst is lower than that of the Ti-Y catalyst, a similar selectivity in gluconic acid is obtained for both catalytic materials, but the selectivity in other acids is less over the Ti-Y catalyst.

## 7.11 CONCLUSIONS

To conclude this short survey, it appears that microporous and mesoporous materials performant catalysts may be suitable for food and nonfood transformation of carbohydrates. Their acidic or basic, as well as their hydrophilic or hydrophobic, properties can be easily modified to take into account the different parameters required for a given reaction. Significant gains in activity and product selectivity are often obtained in the reactions reported except in the oxidation of glucose.

As for other recyclable heterogeneous catalysts, zeolites and related materials can also contribute to the development of environmentally friendly processes in the synthesis of bulk and fine chemicals. The concept of a biomass refinery, capable of separating, modifying and exploiting the numerous constituents of renewable resources, is gaining worldwide acceptance today with a very broad outlook. This chapter has attempted to show that this particular area of carbohydrate chemistry is in itself very rich, both in already acquired knowledge and potential future developments.

## REFERENCES

1. Venuto, P. B. *Microporous Mater.*, **1994**, 2, 297–411.
2. Sheldon, R. A. and van Bekkum, H. (eds) In *Fine Chemicals through Heterogeneous Catalysis*, Wiley-VCH, Weinheim, **2001**, pp. 1–11.
3. Sheldon, R. A. and Blaser, H. U. *Adv. Synth. Catal.*, **2003**, 345, 413.
4. Corma, A. *J. Catal.*, **2003**, 216, 298–312.
5. Bussière, G., Nowak, P. and Cotillon, M. *Ind. Aliment. Agroindust.*, **1990**, 645–649.
6. Hahn-Hägerdal, B., Skoog, K. and Mattiasson, B. *Eur. J. Microbiol. Biotechnol.*, **1983**, 17, 344–348.
7. Masroua, A., Revillon, A., Martin, J. C., Guyot, A. and Descotes, G. *Bull. Soc. Chim. Fr.*, **1988**, 3, 561–566.
8. Satyanarayana, B., Varma, Y. B. G. *Indian J. Technol.*, **1970**, 8, 58–61.
9. Moreau, C., Durand, R., Aliès, F., Cotillon, M., Frutz, T., Théoleyre, M. A. *Ind. Crops Prod.*, **2000**, 11, 237–242.
10. Durand, R., Faugeras, P., Laporte, F., Moreau, C., Neau, M. C. and Roux, G. EP 0 797 686, **1996**; US 5, 888, 306, **1999**, Agrichimie.

11. Abasaheed, A. F., Lee, Y. Y. *Chem. Eng. Technol.*, **1995**, *18*, 440–444.
12. Moreau, C., Durand, R., Duhamet, J., Rivalier, P. *J. Carbohydr. Chem.*, **1997**, *16*, 709–714.
13. Li, S., Kirby, A. J., Deslongchamps, P. *Tetrahedron Lett.*, **1993**, *34*, 7757–7758.
14. Abbadi, A., Gotlieb, K. F., Van Bekkum, H. *Starch/Stärke* **1998**, *50*, 23–28.
15. Heinen, A. W., Peters, J. O., van Bekkum, H. *Carbohydr. Res.*, **2001**, *330*, 381–390.
16. Multon, J. L. (ed.) *Le sucre, les sucres, les édulcorants et les glucides de charge dans les I. A. A.* Lavoisier, Paris, **1992**.
17. Gandini, A., Belgacem, M. N. *Actualité Chimique*, **2002**, *November/December*, 56–61, and references therein.
18. Moreau, C. *Agro-Food-Industry Hi - Tech*, **2002**, *January/February*, 17–26.
19. Moreau, C., Belgacem, M. N., Gandini, A. *Top. Catal.*, **2004**, *27*, 11–30.
20. Moreau, C., Durand, R., Roux, A., Tichit, D. *Appl. Catal.*, *A*, **2000**, *193*, 257–264.
21. Lecomte, J., Finiels, A., Moreau, C. *Starch/Stärke*, *54*, **2002**, 75–79.
22. Wortel, T. M., Van Bekkum, H. *Recl Trav. Chim. Pays-Bas*, **1978**, *97*, 156–158.
23. Neuzil, R. W. and Priegnitz, J. W. US 4 442 285, 1984, UOP, Inc.
24. Ho, C., Ching, C. B., Ruthven, M. *Ind. Eng. Chem. Res.*, **1987**, *26*, 1407–1412.
25. Chang, C. H. US 4 692 514, **1987**, UOP, Inc.
26. Rapp, K. M. EP 0 230 250, **1988**, SüdZucker.
27. Moreau, C., Durand, R., Pourcheron, C., Razigade, S. *Ind. Crops Prod.*, **1994**, *3*, 85–90.
28. Moreau, C., Durand, R., Razigade, S., Duhamet, J., Faugeras, P., Rivalier, P., Ros, P., Avignon, G. *Appl. Catal.*, *A*, **1996**, *145*, 211–224.
29. Avignon, G., Durand, R., Faugeras, P., Geneste, P., Moreau, C., Rivalier, P., Ros, P. FR 2 670 209, **1992**; EP 0 561 928, **1996**, CEA.
30. Rivalier, P., Duhamet, J., Moreau, C., Durand, R. *Catal. Today*, **1995**, *24* 165–171.
31. Antal, M. J., Jr., Leesomboon, T., Mok, W. S., Richards, G. N. *Carbohydr. Res.*, **1991**, *217*, 71–85.
32. Sako, T., Sugeta, T., Nakazawa, N., Okubo, T., Sato, M., Taguchi, T., Hiaki, T. *J. Chem. Eng. Jpn.*, **1992**, *25*, 372–377.
33. Moreau, C., Durand, R., Peyron, D., Duhamet, J., Rivalier, P. *Ind. Crops Prod.*, **1998**, *7*, 95–99.
34. Hensen, H., Busch, P., Krächter, H. U., Tesmann, H. *Tensid. Surf. Det.*, **1993**, *30*, 116–121.
35. Mentech, J., Beck, R. and Burzio, F. In *Carbohydrates as Raw Organic Materials II Catalysis*, G. Descotes (ed.). VCH, Weinheim, **1993**, pp.185–201.
36. Hughes, F. A., Lew, B. W. *J. Am. Oil Chem. Soc.*, **1970**, *47*, 162–167.
37. Fischer, E. *Ber. Deutsch. Chem. Ges.*, **1893**, *26*, 2400–2412.
38. Straathof, A. J. J., Romein, J., van Rantwijk, F., Kieboom, A. P. G., van Bekkum, H. *Starch/Stärke*, **1987**, *39*, 362–368.
39. Straathof, A. J. J., van Bekkum, H., Kieboom, A. P. G. *Starch/Stärke*, **1988**, *40*, 229–234.
40. Corma, A., Iborra, S. In *Fine Chemicals through Heterogeneous Catalysis*, R. A. Sheldon and H. van Bekkum (eds), Wiley-VCH, Weinheim, **2001**, pp. 257–274, and references therein.
41. Hölderich, W. F. and van Bekkum, H. In *Introduction to Zeolite Science and Practice*, Studies in Surface Science and Catalysis, H. van Bekkum, E. M. Flanigen, P. A. Jacobs and J. C. Jansen (eds). Elsevier, Amsterdam, **2001**, Vol. 137, pp. 821–910.
42. Corma, A., Iborra, S., Miquel, S., Primo, J. *J. Catal.*, **1996**, *161*, 713–719.
43. Cambor, M. A., Corma, A., Iborra, S., Miquel, S., Primo, J., Valencia, S. *J. Catal.*, **1997**, *172*, 76–84.
44. Climent, M. J., Corma, A., Iborra, S., Miquel, S., Primo, J., Rey, F. *J. Catal.*, **1999**, *183*, 76–82.

45. Chapat, J. F., Moreau, C. *Carbohydr. Lett.*, **1998**, 3, 25–30.
46. Chapat, J. F., Finiels, A., Joffre, J., Moreau, C. *J. Catal.*, **1999**, 185, 445–453.
47. Le Strat, V., Moreau, C. *Catal. Lett.*, **1998**, 51, 219–222.
48. Corma, A., Iborra, S., Miquel, S., Primo, J. *J. Catal.*, **1998**, 180, 218–224.
49. van der Heiden, A. M., van Rantwijk, F., van Bekkum, H. *J. Carbohydr. Chem.*, **1999**, 18, 131–147.
50. van der Heiden, A. M., Tsz Chung lee, van Rantwijk, F., van Bekkum, H. *Carbohydr. Res.*, **2002**, 337, 1993–1998.
51. Abbadi, A. and van Bekkum, H. In *Fine Chemicals through Heterogeneous Catalysis*, R. A. Sheldon and H. van Bekkum (eds). Wiley-VCH, Weinheim, **2001**, pp. 380–388.
52. Lichtenthaler, F. W. *Acc. Chem. Res.*, **2002**, 35, 728–737.
53. Wen, J-P., Wang, C-L., Liu, Y-X. *J. Chem. Technol. Biotechnol.*, **2004**, 79, 403–406, and references therein.
54. Ruddlesden, J. F., Stewart, A. *J. Chem. Res. (S)*, **1981**, 378–379.
55. Sosa, R. C., Repriels, H. and Jacobs, P. A. In *Proceedings of the XIth Iberoamerican Symposium on Catalysis*, F. Cossio, O. Benudez, G. Del Angel and R. Gomez (eds). Guanajuato, Mexico, **1988**, pp. 1391–1398.
56. Jacobs, P., Hinnekens, H. EP 0 329 923, 1989, Synfina-Oleofina S. A.
57. Besson, M. and Gallezot, P. In *Fine Chemicals through Heterogeneous Catalysis*, R. A. Sheldon and H. van Bekkum (eds). Wiley-VCH, Weinheim, **2001**, pp. 507–518.
58. Corma, A. In *Fine Chemicals through Heterogeneous Catalysis*, R. A. Sheldon and H. van Bekkum (eds). John Wiley & Sons, Ltd, Weinheim, **2001**, pp. 80–91, and references therein.
59. Mombarg, E. J. M., Osnabrug, S. J. M., Van Rantwijk, F. and van Bekkum, H. In *Heterogeneous Catalysis and Fine Chemicals*, Studies in Surface Science and Catalysis, H. U. Blaser, A. Baiker and R. Prins (eds). Elsevier, Amsterdam, **1997**, Vol. 108, pp. 385–390.
60. Martinez Velarde, A., Bartl, P., Niessen, T. E. W., Hölderich, W. F. *J. Mol. Catal., A*, **2000**, 157, 225–233.

---

# 8 One-pot Reactions on Bifunctional Catalysts

---

MICHEL GUISET<sup>a</sup> AND MATTEO GUIDOTTI<sup>b</sup>

<sup>a</sup>*Faculté des Sciences Fondamentales et Appliquées, Université de Poitiers, UMR CNRS 6503, 40 av. du Recteur Pineau, 86022 Poitiers Cedex, France*

<sup>b</sup>*CNR – Istituto di Scienze e Tecnologia Molecolari, via Venezian 21, 20133 Milano, Italy*

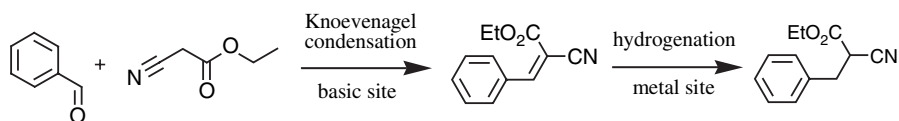
## CONTENTS

8.1	INTRODUCTION . . . . .	157
8.2	EXAMPLES . . . . .	158
8.2.1	One-pot transformations involving successive hydrogenation and acid–base steps . . . . .	158
8.2.2	One-pot transformations involving successive oxidation and acid–base steps . . . . .	166
	REFERENCES . . . . .	168

## 8.1 INTRODUCTION

The environmental and economical benefits of one-pot catalytic fine chemical syntheses, in which various successive chemical steps are accomplished in the same reaction vessel, generally over a bifunctional (or multifunctional) catalyst, are obvious. The reduction in the number of synthetic and separation steps has various positive consequences: environmentally more sustainable processes (higher atom economy and lower environmental factors), lower operating costs, lower production of wastes and in general an improvement in the safety conditions.<sup>[1–3]</sup> The environmental advantages are still more remarkable when the transformation of renewable raw materials, such as mixtures of natural terpenes or carbohydrates are concerned.

The simplest way is to carry out the successive steps, not only in the same pot, but also under the same conditions. However, this is not always possible. Indeed, high yields in the desired product can be obtained only when the last step is quasi irreversibly shifted towards the formation of this product, when, sometimes, the operating conditions satisfying this condition favour the formation of large amounts of undesired products. In this case, the one-pot reaction is carried out in two stages



Scheme 8.1

under different optimized conditions. An example of that is presented in Goettmann *et al.*<sup>[4]</sup> The synthesis of a saturated cyanoester is carried out over a Rh-grafted amino-containing mesoporous silica in two successive steps under different conditions (Scheme 8.1): (1) 1 h under Ar, to allow the Knoevenagel condensation and to avoid the undesired reduction of benzaldehyde; (2) 12 h under 7 bar of hydrogen for the reduction of the unsaturated intermediate.

Once the multi-step reaction sequence is properly chosen, the bifunctional catalytic system has to be defined and prepared. The most widely diffused heterogeneous bifunctional catalysts are obtained by associating redox sites with acid–base sites. However, in some cases, a unique site may catalyse both redox and acid successive reaction steps. It is worth noting that the number of examples of bifunctional catalysis carried out on microporous or mesoporous molecular sieves is not so large in the open and patent literature. Indeed, whenever it is possible and mainly in industrial patents, amorphous porous inorganic oxides (e.g.  $\gamma$ - $\text{Al}_2\text{O}_3$ ,  $\text{SiO}_2$  gels or mixed oxides) are preferred to zeolite or zeotype materials because of their better commercial availability, their lower cost (especially with respect to ordered mesoporous materials) and their better accessibility to bulky reactant fine chemicals (especially when zeolitic materials are used). Nevertheless, in some cases, as it will be shown, the use of ordered and well-structured molecular sieves leads to unique performances.

In the following section, some relevant examples of bifunctional catalytic systems hosted in or supported on either microporous or mesoporous materials are reported. In Tables 8.1 and 8.2 there is a list of the catalysts tested in vapour-phase fixed bed reactor and in liquid-phase batch reactor, respectively.

## 8.2 EXAMPLES

### 8.2.1 ONE-POT TRANSFORMATIONS INVOLVING SUCCESSIVE HYDROGENATION AND ACID–BASE STEPS

A widely studied example of this kind is the synthesis of methyl isobutyl ketone (MIBK, used as a solvent for inks and lacquers) from acetone. The former was previously prepared from the latter through a catalytic three-step process: base-catalysed production of 4-hydroxy-4-methylpentan-2-one, acid dehydration into mesityloxide (MO), then hydrogenation of MO on a Pd catalyst. Since acetone aldolization occurs through acid catalysis as shown over a H-MFI zeolite at 433 K (MO is the main reaction product, the aldolization product being rapidly dehydrated<sup>[5]</sup>), it is possible, by associating with the acid catalyst a hydrogenation phase,

**Table 8.1** One-pot multistep reactions in vapour-phase fixed bed reactor

Catalyst	Reactant	Desired product	Mechanism	C <sup>a</sup> (%)	S <sup>b</sup> (%)	Conditions <sup>e</sup>	Ref.
0.5 %Pd/ZSM-5	Acetone	MIBK	Acid + dehydration + hydrogenation	28	98	41 bar; 453 K H <sub>2</sub> /acetone = 0.6 WHSV = 3.8 h <sup>-1</sup>	[6]
1 % Pd/Cs-H-ZSM-5	Acetone	MIBK	Acid + dehydration + hydrogenation	42	82	1 bar; 523 K H <sub>2</sub> /acetone = 1 WHSV = 2 h <sup>-1</sup>	[7]
0.03 % Pt/H-ZSM-5				—	80 at C = 10	1 bar; 433 K H <sub>2</sub> /acetone = 0.33	[8]
0.5 % Pt/H-[Al]ZSM-5				—	57 at C= 10	1 bar; 433 K H <sub>2</sub> /acetone = 0.33	[36]
0.9 % Pd/SAPO-11	Acetone	MIBK	(Acid or base) + dehydration + hydrogenation	11	72	1 bar; 473 K H <sub>2</sub> /acetone = 1 WHSV = 0.7 h <sup>-1</sup>	[9]
0.2 % Pd/H-FAU	Cyclohexanone	Cyclohexyl Cyclohexanone	Acid + dehydration + hydrogenation	30	75	1 bar; 473 K H <sub>2</sub> /acetone = 0.33	[10]
0.5 % Pd/H-FAU	Acetophenone	1,3-diphenylbutan- 1-one	Acid + dehydration + hydrogenation	10	27	1 bar; 523 K H <sub>2</sub> /acetophenone = 0.25	[11]
0.5 % Pd/AlPO <sub>4</sub> -31	<i>n</i> -Butyraldehyde	2-Ethylhexanal	Acid + dehydration + hydrogenation	50	10	1 bar; 473 K WHSV = 1.2 h <sup>-1</sup>	[14]
0.5 % Pd/KX				70	91	1 bar; 423 K H <sub>2</sub> /aldehyde = 1 WHSV = 0.31 h <sup>-1</sup>	[13]
0.5 % Pd/MnAPSO-31	<i>n</i> -Butyraldehyde + acetone	Heptan-2-one	Acid + dehydration + hydrogenation	70	70	1 bar; 423 K aldehyde/ketone = 0.25; WHSV = 1.6 h <sup>-1</sup>	[14]

(Continued)

**Table 8.1** (Continued)

0.5 % Pd/MnAPSO-31	Acetaldehyde + acetone	Pentan-2-one	Acid + dehydration + hydrogenation	20	89(11) <sup>c</sup>	1 bar; 423 K aldehyde/ketone = 0.25 WHSV = 1.6 h <sup>-1</sup>	[14]
0.5 % Pd/2.3 % Ce/B <sub>2</sub> O <sub>3</sub> -SiO <sub>2</sub> zeolite	3-Hydroxy-2-methylbutan-2-one	MIBK	Dehydration + hydrogenation	>99	95	1 bar; 648 K H <sub>2</sub> /ketone = 10 WHSV = 2 h <sup>-1</sup>	[15]
3.4 % Cu/B <sub>2</sub> O <sub>3</sub> -SiO <sub>2</sub> zeolite	Styrene oxide	2-Phenylethanol	Isomerization + hydrogenation	>99	85	1 bar; 523 K WHSV = 1.5 h <sup>-1</sup>	[16]
1 % Pd/2 % Ce/Na-ZSM-5	$\alpha$ -Limonene	<i>p</i> -Cymene	Isomerization + dehydrogenation	>99	80	Total pressure = 1 bar Partial pressure limonene = 160 mbar; 523 K N <sub>2</sub> carrier gas WHSV = 1.3 h <sup>-1</sup>	[20]
Pd/Ce/Na-ZSM-5	Mixture of dipentene	<i>p</i> -Cymene	Isomerization + dehydrogenation	(70) <sup>d</sup>	—	1 bar; 523 K N <sub>2</sub> carrier gas WHSV = 1.3 h <sup>-1</sup>	[21]

<sup>a</sup>Conversion (%) of reactant.<sup>b</sup>Selectivity (%) to desired product.<sup>c</sup>in parentheses, selectivity to MIBK.<sup>d</sup>global yield to *p*-cymene.<sup>e</sup>all ratios are mol/mol.

MIBK, methyl isobutyl ketone; WHSV, weight hourly space velocity.

**Table 8.2** One-pot multistep reactions in liquid-phase batch reactor

Catalyst	Reactant	Desired product	Mechanism	C <sup>a</sup> (%)	S <sup>b</sup> (%)	Conditions <sup>e</sup>	Ref.
Cu/MFI	1-Propanamine	1-Propanamine- <i>N</i> -(1-propylidene)	Dimerization + dehydrogenation	82	52	66 mbar propanamine 1.3 bar He; 573 K; 2 h gradientless recirculating batch reactor	[22]
0.7 % Pd occluded in SAPO-11	Acetone	MIBK	(Acid or base) + dehydration + hydrogenation	31	84	50 ml acetone 37 bar; 473 K; 4 h H <sub>2</sub> /acetone = 1 Parr reactor; no solvent	[9]
3 % Ru/H-USY	Corn starch	D-glucitol	Hydrolysis + hydrogenation	>99	96	25 % solution in H <sub>2</sub> O 55.2 bar; 453 K; 0.6 h Parr autoclave	[17]
Rh(PNBD)- NH <sub>2</sub> -MCM41	Benzaldehyde + ethylcyanoacetate	Ethyl 2-cyano- 3-phenylpropionate	Base + hydrogenation	(85) <sup>c</sup>	—	1 h under Ar + 12 h under H <sub>2</sub> (7 bar)	[4]
3 % Ir/H-BEA	Citronellal	Menthol	Cyclization + hydrogenation	99	95 (75) <sup>d</sup>	4 h under N <sub>2</sub> 6 h under H <sub>2</sub> (8 bar); 353 K cyclohexane solvent autoclave	[18]
3 % Ni/ Al-MCM-41	Citronellal	Menthol	Hydrogenation + cyclization + hydrogenation	>99	90 (65) <sup>d</sup>	5 bar; 343 K; 5 h toluene solvent Parr autoclave	[19]
Mg(II)Mn(III) AlPO-36	Cyclohexanone + O <sub>2</sub> (air) + NH <sub>3</sub>	ε-Caprolactam	Oxidation + acid oximation + acid rearrangement	23	45	50 g cyclohexanone Cyclohexanone/O <sub>2</sub> = 3 Cyclohexanone/NH <sub>3</sub> = 0.33; 35 bar; 328 K 20 h; no solvent	[23]
Ti,Al-MCM-41; Ti-BEA	Linalool	Furan and pyran hydroxy esters	Epoxidation + ring closure	80	>99	MeCN solvent TBHP/linalool = 1.1 1 bar; 353 K; 24 h glass batch reactor	[24]

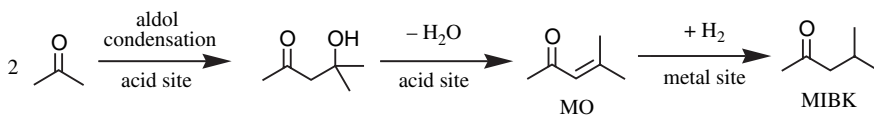
(Continued)



**Table 8.2** (Continued)

Ti-MCM-41	$\alpha$ -Terpineol	2-Hydroxy-1,4-cineol	Epoxidation + ring closure	90	45	MeCN solvent TBHP/ $\alpha$ -terpineol = 1.1 1 bar; 353 K; 24 h	[25]
Ti,Al-BEA	Isopulegol	Substituted tetrahydrofuran	Epoxidation + ring closure	54	61	acetone solvent H <sub>2</sub> O <sub>2</sub> /isopulegol = 1 1 bar; 333 K; 6 h	[26]
Ti,Al-BEA	<i>p</i> -Menth-6-ene-2,8-diol	2,6-Dihydroxy-1,4-cineol	Epoxidation + ring closure	90	95	acetone/CH <sub>2</sub> Cl <sub>2</sub> solvent H <sub>2</sub> O <sub>2</sub> /isopulegol = 1 1 bar; 333 K; 6 h	[26]
Organically modified Ti-MCM-41	<i>cis</i> -4-Hexen-1-ol	Tetrahydro-2-furan-1-ethanol	Epoxidation + ring closure	92	>99	H <sub>2</sub> O solvent, triphase TBHP/substrate = 1 1 bar; 333 K; 12 h	[27]
Ti,Al-MCM-41	$\alpha$ -Pinene	1,2-Pinanediol	Epoxidation + epoxide opening	9	72	chloroform solvent TBHP/pinene=0.33 1 bar; 328 K; 5 h	[32]
Ti-BEA	Camphene	Camphyl aldehyde	Epoxidation + epoxide opening		92	MeCN solvent H <sub>2</sub> O <sub>2</sub> /camphene=0.5 1 bar; 343 K; 1 h	[28]
Ti-HMS	$\alpha$ -Pinene	Campholenic aldehyde	Epoxidation + epoxide opening	30	80	MeCN solvent TBHP/pinene = 1 1 bar; 350 K; 24 h	[33]
Ti-MCM-41	Citronellal	Isopulegol epoxide	Cyclization + oxidation	>99	68	6 h in PhMe 18 h in PhMe + MeCN + TBHP; 1 bar; 363 K	[35]

<sup>a</sup>Conversion (%) of reactant.<sup>b</sup>Selectivity (%) to desired product.<sup>c</sup>Global yield to desired product.<sup>d</sup>Selectivity to the desired (–)-menthol isomer.<sup>e</sup>All ratios are mol/mol.MeCN, acetonitrile; PhMe toluene; TBHP, *tert*-butyl hydroperoxide.



Scheme 8.2

to synthesize MIBK in one apparent step (Scheme 8.2). Most of the studies have been carried out in gas phase by using fixed-bed reactors.

Excellent selectivity to MIBK (98%) is obtained on a 0.5% Pd/HMFI in H<sub>2</sub> stream at 453 K at 29% conversion,<sup>[6]</sup> but the highest yield value so far has been obtained on a 1% Pd/Cs-HMFI catalyst at 523 K under H<sub>2</sub>, with a selectivity to MIBK of 82% at an acetone conversion of 42%.<sup>[7]</sup> The use of Pd supported on other zeolites, such as H-FAU, gives rise to similar conversions, but poorer selectivities (20–30%). The main by-products are propane and 2-methylpentane resulting from three-step transformations of acetone and MIBK, respectively (C=O hydrogenation, dehydration and C=C hydrogenation). For this reason, Pd, which is more selective for the desired hydrogenation of the C=C rather than of the C=O double bonds, is generally chosen. In addition, diisobutyl ketone (DIBK) may also result from trimeric condensation of acetone and was shown to be responsible for the catalyst deactivation.<sup>[8]</sup> However, its formation is minimized on MFI thanks to the narrowness of the zeolite channels, whereas over nonzeolitic catalysts (e.g. Pd/γ-Al<sub>2</sub>O<sub>3</sub>), large amounts of DIBK are obtained<sup>[7]</sup>. Also, Pd supported on aluminophosphate molecular sieves, thanks to their tunable acidity and basicity features, are suitable systems for such a transformation. A good selectivity to MIBK (72%), though at low conversion values (11%), is achieved on Pd/SAPO-11 material. Higher activities, more condensation products and less light hydrocarbons are obtained on the more basic support.<sup>[9]</sup> Tests carried out in liquid-phase batch reactor on a series of catalysts in which Pd was loaded by different techniques (impregnation, ion-exchange or occlusion during synthesis) show that a very uniform distribution of Pd particles is essential to assure the necessary proximity between acid–base and hydrogenation sites and therefore to minimize the formation of undesired products.<sup>[9]</sup>

Similar Pd-containing acidic zeolites were also applied to the vapour-phase synthesis of bulkier ketones, such as cyclohexylcyclohexanone (a precursor of *o*-phenylphenol, an important wide spectrum preservative) from cyclohexanone<sup>[10]</sup> or 1,3-diphenylbutan-1-one (an ingredient for plastifying agents) from acetophenone.<sup>[11]</sup> For these syntheses, a H-FAU-based catalyst (with three-dimensional large pore system) is the catalyst of choice because it is more active and more selective than those based on MOR (one-dimensional large pore) or MFI (three-dimensional average pore) zeolites. On a 0.2% Pd/H-FAU a selectivity to cyclohexylcyclohexanone of 75% at a cyclohexanone conversion of 30% is obtained.<sup>[10]</sup>

Otherwise, by impregnating a Pd precursor onto a basic K-exchanged FAU zeolite a highly selective bifunctional catalyst is obtained for the low-pressure one-step synthesis of 2-ethylhexanal (a component of perfumes and fragrances) from *n*-butyraldehyde and H<sub>2</sub> in a fixed-bed reactor.<sup>[12,13]</sup> Under optimum reaction

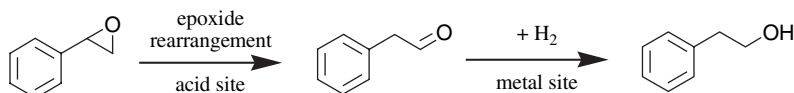
conditions, over a 0.5 % Pd/KX zeolite, 2-ethylhexanal is produced with 91 % selectivity at 70 % conversion. Once again, the zeolitic basic materials show better performances than nonzeolitic ones (under the same conditions 0.5 % Pd/MgO displays a maximum *n*-butyraldehyde conversion of 8 %).

It is worth noting that almost with all of the above-mentioned catalysts a very important loss in activity with the time-on-stream (TOS) can be observed, such a behaviour being more marked when the final product is a bulky ketone. This decrease in activity is ascribed to the strong retention of heavy reaction products inside the zeolite pores ('coke' precursors) as well as to a sintering of the metal particles, owing to the presence of water resulting from the dehydration reaction<sup>[10]</sup>.

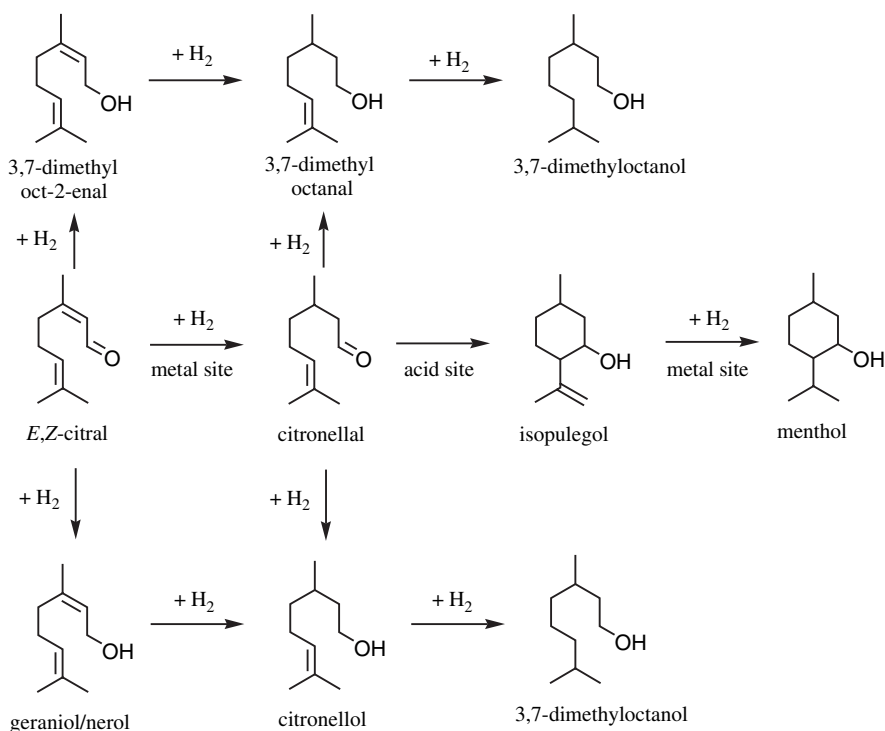
Pd-containing aluminophosphate molecular sieves have been used to carry out crossed aldol condensations between an aldehyde and a ketone by using a 0.5 % Pd/MnAPSO-31 catalyst in a vapour-phase fixed bed reactor.<sup>[14]</sup> Thanks to the excess of the ketone with respect to the aldehyde (4:1), it is possible to get high selectivity to the desired product, i.e. 70 % of heptan-2-one from *n*-butyraldehyde and acetone and 89 % of pentan-2-one from acetaldehyde and acetone, the major by-product being, in both cases, MIBK from acetone self-condensation.

Furthermore, Pd or Cu/ alumino- and borosilicates pentasil zeolites are suitable for catalysing, in one apparent, step the successive dehydration of  $\alpha$ -hydroxyketones to  $\alpha$ ,  $\beta$ -unsaturated ketones and their hydrogenation to unsymmetrical saturated ketones.<sup>[15]</sup> Thus, on a Pd-containing Ce/B-MFI zeolite 3-hydroxy-2-methylbutan-2-one is converted quantitatively to MIBK in a fixed bed reactor at 648 K under H<sub>2</sub>. Under similar conditions, nonzeolitic catalysts, e.g. Pd-containing alumina, show relatively poor performances. The same kind of catalyst displays also interesting results in the consecutive acid-catalysed rearrangement and hydrogenation reaction of terminal aromatic epoxides (Scheme 8.3).<sup>[16]</sup> In particular, over a Cu/borosilicate pentasil zeolite, 2-phenylethanol (a fragrance with a sweet and floral odour) is obtained in high yields (up to 85 %) from styrene oxide.

The bifunctional properties of highly dispersed metal-modified zeolites have also been applied to the transformation of raw materials obtained from renewable sources, such as the one-pot conversion of polysaccharides to polyhydric alcohols, which are important ingredients in pharmaceutical and alimentary use.<sup>[17]</sup> In this process the cleavage of the polysaccharide (e.g. corn starch, sucrose or lactose) by hydrolysis on the acidic sites of the zeolite and the following hydrogenation of the aldehydes and ketones on the metal, such as Ru, Co, Cu or Ni, occur in one apparent step. In particular, a 25 wt % aqueous suspension of corn starch is converted in an autoclave at 453 K and 55 bar of H<sub>2</sub> and in the presence of a 3 % Ru-exchanged H-USY zeolite, after 35 min into a product mixture containing 96 % D-glycitol, 1 % D-mannitol and 2 % xylitol. In this case, the Brønsted acidity required for the



Scheme 8.3



Scheme 8.4

hydrolysis of the polymer could be provided by the outer zeolite surface, whereas the hydrogenation step takes place both on the external surface and within the supercages of the FAU zeolite which are accessible to glucose.

Recently, great attention has been paid to the selective synthesis of menthols (employed in flavouring and pharmaceutical applications) directly from either citronellal or citral in a one-pot process on a bifunctional catalyst (Scheme 8.4). A 3% Ir-impregnated H-BEA zeolite was shown to catalyse both the consecutive acid-catalysed cyclisation of citronellal into isopulegol and the Ir-catalysed hydrogenation of the unsaturated terpenic alcohol.<sup>[18]</sup> To improve the citronellal conversion, the reaction is conducted under  $N_2$  for the first 4 h, after which  $H_2$  is added. In this way, 95% selectivity for the menthol isomers [of which 75% is the desired (–)-menthol] and complete citronellal conversion is achieved after 30 h. The authors underline the high productivity of this catalyst, since up to 17 g of menthol can be obtained per gram of catalyst in a single run. In addition, it is worth noting that the isomerization activity (in absence of  $H_2$ ) clearly increases when the zeolite is loaded with Ir, calcined and reduced. This indicates that not only the protonic acidity of the zeolite, but also the Lewis acidity of nonreduced Ir might play a role in the isomerization step. Furthermore, when other metals, such as Ru or Pd, are used instead of Ir under similar conditions, undesired side products are preferentially

formed: the C=O hydrogenating aptitude of Ru leads to high yields in citronellol, whereas the strong C=C hydrogenating activity of Pd leads to the dominant production of the saturated aldehyde 3,7-dimethyloctanal.

Alternatively, starting from citral, it is possible to exploit a three-step pathway: (1) hydrogenation of citral to citronellal; (2) isomerization/cyclization of citronellal to isopulegol; (3) hydrogenation of isopulegol to menthol.<sup>[19]</sup> For this purpose, a single catalyst (3 % Ni/Al-MCM-41) joins the good selectivity displayed by Ni in hydrogenating the  $\alpha,\beta$  C=C bond in citral and the good activity shown by strong Lewis/weak Brønsted sites of Al-MCM-41 required for an efficient citronellal cyclization. Such a system yields 90 % menthol at 343 K and 5 bar and produces 70–75 % racemic ( $\pm$ )-menthol in the final mixture after 300 min. Under the same conditions, a 3 % Ni/BEA catalyst gives rise to higher formation of by-products, probably via decarbonylation and cracking reactions on the zeolite acid sites, which are stronger than those in Al-MCM-41. Ni is the metal of choice, as it is more selective than Co, Ir or Pt towards the C=C bond hydrogenation (i.e. Ni forms negligible amounts of geraniol/nerol isomers), but not as active as Pd in the hydrogenation of all C=C bonds (i.e. on Ni the formation of 3,7-dimethyloctanal is virtually absent).

Another example in which bifunctional catalysts are applied to the transformation of renewable sources is the manufacture of *p*-cymene (used in the fragrance industry and as intermediate in the *p*-cresol production) from terpenes. High yields (up to 80 %) in *p*-cymene are obtained in vapour phase from  $\alpha$ -limonene by using a multifunctional zeolite system for catalysing the successive double-bond isomerization and dehydrogenation steps.<sup>[20]</sup> In this case, the preparation of the catalyst (1 % Pd/2 % Ce/Na-ZSM-5) and the process conditions have to be properly tuned to avoid secondary product formation and rapid deactivation due to coke deposition and presumably Pd agglomeration. In particular, Ce increases catalyst stability, apparently by an anchoring effect towards the Pd particles, whereas the *p*-cymene selectivity is enhanced by using a quasi neutral support (Na-ZSM-5) and careful ion-exchange and activation procedures. These catalysts can be applied directly to the conversion of mixtures of terpenes from natural sources, such as those obtained as by-product in the pulp and paper industry.<sup>[21]</sup> In this case, Pd-based systems proved to be efficient catalysts, but amorphous supports provide higher yields than zeolitic carriers (90 % versus 70 %, respectively), because of diffusion limitations and significant deposition of carbonaceous compounds over zeolites.

Likewise, *N*-(1-propylidene)-1-propanamine is obtained in liquid phase from 1-propanamine on a Cu-containing MFI zeolite, where the zeolite acidic sites selectively converts 1-propanamine to dipropanamine and the dispersed Cu metal dehydrogenates the amine to imine.<sup>[22]</sup>

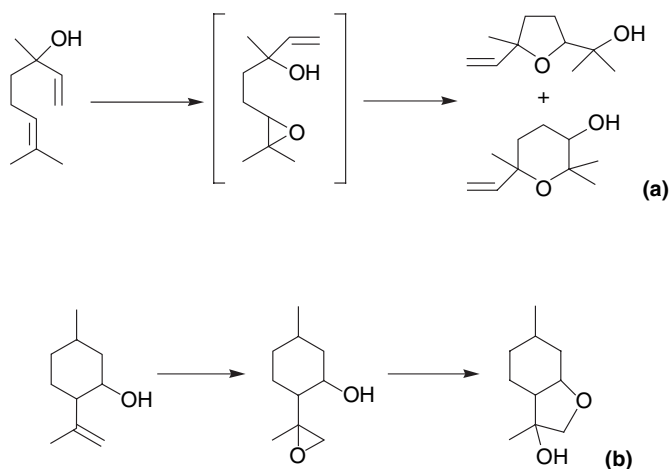
## 8.2.2 ONE-POT TRANSFORMATIONS INVOLVING SUCCESSIVE OXIDATION AND ACID-BASE STEPS

The presence of a metal in low oxidation state is not essential to have a bifunctional system. Indeed, both the acid-base and the redox-active sites can be in high a

oxidation state, as, for example, in Mg(II)Mn(III) AlPO-36 molecular sieve, where M(II) ions with (marked acidity) and M(III) (with oxidizing activity) coexist.<sup>[23]</sup> Such systems were shown to catalyse, in one apparent step, the synthesis of  $\epsilon$ -caprolactam from cyclohexanone, ammonia and oxygen, which involves three successive steps: (1) hydroxylamine formation from  $\text{NH}_3$  and  $\text{O}_2$ ; (2) conversion of cyclohexanone to the related oxime; and (3) its subsequent Beckmann rearrangement.

However, Ti-containing molecular sieves are the high-oxidation state bifunctional systems over which the larger number of organic syntheses have been carried out (Table 8.2). Over such catalysts, where both epoxidizing and acidic sites are present, it is often difficult to get high yields in the desired epoxide because of the production of large amounts of acid-catalysed by-products. Nevertheless, whenever these by-products are commercially valuable compounds, the bifunctional pathway (epoxidation and acid reaction) could be interesting for the synthetic chemist.

The most remarkable examples deal with the formation of substituted tetrahydrofurans, tetrahydropyrans or cineols, which are valuable compounds for the flavours and fragrances industry (two examples in Scheme 8.5).<sup>[24–29]</sup> These types of syntheses are run over Ti-containing large-pore zeolites (especially BEA) or mesoporous materials (mainly of the MCM-41 family) because of the bulkiness of the terpenic substrates. Indeed, Ti medium-pore zeolites (e.g. TS-1) display low conversion rates of bulky alkenes because of diffusion limitations within the micropore and of their too limited external surface.<sup>[28,30,31]</sup> In certain cases, the catalyst contains no aluminium (hence has no protonic acid sites) and the acid-catalysed cyclization is solely due to  $\text{Ti}(\delta+)$  species.<sup>[25,27]</sup> Thus, from a formal point of view, Ti centres act effectively as ‘bifunctional’ catalysts, as the two steps (oxidation and ring closure) are catalysed by the same metal site. The intermediate epoxides can be transformed through acid catalysis into either vicinal diols (by epoxide ring opening) or aldehydes (by rearrangement), such as 1,2-pinenediol or



Scheme 8.5



5. Melo, L., Rombi, E., Dominguez, J. M., Magnoux, P. and Guisnet, M. *Stud. Surf. Sci. Catal.*, **1993**, 78, 701–706.
6. Huang, T. J. and Haag, W. O. US 4339606, 1982, to Mobil Oil Corp.
7. Chen, P. Y., Chu, S. J., Chang, N. S., Chuang, T. K. and Chen, L. Y. *Stud. Surf. Sci. Catal.*, **1984**, 46, 231–239.
8. Melo, L., Giannetto, G., Alvarez, F., Magnoux, P. and Guisnet, M. *Catal. Lett.*, **1997**, 44, 201–204.
9. Yang, S. M. and Wu, Y. M. *Appl. Catal.*, A, **2000**, 192, 211–220.
10. Alvarez, F., Silva, A. I., Ramoa Ribeiro, F., Giannetto G. and Guisnet, M. *Stud. Surf. Sci. Catal.*, **1997**, 108, 609–616.
11. Lavaud, N., Magnoux, P., Alvarez, F., Melo, L., Giannetto, G. and Guisnet, M. *J. Mol. Catal.*, A, **1999**, 142, 223–236.
12. Ko, A. N., Hu, C. H. and Yeh, Y. T. *Catal. Lett.*, **1998**, 54, 207–210.
13. Ko, A. N., Hu, C. H. and Chen, J. Y. *Appl. Catal.*, A, **1999**, 184, 211–217.
14. Olson, K. D. US Patent 4701562, 1987, to Union Carbide Corp.
15. Hoelderich, W., Hupfer, L., Schneider, K., DE Patent 3702483, **1987**, to BASF.
16. Hoelderich, W., Goetz, N. and Hupfer, L. DE Patent 3801106, **1988**, to BASF.
17. Jacobs, P. A., Hinnekens, H. EP Patent 0329923, 1989.
18. Iosif, F., Coman, S., Parvulescu, V., Grange, P., Delsarte, S., De Vos, D. and Jacobs, P. *Chem. Commun.*, **2004**, 1292–1293.
19. Trasarti, A. F., Marchi, A. J. and Apesteguia, C. R. *J. Catal.*, **2004**, 224, 484–488.
20. Weyrich, P. A. and Hölderich, W. F. *Appl. Catal.*, A, **1997**, 158, 145–162.
21. Buhl, D., Weyrich, P. A., Sachtler, W. M. H. and Hölderich, W. F. *Appl. Catal.*, A, **1998**, **171**, 1–11.
22. Guidry, T. F. and Price, G. L. *J. Catal.*, **1999**, 181, 16–27.
23. Raja, R., Sankar, G. and Thomas, J. M. *J. Am. Chem. Soc.*, **2001**, 123, 8153–8154.
24. Corma, A., Iglesias, M. and Sánchez, F. *J. Chem. Soc., Chem. Commun.*, **1995**, 1635–1636.
25. Berlini, C., Guidotti, M., Moretti, G., Psaro, R., and Ravasio, N. *Catal. Today*, **2000**, 60, 219–225.
26. Bhaumik, A. and Tatsumi, T. *J. Catal.*, **1999**, 182, 349–356.
27. Bhaumik, A. and Tatsumi, T. *J. Catal.*, **2000**, 189, 31–39.
28. van der Waal, J. C., Rigutto, M. S. and van Bekkum, H. *Appl. Catal.*, A, **1998**, 167, 331–342.
29. Guidotti, M., Ravasio, N., Psaro, R., Ferraris, G. and Moretti, G. *J. Catal.*, **2003**, 214(2) 247–255.
30. Kumar, R., Pais, G. C. G., Pandey, B. and Kumar, P. *J. Chem. Soc., Chem. Commun.*, **1995**, 1315–1316.
31. Koyano, K. A. and Tatsumi, T. *Stud. Surf. Sci. Catal.*, **1997**, 105, 93–100.
32. Trong On, D., Kapoor, M. P., Joshi, P. N., Bonneviot, L. and Kaliaguine, S. *Catal. Lett.*, **1997**, 44, 171–176.
33. Suh, Y. W., Kim, N. K., Ahn, W. S. and Rhee, H. K. *J. Mol. Catal.*, A, **2001**, 174, 249–254.
34. Suh, Y. W., Kim, N. K., Ahn, W. S. and Rhee, H. K. *J. Mol. Catal.*, A, **2003**, 198, 309–316.
35. Guidotti, M., Moretti, G., Psaro, R. and Ravasio, N. *Chem. Commun.*, **2000**, 1789–1790.
36. Melo, L., Llanos, A., Mediavilla, M. and Moronta, D. *J. Mol. Catal.*, A, **2002**, 177, 281–287.





---

# 9 Base-type Catalysis

---

**DIDIER TICHIT<sup>a</sup>, SARA IBORRA<sup>b</sup>, AVELINO CORMA<sup>b</sup> AND DANIEL BRUNEL<sup>a</sup>**

<sup>a</sup>*Laboratoire de Matériaux Catalytiques et Catalyse en Chimie Organique, ENSCM, UMR CNRS 5618, 8 rue de l'Ecole Normale, 34296 Montpellier Cedex 05, France*

<sup>b</sup>*Instituto de Tecnología Química, UPV, Av. Naranjos s/n, E-46022 Valencia, Spain*

## CONTENTS

9.1 INTRODUCTION . . . . .	171
9.2 CHARACTERIZATION OF SOLID BASES . . . . .	172
9.2.1 Test reactions . . . . .	172
9.2.2 Probe molecules combined with spectroscopic methods . . . . .	174
9.3 SOLID BASE CATALYSTS . . . . .	175
9.3.1 Alkaline earth metal oxides . . . . .	175
9.3.2 Catalysis on alkaline earth metal oxides . . . . .	177
9.3.3 Hydrotalcites and related compounds . . . . .	183
9.3.4 Organic base-supported catalysts . . . . .	187
9.4 CONCLUSIONS . . . . .	195
REFERENCES . . . . .	195

## 9.1 INTRODUCTION

Results obtained since the mid 1990s in the synthesis and characterization of basic solids have resulted in a number of applications.<sup>[1–4]</sup> Solid base catalysts are now able to replace homogeneous bases in many reactions, which can also be performed at higher temperatures or in the vapour phase. This is particularly due to the development of a variety of new solids with less drawbacks than the alkaline or rare earth oxides and alkali-ion exchanged zeolites, the pioneering basic compounds, whose properties were recognized in the early 1970s. A relevant feature is the large range of basic strength now covered by the different available solids. It goes from the so-called superbasic catalysts, with basic sites stronger than  $H_0 = 37$ , to basic solids with strong and medium basicities. These include, in addition to the alkaline and rare earth oxides already mentioned, alkali metals, alkaline oxides or alkali amides loaded on alumina, alkaline earth metal oxides,<sup>[1–4]</sup> as well also imides and nitrides impregnated on alkali exchanged Y-zeolites.<sup>[1,3,4]</sup>

Materials with basic sites of medium or weak strength, or with acid–base pairs constitute the biggest family.<sup>[1]</sup> We will particularly focus on three types of materials within this family: alkaline earth metal oxides,<sup>[5–8]</sup> hydrotalcites<sup>[9,10]</sup> and organic–inorganic hybrids, such as mesoporous silica functionalized by anchored organic bases.<sup>[11,12]</sup> These solids show specific behaviours, such as the great versatility of hydrotalcites,<sup>[13–15]</sup> and the large pore opening and wide distribution of sites of different strengths of hybrid materials. These properties render them very attractive and most promising in applied catalysis.

While much effort has been put into obtaining materials with basic sites of different strength, the exact nature of the basic sites acting on those catalysts is not always known. For instance, reactions like aldolization, hydrogen transfer or double bond isomerization require either Brønsted or Lewis type sites or even the association of strong or medium basic sites with weak acid sites.<sup>[13–16]</sup> Many of these requirements (acid–base associations, versatility of the basic strength) can be accomplished by hydrotalcites and this would explain their significant development as catalysts precursors.<sup>[13–15,17]</sup>

It must also be pointed out that other basic materials have been synthesized which present no surface oxygens and hydroxyls, but other types of active sites whose exact nature remains controversial. These type of solids are, for example, impregnated imides and nitrides on zeolites and alumina, amorphous oxynitrides obtained by treatment with ammonia or aluminium orthophosphate, zirconium phosphate, aluminium vanadate or galloaluminophosphate, and KF supported on alumina.<sup>[1,3,4]</sup> One of the main advantages of these solids with respect to basic oxides is their resistance to carbon dioxide or water.

The development of base catalysis has also resulted from ongoing progress in understanding the behaviour of these materials. It is worth noting that several concurrent methods may be used to fully characterize the basicity of solids. Until recently these characterization methods, titration with indicators,<sup>[18]</sup> adsorption of acid probes followed by spectroscopic techniques, temperature-programmed desorption or XPS measurements<sup>[19–22]</sup> and catalytic tests reactions,<sup>[23–29]</sup> gave information about either the total number or the strength of the basic sites, and rarely about their nature. Nevertheless, significant improvement has been achieved using catalytic reactions and probe molecules able to give insights on both the number and strength of sites. The Knoevenagel condensation of benzaldehyde with molecules containing activated methylenic groups developed by Corma *et al.*<sup>[30]</sup> and the isomerization reaction of  $\beta$ -isophorone to  $\alpha$ -isophorone developed by Figueras *et al.*<sup>[31]</sup> are of particular interest. Besides those, the use of nitromethane as a probe molecule to monitor the basic strength of the surface of oxides with FTIR and NMR spectroscopies is also of interest.<sup>[32,33]</sup>

## 9.2 CHARACTERIZATION OF SOLID BASES

### 9.2.1 TEST REACTIONS

Catalytic test reactions have been widely used to characterize the basicity of catalysts. The decomposition of 2-methyl-3-butyn-2-ol<sup>[29]</sup> and the conversion of

isopropanol<sup>[23,24,26,27]</sup> or acetylacetone<sup>[25]</sup> were mostly used as a qualitative tool to discriminate between acidic and basic surface sites. A different approach was taken by Corma *et al.*<sup>[30]</sup> to evaluate both the number and the strength of basic sites. For doing this, the Knoevenagel condensation of benzaldehyde was carried out with a family of molecules requiring different basic strengths to abstract the proton and to form the corresponding carbanion. The kinetic rate constants thus obtained with different catalysts using benzaldehyde and molecules with activated methylenic groups, i.e. ethyl cyanoacetate ( $pK_a \leq 9$ ), ethyl acetoacetate ( $pK_a \leq 10.7$ ), ethyl malonate ( $pK_a \leq 13.3$ ), ethyl bromoacetate ( $pK_a = 16.5$ ) could be correlated with the  $pK$ s of the catalysts in order to evaluate their basic strength distribution. Moreover, a quantification of the number of sites possessing different  $pK$ s could also be done. By measuring the amount of benzoic acid necessary to completely poison the condensation reaction with the molecules having the different activated methylenic groups it was indeed possible to evaluate the number of sites in the various  $pK$  ranges. For example, the amount of benzoic acid necessary to stop the reaction of benzaldehyde and ethyl acetoacetate in the presence of calcined hydrotalcite corresponds to 12 mmol basic site  $m^{-2}$ , which is in agreement with determinations performed using Hammet indicators. This method is therefore a useful tool to evaluate the number of basic sites with different strengths.

One of the main drawbacks generally mentioned when using catalytic test reactions to evaluate the basicity of solids is the interaction between acid and basic sites, thus leading to somewhat biased results. Indeed, in the case of a reaction for which the driving forces are both acidic or electrophilic and basic or nucleophilic activations for the formation of the transition state, the reaction is catalysed by the cooperative action of both acid and base sites. Hence, the catalytic activity cannot reflect either the acid or base strength of each type of catalytic site. Moreover, in the case of bimolecular test reactions, the competitive adsorption between the two substrates could lead to unreliable results when catalysts of very different basic strengths are compared. In a competitive mechanism the adsorption coefficients and the concentrations of the substrates are in an inverse ratio when the reaction rate goes through its maximum.<sup>[14,34]</sup> Besides, the adsorption coefficients depend on the basic strength distribution of sites at the surface of the solids. Figueras *et al.*<sup>[31]</sup> suggested a more responsive test reaction, the monomolecular isomerization of  $\beta$ -isophorone to  $\alpha$ -isophorone. The kinetics of this reaction catalysed by basic solids is zero order relative to  $\beta$ -isophorone at different temperatures, the initial rate being then equal to the rate constant. The Arrhenius plot of the kinetic rate constants obtained at different reaction temperatures allows the true activation energy to be calculated. The number of basic sites could thus be calculated from the activation energy by application of Eyring's theory. A simplified formula gives direct access to the number of sites assuming that the activation entropy is negligible, which is quite acceptable for zero-order kinetics:

$$k_r = k_T/hB_0 \exp(-E/RT) \exp(\Delta S/R)$$

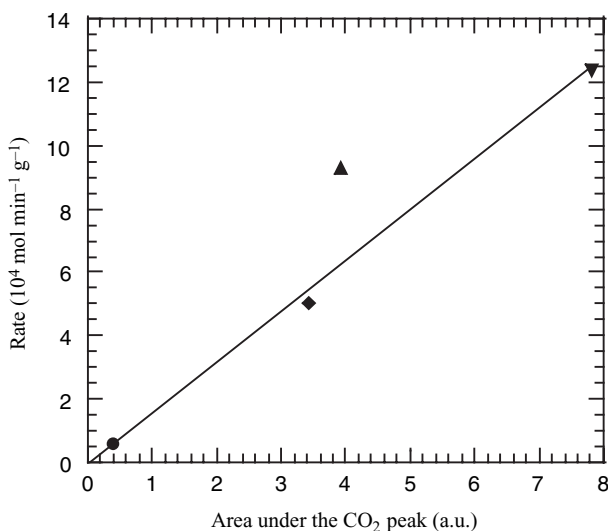


**Figure 9.1** Rate constant for isophorone isomerization at 308 K as a function of the number of sites determined by CO<sub>2</sub> adsorption for a series of basic solids: (●) KF; (◆) Mg(La)O; (▲) Mg(Al)O; and (▼) Ba(Al)O. Reprinted from *Journal of Catalysis*, vol. 211, Figueras *et al.*, Isophorone isomerization as model reaction for the characterization of solid bases: application to the determination of the number of sites, pp. 144–149, Copyright (2002), with permission from Elsevier

where  $k$  and  $h$  are the Boltzmann and Planck constants; respectively,  $E$  and  $\Delta S$  are the enthalpy and entropy of activation and  $B_0$  is the number of sites.

The accuracy of this method used to determine the number of basic sites has been confirmed by the good agreement between these results and those obtained by CO<sub>2</sub> adsorption on basic solids of different types, i.e. MgAl, BaAl and MgLa mixed oxides and KF/alumina (Figure 9.1).<sup>[31]</sup>

## 9.2.2 PROBE MOLECULES COMBINED WITH SPECTROSCOPIC METHODS

FTIR and NMR spectroscopies have been used to study the surface basicity of solids by adsorbing different probe molecules such as pyrrole, but-1-yne, acetonitrile, chloroform, CO, CO<sub>2</sub> and thiols.<sup>[19,22]</sup> Limitations arise from the formation of various adsorbate structures leading to complicated patterns, or complete dissociation of the molecule with the disappearance of the signal, or polymerization of the molecule upon heating.

Though scarcely used up to now, nitromethane has nevertheless been an interesting probe to obtain information about the strength and nature of basic sites. FTIR and NMR spectroscopies have been used in combination with this probe molecule.<sup>[32,33]</sup> The <sup>13</sup>C CP-MAS NMR has been the most interesting because it is a

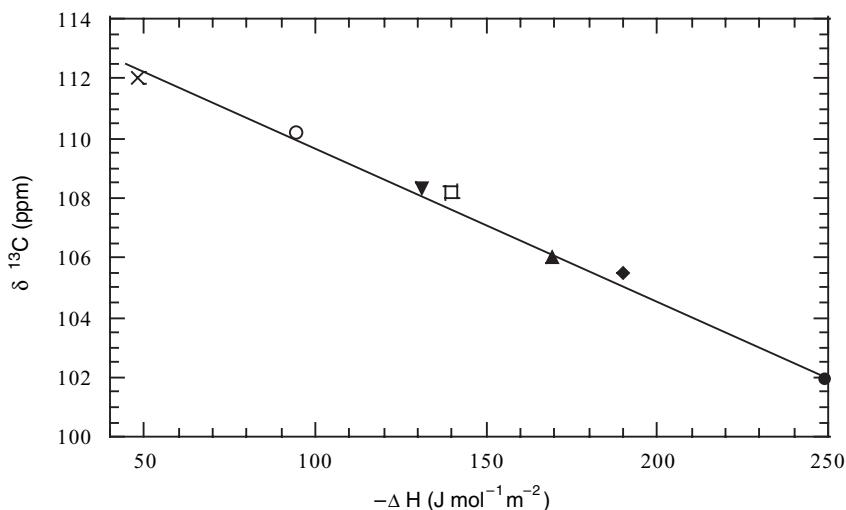


**Figure 9.2**  $^{13}\text{C}$  isotopic chemical shift of the adsorbed aci-anion of nitromethane as a function of the heats of adsorption of  $\text{CO}_2$  measured by microcalorimetry on: (X)  $\gamma\text{-Al}_2\text{O}_3$ ; (○)  $\text{Mg}(\text{Al})\text{O}$  ( $\text{Mg}/\text{Al} = 2.0$ ); (▼)  $\text{Mg}(\text{Al})\text{O}$  ( $\text{Mg}/\text{Al} = 2.2$ ); (□)  $\text{Mg}(\text{Al})\text{O}$  ( $\text{Mg}/\text{Al} = 2.3$ ); (▲)  $\text{Mg}(\text{Al})\text{O}$  ( $\text{Mg}/\text{Al} = 2.5$ ); (◆)  $\text{Mg}(\text{Al})\text{O}$  ( $\text{Mg}/\text{Al} = 3.0$ ); and (●)  $\text{MgO}$

nondestructive way of characterizing the basic sites, as opposed to the thermal decomposition required for FTIR analysis.

Nitromethane ( $\text{p}K_{\text{a}} 10.2$ ) requires stronger basic strength for the abstraction of a proton leading to the aci-anion nitromethane than its tautomeric form aci nitromethane ( $\text{p}K_{\text{a}} 3.2$ ). Except on weakly basic solids, e.g.  $\text{NaX}$  or  $\text{CsX}$  zeolites, where only physisorbed species are detected upon adsorption, aci-anion nitromethane is always formed on basic surfaces. Methazonate anion also appears when strong basic sites, likely isolated  $\text{O}^{2-}$ , are present. Interestingly a unique relationship exists between the  $^{13}\text{C}$  CP-MAS NMR chemical shift of the chemisorbed aci-anion nitromethane and the strength of basic sites. A good correlation has indeed been found between this chemical shift and the heat of adsorption of  $\text{CO}_2$  at 373 K on various solid samples as depicted in Figure 9.2. Therefore the  $^{13}\text{C}$  CP-MAS NMR chemical shift of the methylene group of chemisorbed aci-anion nitromethane has provided an efficient and easy method to probe the basic strength of the surface oxides.

### 9.3 SOLID BASE CATALYSTS

#### 9.3.1 ALKALINE EARTH METAL OXIDES

Alkaline earth metal oxides have been used as solid base catalysts for a variety of organic transformations. The basic sites able to abstract protons from a reactant molecule are those associated with  $\text{O}^{2-} \text{M}^{2+}$  ion pairs and OH groups, whereas the

adjacent metal ion acts to stabilize the resultant anionic intermediate. Concerning the nature of Lewis basic sites Coluccia and Tench<sup>[35]</sup> proposed a model of the MgO surface that shows Mg-O ion pairs of various coordination numbers. MgO has a defective surface structure showing steps, edges, corners, etc., which provide O<sup>2-</sup> sites of low coordination numbers (O<sup>2-</sup><sub>(5c)</sub> on faces, (O<sup>2-</sup><sub>(4c)</sub> on edges, and (O<sup>2-</sup><sub>(3c)</sub> on corners). These low-coordinated O<sup>2-</sup> sites are expected to be responsible for the presence of basic sites with different strengths. Base strength of surface O<sup>2-</sup> sites increases as the coordination number becomes lower. However, the surfaces of these materials, when they are in contact with the atmosphere, are covered with CO<sub>2</sub>, water, and in some cases oxygen. An important catalyst preparation variable is the treatment temperature which influences not only the total number of such sites, but also the base strength.<sup>[5]</sup> This is due to the surface basic sites being exposed when the oxide is pretreated at high temperature. Thus, evacuation of MgO at high temperature (673–1273 K)<sup>[5]</sup> leads to the appearance of three different types of basic sites exposing O<sup>2-</sup> ions with different coordination numbers and therefore with different base strengths. This is reflected in the variation of the catalytic activities for various reactions<sup>[7,8,36]</sup> as a function of the catalyst treatment temperature.

According to the model presented above, these materials show heterogeneity with respect to the basic sites and with respect to catalysis due to different types of basic sites of different nature and base strength that exist on the surfaces of alkaline earth metal oxides. Therefore, this means that if several competitive reactions that require basic sites of different strength can occur, different MgO samples with different relative populations of sites of different coordination numbers should give different selectivities. Then, the population of basic sites and consequently the activity and selectivity of the catalyst can also be changed by control of the size and shape of the MgO crystals through the preparation procedure, because this controls the relative number of atoms located at corners, edges or faces.

The most general methodology followed to prepare alkaline earth metal oxides as basic catalysts consists of the thermal decomposition of the corresponding hydroxides or carbonates in air or under vacuum. BaO and SrO are prepared from the corresponding carbonates as precursor salts, whereas decomposition of hydroxides is frequently used to prepare MgO and CaO. Preparation of alkaline earth metal oxides with high surface areas is especially important when the oxide will be used as a basic catalyst, because the catalytic activity will depend on the number and strength of the basic sites accessible to the reactant molecules, which is dependent on the accessible surface area.

From the reported data, only MgO has been synthesized with high surface areas (usually between 130 and 300 m<sup>2</sup> g<sup>-1</sup>) whereas for CaO, SrO and BaO only very low surface areas have been achieved (~60, 10 and 2 m<sup>2</sup> g<sup>-1</sup>, respectively).<sup>[37–39]</sup> For the preparation of high-surface-area MgO, the thermal decomposition of magnesium salts such as oxalates, hydroxycarbonates, sulfates and preferentially Mg(OH)<sub>2</sub> has been frequently selected. The surface area is strongly dependent on the nature of the precursor salt,<sup>[40,41]</sup> the method and conditions of its preparation<sup>[42]</sup> as well as the conditions of the thermal decomposition of the precursor salt.<sup>[43]</sup>

The possibility of synthesizing MgO powders from liquid precursors by a sol-gel route involving the hydrolysis and condensation of magnesium ethoxide has been examined by several researchers.<sup>[44,45]</sup> Excellent results were reported by Klambunde *et al.*<sup>[46,47]</sup> using a method involving the formation of Mg(OH)<sub>2</sub> gel from Mg(OCH<sub>3</sub>)<sub>2</sub>. Heat treatment of Mg(OH)<sub>2</sub> precursor at 773 K under vacuum yielded the dehydrated MgO with a 500 m<sup>2</sup> g<sup>-1</sup> surface area and 4.5 nm crystallite size.

Extensive reviews by Hattori<sup>[5-7]</sup> and Tanabe<sup>[8]</sup> and more recently by Corma and Iborra<sup>[48]</sup> provide detailed information about the catalytic behaviour of alkaline earth metal oxides for several organic reactions of importance for industrial organic synthesis. In this section, we describe in more detail reactions that have been reported recently to be catalysed by alkaline earth metal oxides.

### 9.3.2 CATALYSIS ON ALKALINE EARTH METAL OXIDES

#### Aldol Condensations

The self-condensation of acetone is an important industrial reaction for the production of diacetone alcohol (DA), which is an intermediate in the synthesis of industrially important products, such as mesityl oxide (MO). It has been reported that alkaline earth metal oxides are active for this process at 273 K, the order of activity being: BaO > SrO > CaO > MgO,<sup>[16]</sup> which agrees with the order of basicity of the oxides. It was found that the rate-determining step for this condensation is the formation of a new C—C bond between two molecules of acetone rather than the abstraction of a proton from the methyl group of the acetone. Besides, when the catalyst was MgO, addition of CO<sub>2</sub> and water did not inhibit the aldol condensation. However, addition of small amounts of water or ammonia led to marked increases in activity and selectivity to diacetone alcohol. It was suggested that the active sites for the aldol condensation are the basic OH groups retained on the surface of MgO or formed by dissociation of water resulting from the condensation process itself.<sup>[49]</sup> Di Cosimo *et al.*<sup>[50]</sup> have investigated the self-condensation of acetone in the gas phase at 573 K, with the catalysts being MgO or MgO promoted with alkali metal ions. On pure MgO, the acetone conversion was initially 17 %, and this decreased to about 8 % after 10 h of reaction with a selectivity to MO of 67 % due to a progressive deactivation by coke.<sup>[51]</sup> Alkali metal promoted MgO gave an increase of the initial rates of conversion of acetone but the addition of such promoters increased the rate of deactivation.

Condensation of butanal has been carried out on alkaline earth metal oxides at 273 K<sup>[52,53]</sup> yielding 2-ethyl-3-hydroxy-hexanal as a main product; the order of activity per unit surface area was equal to that in the case of self-condensation of acetone and in agreement with the order of basicity of the solids, namely, SrO > CaO > MgO. The authors found that for aldol condensation of *n*-butyraldehyde, the active sites are the surface O<sup>2-</sup> ions and the rate-determining step is the  $\alpha$ -hydrogen abstraction. The differences in rate-determining step and active sites in the condensation of butyraldehyde and self-condensation of the acetone were attributed to differences in acidity of the  $\alpha$ -hydrogen in the two molecules. CaO was slightly



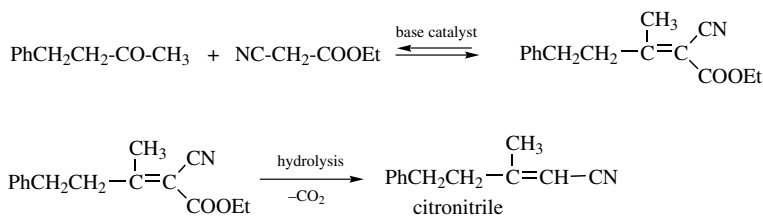
more active than MgO at 273 K; after a reaction time of 1 h, maximum conversions of 41 % were observed with a selectivity for 2-ethyl-3-hydroxy-hexanal of 39.8 %.

Cross-aldol condensations have been performed with alkaline earth metal oxide, as base catalysts. A limitation of the cross-aldol condensation reactions is the formation of by-products through the self-condensation of the carbonyl compounds, resulting in low selectivities for the cross-aldol condensation product. Thus, the cross-condensation of heptanal with benzaldehyde, which leads to jasminaldehyde ( $\alpha$ -*n*-amylcinnamaldehyde), with a violet scent, has been performed with various solid base catalysts,<sup>[13,54]</sup> particularly MgO, which gave excellent conversions of heptanal (97 %) at 398 K in the absence of a solvent (but the selectivity to jasminaldehyde was only 43 %). A low selectivity was also reported (40 %) for the cross-aldol condensation of acetaldehyde and heptanal catalysed by MgO.<sup>[55]</sup>

Another example of cross-aldol condensation is the reaction between citral and acetone, which yields pseudoionone, an intermediate in the production of vitamin A. Noda *et al.*<sup>[56]</sup> working at 398 K with a 1:1 molar ratio of reagents and 2 wt % of catalyst, obtained high conversions (98 %) with selectivities to pseudoionone close to 70 % with CaO and an Al-Mg mixed oxide catalyst; these pseudoionone yields are greater than those reported for the homogeneous reaction. MgO exhibited poor activity, and under these conditions only 20 % citral conversion was obtained after 4 h in a batch reactor. Nevertheless, Climent *et al.*,<sup>[57]</sup> working with 16 wt % MgO as a catalyst, a molar ratio of acetone to citral close to 3 and at 333 K, achieved 99 % conversion and 68 % selectivity to pseudoionone after 1 h.

Reaction between 2'-hydroxyacetophenone and benzaldehyde (Claisen-Schmidt condensation) in the absence of a solvent at 423 K giving 2'-hydroxy chalcones and flavanones has been successfully performed with MgO as a solid base catalyst.<sup>[58]</sup> A conversion of 40 % after 1 h with 67 % selectivity to chalcone was achieved. The influence of the solvent and the effects of a substituent on the aromatic ring were investigated by Amiridis *et al.*<sup>[59,60]</sup> The reaction was carried out on MgO at 433 K. Dimethyl sulfoxide (DMSO) showed a strong promoting effect on the reaction, which was attributed to the ability of this dipolar aprotic solvent to weakly solvate anions and stabilize cations so that both become available for reaction. In this case, a conversion of 2-hydroxyacetophenone of 47 % with a selectivity to flavanone of 78 % was achieved after 30 min in a batch reactor. Further investigations<sup>[61]</sup> showed that DMSO significantly increases the rate of the subsequent isomerization of the 2'-hydroxychalcone intermediate to flavanone.

2-Nitroalkanols are intermediate compounds of  $\beta$ -amino alcohols that are used extensively in many important syntheses. They are obtained by Henry's reaction through the condensation of nitroalkanes with aldehydes. Different nitro compounds have been reacted with carbonyl compounds in reactions catalysed by alkaline earth metal oxides and hydroxides.<sup>[62]</sup> Among the catalysts examined, MgO, CaO, Ba(OH)<sub>2</sub>, and Sr(OH)<sub>2</sub>, exhibited high activity for the reaction of nitromethane with propionaldehyde. The yields were between 60 % (for MgO) and 26 % [for Sr(OH)<sub>2</sub>] at 313 K after 1 h in a batch reactor. The study of the influence of the pretreatment temperature of the solid showed that for MgO and CaO a



Scheme 9.1

considerable fraction of activity remained even after pretreatment at low temperature (473 K). This result indicates that for the nitroaldol reaction the removal of the surface OH groups is not a prerequisite for the preparation of active catalysts.

### Knoevenagel, Wittig and Wittig–Horner Reactions

The Knoevenagel condensation is the reaction between a carbonyl compound with an active methylene compound leading to C–C bond formation. This reaction has wide application in the synthesis of fine chemicals. An example of commercial interest is the synthesis of citronitrile (Scheme 9.1), a compound with a citrus-like odour, which is used in the cosmetic and fragrance industries.

The first step in the synthesis of citronitrile is the Knoevenagel condensation of benzyl acetone and ethyl cyanoacetate. This condensation has been carried out with MgO and Al-Mg calcined hydrotalcites as catalysts.<sup>[63]</sup> Similar results were obtained with the two solid catalysts, with yields of 75 % of the Knoevenagel adduct.

The method of choice for the synthesis of unsaturated arylsulfones is the Knoevenagel condensation of arylsulfonylalkanes with aldehydes. The condensation between aldehydes and phenylsulfonyl acetonitrile, has been performed in the presence of various solid base catalysts (MgO, Cs-exchanged X zeolite, Al-Mg mixed oxide, and aluminophosphate oxynitride) at 373 K in the absence of solvents.<sup>[64]</sup> The most active catalyst for this transformation was the aluminophosphate oxynitride, but MgO and the Al-Mg mixed oxide also were found to have excellent activity, yielding the Knoevenagel adduct in yields of 86 and 71 %, respectively, after 2 h in a batch reactor.

MgO has been reported to be an efficient basic catalyst for Knoevenagel, Wittig and Wittig–Horner reactions for the preparation of alkenes at temperatures between 293 and 333 K.<sup>[65]</sup> Recently, competitive Wittig–Horner and Knoevenagel reactions of benzaldehyde with diethyl cyanomethylphosphonate and tetraethyl methylenediphosphonate on different solid base catalysts [C<sub>2</sub>CO<sub>3</sub>, BaO, Ca(OH)<sub>2</sub>, CaO, MgO, MgCl<sub>2</sub>, BaF<sub>2</sub>, KF, CaF<sub>2</sub>, and CsF] in the absence of a solvent have been reported.<sup>[66]</sup> Tetraethyl methylenediphosphonate reacting with benzaldehyde at similar conditions gave only the product of Horner's reaction. The basicity of the solid and the nature of the cation (mono- or divalent) of the base strongly influence the ratio of products formed in the Horner–Knoevenagel reactions.

### Michael Additions

Dimerization of methyl crotonate has been carried out on various base catalysts (MgO, CaO, SrO, BaO, ZrO<sub>2</sub>, La<sub>2</sub>O<sub>3</sub>, KF/alumina, KOH/alumina, and KX zeolite) at 323 K.<sup>[67]</sup> The reaction proceeds by Michael addition, which form a methyl diester of 3-methyl-2-vinylglutaric acid. The diester undergoes a double bond migration to form the final *E*- and *Z*- isomers of 3-ethylidene-3-methylglutaric acid dimethyl ester (MEG). MgO exhibited the highest activity when it was pretreated at 873 K. In this case the conversion of methyl crotonate was 36.5 % after a 2 h reaction time in a batch reactor with a selectivity to *E,Z*-MEG isomers of 93 %. However, MgO pretreated at 673 K exhibited considerable activity for the Michael addition. Because at this pretreatment temperature the catalyst still retains a large number of OH groups, it was assumed that basic hydroxyl groups can act as active sites. The same authors<sup>[38]</sup> also investigated the Michael addition of nitromethane to  $\alpha,\beta$ -unsaturated carbonyl compounds such as methyl crotonate, 3-buten-2-one, 2-cyclohexen-1-one and crotonaldehyde in the presence of various solid base catalysts (alumina-supported potassium fluoride and hydroxide, alkaline earth metal oxides and lanthanum oxide).

Nucleophilic additions of alcohols to  $\alpha,\beta$ -unsaturated compounds have been performed on alkali metal oxides and hydroxides. Cyanoethylation of various alcohols with acrylonitrile to form 3-alkoxypropanenitriles has been carried out efficiently in the presence of these solid base catalysts at a temperature of 323 K.<sup>[68,69]</sup> In cyanoethylation of methanol, conversions of 98 % after 2 h in a batch reactor were obtained with MgO, CaO and SrO; in contrast, with BaO the conversion was only 68 %.

Conjugate addition of methanol to  $\alpha,\beta$ -unsaturated carbonyl compounds forms a new carbon–oxygen bond to yield valuable ethers. Kabashima *et al.*<sup>[70]</sup> reported the conjugate addition of methanol to 3-buten-2-one on alkaline oxides, hydroxides and carbonates at a temperature of 273 K. The activities of the catalyst follow the order: alkaline earth metal oxides > alkaline earth metal hydroxides > alkaline earth metal carbonates. All alkaline earth metal oxides exhibited high catalytic activities. The yields obtained after 10 min in a batch reactor with MgO, CaO or SrO exceeded 92 %, whereas with BaO the yield was lower (72 %), probably because of its low surface area (2 m<sup>2</sup> g<sup>-1</sup>). As observed for other reactions, the catalytic activity of MgO strongly depends on the pretreatment temperature.

### Transesterification Reactions

Fatty acid methyl and ethyl esters derived from vegetable oils are considered to be a promising fuel for direct injection diesel engines. Moreover, they are valuable compounds for the production of fine chemicals for food, pharmaceutical and cosmetic products. Leclercq *et al.*<sup>[71]</sup> showed that the methanolysis of rapeseed oil can be carried out with MgO, although its activity depends strongly on the pretreatment temperature of this oxide. Thus, with MgO pretreated at 823 K and a methanol to oil molar ratio of 75 at methanol reflux, a conversion of 37 % with 97 % selectivity to methyl esters was achieved after 1 h in a batch reactor.

Triglycerides react with glycerol to give fatty acid monoesters and diesters of glycerol, which are valuable compounds with wide applications as emulsifiers in the food, pharmaceutical and cosmetic industries. Corma *et al.*<sup>[72]</sup> performed the glycerolysis of triolein and rapeseed oil in the absence of a solvent on various solid base catalysts (Cs-exchanged MCM-41, Cs-exchanged Sepiolite, MgO, and calcined hydrotalcites with various Al/Mg ratios). The results showed that the most active catalysts were MgO and calcined hydrotalcites with an Al/(Al + Mg) ratio of 0.20. The authors showed that using MgO as a solid base catalyst and optimizing the main process variables, such as temperature and the glycerol/oil ratio, it is possible to obtain 96 % conversion of rapeseed oil with 68 % selectivity to monoglycerides after 5 h in a batch reactor by working at 513 K with a glycerol/triglyceride molar ratio of 12.

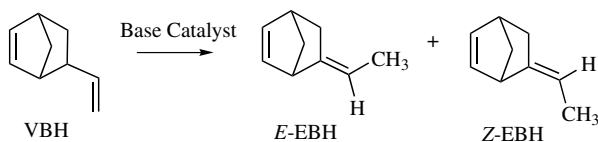
Monoglycerides can alternatively be prepared by glycerolysis of fatty acid methyl esters. Bancquart *et al.*<sup>[73,74]</sup> showed that basic solid catalysts such as MgO, ZnO, CeO<sub>2</sub> and La<sub>2</sub>O<sub>3</sub>, as well as MgO doped with alkali metals (Li/MgO and Na/MgO), are active catalysts for the transesterification of methyl stearate with glycerol. The reactions were performed at 493 K in the absence of solvent, the order of activity being: La<sub>2</sub>O<sub>3</sub> > MgO  $\approx$  CeO<sub>2</sub> > ZnO, which correlates with the intrinsic basicity of these solids.

Esters such as di(2-ethylhexyl) adipate and an oligomeric ester of neopentyl glycol find application as lubricants, and it is suggested that they can be used as environmentally friendly substitutes for petroleum-derived lubricants. They have been synthesized recently by alcoholysis of dimethyl adipate ester and the corresponding alcohols, with alkaline earth metal compounds as the catalysts.<sup>[75]</sup> MgO does not show any activity for either transesterification reaction, whereas CaO gives yields of both diesters near 100 % after 4 h in a batch reactor.

Alcoholysis of ester and epoxide with various basic catalysts including alkaline earth metal oxides and hydroxides was reported recently by Hattori *et al.*<sup>[76]</sup> Various alcohols were transesterified with ethyl acetate at 273 K. The results show that in the presence of strongly basic catalysts such as CaO, SrO and BaO, propan-2-ol reacted much faster than methanol, whereas in the presence of more weakly basic catalysts such as MgO, Sr(OH)<sub>2</sub>·8H<sub>2</sub>O and Ba(OH)<sub>2</sub>·8H<sub>2</sub>O, methanol reacted faster than propan-2-ol. When the alcoholysis was performed with propene oxide, alkaline earth metal oxides were found to be more reactive than hydroxides; the reactivity of the alcohols was in the order: methanol > ethanol > propan-2-ol > 2-methylpropan-2-ol, regardless of the type of catalyst.

### Isomerization Reactions

Alkaline earth metal oxides are active catalysts for double bond isomerization.<sup>[77-80]</sup> It has been reported<sup>[37]</sup> that MgO, CaO, SrO and BaO catalyse the double bond isomerization of 5-vinylbicyclo-[2.2.1]-hept-2-ene (VBH) leading to 5-ethylidenebicyclo-[2.2.1]-hept-2-ene (EBH) (Scheme 9.2), which is used as a comonomer of ethene-propene synthetic rubber.



Scheme 9.2

The order of activity was:  $\text{CaO} > \text{MgO} > \text{SrO} > \text{BaO}$ , which is attributed to the trends in the base strength of oxides ( $\text{BaO} > \text{SrO} > \text{CaO} > \text{MgO}$ ) and their surface area, the latter decreasing in the order:  $\text{MgO} > \text{CaO} > \text{SrO} > \text{BaO}$ . The activity of MgO varied with pretreatment temperature, reaching a maximum at 873 K; then a 99.7 % conversion of VBH was observed after 2 h of reaction in a batch reactor at 323 K.

### The Meerwein–Pondorff–Verley Reduction

The Meerwein–Pondorff–Verley (MPV) reduction of carbonyl compounds is a hydrogen transfer reaction between carbonyl compounds and alcohols that can be applied avoiding the possibility of reducing or oxidizing other functional groups present in the molecules. The hydrogen donors are secondary alcohols (e.g. propan-2-ol and butan-2-ol), and the oxidants are simple ketones (e.g. acetone and cyclohexanone). Basic catalysts, such as oxides and zeolites, have been used for this reaction;<sup>[81]</sup> among them, special attention has been paid to MgO which appears to be an excellent catalyst for the hydrogenation of ketones using secondary alcohols with reactants in the vapour phase. However, an important drawback of the reaction is that MgO gradually deactivates, ultimately leading to a complete loss of activity. Szölloši and Bartok<sup>[82,83]</sup> showed that deactivation of MgO during the catalytic transfer hydrogenation of various ketones with propan-2-ol could be prevented by pretreatment with chloromethanes. It was suggested that modification of the MgO surface with chloroform resulted in blocking of the Lewis acid centres responsible for poisoning and also in the generation of surface OH groups with proper acidity for the reaction.<sup>[84]</sup>

The reaction of benzaldehyde with ethanol in the presence of MgO, CaO, and mixed oxides obtained by calcination of double layered hydroxides was investigated by Aramendia *et al.*<sup>[85]</sup> in liquid phase. CaO was found to be the most active catalyst for the process.

The influence of the preparation method of various MgO samples on their catalytic activity in the MPV reaction of cyclohexanone with 2-propanol has been recently reported.<sup>[86]</sup> It was concluded that the efficiency of the catalytic hydrogen transfer process was directly related to the number of basic sites in the solid.

The reduction of citral with alkanols and cycloalkanols to the Z- and E-alcohol isomers nerol and geraniol using MgO and CaO as catalysts has also been reported.<sup>[86]</sup> When the reactions were performed by refluxing the mixture with an alcohol/citral molar ratio of 20, excellent yields to the corresponding alcohol

isomers were obtained. Reaction yield and selectivity on MgO and on CaO exceeded 95 and 85 %, respectively, in all the experiments.

### Tishchenko Reaction

The Tishchenko reaction is a dimerization of aldehydes to the corresponding esters, which is classically performed in homogeneous media using aluminium alkoxides as catalysts.<sup>[87,88]</sup> Mixed Tishchenko reactions with various aldehydes: (i) benzaldehyde and pivalaldehyde; (ii) pivalaldehyde and cyclopropane carbaldehyde; and (iii) cyclopropane carbaldehyde and benzaldehyde, have been investigated with various solid base catalysts including alkaline earth metal oxides.<sup>[89]</sup> The reactions were performed using equimolar mixtures of two kinds of aldehydes, at 353 K *in vacuo* without solvent. Alkaline earth metal oxides were the most active catalysts. In all the combinations, the activity of the catalysts was found to increase in the order BaO  $\ll$  MgO < CaO < SrO. This result indicates that strongly basic sites and high surface areas are indispensable for high activity.

The Tishchenko reaction of furfural has been found to be difficult when carried out by traditional homogeneous catalysis, but excellent results for the Tishchenko reaction of furfural and 3-furaldehyde<sup>[90,91]</sup> using CaO and SrO as catalysts have been obtained. The use of other solid base catalysts such as La<sub>2</sub>O<sub>3</sub>, ZrO<sub>2</sub>, ZnO,  $\gamma$ -alumina, hydrotalcite and KOH/alumina, was unsuccessful. An investigation of the influence of the pretreatment temperature of the MgO and CaO catalysts showed that the active basic sites for this transformation are not OH groups, but rather O<sup>2-</sup> ions on the MgO surface.

Tishchenko reaction of dialdehydes gives lactones via intramolecular catalytic esterification. MgO, CaO, and SrO exhibited good catalytic properties for the Tishchenko reaction of *o*-phthalaldehyde to phthalide<sup>[92]</sup> at 313 K, affording phthalide exclusively with yields between 86 and 100 % after a short time (15 min) in a batch reactor.

## 9.3.3 HYDROTALCITES AND RELATED COMPOUNDS

### Preparation and Catalytic Properties

Layered double hydroxides (LDH), also called hydrotalcite-like compounds, are potential substitutes for common liquid bases in environmentally friendly processes since their basic properties, i.e. number, strength and nature of sites are extremely versatile and can be tailored at will. Their interest from a practical point of view also arises from their easy synthesis procedures, their nontoxicity and their low cost.<sup>[9,10]</sup>

LDH of general formula  $[M_{1-x}^{II}M_x^{III}(OH)_2]^{x+}[A_{x/m}^{m-}]_x \cdot nH_2O$  exhibit a layer structure whose positively charged brucite-like layers contain edge-shared metal M<sup>II</sup> and M<sup>III</sup> hydroxide octahedra, with charges neutralized by A<sup>m-</sup> anions located in interlayer spacings. The layers are stacked one on top of the other and are held together by weak interactions. The Mg/Al LDH exchanged with CO<sub>3</sub><sup>2-</sup> corresponding to the natural mineral hydrotalcite was extensively used to obtain basic catalysts

since the pioneering work of Reichle.<sup>[93]</sup> This results from its peculiar ability to give active and selective catalysts either in its lamellar form containing either  $\text{CO}_3^{2-}$ ,  $\text{OH}^-$  or *tert*-butoxide anions ( $^- \text{O}-t\text{-Bu}$ ), or in its mixed oxide form  $[\text{Mg}(\text{Al})\text{O}]$  obtained by thermal decomposition. These different forms differ by their structure, the nature and the environment of the active sites. The catalytic applications of these materials include a wide range of reactions which have been recently reviewed,<sup>[10,17]</sup> e.g. C—C bond formation by condensation of aldehydes and/or ketones, oxidation, selective reductions by hydrogen transfer, polymerizations. This section focusses on the results obtained in various well known base-catalysed reactions (Table 9.1), where comparative data obtained with the different catalytically active forms were available. This allows their specific behaviour to be highlighted.

Mixed oxides obtained after calcination of Mg/Al LDH in the temperature range between 673 and 773 K have been for a long time the only catalytic form used. The as synthesized Mg/Al- $\text{CO}_3^{2-}$  LDH treated at temperatures below the structural decomposition point were generally found inactive or poorly active in most of the basic reactions. However, they show after outgassing at 423 K or drying at 383 K, respectively, a remarkable activity for disproportionation of 2-methyl-3-butyn-2-ol (MBOH)<sup>[94,95]</sup> and for epoxidation of olefins using hydrogen peroxide and benzonitrile.<sup>[96]</sup> Therefore they possess basic catalytic properties,<sup>[29]</sup> though the nature of basic sites in dehydrated crystalline Mg/Al- $\text{CO}_3^{2-}$  was not well understood. It was suggested by Constantino and Pinnavaia<sup>[94,95]</sup> that the  $\text{CO}_3^{2-}$  ions at the external surface act as strong basic sites.

The crystalline structure containing  $\text{OH}^-$  as compensating anions which corresponds to the natural mineral meixnerite (Mg/Al-OH) has been the most active catalyst for aldol, Claisen-Schmidt and Knoevenagel condensations,<sup>[13,14,57,97-101]</sup> Michael additions,<sup>[102,103]</sup> and epoxidation of activated olefins<sup>[104]</sup> (Table 9.1). This resulted from the Brønsted nature of the basic sites, known to be particularly efficient in these reactions.<sup>[14,16,17,101]</sup> The meixnerite-like form, which could not be prepared by ion exchange, was obtained by rehydration of Mg(Al)O mixed oxides resulting in the reconstruction of the layered structure taking advantage of its 'memory effect'.<sup>[9,10]</sup>

It was established that less than 5% of the  $\text{OH}^-$  compensating anions of the reconstructed Mg/Al LDH were active catalytic sites in the aldol condensation reaction.<sup>[100]</sup> This suggested that the active hydroxyls were most likely situated on the defective sites at the edge of the layers. Consequently enhanced catalytic activity could be expected from highly disordered Mg/Al-LDH with 'house of cards' type structure or possessing small particle sizes. Several attempts have been carried out in order to synthesize LDH, the corresponding mixed oxides and their rehydrated form with high surface areas. An increase of about 20% of the surface area of Mg(Al)O mixed oxide was thus obtained by performing the synthesis of the Mg/Al-LDH precursor under sonication at 298 K.<sup>[105]</sup> Accordingly these rehydrated mixed oxides are more active in the condensation reaction of citral and acetone than those conventionally prepared, due to their larger amount of accessible Brønsted basic sites.<sup>[105]</sup>

**Table 9.1**

Reactants ( $T_{\text{react}}$ , solvent)	Product (%)	Yield % (time)				Ref.
		Mg/ Al-CO <sub>3</sub> <sup>2-</sup>	Mg (Al)O	Mg/ Al-OH	Mg/ Al-O- <i>t</i> -Bu	
<i>Aldolization and Claisen-Schmidt condensations</i>						
Acetone (273 K, without)	Diacetone alcohol	0.2 (10 h)	9 (10 h)	23 (1 h)		[101]
Benzaldehyde + heptanal (398 K, without)	Jasminaldehyde ( $\alpha$ - <i>n</i> - amylcinnamaldehyde)		44 (8 h)	60 (4 h)		[13]
Citral + acetone (333 K, without)	Pseudoionone (6,7-dimethyl-3,5, 9-undecatrien-2-one)		58.5 (1 h)	91 (1 h)		[13]
Heptanal + acetaldehyde (393 K, ethanol)	2-Nonenal		21 (6 h)	17 (6 h)		[55]
Benzaldehyde + acetone (273 K, THF)	Aldol		1.2 (1 h)	61 (1 h)	95 (0.25 h) <sup>d</sup>	[98,112]
2,4-Dimethoxy acetophenone + 4-methoxy benzaldehyde (without)	Vesidryl (2',4,4'- trimethoxychalcone)		20 (4 h) <sup>b</sup>	78 (4 h) <sup>c</sup>		[13]
Acetophenone + benzaldehyde (323 K, without)	Chalcone		4 (1 h)	82 (1 h)		[109]
<i>Michael addition</i>						
Nitromethane + cyclo-2- en-1-one (353 K, DMSO)	Monoadduct	No reaction	15 (8 h)	76 (8 h)		[103]
<i>Cyanoethylation of alcohols</i>						
Acrylonitrile + methanol (323 K, CH <sub>2</sub> Cl <sub>2</sub> )	3-Methoxy- propionitrile	2.5 (2 h) <sup>d</sup>	20 (2 h) <sup>d</sup>	99.8 (0.75 h) <sup>d</sup>	92 (0.6 h) <sup>d</sup>	[110]
<i>Wadsworth-Emmons reaction</i>						
2-Methoxybenzaldehyde + diethylcyanomethyl- phosphonate (reflux, DMF)	2-Methoxy- cinnamonnitrile	No reaction	5 (2 h)	18 (2 h)	92 (2 h)	[110,113]
<i>Epoxidation</i>						
Cyclohexen-1-one + TBHP (298 K, CH <sub>3</sub> OH)	Epoxide	20 (6 h)	33.5 (6 h)	87 (6 h)		[104,110]
<i>Meerwein-Ponndorf-Verley reduction</i>						
4- <i>tert</i> -Butylcyclohexanone (355 K, isopropanol)	4- <i>tert</i> -Butylcyclo- hexanol		93 (4 h)	No reaction		[110,115]
<i>Transesterification</i>						
Methyl acetoacetate + 1-hexanol (363 K, toluene)	Ester	No reaction	55 (12 h)	77 (12 h)	98 (2 h)	[110,111]

<sup>a</sup>Without solvent.<sup>b</sup>393 K.<sup>c</sup>353 K.<sup>d</sup>Conversion.



A dramatic increase of the specific area has also accounted for the higher activity reached in the condensation of citral and acetone with samples rehydrated in liquid phase rather than in vapour phase.<sup>[106]</sup> The specific surface area of the former samples could be 30 times higher than in the latter and reach  $440 \text{ m}^2 \text{ g}^{-1}$ . Smaller particles than in the used as-prepared LDH precursor, forming thin platelets, were indeed observed in the sample rehydrated in liquid phase using a higher stirring speed or ultrasound during rehydration.<sup>[107]</sup> In these cases, an increase of exposed OH sites has been generated due to the exfoliation of the platelets, thus leading to an improved catalytic activity.

It must also be noticed that the rehydrated Mg/Al-LDH, in spite of their moderate basic strength,<sup>[108]</sup> due to the Brønsted nature of the active sites have been able to catalyse Michael additions normally requiring basic Lewis sites of high strength.<sup>[30]</sup>

Rehydrated Mg/Al LDH have also been used successfully for the synthesis of several fine chemicals of industrial or pharmacological interest, i.e. jasminaldehyde ( $\alpha$ -*n*-amylcinnamaldehyde), chalcones such as vesidryl (2',4,4'-trimethoxychalcone) and pseudoionones (6,7-dimethyl-3,5,9-undecatrien-2-one) by aldol and Claisen-Schmidt condensations.<sup>[13,109]</sup>

Mg/Al-O-*t*-Bu-LDH obtained by exchange of nitrate-intercalated Mg/Al LDH have been found much more active than rehydrated Mg/Al-OH LDH in cyanoethylation,<sup>[110]</sup> transesterification<sup>[111]</sup>, aldol condensation<sup>[112]</sup> and Wadsworth-Emmons<sup>[113]</sup> reactions, i.e. the condensation of an aldehyde or a ketone with a phosphonate into an unsaturated nitrile or ester (Table 9.1). This has initially been assigned to a higher basicity of the *tert*-butoxide anions than hydroxides.<sup>[111,112]</sup> However, investigations using *ab initio* plane-wave density functional theory of the transesterification reaction of methyl acetoacetate with prop-2-en-1-ol have led Greenwell *et al.*<sup>[114]</sup> to suggest an alternative to the classic base-catalysed reaction mechanism. The latter involves the initial step, a deprotonation of prop-2-en-1-ol by *tert*-butoxide anion located in the interlayer space as proposed by Choudary *et al.*<sup>[111]</sup> The new mechanism proposed by Greenwell *et al.*<sup>[114]</sup> relies on the bipolar nature of the Mg/Al-O-*t*-Bu-HDL. They have indeed showed that these materials consist of a hydrophilic layer of OH<sup>-</sup> groups and water molecules along the brucite-like layer, with an organophilic layer of *tert*-butyl groups between them. The charge balancing anions are OH<sup>-</sup> generated through the reaction of interlayer water and *tert*-butoxide. The resultant *tert*-butyl alcohol gives rise to the intercalated organophilic layer. The organic substrates interact with the LDH layer through their polar groups and decrease the binding energy of the OH<sup>-</sup>, whose catalytic activity thus increases. Therefore, the samples intercalated by O-*t*-Bu anions exhibit a higher catalytic activity than that of the samples intercalated by OH<sup>-</sup> due to the presence of the hydrophilic interlayer region.

In some few cases, the acid-base bifunctional Mg(Al)O mixed oxides have been more active and selective than the rehydrated Mg/Al-LDH (Mg/Al-OH) (Table 9.1). This has been observed in the condensation reaction of heptanal and acetaldehyde yielding 2-nonenal<sup>[55]</sup> and in MPV reductions.<sup>[115]</sup> In the former reaction, obtention of 2-nonenal requires in the first step the  $\alpha$ -hydrogen abstraction from acetaldehyde. Lewis-type basic sites of moderate strength appear more efficient than Brønsted-

type sites to perform to a greater extent the proton abstraction from acetaldehyde in competition with heptanal.

Rehydrated Mg/Al-OH catalysts have been found to be inactive in the MPV reduction of 4-*tert*-butylcyclohexanone by isopropanol, whereas the bifunctional character of the Mg(Al)O mixed oxides made them highly active in this reaction. The aluminium alkoxide intermediate of the MPV reaction indeed involves a cooperation between basic and acidic sites. On mixed oxides, the abstraction of a proton from isopropanol on  $O^{2-}$  sites gives isopropoxide anions, which are then stabilized on  $Al^{3+}$  and form intermediates with the aldehyde. The high activity of mixed oxide comes from the synergetic effect of strong Lewis basicity and mild acidity.

### 9.3.4 ORGANIC BASE-SUPPORTED CATALYSTS

#### Polymer-supported Catalysts

Polymer-supported quaternary ammonium hydroxides have been used to catalyse Michael reactions between various alkyl methacrylates, acrylonitrile, and methyl vinyl ketone as acceptors and nitro or keto derivatives as donors.<sup>[116,117]</sup>

With the purpose of gaining access to polymer bearing a primary amine function, Rich and Gurwara<sup>[118]</sup> reported a relatively facile route which consists of reacting a chloromethyl polystyrene-divinylbenzene (PS-DVB) resin with excess of ammonia. Another possible route is based on the conversion of phthalimidomethyl PS-DVB resin by hydrazinolysis leading to aminomethyl PS-DVB, the starting resin being produced either by direct treatment of PS-DVB by *N*-(chloromethyl)phthalimide or by reacting chloromethyl PS-DVB with potassium phthalimide.<sup>[119]</sup> More recently, Luis *et al.*<sup>[120]</sup> have proposed a novel method for the functionalization of PS resins through long aliphatic spacers, which provides polymers of variable and controlled functionalization degrees and high mobility of the functional chains with a large variety of functionalities.

Guanidines and biguanidines are strong organic bases as their basic strength is in the range of the common inorganic bases, such as alkaline hydroxides and carbonates. In homogeneous conditions, they have been used as catalysts for several types of base-catalysed reactions, such as alkylation and elimination,<sup>[120–123]</sup> Michael-type reactions,<sup>[124,125]</sup> esterification and transesterification.<sup>[126]</sup> Hence, the design of supported guanidines on insoluble polymeric matrices have been investigated to provide heterogenized strong base catalysts for the synthesis of fine chemicals. Firstly, heterogenization of various guanidines, such as 1,1,3,3-tetramethylguanidine (TMG) and 1,5,7-triazabicyclo[4.4.0]dec-5ene (TBD) by chlorine substitution was achieved on different types of chloromethylated PS-DVB or by 1,3-dicyclocarbodiimide (DCC) on linear PS with the use of a 'space linker' bearing amine function.<sup>[127]</sup> The catalysts possessing guanidine linked through a space linker were less active. Furthermore, they suffer substitution reactions during recycling runs which give inactive hexasubstituted guanidinium derivatives. On the other hand, it should be noted that there is a loss of base capacity for polymer [PS]-CH<sub>2</sub>-TMG during transesterification of soybean with methanol due to an attack of methoxide on benzylic CH<sub>2</sub> groups leading to TMG leaching.

Resins carrying the guanidine function have been patented as catalyst<sup>[128]</sup> for the preparation of organic disulfides and polysulfides<sup>[129]</sup> and the preparation of sulfonated olefins.<sup>[130]</sup>

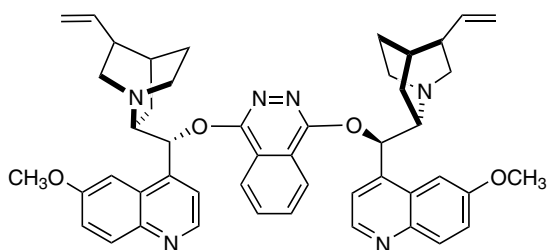
A new and convenient method was developed to prepare polystyrene-supported biguanidine by addition of TMG on supported carbodiimide or by *N*-addition of diazetidinium triflate salts on supported  $\omega$ -methylaminoethyl-PS.<sup>[131,132]</sup> The PS-bound biguanides were checked in exactly the same conditions and exhibited excellent catalytic properties. The yields of methyl esters in the transesterification of several vegetable oils are above 94 %, even before 15 min reaction time. These biguanide-supported catalysts are, by far, more reactive and more stable than the previously described guanidines. This confirms the higher basicity of biguanides versus guanidines and that their immobilization induces only a very limited decrease in reactivity (90 % instead of 94 % yield after 30 min reaction time). Even more interestingly, the recycling of polymer-bound biguanidines could be performed 17 times and the efficiency remains unaffected for >10 cycles, after which alterations begin to appear.

Pyridine-bound resins were also prepared and successfully employed as polymer-supported phase transfer catalysts in bromide displacement from 1-bromoalkanes by salt phenoxide or naphthoxide, even though the controlling factor (diffusivity or preferential sorption) for the observed substrate selectivity effects was difficult to determine.<sup>[133]</sup>

Another interesting feature of polymer-supported catalysts containing quaternary ammonium salts involves the development of enantioselective catalysis using salts derived from cinchonia or ephedra alkaloids.<sup>[134]</sup> The first application of such chiral supported catalysts in the Michael reaction between methyl 1-oxoindan-2-carboxylate and methyl vinyl ketone revealed a high chemical yield in condensation product (60–100 %) although the enantioselectivities were only moderate (ee <27 %).

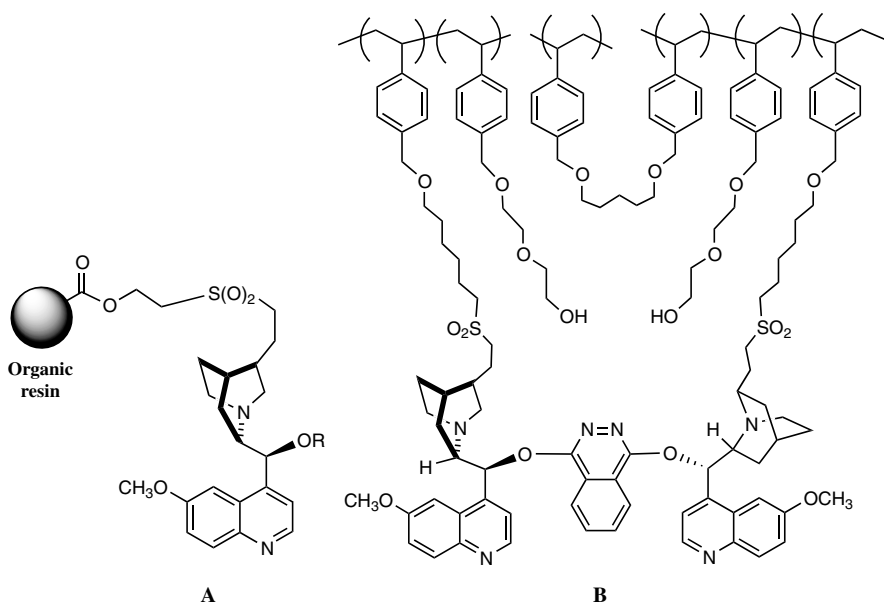
The use of numerous polymer-supported optically active phase transfer catalysts was further extended by Kelly and Sherrington<sup>[135]</sup> in a range of phase transfer reactions including a variety of displacement reactions, such as sodium borohydride reductions of prochiral ketones, epoxidation of chalcone, addition of nitromethane to chalcone and the addition of thiophenol to cyclohexanone. Except in the chalcone epoxidation, all the examined resin catalysts proved to be very effective. However, with none of the chiral catalyst system examined was any significant ee achieved. The absence of chiral induction is a matter of debate, in particular over the possible reversibility of a step and the minimal interaction within an ion pair capable of acting as chiral entities in the transition state and/or the possible degradation of catalysts and leaching.

More recently, Petri *et al.*<sup>[136]</sup> have copolymerized the chiral ligand (QHN)<sub>2</sub>-PHAL (Scheme 9.3) directly with ethylglycol dimethacrylate using AIBN as radical initiator. This material revealed high activities (68–80 % yield) and enantioselectivities (ee  $\geq$  98 %) for asymmetric dihydroxylation of *trans*-stilbene using K<sub>3</sub>Fe(CN)<sub>6</sub> as secondary oxidant. However, the authors noted that the catalytic material still contained unbound bis-alkaloid.

(QHN)<sub>2</sub>-PHAL

Scheme 9.3

Subsequently, Song *et al.*<sup>[137]</sup> have prepared a similar polymer by copolymerization of (QHN)<sub>2</sub>-PHAL and methyl methacrylate, claiming a more facile copolymerization than with 2-hydroxyethyl methacrylate. They observed also excellent enantioselectivities in the dihydroxylation of *trans*-stilbene. However, the genuine heterogeneous catalysis was disproven by Sherrington *et al.*<sup>[138]</sup> who showed that the polymer catalyst contains some physically trapped unreacted alkaloid monomer in agreement with Salvadori's observations. Finally, the problem of ligand leaching was addressed and a prominent homogeneous contribution was confirmed in the case of immobilized alkaloid type ligand A<sup>[139]</sup> (Scheme 9.4).



Scheme 9.4

On the other hand, a significant homogeneous catalysis was ruled out by specific requirements for the immobilized alkaloid type B, which can deliver uniformly high activity and enantioselectivity levels after recycling, thanks to substantial chemical stability and effective swelling due to the hydrophilic diethylene glycol side-chains<sup>[140]</sup> (Scheme 9.4).

A more chemically robust polymer-supported chiral catalyst, based on  $\alpha,\alpha$ -diphenyl-L-prolinol, was designed by Kell *et al.*<sup>[141]</sup> for reduction of prochiral ketones with borane.

The Julia–Colonna asymmetric epoxidation<sup>[142,143]</sup> of (*E*)- $\alpha,\beta$ -unsaturated ketones, catalysed by polyamino acids, such as poly-L-leucine, is one of the more commonly employed methods for epoxidation of electron-deficient substrates<sup>[144,145]</sup> among the three protocols that were reported.<sup>[146]</sup> The first involves a triphasic system consisting of insoluble catalyst (generally polyalanine or polyleucine), a solution of the enone in an organic solvent (such as hexane, carbon tetrachloride or toluene) and an aqueous layer containing H<sub>2</sub>O<sub>2</sub> and NaOH.<sup>[147]</sup> More recently, Allen *et al.*<sup>[148]</sup> have reported two protocols that lead to greatly reduced reaction times and a significant expanded substrate range. The biphasic consists of insoluble catalyst and a solution of tetrahydrofuran (THF), 1,8-diaza-7-bicyclo[5.4.0]undecene and H<sub>2</sub>O<sub>2</sub> (added in the form of anhydrous urea–H<sub>2</sub>O<sub>2</sub>).<sup>[149]</sup> Another method carried out in a homogeneous solvent mixture of water and 1,2-dimethoxyethane (DME), utilizes sodium percarbonate as both oxidant and base.<sup>[148]</sup>

Preparation and activation of silica-supported poly-L-leucine<sup>[150]</sup> has been studied under a variety of reaction conditions leading to an efficient procedure for the preparation of material suitable for use in the Julia–Colonna asymmetric epoxidation reaction. Poly-L-leucine, can be added to the list of natural<sup>[151]</sup> and non-natural<sup>[152]</sup> oxidation catalysts that benefit from being supported on commercially available silica gel.

Even though there is great interest in such systems based on polymers as supporting materials, this chapter essentially focuses on the use of minerals as support. The use of silica has been historically investigated, mainly for its large surface area. As mentioned later, micelle-templated silica (MTS) has recently been disclosed.

### Hybrid Mesoporous Micelle-templated Silicas (MTS) Containing Organic Base Moieties

**Organically modified mesoporous silicas** Recently, modification of MCM-41 with covalently bonded organic species, especially functional organosilanes, has attracted much attention in order to design hybrid materials with engineered properties for advanced applications, e.g. in catalysis,<sup>[153–158]</sup> and selective adsorption of organics<sup>[159]</sup> and metals.<sup>[155]</sup> At the same time, the grafting of alkylsilane on the MCM-41 surface has provided an opportunity to obtain hydrophobic materials with tailored pore size and high surface area.<sup>[160,161]</sup>

On the other hand, the functionalization of various silicas with covalently bonded organosilanes by different procedures has been studied in the past for various applications.<sup>[162–165]</sup> The synthesis of organically modified mesoporous

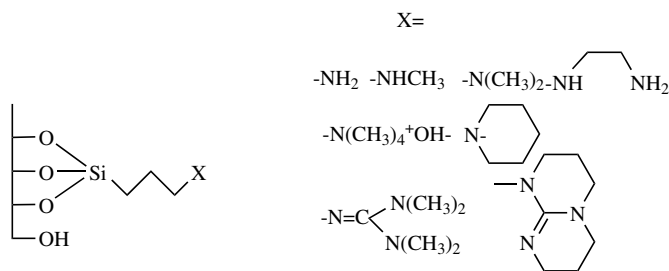
siliceous materials has been performed via three different routes: (i) silylation; (ii) coating of the nanostructured silica surface with alkyl trialkoxysilane; (iii) mono-phasic sol-gel assembly of alkyl trialkoxysilane and silica precursor  $(\text{RO})_4\text{Si}$  in the presence of surfactants as templating agents.

*Silylation of MTS surface* Firstly, the wall of preformed MTS is functionalized by the covalent linkage of organic moieties carried out by silylation of the surface with alkyl trialkoxysilane in anhydrous conditions in apolar solvent (biphasic conditions).

*Monophasic preparation of mesoporous hybrid materials* Incorporation of organic functionalities has been achieved by co-condensation of organically functionalized silica precursors leading to hybrid materials, i.e.  $\text{RSi}(\text{OR})_3$  silica and a series of hydrolysis and self-assembly condensations in the presence of surfactants (mono-phasic conditions). Macquarrie first reported the preparation of hybrid organic-mineral mesoporous materials with alkyl groups bearing amine functionality in the presence of nonionic templates.<sup>[166]</sup> The synthesis of nanostructured silicate (hexagonal mesoporous silica, HMS) in the presence of neutral surfactants had been already performed by Tanev and Pinnavaia<sup>[167]</sup> in order to remove easily the templating agent by solvent washing in place of calcinations. Hence, the anchored 3-aminopropyl chain<sup>[166]</sup> and the 3-mercaptopropyl chain<sup>[168]</sup> remain intact during the removal of surfactants.

*Organic bases attached to mesoporous silica surface* Primary, secondary and tertiary amines,<sup>[169–171]</sup> diamines,<sup>[172]</sup> ammonium hydroxide<sup>[173]</sup> and guanidines<sup>[157,174–178]</sup> have been grafted onto MTS surfaces through direct or postsilylation methodology (Scheme 9.5).

Hybrid organic/mineral solid base catalysts bearing primary and tertiary amino functions have been used as catalysts in the Knoevenagel condensation of benzaldehyde and ethyl cyanoacetate at 375 K in the presence of DMSO as solvent. Both catalysts exhibited a selectivity of approximately 100 % in ethyl *trans*- $\alpha$ -cyanocinnamate and could be recycled several times, after filtration and washing, without decrease in their catalytic performance.<sup>[171]</sup> The activity was found to be



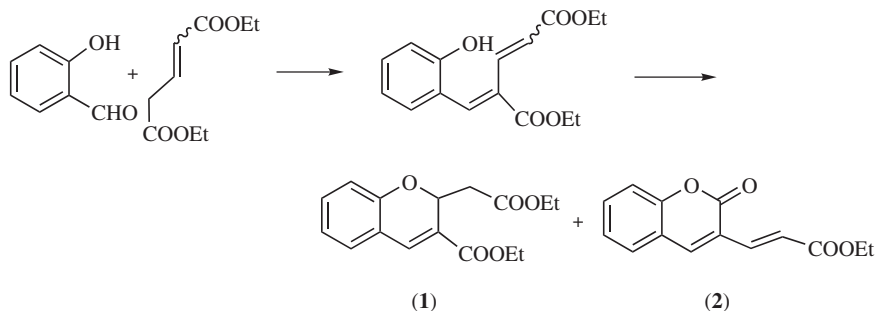
**Scheme 9.5**

directly proportional to the amount of base grafted indicating constant turnover numbers (TONs) over a wide range of surface coverage. TONs were significantly higher in the case of the primary amine grafted solid than in the case of the formed from a tertiary amine one. This resulted from the transient formation of imine groups with enhanced catalytic activity. The reaction pathway proposed involves a concerted mechanism – which is probably favoured under heterogeneous conditions – and is consistent with an enhanced base strength of the transiently formed imine groups. It also suggests that only one site is involved in each catalytic cycle. When the amine group was previously converted into imine by reaction of benzaldehyde in toluene under azeotropic distillation, the isolated material exhibited higher initial activity than the parent grafted amine under the same conditions. A similar type of mechanism which encompasses an imine intermediate in the catalytic cycle has been also proposed by Bigi *et al.*<sup>[169]</sup> for the nitroaldol condensation of benzaldehyde and nitromethane using primary amine tethered to amorphous silica or MCM-41-type materials. Recent results suggest that the silanol groups of the uncovered silica surface play a role in the imine formation.<sup>[179]</sup>

Amine containing MTS has been also used for the synthesis of monoglycerides via a reaction route involving epoxide ring opening of glycidol with fatty acids.<sup>[170]</sup> Selective synthesis of  $\alpha$ -monoglycerides constitutes a major challenge for agrochemical and pharmaceutical products. The reaction of glycidol with lauric acid ( $n = 10$ ) was performed at 293 K using toluene as solvent. Despite very high selectivities in  $\alpha$ -monoglyceride, low yields were obtained on the fresh catalyst due to extensive consumption of glycidol by polymerization of the residual silanol groups. Reuse of the catalyst, after washing with toluene, ethanol and diethyl ether, led to enhanced yields on account of the passivation of the acidic surface sites by strongly adsorbed polymer. The initial performance of the catalysts could be significantly improved after silylation of the surface by chemical vapour deposition (CVD) using hexamethyldisilazane (HMDS) as the reagent.<sup>[180]</sup> Yields up to 90 % of isolated pure  $\alpha$ -monoglyceride could then be reached and the catalysts proved to be very stable after several recycles.<sup>[170]</sup> Such catalytic reaction induced by an amine has never been described in the literature even though it was reported for reactions in homogeneous conditions.

Diamines grafted on MCM-41 revealed higher base catalytic activity because they were able to catalyse condensation between benzaldehyde and ethyl malonate which is usually less active than ethyl cyanoacetate. The catalytic activity was also high with less reactive carbonyl derivatives, such as cyclic or aliphatic ketones. Moreover, aldolization between acetone and aromatic aldehyde was also possible.<sup>[172]</sup>

Quaternary ammonium hydroxides anchored on MCM-41 provide stronger base catalysts than amine analogues<sup>[173]</sup> and were able to catalyse the same reaction as previously reported namely for the intermolecular Michael reaction leading to flavanone.<sup>[181]</sup> Moreover, this catalyst induced the successive intramolecular olefinic attack of the phenolic group from the Knoevenagel condensation product of salicylaldehyde and diethyl glutaconate (Scheme 9.6). This fast cyclization leads to chromene derivatives (**1**) from which subsequent conversions induced by proton abstraction from the alpha position of the ester function gives coumarin

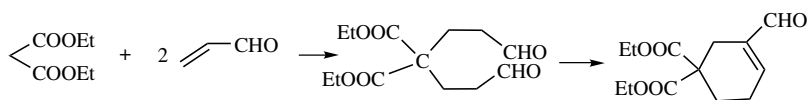


Scheme 9.6

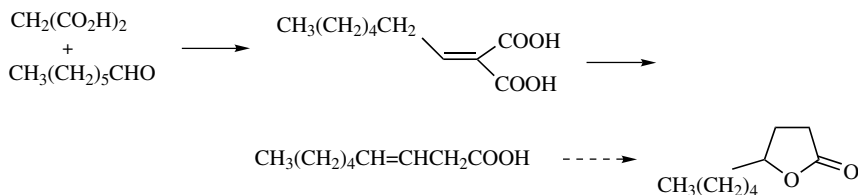
derivatives (2). The ratio of chromene/coumarin produced should be influenced by the base strength of the catalyst. Hence, the possible control of the selective formation of one or other of these compounds would be very useful because of growing interest in them for the preparation of pharmaceuticals.

Guanidines are stronger organic bases, which have already been immobilized on polymers in order to develop supported catalysis in organic synthesis.<sup>[127,132]</sup> The anchored guanidines on MTS provide useful catalysts for difficult reactions such as Michael reactions<sup>[157]</sup> or transesterification reactions.<sup>[178]</sup> Hence, during the reaction between cyclopentenone and ethyl cyanoacetate, the strong basic sites selectively catalyse 1-4 addition versus undesirable secondary reactions (dimerizations and rearrangements). Another interesting application of guanidine containing MTS reported by Rao *et al.*<sup>[157]</sup> involves the double Michael addition of acrolein on diethylmalonate followed by aldol condensation leading to ring formation (Scheme 9.7).

The Linstead variation of the Knoevenagel condensation catalysed by a series of supported guanidines prepared via different routes, was also investigated by us in collaboration with Macquarrie's group, and revealed excellent results. This condensation reaction can be used for the synthesis of the precursor of coconut oil lactone, a fragrance component (Scheme 9.8).<sup>[174]</sup>

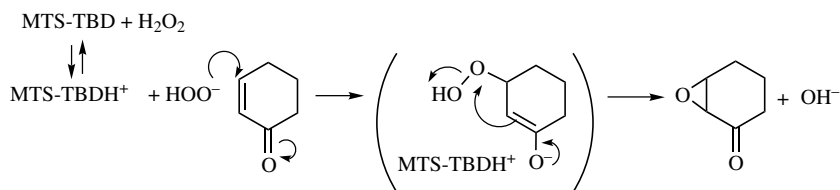


Scheme 9.7



Scheme 9.8





Scheme 9.9

The base-catalysed epoxidation of electron-deficient alkenes was also described<sup>[157,174]</sup> and proceeded with excellent conversions and selectivities, when the surface was passivated by silylation. Their high efficiency in the epoxidation of alken-2-one results from their ability to deprotonate  $\text{H}_2\text{O}_2$  leading to an ion pair ( $\text{HOO}^-$ ,  $\text{MTS-TBDH}^+$ ) and from their lipophilic character, which favours the adsorption of olefin which then reacts via 1-4 addition (Scheme 9.9).

The proton sponge, 1,8-bis(dimethylaminonaphthalene) (DMAN), has been anchored onto amorphous and pure silica MCM-41.<sup>[182]</sup> DMAN supported on MCM-41 is an excellent base catalyst for the Knoevenagel condensation between benzaldehyde and different active methylene compounds, as well as for the Claisen–Schmidt condensation of benzaldehyde and 2'-hydroxyacetophenone to produce chalcones and flavanones. It was found that the activity of the supported catalyst is directly related to the polarity of the inorganic support. Moreover, the support can also preactivate the reagents by interaction of the carbonyl groups with the weakly acidic silanol groups of MCM-41. This preactivation step enables DMAN, anchored onto MCM-41, to abstract protons with a higher  $\text{p}K$  than that of the DMAN.

It is noteworthy that chiral organic bases such as pyrrolidines and cinchonines or cinchonidines were recently grafted onto a MCM-41 support.<sup>[183,184]</sup> These materials catalyse enantioselective Michael-type addition between ethyl 2-oxocyclopentanecarboxylate and methyl vinyl ketone<sup>[183]</sup> as well as thiol and 5-methoxy-2(5H)-furanone.<sup>[184]</sup> Although ee was only modest (maximum ee 35%), these attempts are very promising.

Other basic catalysis performed with *in situ*-prepared hybrid materials (HMS) have also been successfully developed by Macquarrie *et al.*<sup>[185,186]</sup>

In the case of base catalysis, the stabilization of MCM-41 by hydrophobization could provide access to more base resistant materials. Other strategies would include the use of other supports, such as  $\text{TiO}_2$  or  $\text{ZrO}_2$ .

The main advantages of these new hybrid mesoporous materials lie in their extremely high surface areas and free accessibility of their pore systems. The design of anchored catalytic sites possessing chirality and higher acid or base strength is in progress and will extend their application in fine chemical synthesis. However, the challenging task which needs to be addressed is the improvement of the chemical stability and the price of MTS versus silica gel in order to allow regeneration and reuse without loss of activity.

## 9.4 CONCLUSIONS

Solid base catalysts with a variety of base strengths are now available. Characterization of base strength relies mainly on probe molecules combined with spectroscopies and on catalytic test reactions. A large variety of reactions of industrial interest can be catalysed by solid catalysts, but in most cases they have to compete reactions using NaOH as a base. Since costwise it is not possible to compete with NaOH, specially when production is relatively low or product added value is small, solid base catalysts should show clear selectivity and/or yield advantages. For highly demanding base-catalysed reactions, problems associated with catalyst poisoning by CO<sub>2</sub> and H<sub>2</sub>O are still dominant.

## REFERENCES

1. Ono, Y. Solid base catalysts for the synthesis of fine chemicals. *J. Catal.*, **2003**, *216*, 406–415.
2. Hattori, H. Solid base catalysts: generation of basic sites and application to organic synthesis. *Appl. Catal., A*, **2001**, *222*, 247–253.
3. Ono, Y. and Baba, T. Selective reactions over solid base catalysts. *Catal. Today*, **1997**, *38*, 321–337.
4. Weitkamp, J., Hunger, M. and Rymasa, U. Base catalysis on microporous and mesoporous materials: recent progress and perspectives. *Microporous Mesoporous Mater.*, **2001**, *48*, 255–270.
5. Hattori, H. Catalysis by basic metal oxides. *Mater. Chem. Phys.*, **1988**, *18*, 533–52.
6. Hattori, H. Catalysis by alkaline earth metal oxides. *Stud. Surf. Sci. Catal.*, **1985**, *21*, 319–330.
7. Hattori, H. Heterogeneous basic catalysts. *Chem. Rev.*, **1995**, *95*, 537–558.
8. Tanabe, K. Catalysis by solid bases and related subjects. In *Catalysis by Acids and Bases*, B. Imelik *et al.* (eds). Elsevier, Amsterdam, **1985**.
9. Cavani, F., Trifiro, F. and Vaccari, A. Hydrotalcite-type anionic clays: preparation, properties and applications, *Catal. Today*, **1991**, *11*, 173–301.
10. Rives, V. E. *Layered Double Hydroxydes: Present and Future*. Nova Sci., New York, **2001**.
11. Brunel, D. Functionalized micelle-templated silicas (MTS) and their use as catalysts for fine chemicals. *Microporous Mesoporous Mater.*, **1999**, *27*, 329–344.
12. Brunel, D., Blanc, A. C., Galarneau, A. and Fajula, F. New trends in the design of supported catalysts on mesoporous silicas and their applications in fine chemicals. *Catal. Today*, **2002**, *73*, 139–152.
13. Climent, M. J., Corma, A., Iborra, S. and Velty, A. Designing the adequate base solid catalyst with Lewis or Bronsted basic sites or with acid–base pairs, *J. Mol. Catal., A*, **2002**, *182–183*, 327–342.
14. Figueras, F. Base catalyst in the synthesis of fine chemicals, *Top. Catal.*, **2004**, *29*, 189–196.
15. Tichit, D. and Coq, B. Catalysis by hydrotalcites and related materials, *Cattech*, **2003**, *7*, 206–217.
16. Zhang, G., Hattori, H. and Tanabe, K. Aldol addition of acetone, catalyzed by solid base catalysts: magnesium oxide, calcium oxide, strontium oxide, barium oxide, lanthanum-(III) oxide and zirconium oxide, *Appl. Catal.*, **1988**, *36*, 189–97.

17. Sels, B. F., De Vos, D. E. and Jacobs, P. A. Hydrotalcite-like anionic clays in catalytic organic reactions, *Cat. Rev. - Sci. Eng.*, **2001**, *43*, 443–488.
18. Tanabe, K. In *Catalysis Science and Technology*, Anderson, J. R. and Boudart, M. (eds). Springer-Verlag, Berlin, **1981**.
19. Barthoomeuf, D. Basic zeolites: characterization and uses in adsorption and catalysis, *Cat. Rev. - Sci. Eng.*, **1996**, *38*, 521–612.
20. Huang, M., Adnot, A. and Kaliaguine, S. Characterization of basicity in alkaline cation faujasite zeolites - An XPS study using pyrrole as a probe molecule, *J. Catal.*, **1992**, *137*, 322–332.
21. Knözinger, H. and Huber, S. IR spectroscopy of small and weakly interacting probes for acidic and basic zeolites. *J. Chem. Soc., Faraday Trans.*, **1998**, *94*, 2047.
22. Lavalley, J. C. Infrared spectrometric studies of the surface basicity of metal oxides and zeolites using adsorbed probe molecules. *Catal. Today*, **1996**, *27*, 377–401.
23. Ai, M. Oxidation activity and acid–base properties of SnO<sub>2</sub>-based binary catalysts. 1. SnO<sub>2</sub>-V<sub>2</sub>O<sub>5</sub> system. *J. Catal.*, **1975**, *40*, 318–326.
24. Corma, A., Fornes, V. and Rey, F. Hydrotalcites as base catalysts: influence of the chemical composition and synthesis conditions on the dehydrogenation of isopropanol, *J. Catal.*, **1994**, *148*, 205–12.
25. Dessau, R. M., Base-catalyzed and acid catalyzed cyclization of diketones over ZSM-5. *Zeolites*, **1990**, *10*, 205.
26. Diez, V. K., Apesteguia, C. R. and Di Cosimo, J. I. Acid–base properties and active site requirements for elimination reactions on alkali-promoted MgO catalysts. *Catal. Today*, **2000**, *63*, 53–62.
27. Gervasini, A. and Auroux, A. Acidity and basicity of metal-oxide surfaces. 2. Determination by catalytic decomposition of isopropanol, *J. Catal.*, **1991**, *131*, 190–198.
28. Handa, H., Fu, Y., Baba, T. and Ono, Y. Characterization of strong solid bases by test reactions, *Catal. Lett.*, **1999**, *59*, 195–200.
29. Lauronpernot, H., Luck, F. and Popa, J. M. Methylbutynol—A new and simple diagnostic-tool for acidic and basic sites of solids, *Appl. Catal.*, **1991**, *78*, 213–225.
30. Corma, V., Fornes, V., Martin-Aranda, R. M. and Rey, F. Determination of base properties of hydrotalcites: condensation of benzaldehyde with ethyl acetoacetate, *J. Catal.*, **1992**, *134*, 58–65.
31. Figueras, F., Lopez, J., Sanchez-Valente, J., Vu, T. T. H., Clacens, J. M. and Palomeque, J. Isophorone isomerization as model reaction for the characterization of solid bases: application to the determination of the number of sites, *J. Catal.*, **2002**, *211*, 144–149.
32. Lima, E., de Menorval, L. C., Tichit, D., Lasperas, M., Graffin, P. and Fajula, F. Characterization of the acid–base properties of oxide surfaces by C-13 CP/MAS NMR using adsorption of nitromethane, *J. Phys. Chem., B*, **2003**, *107*, 4070–4073.
33. Nesterenko, N., Lima, E., Graffin, P., de Menorval, L. C., Lasperas, M., Tichit, D. and Fajula, F. Probing the basicity of oxide surfaces by FTIR spectroscopy of isocyanic acid generated in situ by thermal decomposition of nitromethane. *New J. Chem.*, **1999**, *23*, 665–666.
34. Guida, A., Lhouty, M. H., Tichit, D., Figueras, F. and Geneste, P. Hydrotalcites as base catalysts. Kinetics of Claisen–Schmidt condensation, intramolecular condensation of acetylacetone and synthesis of chalcone, *Appl. Catal., A*, **1997**, *164*, 251–264.
35. Coluccia, S. and Tench, A. J. *Proc. 7th Int. Congr. Catal., Tokyo*, **1980**, 1157.
36. Tanabe, K., Misono, M., Ono, Y. and Hattori, H. *New Solid Acids and Bases*. Kodansha-Elsevier, Tokyo, **1989**.

37. Kabashima, H., Tsuji, H. and Hattori, H. Double bond isomerization of 5-vinylbicyclo[2.2.1]hept-2-ene to 5-ethylidenebicyclo[2.2.1]hept-2-ene over alkaline earth oxides. *React. Kinet. Catal. Lett.*, **1996**, 58, 255–259.
38. Kabashima, H., Tsuji, H., Shibuya, T. and Hattori, H. Michael addition of nitromethane to  $\alpha,\beta$ -unsaturated carbonyl compounds over solid base catalysts, *J. Mol. Catal., A*, **2000**, 155, 23–29.
39. Kabashima, H., Katou, T. and Hattori, H. Conjugate addition of methanol to 3-buten-2-one over solid base catalysts. *Appl. Catal., A*, **2001**, 214, 121–124.
40. Aramendia, M. A., Borau, V., Garcia, I. M., Jimenez, C., Marinas, A., Marinas, J. M., Porras, A. and Urbano, F. J. Comparison of different organic test reactions over acid–base catalysts, *Appl. Catal., A*, **1999**, 184, 115–125.
41. Choudhary, V. R., Pataskar, S. G., Zope, G. B. and Chaudhari, P. N. Surface properties of magnesium oxide obtained from basic magnesium carbonate – influence of preparation conditions of magnesium carbonate. *J. Chem. Technol. Biotechnol.*, **1995**, 64, 407–413.
42. Choudhary V. R. and Pandit, M. Y. Surface properties of magnesium oxide obtained from magnesium hydroxide – influence on preparation and calcination conditions of magnesium-hydroxide. *Appl. Catal.*, **1991**, 71, 265–274.
43. Shastri, A. G., Chae, H. B., Bretz, M. and Schwank, J. Morphology and surface uniformity growth in MgO dehydration, *J. Phys. Chem., B* **1985**, 89, 3761–3766.
44. Menon, M., Warren, J. L. and Bullard, J. W. Synthesis of magnesia powders from an alkoxide precursor, *Ceram. Trans.*, **1998**, 95, 217–223.
45. Lopez, T., Marmolejo, R., Asomoza, M., Solis, S., Gomez, R., Wang, J. A., Bokhimi, Novaro, O., Navarrete, J., Llano, M. E. and Lopez, E. Preparation of a complete series of single phase homogeneous sol-gels of  $\text{Al}_2\text{O}_3$  and MgO for basic catalysts. *Mater. Lett.*, **1997**, 32, 325–334.
46. Stark, J. V., Park, D. G., Lagadic, I. and Klabunde, K. J. Nanoscale metal oxide particles/clusters as chemical reagents. Unique surface chemistry on magnesium oxide as shown by enhanced adsorption of acid gases (sulfur dioxide and carbon dioxide) and pressure dependence, *Chem. Mater.*, **1996**, 8, 1904–1912.
47. Klabunde, K. J., Stark, J., Koper, O., Mohs, C., Park, D. G., Decker, S., Jiang, Y., Lagadic, I. and Zhang, D. J. Nanocrystals as stoichiometric reagents with unique surface chemistry, *J. Phys. Chem., B* **1996**, 100, 12142–12153.
48. Corma A. and Iborra, S. Optimization of alkaline earth metal oxide and hydroxide catalysts for base-catalyzed reactions, *Adv. Catal.* **2006**, 49, 239–302.
49. Zhang, G., Hattori, H. and Tanabe, K. Aldol condensation of acetone/acetone-d6 over magnesium oxide and lanthanum oxide. *Appl. Catal.*, **1988**, 40, 183.
50. Di Cosimo, J. I., Diez, V. K. and Apesteguia, C. R. Base catalysis for the synthesis of  $\alpha,\beta$ -unsaturated ketones from the vapor-phase aldol condensation of acetone, *Appl. Catal., A*, **1996**, 137, 149–66.
51. Di Cosimo J. I. and Apesteguia, C. R. Study of the catalyst deactivation in the base-catalyzed oligomerization of acetone, *J. Mol. Catal., A*, **1998**, 130, 177–185.
52. Zhang, G., Hattori, H. and Tanabe, K. Aldol addition of butyraldehyde over solid base catalysts, *Bull. Chem. Soc. Jpn.*, **1989**, 62, 2070–2072.
53. Tsuji, H., Yagi, F., Hattori, H. and Kita, H. Self-condensation of n-butyraldehyde over solid base catalysts, *J. Catal.*, **1994**, 148, 759–70.
54. Climent, M. J., Corma, A., Fornes, V., Guil-Lopez, R. and Iborra, S. Aldol condensations on solid catalysts: a cooperative effect between weak acid and base sites. *Adv. Synth. Catal.*, **2002**, 344, 1090–1096.

55. Tichit, D., Lutic, D., Coq, B., Durand, R. and Teissier, W. The aldol condensation of acetaldehyde and heptanal on hydrotalcite-type catalysts. *J. Catal.*, **2003**, *219*, 167–175.
56. Noda, C., Alt, G. P., Werneck, R. M., Henriques, C. A. and Monteiro, J. L. F. Aldol condensation of citral with acetone on basic solid catalysts. *Braz. J. of Chem. Eng.*, **1998**, *15*, 120–125.
57. Climent, M. J., Corma, A., Iborra, S. and Velty, A. Synthesis of pseudoionones by acid and base solid catalysts, *Catal. Lett.*, **2002**, *79*, 157–163.
58. Climent, M. J., Corma, A., Iborra, S. and Primo, J. Base catalysis for fine chemicals production: Claisen–Schmidt condensation on zeolites and hydrotalcites for the production of chalcones and flavanones of pharmaceutical interest, *J. Catal.*, **1995**, *151*, 60–6.
59. Drexler, M. T. and Amiridis, M. D. Kinetic investigation of the heterogeneous synthesis of flavanone over MgO, *Catal. Lett.*, **2002**, *79*, 175–181.
60. Hargrove-Leak S. C. and Amiridis, M. D. Substitution effects in the heterogeneous catalytic synthesis of flavanones over MgO, *Catal. Commun.*, **2002**, *3*, 557–563.
61. Drexler, M. T. and Amiridis, M. D. The effect of solvents on the heterogeneous synthesis of flavanone over MgO. *J. Catal.*, **2003**, *214*, 136–145.
62. Akutu, K., Kabashima, H., Seki, T. and Hattori, H. Nitroaldol reaction over solid base catalysts, *Appl. Catal., A*, **2003**, *247*, 65–74.
63. Corma, A., Iborra, S., Primo, J. and Rey, F. One-step synthesis of citrionitrile on hydrotalcite derived base catalysts, *Appl. Catal., A*, **1994**, *114*, 215–225.
64. Climent, M. J., Corma, A., Guil-Lopez, R., Iborra, S. and Primo, J. Solid catalysts for the production of fine chemicals: the use of ALPON and hydrotalcite base catalysts for the synthesis of aryl sulfones, *Catal. Lett.*, **1999**, *59*, 33–38.
65. Moison, H., Texier-Boullet, F. and Foucaud, A. Knoevenagel, Wittig and Wittig–Horner reactions in the presence of magnesium oxide or zinc oxide. *Tetrahedron*, **1987**, *43*, 537–542.
66. Hachemi, M., Puciova-Sebova, M., Toma, S. and Villemin, D. Dry reaction of diethyl cyanomethylphosphonate and tetraethyl methylenediphosphonate with benzaldehyde on solid bases, *Phosphorus, Sulfur Silicon Relat. Elem.*, **1996**, *113*, 131–136.
67. Kabashima, H., Tsuji, H. and Hattori, H. Michael addition of methyl crotonate over solid base catalysts, *Appl. Catal., A*, **1997**, *165*, 319–325.
68. Kabashima, H. and Hattori, H. Cyanoethylation of methanol catalyzed by alkaline earth oxides and alumina-supported K catalysts, *Appl. Catal., A*, **1997**, *161*, L33–L35.
69. Kabashima, H. and Hattori, H. Cyanoethylation of alcohols over solid base catalysts, *Catal. Today*, **1998**, *44*, 277–283.
70. Kabashima, H., Katou, T. and Hattori, H. Conjugate addition of methanol to 3-buten-2-one over solid base catalysts, *Appl. Catal., A*, **2001**, *214*, 121–124.
71. Leclercq, E., Finiels, A. and Moreau, C. Transesterification of rapeseed oil in the presence of basic zeolites and related solid catalysts, *J. Am. Oil Chem. Soc.*, **2001**, *78*, 1161–1165.
72. Corma, A., Iborra, S., Miquel, S. and Primo, J. Catalysts for the production of fine chemicals. Production of food emulsifiers, monoglycerides, by glycerolysis of fats with solid base catalysts, *J. Catal.*, **1998**, *173*, 315–321.
73. Bancquart, S., Vanhove, C., Pouilloux, Y. and Barrault, J. Glycerol transesterification with methyl stearate over solid basic catalysts. I. Relationship between activity and basicity, *Appl. Catal., A*, **2001**, *218*, 1–11.
74. Barrault, J., Pouilloux, Y., Clacens, J. M., Vanhove C. and Bancquart, S. Catalysis and fine chemistry, *Catal. Today*, **2002**, *75*, 177–181.

75. Gryglewicz, S. Alkaline earth metal compounds as alcoholysis catalysts for ester oils synthesis, *Appl. Catal., A*, **2000**, 192, 23–28.
76. Hattori, H., Shima, M. and Kabashima, H. Alcoholysis of ester and epoxide catalyzed by solid bases, *Stud. Surf. Sci. Catal.*, **2000**, 130D, 3507–3512.
77. Morishige, K., Hattori, H. and Tanabe, K. Pronounced catalytic activity of magnesium oxide and calcium oxide in isomerization of penta-1,4-diene to penta-1,3-diene, *J. Chem. Soc., Chem. Commun.*, **1975**, 559–560.
78. Hattori, A., Hattori, H. and Tanabe, K. Double-bond migration of allylamine to enamine over basic solid catalysts, *J. Catal.*, **1980**, 65, 245.
79. Matsushashi, H., Hattori, H. and Tanabe, K. Double-bond migration of allyl ethers over solid base catalysts, *Chem. Lett.*, **1981**, 341.
80. Matsushashi, H. and Hattori, H. Double-bond migration of 2-propenyl ethers to 1-propenyl ethers over solid base catalysts, *J. Catal.*, **1984**, 85, 457.
81. Creighton, E. J., Huskens, J., van der Waal, J. C. and van Bekkum, H. Meerwein–Ponndorf–Verley and Oppenauer reactions catalysed by heterogeneous catalyst. *Stud. Surf. Sci. Catal.*, **1997**, 108, 531.
82. Szollosi, G. and Bartok, M. Vapour-phase heterogeneous catalytic transfer hydrogenation of alkyl methyl ketones on MgO: prevention of the deactivation of MgO in the presence of carbon tetrachloride, *Appl. Catal., A*, **1998**, 169, 263–269.
83. Szollosi, G. and Bartok, M. Catalytic transfer hydrogenation of 2-butanone on MgO. New active surface sites generated by treatment with chloroform, *Catal. Lett.*, **1999**, 59, 179–185.
84. Szollosi, G. and Bartok, M. Role of basic and acidic centers of MgO and modified MgO in catalytic transfer hydrogenation of ketones studied by infrared spectroscopy, *J. Mol. Struct.*, **1999**, 483, 13–17.
85. Aramendia, M. A., Borau, V., Jimenez, C., Marinas, J. M., Ruiz, J. R. and Urbano, F. J. Activity of basic catalysts in the Meerwein–Ponndorf–Verley reaction of benzaldehyde with ethanol, *J. Colloid Interface Sci.*, **2001**, 238, 385–389.
86. Aramendia, M. A., Borau, V., Jimenez, C., Marinas, J. M., Ruiz, J. R. and Urbano, F. J. Influence of the preparation method on the structural and surface properties of various magnesium oxides and their catalytic activity in the Meerwein–Ponndorf–Verley reaction, *Appl. Catal., A*, **2003**, 244, 207–215.
87. Ogata, Y. and Kawasaki, A. Alkoxide transfer from aluminum alkoxide to aldehyde in the Tishchenko reaction. *Tetrahedron*, **1969**, 25, 929.
88. Saegusa, T. and Ueshima, T. Tishchenko reaction of chloral by aluminum haloalcohols, *J. Org. Chem.*, **1968**, 33, 3310.
89. Seki, T., Kabashima, H., Akutsu, K., Tachikawa, H. and Hattori, H. Mixed Tishchenko reaction over solid base catalysts, *J. Catal.*, **2001**, 204, 393–401.
90. Seki, T., Akutsu, K. and Hattori, H. Calcium oxide and strontium oxide as environmentally benign and highly efficient heterogeneous catalysts for the Tishchenko reaction of furfural, *Chem. Commun.*, **2001**, 1000–1001.
91. Seki, T. and Hattori, H. Tishchenko reaction over solid base catalysts, *Catal. Surv. Asia*, **2003**, 7, 145–156.
92. Seki, T., Tachikawa, H., Yamada, T. and Hattori, H. Synthesis of phthalide-skeleton using selective intramolecular Tishchenko reaction over solid base catalysts, *J. Catal.*, **2003**, 217, 117–126.
93. Reichle, W. T. Pulse microreactor examination of the vapor-phase aldol condensation of acetone, *J. Catal.*, **1980**, 63, 295.

94. Constantino V. R. L. and Pinnavaia, T. J. Structure–reactivity relationships for basic catalysts derived from a  $\text{Mg}^{2+}/\text{Al}^{3+}/\text{CO}_3^{2-}$  layered double hydroxide, *Catal. Lett.*, **1994**, 23, 361–67.
95. Constantino V. R. L. and Pinnavaia, T. J. Basic properties of  $\text{Mg}_{1-x}\text{Al}_x^{3+}$  layered double hydroxides intercalated by carbonate, hydroxide, chloride, and sulfate anions, *Inorg. Chem.*, **1995**, 34, 883–92.
96. Ueno, S., Yamaguchi, K., Yoshida, K., Ebitani, K. and Kaneda, K. Hydrotalcite catalysis: heterogeneous epoxidation of olefins using hydrogen peroxide in the presence of nitriles, *Chem. Commun.*, **1998**, 295–296.
97. Lakshmi Kantam, M., Choudary, B. M., Reddy, C. V., Koteswara Rao, K. and Figueras, F. Aldol and Knoevenagel condensations catalyzed by modified Mg–Al hydrotalcite: a solid base as catalyst useful in synthetic organic chemistry, *Chem. Commun.*, **1998**, 1033–1034.
98. Lopez, J., Jacquot, R. and Figueras, F. Heterogeneous catalysis of aldolizations on activated hydrotalcites, *Stud. Surf. Sci. Catal.*, **2000**, 130A, 491–496.
99. Roelofs, J. C. A. A., van Dillen, A. J. and de Jong, K. P. Base-catalyzed condensation of citral and acetone at low temperature using modified hydrotalcite catalysts, *Catal. Today*, **2000**, 60, 297–303.
100. Roelofs, J. C. A. A., Lensveld, D. J., van Dillen, A. J. and de Jong, K. P. On the structure of activated hydrotalcites as solid base catalysts for liquid-phase aldol condensation. *J. Catal.*, **2001**, 203, 184–191.
101. Tichit, D., Bennani, M. N., Figueras, F., Tessier, R. and Kervennal, J. Aldol condensation of acetone over layered double hydroxides of the meixnerite type. *Appl. Clay Sci.*, **1998**, 13, 401–415.
102. Choudary, B. M., Lakshmi Kantam, M., Venkat Reddy, C. R., Koteswara Rao, K. and Figueras, F. The first example of Michael addition catalyzed by modified Mg–Al hydrotalcite, *J. Mol. Catal., A*, **1999**, 146, 279–284.
103. Lima, E., Lasperas, M., de Menorval, L. C., Tichit, D. and Fajula, F. Characterization of basic catalysts by the use of nitromethane as NMR probe molecule and reactant, *J. Catal.*, **2004**, 223, 28–35.
104. Palomeque, J., Lopez, J. and Figueras, F. Epoxidation of activated olefins by solid bases, *J. Catal.*, **2002**, 211, 150–156.
105. Climent, M. J., Corma, A., Iborra, S., Epping, K. and Velty, A. Increasing the basicity and catalytic activity of hydrotalcites by different synthesis procedures, *J. Catal.*, **2004**, 225, 316–326.
106. Abello, S., Medina, F., Tichit, D., Perez-Ramirez, J., Groen, J. C., Sueiras, J. E., Salagre, P. and Cesteros, Y. Aldol condensations over reconstructed Mg–Al hydrotalcites: structure–activity relationships related to the rehydration method, *Chem. Eur. J.*, **2005**, 11, 728–739.
107. Abello, S., Medina, F., Tichit, D., Perez-Ramirez, J., Cesteros, Y., Salagre, P. and Sueiras, J. E. Nanoplatelet-based reconstructed hydrotalcites: towards more efficient solid base catalysts in aldol condensations, *Chem. Commun.*, **2005**, 1453–1455.
108. Valente, J. S., Figueras, F., Gravelle, M., Kumbhar, P., Lopez, J. and Besse, J. P. Basic properties of the mixed oxides obtained by thermal decomposition of hydrotalcites containing different metallic compositions, *J. Catal.*, **2000**, 189, 370–381.
109. Climent, M. J., Corma, A., Iborra, S. and Velty, A. Activated hydrotalcites as catalysts for the synthesis of chalcones of pharmaceutical interest, *J. Catal.*, **2004**, 221, 474–482.
110. Choudary, B. M., Kantam, M. L. and Kavita, B. Mg–Al–O–Bu–t–Hydrotalcite: a mild and ecofriendly catalyst for the cyanoethylation of alcohols and thiols. *Green Chem.*, **1999**, 1, 289–292.

111. Choudary, B. M., Kantam, M. L., Reddy, C. V., Aranganathan, S., Santhi, P. L. and Figueras, F. Mg-Al-O-t-Bu hydrotalcite: a new and efficient heterogeneous catalyst for transesterification, *J. Mol. Catal., A*, **2000**, *159*, 411–416.
112. Choudary, B. M., Kantam, M. L., Kavita, B., Reddy, C. V., Rao, K. K. and Figueras, F. Aldol condensations catalysed by novel Mg-Al-O-t-Bu hydrotalcite, *Tetrahedron Lett.*, **1998**, *39*, 3555–3558.
113. Choudary, B. M., Kantam, M. L., Reddy, C. R. V., Bharathi, B. and Figueras, F. Wadsworth–Emmons reaction: the unique catalytic reaction by a solid base, *J. Catal.*, **2003**, *218*, 191–200.
114. Greenwell, H. C., Stackhouse, S., Coveney, P. V. and Jones, W. A density functional theory study of catalytic *trans*-esterification by tert-butoxide MgAl anionic clays. *J. Phys. Chem. B*, **2003**, *107*, 3476–3485.
115. Kumbhar, P. S., Sanchez-Valente, J., Lopez, J. and Figueras, F. Meerwein–Ponndorf–Verley reduction of carbonyl compounds catalysed by Mg-Al hydrotalcite. *Chem. Commun.*, **1998**, 535–536.
116. Bergmann, E. D. and Corett, R. Basic exchange resins as catalysts in the Michael reaction. 1. *J. Org. Chem.*, **1956**, *21*, 107–110.
117. Bergmann, E. D. and Corett, R. Basic exchange resins as catalysts in the Michael reaction. 2. *J. Org. Chem.*, **1958**, *23*, 1507–1510.
118. Rich, D. H. and Gurwara, S. K. Preparation of a new omicron-nitrobenzyl resin for solid-phase synthesis of tert-butyloxycarbonyl-protected peptide acids, *J. Am. Chem. Soc.*, **1975**, *97*, 1575–1579.
119. Mitchell, A. R., Kent, S. B. H., Erickson, B. W. and Merrifield, R. B. Preparation of aminomethyl-polystyrene resin by direct amidomethylation, *Tetrahedron Lett.*, **1976**, 3795–3798.
120. Luis, S. V., Burguete, M. I. and Altava, B. A novel method for the functionalization of polystyrene resins through long aliphatic spacers, *React. Funct. Polym.*, **1995**, *26*, 75–83.
121. Barton, D. H. R., Elliott, J. D. and Gero, S. D. The synthesis and properties of a series of strong but hindered organic bases, *J. Chem. Soc., Chem. Commun.*, **1981**, 1136–1137.
122. Barton, D. H. R., Elliott, J. D. and Gero, S. D. Synthesis and properties of a series of sterically hindered guanidine bases, *J. Chem. Soc., Perkin Trans. I*, **1982**, 2085–2090.
123. Flynn, K. G. and Neortas, D. R. Kinetics and mechanism of reaction between phenyl isocyanate and alcohols – strong base catalysis and deuterium isotope effects, *J. Org. Chem.*, **1963**, *28*, 3527–3530.
124. Pollini, G. P., Barco, A. and De Giuli, G. Tetramethylguanidine-catalyzed addition of nitromethane to  $\alpha,\beta$ -unsaturated carboxylic acid esters, *Synthesis*, **1972**, 44–45.
125. Vanaken, E., Wynberg, H. and Vanbolhuis, F. Nitroalkanes in C-C bond forming reactions – A crystal-structure of a complex of a guanidine catalyst and a nitroalkane substrate, *J. Chem. Soc., Chem. Commun.*, **1992**, 629–630.
126. Schuchardt, U., Vargas, R. M. and Gelbard, G. Alkylguanidines as catalysts for the transesterification of rapeseed oil, *J. Mol. Catal., A*, **1995**, *99*, 65–70.
127. Schuchardt, U., Vargas, R. M. and Gelbard, G. Transesterification of soybean oil catalyzed by alkylguanidines heterogenized on different substituted polystyrenes, *J. Mol. Catal., A*, **1996**, *109*, 37–44.
128. Le Perche, P., Abusio, M., Arretz, E. Resins having a primary amine or guanidine function and their preparation. **1996**, WO 9721740.
129. Arretz, E., Lopez, F. Method for preparing organic disulfides and polysulfides from mercaptans and sulfur in the presence of heterogeneous styrene-divinylbenzene copolymer catalysts having pendant guanidine or amidine groups. **1996**, WO 9721673.



130. Luyendijk, P., Devaux, J. F., Monguillon, B. Process for the preparation of sulfurized olefins using solid acid and solid base catalysts simultaneously, **2001**, EP 1149813.
131. Gelbard, G. and Vielfaure-Joly, F. Polynitrogen strong bases as immobilized catalysts, *React. Funct. Polym.*, **2001**, 48, 65–74.
132. Gelbard, G. and Vielfaure-Joly, F. Polynitrogen strong bases as immobilized catalysts for the transesterification of vegetable oils, *Compt. Rend. Acad. Sci., Ser. IIc*, **2000**, 3, 563–567.
133. Mackenzie W. M. and Sherrington, D. C. Substrate selectivity effects involving polymer-supported phase-transfer catalysts, *Polymer*, **1981**, 22, 431–433.
134. Hodge, P., Khoshdel, E. and Waterhouse, J. Michael reactions catalyzed by polymer-supported quaternary ammonium-salts derived from cinchona and ephedra alkaloids, *J. Chem. Soc., Perkin Trans. 1*, **1983**, 2205–2209.
135. Kelly, J. and Sherrington, D. C. Some novel polymer-supported optically-active phase-transfer catalysts. 2. Use in displacement, reduction, epoxidation and addition reactions, *Polymer*, **1984**, 25, 1499–1504.
136. Petri, A., Pini, D. and Salvadori, P. Heterogeneous enantioselective dihydroxylation of aliphatic olefins – A comparison between different polymeric cinchona alkaloid derivatives, *Tetrahedron Lett.*, **1995**, 36, 1549–1552.
137. Song, C. E., Yang, J. W., Ha, H. J. and Lee, S. G. Efficient and practical polymeric catalysts for heterogeneous asymmetric dihydroxylation of olefins, *Tetrahedron: Asymmetry*, **1996**, 7, 645–648.
138. Canali, L., Song, C. E. and Sherrington, D. C. Polymer-supported bis-cinchona alkaloid ligands for asymmetric dihydroxylation of alkenes – a cautionary tale. *Tetrahedron: Asymmetry*, **1998**, 9, 1029–1034.
139. Sheldon, R. A., Wallau, M., Arends, I. W. C. E. and Schuchardt, U. Heterogeneous catalysts for liquid-phase oxidations: Philosophers' stones or Trojan horses? *Acc. Chem. Res.*, **1998**, 31, 485–493.
140. Mandoli, A., Pini, D., Fiori, M. and Salvadori, P. Asymmetric dihydroxylation with recoverable cinchona alkaloid derivatives: a warning note and an improved, insoluble polymer-bound ligand 5 architecture, *Eur. J. Org. Chem.*, **2005**, 1271–1282.
141. Kell, R. J., Hodge, P., Snedden, P. and Watson, D. Towards more chemically robust polymer-supported chiral catalysts: alpha,alpha-diphenyl-L-prolinol based catalysts for the reduction of prochiral ketones with borane. *Org. Biomol. Chem.*, **2003**, 1, 3238–3243.
142. Julia, S., Guixer, J., Masana, J., Rocas, J., Colonna, S., Annuziata, R. and Molinari, H. Synthetic enzymes. 2. Catalytic asymmetric epoxidation by means of polyamino-acids in a triphase system, *J. Chem. Soc., Perkin Trans. 1*, **1982**, 1317–1324.
143. Julia, S., Masana, J. and Vega, J. C. Synthetic enzyme: highly stereoselective epoxidation of chalcone in the three-phase system toluene-water-poly-(S)-alanine, *Angew. Chem.*, **1980**, 92, 968–969.
144. Chen, R., Qian, C. and de Vries, J. G. Asymmetric epoxidation of  $\alpha,\beta$ -unsaturated ketones catalyzed by chiral ytterbium complexes, *Tetrahedron Lett.*, **2001**, 42, 6919–6921.
145. Porter M. J. and Skidmore, J. Asymmetric epoxidation of electron-deficient olefins, *Chem. Commun.*, **2000**, 1215–1225.
146. Savizky, R. M., Suzuki, N. and Bove, J. L. The use of sonochemistry in the asymmetric epoxidation of substituted chalcones with sodium perborate tetrahydrate. *Tetrahedron: Asymmetry*, **1998**, 9, 3967–3969.

147. Flisak, J. R., Gombatz, K. J., Holmes, M. M., Jarmas, A. A., Lantos, I., Mendelson, W. L., Novack, V. J., Remich, J. J. and Snyder, L. A Practical, enantioselective synthesis of SK-and-F 104353. *J. Org. Chem.*, **1993**, 58, 6247–6254.
148. Allen, J. V., Drauz, K. H., Flood, R. W., Roberts, S. M. and Skidmore, J. Polyamino acid-catalysed asymmetric epoxidation: sodium percarbonate as a source of base and oxidant. *Tetrahedron Lett.*, **1999**, 40, 5417–5420.
149. Lauret, C. and Roberts, S. M. Asymmetric epoxidation of alpha,beta-unsaturated ketones catalyzed by poly(amino acids), *Aldrichim. Acta*, **2002**, 35, 47–51.
150. Baars, S., Drauz, K. H., Krimmer, H. P., Roberts, S. M., Sander, J., Skidmore, J. and Zanardi, G. Development of the Julia-Colonna asymmetric epoxidation reaction: Part I. Preparation and activation of the polyleucine catalyst. *Org. Proc. Res. Dev.*, **2003**, 7, 509–513.
151. Heller, J. and Heller, A. Loss of activity or gain in stability of oxidases upon their immobilization in hydrated silica: significance of the electrostatic interactions of surface arginine residues at the entrances of the reaction channels. *J. Am. Chem. Soc.*, **1998**, 120, 4586–4590.
152. Song, C. E., Oh, C. R., Lee, S. W., Lee, S. G., Canali, L. and Sherrington, D. C. Heterogeneous asymmetric aminohydroxylation of alkenes using a silica gel-supported bis-cinchona alkaloid. *Chem. Commun.*, **1998**, 2435–2436.
153. Corma, A. From microporous to mesoporous molecular sieve materials and their use in catalysis. *Chem. Rev.*, **1997**, 97, 2373–2419.
154. Corma, A. Preparation and catalytic properties of new mesoporous materials. *Top. Catal.*, **1998**, 4, 249–260.
155. Mercier, L. and Pinnavaia, T. J. Access in mesoporous materials: advantages of a uniform pore structure in the design of a heavy metal ion adsorbent for environmental remediation. *Adv. Mater.*, **1997**, 9, 500-&.
156. Moller, K. and Bein, T. Inclusion chemistry in periodic mesoporous hosts. *Chem. Mater.*, **1998**, 10, 2950–2963.
157. Rao, Y. V. S., De Vos, D. E. and Jacobs, P. A. 1,5,7-Triazabicyclo[4.4.0]dec-5-ene immobilized in MCM-41: a strongly basic porous catalyst, *Angew. Chem. Int. Ed.*, **1997**, 36, 2661–2663.
158. Ying, J. Y., Mehnert, C. P. and Wong, M. S. Synthesis and applications of supramolecular-templated mesoporous materials, *Angew. Chem. Int. Ed.*, **1999**, 38, 56–77.
159. Zhao, X. S., Lu, G. Q. and Hu, X. Characterization of the structural and surface properties of chemically modified MCM-41 material, *Microporous Mesoporous Mater.*, **2000**, 41, 37–47.
160. Impens, N. R. E. N., Van Der Voort, P. and Vansant, E. F. Silylation of microporous, meso- and non-porous oxides: a review. *Microporous Mesoporous Mater.*, **1999**, 28, 217–232.
161. Jaroniec, C. P., Kruk, M., Jaroniec, M. and Sayari, A. Tailoring surface and structural properties of MCM-41 silicas by bonding organosilanes, *J. Phys. Chem. B*, **1998**, 102, 5503–5510.
162. Berezniński, Y., Jaroniec, M., Kruk, M. and Buszewski, B. Adsorption characterization of octyl bonded phases for high performance liquid chromatography, *J. Liq. Chromatogr. Related Technol.*, **1996**, 19, 2767–2784.
163. Hertl, W. and Hair, M. L. Reaction of hexamethyldisilazane with silica. *J. Phys. Chem. B*, **1971**, 75, 2181–2185.
164. Tundo, P. and Venturello, P. Catalysis mechanism of phosphonium salts supported on silica-gel in organic-aqueous 2-phase systems, *J. Am. Chem. Soc.*, **1981**, 103, 856–861.

165. Waddell, T. G., Leyden, D. E. and DeBello, M. T. The nature of organosilane to silica-surface bonding, *J. Am. Chem. Soc.*, **1981**, *103*, 5303–5307.
166. Macquarrie, D. J. Direct preparation of organically modified MCM-type materials. Preparation and characterisation of aminopropyl-MCM and 2-cyanoethyl-MCM. *Chem. Commun.*, **1996**, 1961–1962.
167. Tanev, P. T. and Pinnavaia, T. J. A neutral templating route to mesoporous molecular sieves. *Science*, **1995**, *267*, 865–867.
168. Richer, R. and Mercier, L. Direct synthesis of functionalized mesoporous silica by non-ionic alkylpolyethyleneoxide surfactant assembly, *Chem. Commun.*, **1998**, 1775–1776.
169. Bigi, F., Carloni, S., Maggi, R., Mazzacani, A. and Sartori, G. Nitroaldol condensation promoted by organic bases tethered to amorphous silica and MCM-41-type materials. *Stud. Surf. Sci. Catal.*, **2000**, *130D*, 3501–3506.
170. Cauvel, A., Renard, G. and Brunel, D. Monoglyceride synthesis by heterogeneous catalysis using mcm-41 type silicas functionalized with amino groups. *J. Org. Chem.*, **1997**, *62*, 749–751.
171. Lasperas, M., Llorett, T., Chaves, L., Rodriguez, I., Cauvel, A. and Brunel, D. Amine functions linked to MCM-41-type silicas as a new class of solid base catalysts for condensation reactions. *Stud. Surf. Sci. Catal.*, **1997**, *108*, 75–82.
172. Choudary, B. M., Kantam, M. L., Sreekanth, P., Bandopadhyay, T., Figueras, F. and Tuel, A. Knoevenagel and aldol condensations catalysed by a new diamino-functionalised mesoporous material, *J. Mol. Catal., A*, **1999**, *142*, 361–365.
173. Rodriguez, I., Iborra, S., Rey, F. and Corma, A. Heterogeneized Brønsted base catalysts for fine chemicals production: grafted quaternary organic ammonium hydroxides as catalyst for the production of chromenes and coumarins, *Appl. Catal., A*, **2000**, *194–195*, 241–252.
174. Blanc, A. C., Macquarrie, D. J., Valle, S., Renard, G., Quinn, C. R. and Brunel, D. The preparation and use of novel immobilised guanidine catalysts in base-catalysed epoxidation and condensation reactions, *Green Chem.*, **2000**, *2*, 283–288.
175. Derrien, A., Renard, G. and Brunel, D. Guanidine linked to micelle-templated mesoporous silicates as base catalyst for transesterification. *Stud. Surf. Sci. Catal.*, **1998**, *117*, 445–452.
176. Jaenicke, S., Chuah, G. K., Lin, X. H. and Hu, X. C. Organic–inorganic hybrid catalysts for acid- and base-catalyzed reactions. *Microporous Mesoporous Mater.*, **2000**, *35–36*, 143–153.
177. Lin, X., Chuah, G. K. and Jaenicke, S. Base-functionalized MCM-41 as catalysts for the synthesis of monoglycerides, *J. Mol. Catal., A*, **1999**, *150*, 287–294.
178. Sercheli, R., Vargas, R. M., Sheldon, R. A. and Schuchardt, U. Guanidines encapsulated in zeolite Y and anchored to MCM-41: synthesis and catalytic activity, *J. Mol. Catal., A*, **1999**, *148*, 173–181.
179. Blanc, A. C., Brunel, D. and Macquarrie, D. J. in preparation.
180. Sutra, P., Fajula, F., Brunel, D., Lentz, P., Daelen, G. and Nagy, J. B. Si-29 and C-13 MAS-NMR characterization of surface modification of micelle-templated silicas during the grafting of organic moieties and end-capping, *Colloids Surf., A*, **1999**, *158*, 21–27.
181. Kloetstra, K. R. and Vanbekkum, H. Base and acid catalysis by the alkali-containing MCM-41 mesoporous molecular-sieve, *J. Chem. Soc., Chem. Commun.*, **1995**, 1005–1006.
182. Corma, A., Iborra, S., Rodriguez, I. and Sanchez, F. Immobilized proton sponge on inorganic carriers, *J. Catal.*, **2002**, *211*, 208–215.

183. Corma, A., Iborra, S., Rodriguez, I., Iglesias, M. and Sanchez, F. MCM-41 heterogenized chiral amines as base catalysts for enantioselective Michael reaction, *Catal. Lett.*, **2002**, 82, 237–242.
184. Iglesias-Hernandez M. and Sanchez-Alonso, F. New environmentally friendly base catalyst for enantioselective reactions. Heterogenization of chiral amines to USY and MCM-41 zeolites, *Stud. Surf. Sci. Catal.*, **2000**, 130D, 3393–3398.
185. Macquarrie, D. J. and Jackson, D. B. Aminopropylated MCMs as base catalysts: a comparison with aminopropylated silica, *Chem. Commun.*, **1997**, 1781–1782.
186. Medoe, J. E. G., Clark, J. H. and Macquarrie, D. J. Michael additions catalysed by *N,N*-dimethyl-3-aminopropyl – derivatised amorphous silica and hexagonal mesoporous silica (HMS). *Synlett*, **1998**, 625–631.



---

# 10 Hybrid Oxidation Catalysts from Immobilized Complexes on Inorganic Microporous Supports

---

DIRK DE VOS, IVE HERMANS, BERT SELS AND PIERRE JACOBS

*Centrum voor Oppervlaktechemie en Katalyse, K.U.Leuven, Kasteelpark Arenberg 23,  
B-3001 Leuven, Belgium*

## CONTENTS

10.1 INTRODUCTION AND SCOPE . . . . .	207
10.2 OXYGENATION POTENTIAL OF HEME-TYPE COMPLEXES IN ZEOLITE . . . . .	211
10.2.1 Metallo-phthalocyanines encapsulated in the cages of faujasite-type zeolites . . . . .	211
10.2.2 Oxygenation potential of metallo-phthalocyanines encapsulated in the mesopores of VPI-5 AlPO <sub>4</sub> . . . . .	215
10.2.3 Oxygenation potential of zeolite encapsulated metallo-porphyrins . . . . .	216
10.3 OXYGENATION POTENTIAL OF ZEOLITE ENCAPSULATED NONHEME COMPLEXES . . . . .	220
10.3.1 Immobilization of <i>N,N'</i> -bidentate complexes in zeolite Y . . . . .	220
10.3.2 Ligation of zeolite exchanged transition ions with bidentate aza ligands . . . . .	224
10.3.3 Ligation of zeolite exchanged transition ions with tri- and tetra-aza(cyclo)alkane ligands . . . . .	225
10.3.4 Ligation of zeolite exchanged transition ions with Schiff base-type ligands . . . . .	228
10.3.5 Zeolite effects with <i>N,N'</i> -bis(2-pyridinecarboxamide) complexes of Mn and Fe in zeolite Y . . . . .	231
10.3.6 Zeolite encapsulated chiral oxidation catalysts . . . . .	233
10.4 CONCLUSIONS . . . . .	235
ACKNOWLEDGEMENTS . . . . .	235
REFERENCES . . . . .	235

### 10.1 INTRODUCTION AND SCOPE

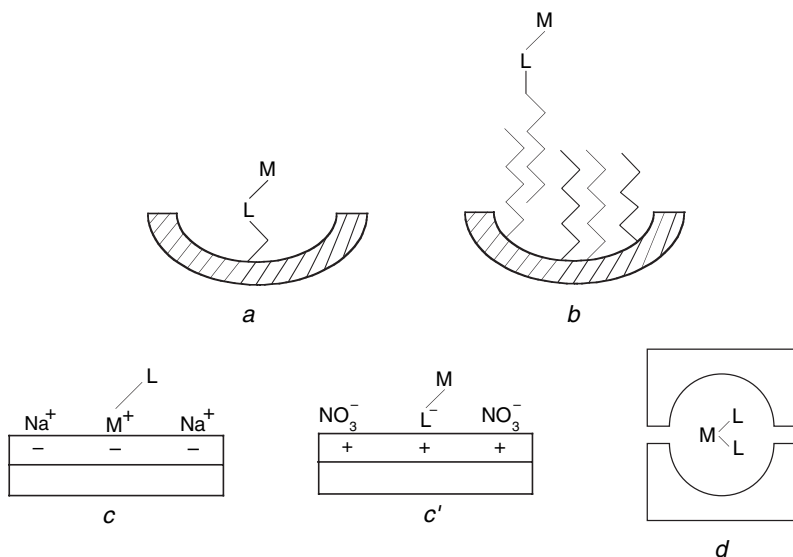
Traditionally, a comparison between homogeneous and heterogeneous catalysis for each methodology stresses a number of weak and strong points.<sup>[1]</sup> The definition of the active site at the molecular level and the variability in design are generally

considered as advantageous for homogeneous catalysis, while limited activity and stability of the catalysts in batch procedures often represent its weak points. On the other hand, ease of separation, recovery, recycling, and stability of heterogeneous catalysts are in favour of using such solids. Difficulties in the characterization at the molecular level, complexity and reproducibility in preparation, negative effects on selectivity resulting from the occurrence of diffusion limitations, are without any doubt disadvantageous when designing heterogeneous processes.

In principle, immobilization of homogeneous catalysts allows combining of all advantages of homogeneous and heterogeneous catalysts. In this frame, requirements for successful immobilization of catalysts are the following:<sup>[2]</sup>

- Preparation should be simple, efficient and generally applicable.
- Performance should at least be comparable to that of the free catalyst.
- Catalyst recovery or separation should occur via simple techniques, such as filtration.
- Leaching of the active species, often a transition metal, from the catalyst support should be negligible.
- Catalyst supports should be chemically, thermally and mechanically stable.
- Catalyst re-use should be feasible without activity or selectivity loss; activity and selectivity should be stable in case of operation in a continuous flow reactor.

Several methods have been proposed combining the best properties of homogeneous and heterogeneous catalysts. The popular ones are schematically shown in Scheme 10.1.<sup>[1]</sup>



**Scheme 10.1** Schematic representation of often used catalyst immobilization methodologies (after Blaser *et al.*<sup>[1]</sup>) via: a, covalent bonding, b, adsorption; c and c', ion pair formation; and d, entrapment. L and M stand for the ligand and transition metal of the active complex,  $ML_x$ , respectively.

Immobilization via covalent bonding or tethering of a ligand to the catalyst support, has a broad applicability, but often requires redesign of the ligand to get the appropriate functionalization. In general, the hybrid catalyst thus obtained is thermally labile, limiting regeneration or rejuvenation to mild solvent washing and inhibiting regeneration by thermal treatment.

Occasionally, immobilization via adsorption is possible, provided the complex is not removed from its support as a result of competition effects with solvents and substrates. Provided the suitable solvents and reactants are available preventing catalyst leaching from the support surface, the often-expensive catalyst can be easily desorbed and re-adsorbed on fresh support.

Solid supports showing ion exchange capacity can be used to immobilize charged catalytic complexes via ion pair formation or electrostatic retention. Although competition with ionic substrates and salts in solution is obvious, cheap inorganic cation as well as anion exchangers are available, namely zeolites, clays, and layered double hydroxides (LDHs), respectively. In the former case, direct linking of the transition metal to the inorganic entity allows heterogenization, while in the latter case the presence of negatively charged ligands is a prerequisite for immobilization via electrostatic retention. Only the former category of solids will be considered in this Chapter.

In microporous supports or zeolites, catalyst immobilization is possible by steric inclusion or entrapment of the active transition metal complex. As catalyst retention requires the encapsulation of a relatively large complex into cages only accessible through windows of molecular dimensions, the term ‘ship-in-a-bottle’ has been coined for this methodology. Intrinsically, the size of the window not only determines the retention of the complex, but also limits the substrate size that can be used. The sensitivity to diffusion limitations of zeolite-based catalysis remains unchanged with the ship-in-a-bottle approach. In many cases, complex deformation upon heterogenization may occur.

The area of catalyst immobilization has received considerable attention as can be judged from the available literature reviews.<sup>[1–30]</sup> Immobilization of oxidation catalysts shows intrinsic advantages over other catalysts as the tendency for self-oxidation will decrease. Moreover, complexes with generally low solubility, such as heme-type transition metal complexes, can be dispersed molecularly on supports. It is the aim of the present work to overview the state of knowledge on the immobilization of transition metal complexes using microporous supports, such as zeolites and laminar supports like clays. The wealth of information available for complexes immobilized on LDHs or tethered to the mesopore walls in hierarchically organized oxides will not be dealt with.

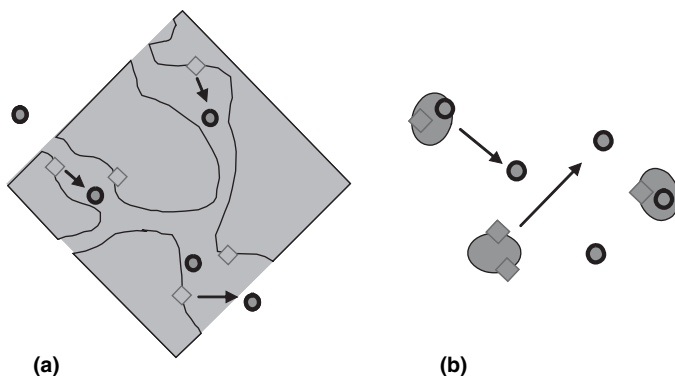
The most straightforward immobilization method for catalytically active redox elements for liquid phase oxidation reactions consists of isomorphic substitution. Well-known systems with very peculiar properties that will not be treated in further detail are:

- Ti-substituted silicalite, used for selective oxygenation of numerous substrate types with aqueous hydrogen peroxide; although the geometric environment of



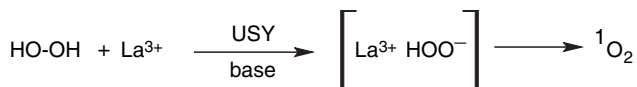
the active site limits its use to relatively small substrates, such as linear alkenes, excluding the use of substrates like cyclohexane and cyclohexene, the active site is quite stable under the reaction conditions;<sup>[31, 32]</sup> on the other hand, Ti-substituted in meso-structured silica, although being accessible to much larger substrate molecules, is very prone to leaching.<sup>[33]</sup>

- Fe-substituted ZSM-5 type zeolites, allowing the hydroxylation of benzene with  $N_2O$  with the help of the so-called redox properties of lattice substituted  $\alpha$ -iron [34].
- Microporous and crystalline alumino-phosphates with  $AlPO_4-n$  topology, substituted by transition ions like Mn, Co, Cr, and V. Although most transition metals do not fulfil the conditions for isomorphic substitution, catalysts with interesting properties may arise; extreme caution should, however, be exercised in applying such materials to liquid phase oxidation reactions, particularly involving solubilizing agents such as hydroperoxides and acids, such as adipic and acetic acid.<sup>[35]</sup> In particular, early claims on the heterogeneous nature of many of these redox molecular sieves in reaction conditions were withdrawn,<sup>[36]</sup> converting the materials from philosopher's stones into Trojan horses; exciting claims on the potential of shape selective redox molecular sieves in the selective oxidation of primary alkane carbons,<sup>[37,38]</sup> require also subtraction by other groups.
- Sn-substituted zeolite  $\beta$ ,<sup>[27, 39, 40]</sup> this material shows exceptional Lewis acidity, allowing Baeyer–Villiger oxidations of ketones into the corresponding lactones.
- La and Ca exchanged in zeolites, and more particularly in USY (ultrastable Y) and Beta, functioning as dark sources of singlet oxygen ( $^1O_2$ ) from hydrogen peroxide;<sup>[41–43]</sup> the  $^1O_2$  formed is able to react in an efficient way with olefinic substrates, provided the sites generating the short living electrophilic oxidant are close to the organic substrate. This is possible in the mesopores of USY



**Scheme 10.2** Efficient use of  $^1O_2$  ( $\diamond$ ), generated near La or Ca cations in the mesopores of zeolite USY (a) or at the external surface of small zeolite Beta crystals (b), in the oxygenation of alkenes ( $\circ$ ).

zeolite or at the external surface of the small crystals of zeolite Beta (Scheme 10.2). The generation of singlet oxygen seems to occur via the following undetailed reaction scheme:



## 10.2 OXYGENATION POTENTIAL OF HEME-TYPE COMPLEXES IN ZEOLITE

### 10.2.1 METALLO-PHTHALLOCYANINES ENCAPSULATED IN THE CAGES OF FAUJASITE-TYPE ZEOLITES

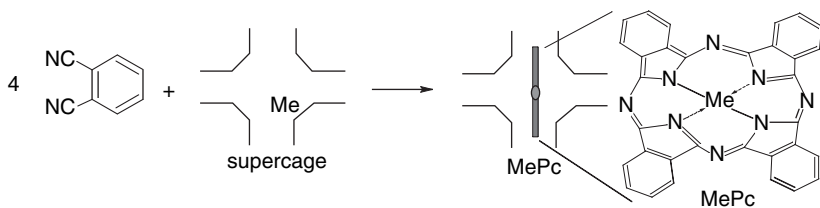
Metallo-phthalocyanine (MePc) complexes are known as mild oxygenation catalysts for alkanes and alkenes and as functional models for enzymes, more in particular for monooxygenases like Cytochrome P450.<sup>[44]</sup> Among the many possible supports for such complexes, zeolite FAU topologies<sup>[45]</sup> are excellent materials for their encapsulation.<sup>[46–50]</sup> The low solubility of MePc complexes in general and their tendency to form adducts even in solution, giving rise to self-oxidation and subsequent self-destruction phenomena, make them the ideal candidates for their distribution as individual species on a solid support.

Upon exposure of transition metal ( $\text{Mn}^{\text{II}}$ ,  $\text{Fe}^{\text{III}}$ ,  $\text{Cu}^{\text{II}}$ ,  $\text{Co}^{\text{II}}$ ) exchanged zeolites to dicyanobenzene (DCB), encapsulated MePc complexes are formed in the faujasite supercages, according to the following stoichiometry:



The complex formation is accompanied by a two-electron oxidation of sorbed (residual) water molecules. Dicyanobenzene entering the supercages via the 12-membered rings (12-MR) of oxygen atoms, undergo a tetramerization reaction around the transition metal, resulting in encapsulated MePc with the four phenyl groups protruding into the four 12-MR giving access to each supercage, this way irreversibly retaining the complex (Scheme 10.3).

This form of encapsulation is known as ‘ship-in-a-bottle’.<sup>[46, 49]</sup> This method, where a catalytic complex is assembled and irreversibly retained inside the pores (cages) of a support material, is generally known as the ‘flexible ligand method’, assuming that ligand precursors can freely diffuse towards the transition metal. Crucial to the successful development of a zeolite encapsulated MePc complex is the thorough washing of the product after reaction, preferably with several solvents, such as acetone, dimethylformamide and alkane. A degree of filling amounting to

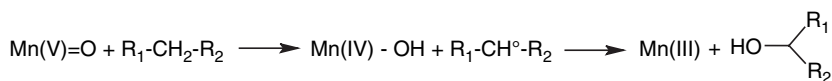


**Scheme 10.3** Formation of MePc complexes in the supercages of FAU-type zeolites via tetramerization of 1,2-dicyanobenzene around transition metal exchanged zeolite.

1 MePc per every 10 supercages, yields a material with acceptable diffusional properties in subsequent reactions.<sup>[51]</sup>

The question whether immobilized complexes in the faujasite topology really reside within the zeolite cages has been addressed for the CuPcY system.<sup>[50]</sup> The flexible ligand method allowed to fix 0.8 CuPc entities per unit cell (UC) corresponding to one complex per 8 supercages, next to 0.5 unmetallated ligands per UC. The presence of hyperfine features in the ESR spectrum, allowed the presence of uncomplexed  $\text{Cu}^{2+}$  to be established. On one hand, the presence of nine hyperfine features in the second derivative ESR spectrum of Cu in CuPcY, point to the presence of four equivalent N atoms coordinated to Cu, indicating the absence of intermolecular interactions between the complexes and consequently the presence of isolated complexes. On the other hand, the red shift from 545 to 581 nm of the Q bands of Pc ( $\pi - \pi^*$  transitions) upon encapsulation and the existence of a tetrahedrally elongated square pyramidal geometry for Cu in CuPcY (as derived from the ESR Cu spin Hamiltonian parameters), are both in favour of puckering of the planar Pc geometry upon encapsulation.<sup>[50,52]</sup> These observations confirm earlier conclusions based on geometric considerations and mechanical modelling, stimulating the proposal of a saddle-type structure.<sup>[53]</sup> Thermal stability up to 400 °C was reported upon encapsulation.<sup>[54]</sup> Starting with 4-nitro-1,2-dicyanobenzene and zeolite Y adsorbed ferrocene, the so-formed Fe-tetra-nitro-substituted phthalocyanine is easily extractable and therefore should be formed at the external surface of the zeolite crystals, the bulky substituents precluding the complex from encapsulation.<sup>[55]</sup>

Alkane oxygenation with Cytochrome P450 mimics occurs with monooxygenatom donors like iodosobenzene and peroxides. Groves' oxygen-rebound mechanism involves  $\text{H}^\circ$  abstraction from an alkane  $\text{sp}^3$  C-H bond upon interaction with a high valent oxo-iron (or oxo-manganese), followed by fast recombination of the  $\text{OH}^\circ$  radicals formed with  $^\circ\text{C}$  of the alkane to form the corresponding alcohols, the high valent oxo species being formed by reaction of the oxidant with the chelated transition metal:<sup>[56]</sup>

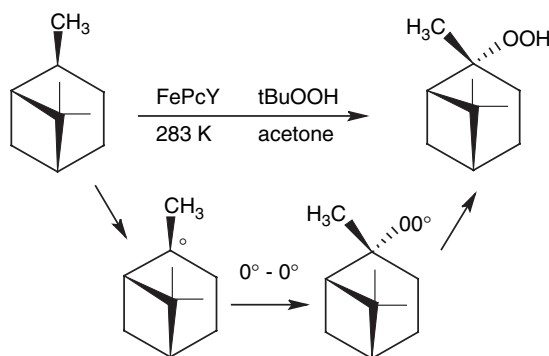


The radicals formed stay with the complex, and do not start a radical chain reaction in solution. The observed kinetic isotope effects (KIE) are of the order of 10–12, compared with values of 2–4 observed for a radical chain reaction, confirming that C–H bond breaking in the alkane substrate is rate determining. High KIE values and product similarities obtained from alkane oxygenation with organic hydroperoxides using FePcY as catalysts confirm the role of this system as a monooxygenase mimic. With dioxygen as oxidant, the same mechanism can only occur in the presence of a sacrificial reductants, supplying the required electrons forming a superoxo-metal species, and of an activator (acid; anhydride) generating the highvalent metal-oxo species.<sup>[56]</sup>

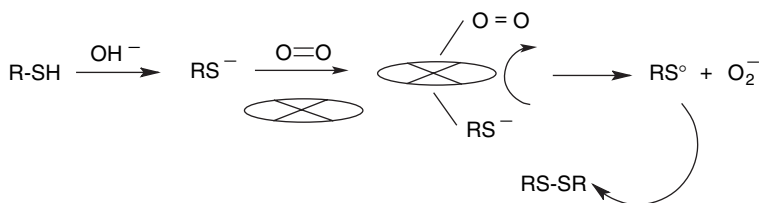
A FePc complex encaged in the zeolite Y supercages, in its turn, can be wrapped in a polydimethylsiloxane membrane, thus acting not only as a mechanistic but also as a formal mimic of Cytochrome P450 often found in cell membranes.<sup>[57]</sup> Such membranes, contacted on one side with substrate and on the other side with oxidant, catalyse oxygenation reactions in a membrane reactor in the absence of any solvent, the majority of the product amount being recovered from the more polar phase.

Alternatively, the initial formation of hydroperoxides could be indicative of the presence of radicals trapped by dissolved oxygen. This phenomenon definitely occurs during the subambient oxygenation of *cis*-pinane (Scheme 10.4).<sup>[58]</sup>

With CoPc encapsulated in zeolite X thiols can undergo autoxidation.<sup>[3,59,60]</sup> Thiol deprotonated in a basic reaction medium coordinates to Co in CoPc. Co in the CoPc macrocycle mediates an electron transfer from dioxygen to thiol, *trans* coordinated on the macrocycle with respect to dioxygen. Finally, two formed thiol radicals combine, forming disulfide (Scheme 10.5). Oxidation of mercaptanes with dioxygen to disulfide, used in the sweetening of petroleum fractions in the MEROX process, is possible as well. Zeolite supported CoPc shows better dispersion, because of the low solubility of CoPc in the reaction medium.<sup>[61]</sup> As this constitutes a two-phase process consisting of an alkali and hydrocarbon phase, the use of CoPcY would imply zeolite modification to position it at the interphase.



**Scheme 10.4** Rationalization of hydroperoxide formation during oxygenation of *cis*-pinane with FePcY and *tert*-butylhydroperoxide as oxidant.



**Scheme 10.5** Autoxidation of thiols in a basic medium with dioxygen and CoPc(Y).

It has often been claimed that MePc encaged in zeolites shows enhanced activity compared with that of a homogeneous system. The oxidation of cumene, cysteine, and CO<sub>2</sub> with dioxygen showed a 25-, 3- and 4-fold enhanced activity, respectively.<sup>[46]</sup> The formation of styrene epoxide from styrene with *tert*-butylhydroperoxide was increasing from 8 up to 50 turnovers (TON) per hour, substituting CuPc for CuPcY.<sup>[52]</sup> By-products, such as phenylacetaldehyde and benzaldehyde, are formed. The first product possibly stems from acid isomerization of the primary product, catalysed by residual zeolite proton acidity. The second product probably is the result of a homogeneous autoxidation reaction with dioxygen formed from decomposed peroxide. The decreased epoxide yields with CoPcY in alkene epoxidations compared with CoPc probably reflects the increasing sensitivity of the respective transition ions to hydrolysis, probably during the ion exchange in the parent zeolite.<sup>[62]</sup>

From chromatographic measurements on the system in pre-catalytic conditions, it follows that reversible deactivation of such catalysts is the result of selective adsorption of the polar products (alkanols/alkanols).<sup>[63]</sup> Extensive washing with the appropriate solvents can be used as a catalyst regeneration procedure. It follows that proper design of the host–guest couple by using less polar zeolites should be able to remediate deactivation. The selective sorption of products and also of reactants in the zeolite cages, and the resulting enhancement of substrate close to the active sites, points to the existence of a zeolite sorption effect that can be at the origin of the systematically reported activity enhancement for encaged complexes.

The catalytic activity of MePc depends on the nature of the ligand in the apical position and should therefore be solvent dependent.<sup>[56]</sup> From the chromatographic determination of the respective adsorption coefficients of the reaction partners in pre-catalytic conditions, a very pronounced activity difference is found depending on the nature of the solvent used.<sup>[64]</sup> However, the sequence of the adsorption coefficients is of zeolitic origin and reflects a sorption effect rather than a coordination effect. The respective values of the adsorption coefficients indicate that for the oxidation of alkanes, cyclohexane, with organic peroxide for example, in acetone the oxidant is enriched in the intracrystalline voids, resulting preferentially in peroxide decomposition. In excess cyclohexane, the substrate is enriched in the pores, so that every adsorbed peroxide molecule results in an efficient oxygenation.

With electron-withdrawing groups substituted at the phenyl groups of the MePc macrocycles like tetra-nitro [Pc(NO<sub>2</sub>)<sub>4</sub>] and perchloro-phthalocyanine (PcCl<sub>14</sub>), the metal-oxo species of the MePc complex becomes considerably more active, also as

a zeolite encaged species.<sup>[65,66]</sup> However, the entrapment of such bulky complexes in the faujasite supercage could be questioned. Indirectly, it follows from the product distribution in phenol hydroxylation with H<sub>2</sub>O<sub>2</sub> that encapsulation occurs.<sup>[66]</sup> When the catechol / hydroquinone ratio is compared, the selectivity for the slimmer product, hydroquinone, is enhanced.<sup>[13,66]</sup> It seems that when more space is available in the supercages close to encapsulated MePc, relatively more catechol formation is observed.

An important claim has been made on the regioselectivity in the *n*-alkane reaction with dioxygen using CuPcCl<sub>17</sub>Y as catalyst.<sup>[65]</sup> A remarkable selectivity for formation of primary alcohols, in other words of selective oxygenation of primary C atoms, has been reported.

An alternative method used for entrapment of large complexes into zeolite crystals is known as the so-called 'zeolite synthesis method'.<sup>[67-70]</sup> In this method transition metal complexes are added to the synthesis mixture from which a faujasite zeolite is obtained. Therefore, the complex should be stable and dissolved in the medium in the conditions of zeolite synthesis, i.e. at elevated pH (>12) and temperature (around 100 °C). It is not entirely clear whether occluded complexes are positioned in faujasite supercages or in cracks or defects of the crystals. To assure occlusion of isolated MePc complexes rather than of their clusters, the occluded amounts must be limited, implying the use of very active complexes. Ru and CoPcF<sub>17</sub> complexes have been reported to show good activity and resistance to leaching.<sup>[67-70]</sup>

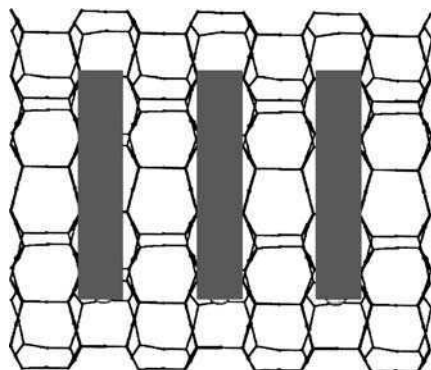
## 10.2.2 OXYGENATION POTENTIAL OF METALLO-PHTHALLOCYANINES ENCAPSULATED IN THE MESOPORES OF VPI-5 AIPO<sub>4</sub>

VPI-5 is a crystalline mesoporous AIPO<sub>4</sub> with VFI topology and monotubular 18-MR rings with an inner diameter of 1.27 nm.<sup>[71]</sup> Partially dehydrated samples were filled with ferrocene molecules and subsequently exposed to DCB.<sup>[72,73]</sup>

Exhaustive physicochemical characterization of the exhaustively washed samples showed that FePc occlusion had occurred in a very particular way:

- The expected structural transformation of VPI-5 into the more stable AIPO<sub>4</sub>-8 structure upon dehydration no longer occurred, while the porosity disappeared almost completely. This was attributed to presence of stacks of FePc complexes, filling the pores. No such effects were found upon adsorption of pre-synthesized complex into the VPI-5 voids. Indeed, application of the washing procedures that remove FePc from the external surface of zeolite crystals<sup>[59]</sup> do not result in any extraction of FePc from VPI-5.
- <sup>1</sup>H-<sup>27</sup>Al CP DOR NMR measurements on the FePcVPI-5 samples showed a remarkable enhancement of the NMR signal intensity, pointing to the existence of a very tight fit between occluded FePc and the VPI-5 pore walls.

The stacks of occluded FePc molecules in the monodimensional 18-MR pore of VPI-5 is schematically shown in Scheme 10.6.



**Scheme 10.6** Schematic drawing of the stacks of occluded MePc in a VPI-5 pore (after<sup>[71]</sup>).

It has been shown<sup>[72,73]</sup> that the FePcVPI-5 catalyst was not only active in the room temperature oxygenation of cyclohexane with *tert*-butylhydroperoxide, but also could convert cyclododecane, a large molecule that is inert when a FePcY-type catalyst is used. The respective TON for both substrates are 313 and 125. Taking into account that per pore only the two complexes at the pore entrance/exit are active, unsurpassed TOF amounting to a few 100 000 a minute, are achieved. Even on a mere weight basis, acceptable catalytic activity is present. Although this phenomenon is not understood in detail, the stacked FePc complexes are expected to exert an electronic influence, resulting in highly electron-deficient and reactive Fe-oxo species of the complexes located at the pore mouths.

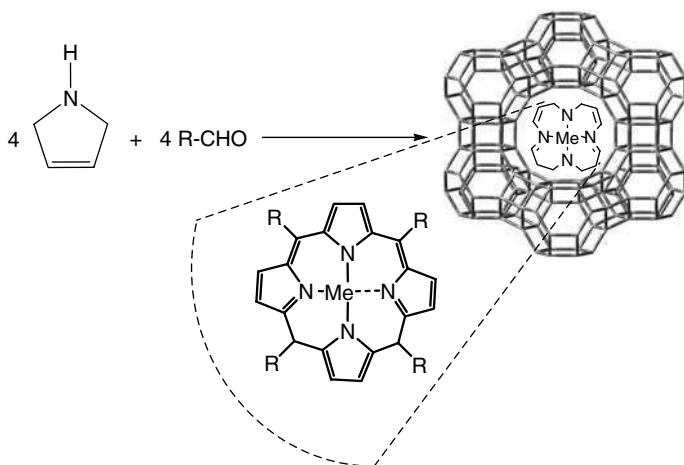
### 10.2.3 OXYGENATION POTENTIAL OF ZEOLITE ENCAPSULATED METALLO-PORPHYRINS

The flexible ligand method, consisting of the tetramerization of pyrrole and an aldehyde, can be used for the entrapment of metallo-porphyrins (MePOR) *in situ* in the supercages of faujasite-type zeolites (Scheme 10.7).<sup>[74]</sup>

This method although straightforward, yields less clean products compared with the encapsulation of MePc, as it is difficult to remove debris that fills the pores.

More than MePc complexes, MePOR complexes have offered a great contribution to the understanding of monooxygenase and peroxidase enzymes.<sup>[75,76]</sup> The similarity in behaviour in selective oxidations with synthetic and natural systems has been the impetus for the search of mimicking the protein cavity of natural enzymes. In this context zeolites have always had a privileged role. Next to the *in situ* synthesis, zeolite adsorption of pre-synthesized Fe<sup>III</sup>POR has been attempted as well.

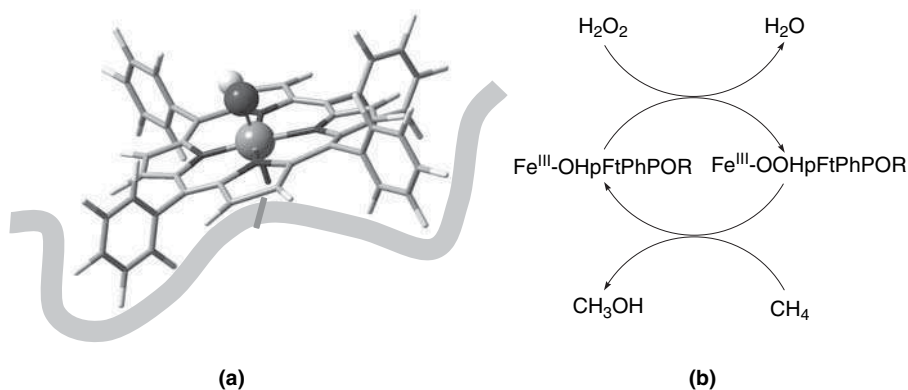
In the case of perfluoro-tetraphenyl porphyrin (pFtPhPOR),<sup>[77]</sup> because of evident stereolimitations, the intracrystalline voids of faujasite will not be available and adsorption will be confined to the external crystal surface. The zeolite adsorbed



**Scheme 10.7** Co-tetramerization of pyrrole and aldehydes in the presence of transition metal exchanged Y zeolite (MeY), yielding entrapped metalloporphyrin (after Jacobs<sup>[13]</sup>).

complex, Me (pFtPhPOR), has been reported to perform extremely well as a methane monooxygenase mimic working at an average rate of 1.7 TON a minute (Scheme 10.8).

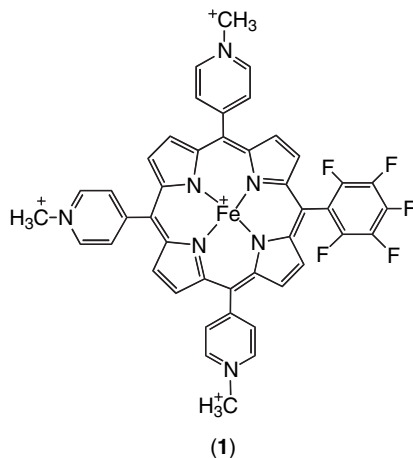
The potential of cationic metallo-porphyrins as structure directing agent (SDA) for zeolite synthesis has been explored as well.<sup>[78]</sup> Macrocycles like tetrakis(*n*-pyridyl)porphyrin, tetrakis(*N*-methyl-*n*-pyridyl)porphyrin with  $n = 2-4$ , tetrakis(*N,N,N*-trimethylanilinium)porphyrin, and tris(4-methylpyridyl)-mono(pentafluorophenyl) porphyrin (trMePypmFPOR)(1)<sup>[78,79]</sup> seem to be suitable SDA for zeolite synthesis, thus yielding the occluded corresponding porphyrins. They show good stability in synthesis conditions and the very successful easily, controllable nano-inclusion of this large cation in the zeolite Y supercages seems to be driven by



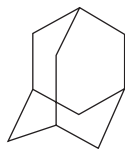
**Scheme 10.8** Schematic representation of pFtPhPOR adsorbed at the external crystal surface of zeolites (a) and of the methane monooxygenase catalysed cycle (b) (after Nagiev *et al.*<sup>[77]</sup>).



the electrostatic interaction between the anionic aluminosilicate species and the cationic peripheral substituents on the porphyrin macrocycle.<sup>[80]</sup> Good quality zeolites (X, Y, VPI-5) (XRD) with occluded intact porphyrin (UV-VIS; IR) can be obtained this way.<sup>[78]</sup> On average, one MePOR per unitcell of zeolite X or Y could be entrapped (1 per 8 supercages) as evidenced by TGA. This route offers a large scope for the preparation of zeolite encapsulated macrocycles and their use as mimics for biomimetic oxidations.



In the cyclohexane oxidation with iodobenzene and  $\text{Fe}^{\text{III}}(\text{trMePympFPOR})\text{Y}$  as catalyst, evidence for the occurrence of the oxygen rebound mechanism is found as high yields of cyclohexanol are obtained.<sup>[79]</sup> The encapsulated system resulting from a porphyrin templated synthesis shows significantly enhanced performance when compared with either the complex impregnated on the same zeolite or the homogeneous system. With *Z*-cyclooctene equally high yields of *cis*-epoxycyclooctane are obtained for the encapsulated and the homogeneous complex, indicating neither residual acidity nor diffusional limitations are hindering the heterogeneous reaction. In the oxygenation of adamantane (2), the 1-adamantol to 2-adamantol molar ratio, corrected for the different number of secondary and primary hydrogen atoms available, amounts in each of the three cases to 19:1, a value expected for a P 450 model where the tertiary hydrogen atoms are preferentially abstracted via a radical mechanism.<sup>[79]</sup> No ketones nor any other side-products are observed, pointing to the absence of structural degradation via, e.g., self-oxidation.

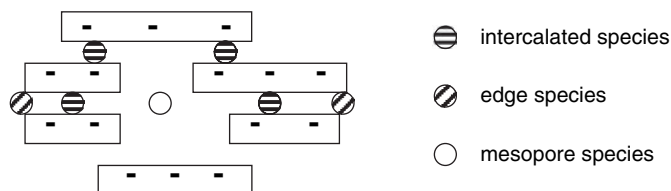


A series of metalloporphyrins of the tetraphenylporphyrin-type, encapsulated via the zeolite synthesis method<sup>[81]</sup> in zeolite X, was characterized and tested in the cyclohexane/cyclooctane oxidation with dioxygen in the absence of any sacrificial co-reductant.<sup>[82]</sup> In the case of oxidation of cyclooctane with dioxygen the on/ol ratio is in the range 8–10 as normally been observed for this type of reaction in the presence of metalloporphyrins. The product yield showed an almost linear increase with the electronegativity of the axial ligands ( $I < Br < Cl < F$ ). The same is true when the number of peripheral halogen substituents on increases. Shifts of the Soret bands of porphyrin (460–500 nm) occur in a parallel way. As the effect of the support on these parameters was nonexistent upon encapsulation, it is clear that the porphyrin ring is not altered during such a process.

The data seem to support an alternative mechanism compared with the so-called Lyons mechanism in which  $O_2$  is activated forming a metal-oxo ( $M=O$ ) species.<sup>[83]</sup> Via reaction of a second metalloporphyrin with a primarily formed superoxo ( $Me-OO^\ominus$ ) or peroxy species, a metal-oxo is formed, reacting eventually with an alkane according to the oxygen rebound mechanism. Alternatively, radicals present in solution, upon reaction with dioxygen, may form alkyl hydroperoxides that are decomposed by metalloporphyrins.<sup>[83]</sup>

In the autoxidation reaction of mercaptoethanol with dioxygen, cationic  $Co^{II}$  (tetraarylporphyrin) complexes supported on montmorillonite clay yield the expected disulfide and again the catalyst activity was significantly enhanced. It seems that the better distribution of the porphyrin on the clay platelet edges prevents the formation of inactive  $\mu$ -oxo dimers ( $Me-O-O-Me$ ) and avoids self-oxidation which commonly occurs in homogeneous solution.<sup>[84]</sup> For the same reasons, tetrakis(tetramethylpyridino) porphyrin was immobilized (via cation exchange) on a montmorillonite clay.<sup>[85]</sup> The immobilized catalyst functioned as an active and stable suprabiotic catalyst for the oxidation of lignin model compounds with  $H_2O_2$ .

MePOR species and other complexes in cationic clays can be located at the edges of packed platelets, in the interlamellar space or in the mesopores present (Scheme 10.9). A review of the early data in this area is available.<sup>[86]</sup> The flat metallo macrocycles under clay synthesis conditions help to induce layer silicate formation, the complexes being intercalated between the layers. Whereas with monooxygen atom donors, alkanes can be oxygenated with significantly enhanced activities compared with the homogeneous case, in every case the expected products (ol/on) were obtained. Competitive oxygenation of adamantane and pentane shows lower



**Scheme 10.9** Possible location of MePOR and other complexes in a montmorillonite-type clay (after Bedoui<sup>[86]</sup>).

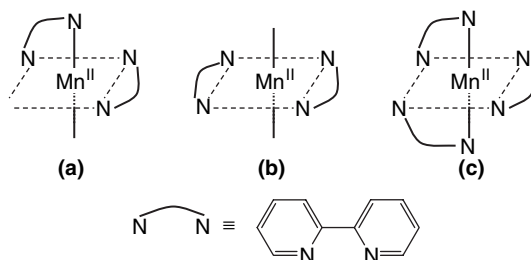
(adamantol + adamantone)/(pentanol + pentanone) ratios for the clays, compared with the homogeneous case,<sup>[87]</sup> pointing to the existence of shape selective effects or reduced access to the active complexes. The available data are not of sufficient detail to definitively locate MePOR complexes in terms of the sites shown in Scheme 10.9.

### 10.3 OXYGENATION POTENTIAL OF ZEOLITE ENCAPSULATED NONHEME COMPLEXES

After a very extensive research examining period on porphyrin and related chemistry, emphasis moved somewhat to Fe and Mn chemistry in a nonporphyrin environment.<sup>[88]</sup> In the nonheme environment, dinuclear Mn is the active centre in catalase, while plants and algae use a tetranuclear Mn complex in the oxidation of water with photosystem II.<sup>[89, 90]</sup> In contrast to the wealth of information available from biology, the data on metal complexes for epoxidation and in particular for alkane oxygenation and their immobilization on supports are less abundant. Typical nonheme type ligands are 2,2'-bipyridine (bpy), tri- and tetraazacycloalkanes, as well as Salen and Saloph ligands for Schiff bases.<sup>[3]</sup> Their Mn (and Fe) complexes often activate peroxides heterolytically making use of Mn<sup>II</sup>/Mn<sup>IV</sup> or Mn<sup>III</sup>/Mn<sup>V</sup> redox couples.<sup>[13]</sup>

#### 10.3.1 IMMOBILIZATION OF *N,N'*-BIDENTATE COMPLEXES IN ZEOLITE Y

Addition of stoichiometric amounts of bpy ligand to Mn exchanged zeolite Y results in the stabilization of a Mn(bpy)<sub>2</sub> complex which otherwise is unstable in solution.<sup>[91]</sup> Mn<sup>II</sup> ions located in zeolite 6-MR, are lifted out of their positions and coordinate to 2 bpy ligands. ESR shows that the 16-line spectrum typical for aerated Mn containing solutions (pointing to the generation of a Mn<sup>III</sup>-Mn<sup>IV</sup> dimer via oxidation and dimerization of Mn<sup>II</sup>), does not occur when Mn<sup>II</sup>(bpy)<sub>2</sub> is located in the zeolite supercages.<sup>[92]</sup> Characteristic IR features show the exclusive presence of a zeolite encapsulated *cis*-Mn(bpy)<sub>2</sub> complex (Scheme 10.10), as can be derived from the



**Scheme 10.10** Representation of *cis*- (a), *trans*-Mn<sup>II</sup>(bpy)<sub>2</sub> (b) and Mn<sup>II</sup>(bpy)<sub>3</sub> (c) complexes (after Knops-Gerrits *et al.*<sup>[92]</sup>).

intensity of the split out-of-plane C-H deformations for *cis*- and *trans*-complexes at 772 and 757  $\text{cm}^{-1}$ , respectively. Zeolite encapsulation not only has an impact on nuclearity but also on valency as low temperature ESR shows the absence of high valent species and doubly integrated room temperature spectra yield values for  $\text{Mn}^{\text{II}}$  corresponding to the total Mn content of the sample.<sup>[92]</sup> The bpy metal to ligand charge transfer bands at 530 and 486 nm for the zeolite occluded complex are not broadened compared with, e.g., the case of the stiffer phenanthroline (phen) ligand, pointing to a very low degree of distortion of the ideal symmetry in the bpy case.

Whereas alkenes can be oxidized with aqueous  $\text{H}_2\text{O}_2$  into the corresponding epoxides, zeolite residual acidity in the presence of sorbed water converts them into the corresponding *trans*-1,2-diols.<sup>[91,93]</sup> With excess oxidant, such diols are converted into the corresponding 1,2-diketones, which easily undergo bond cleavage yielding organic acids. Known zeolite manipulation procedures, such as a decrease of the Si/Al ratio of the faujasite topology and exchange with more basic ions, allows reduction of these epoxide opening consecutive reactions. In this way, selective cyclohexene epoxidation is possible with  $\text{Mn}(\text{bpy})_2$  occluded in KX, while almost selective adipic acid formation is possible with NaY.<sup>[94]</sup> In the latter case the catalyst is gradually fouled by strongly adsorbed acid. Generally, the stability of  $\text{Mn}(\text{bpy})_2\text{X}$  and Y is determined by sorption of polar by-products. If effective solvent washing procedures can be established, the catalyst is regenerable. Suppression of the reactivity of the smaller substrate in competitive experiments with cyclohexene and 1-octene,<sup>[93]</sup> indicates that zeolite sorption effects again dominate the events.

Cyclohexane is oxygenated into cyclohexanone as the major product,<sup>[94]</sup> pointing to the occurrence of Mn-oxo type catalysis. HCl treatment of the zeolite prior to ion exchange and ligand addition, shows a 4-fold increase in TOF, indicating that creation of mesopores with access to the external crystal rim enhances mass transfer without affecting the specific zeolitic sites needed for complex retention.<sup>[95]</sup>

Upon addition of stoichiometric amount of bpy to  $\text{Cu}^{\text{II}}$  exchanged smectite-type montmorillonite, the formation of a  $\text{Cu}^{\text{II}}(\text{bpy})_2$  complex was claimed, which was very active and selective for the oxidation of alcohols into the corresponding ketones.<sup>[96]</sup> Unfortunately, neither the nature of the secondary porosity, the complex geometry nor its location was investigated in further detail.

An analogous ship-in-bottle complex,  $[\text{VO}(\text{bpy})_2]^{2+}\text{-NaY}$ , could be designed starting from a vanadyl exchanged Y zeolite upon bpy addition.<sup>[97]</sup> Strong spectroscopic proof for the formation of such complex was evident from FT-Raman, FTIR, diffuse reflectance spectroscopy, XPS and EPR; as follows:

- An intense Raman band at 1042  $\text{cm}^{-1}$  can be assigned to  $\nu_{\text{V=O}}$  in  $\text{VO}(\text{bpy})_2$ .
- IR shifts to lower wavenumbers observed for ligand C=N vibrations, in contrast to the unchanged positions of all C=C vibrations, are indicative of N-ligation.
- The position of the C-H out-of-plane for the complex (786  $\text{cm}^{-1}$ ) is indicative of the presence of a *cis*-bis complex.
- XPS data of the encapsulated complex show the V  $2p_{3/2}$  peak at 516 eV, typical for  $\text{V}^{\text{IV}}$ ; comparable V contents obtained by ICP as well as by XPS, amounting to about 1 V per unit cell, are evidence for the homogeneous distribution of V across

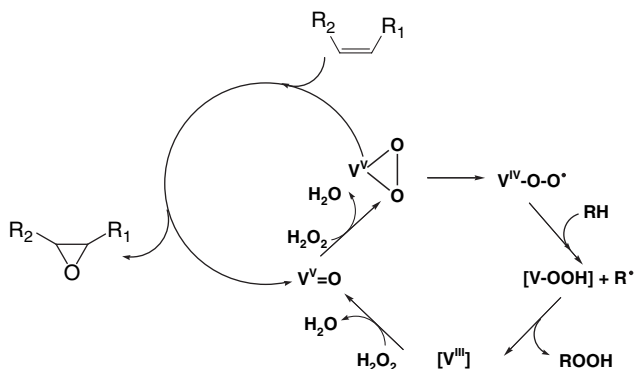
the zeolite crystals. Curie–Weiss behaviour for the occluded complexes, as evidenced by the linear temperature dependence of the inverse of the integrated ESR signal intensity and the intersection of the straight line with the abscissa around 0 K, also points to the existence of a homogeneous distribution of  $V^{IV}$  in the zeolite crystals.

- $V^{IV}$  in VO-NaY shows anisotropic and eight equally spaced hyperfine ESR splittings indicative of  $V^{IV}$  in a square pyramidal configuration. Upon coordination with bpy the in-plane coordination becomes more covalent, while  $V=O$  shows decreased covalency. All this is evidence for the existence of square pyramidal  $VO(bpy)_2$  complexes with tetragonal planar distortion.

Upon  $H_2O_2$  addition, vanadyl ions are transformed into vanadyl monoperoxo species as evidenced by the new IR  $V_{O-O}$  bond appearing at  $873\text{ cm}^{-1}$ . The cyclohexane oxidation with  $H_2O_2$  amounting to around 1 TON a minute, is much higher than that of zeolite ligated vanadyl or of the homogeneous complex, representing activity comparable to that of dioxygenase enzymes.<sup>[98]</sup> Primarily formed cyclohexyl hydroperoxide is decomposed into alcohol/ketone mixture. All this is in line with Shulpin's stoichiometric sequences,<sup>[98]</sup> implying the formation of an open peroxy radical species that abstracts H from an alkane, forming an alkyl radical that is able to abstract  $^{\circ}OOH$  from V-hydroperoxide. Thus it seems that upon encapsulation a closed cycle can be formed (Scheme 10.11).

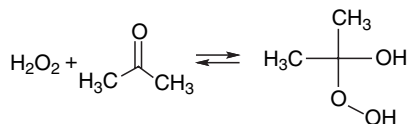
With alkenes and peroxides room temperature epoxidation can be performed, the selectivity with respect to ring-opened products being dependent on solvent and hydroperoxide nature.<sup>[96]</sup> With organic peroxides the epoxide selectivity is high, while with  $HO_2H$  in acetone high diol selectivity is evident with the *cis/trans* diol isomer ratio at its equilibrium value.

The absence of allylic oxidation products seems to point to the heterolytic ring opening of the peroxide as dominant pathway. The excellent properties of



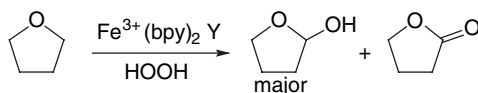
**Scheme 10.11** Mixed catalytic cycle for hydroperoxide formation in alkane oxygenation and alkene epoxidation with  $HO_2H$  and *cis*- $VO(bpy)_2Y$ , via a homolytic and heterolytic cleavage of peroxy intermediates, respectively (after Knops-Gerrits *et al.*<sup>[97]</sup>).

acetone as solvent for HOOH, are attributed to the following equilibrium reaction:<sup>[92]</sup>



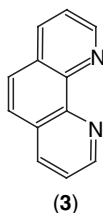
Formed 2-hydroxy-2-hydroperoxypropane gradually releases HOOH, keeping its concentration in solution low, and favouring its use as efficient monooxygen atom donor.

Fe<sup>III</sup> and Mn<sup>II</sup> bpy complexes in zeolite Y and bentonite, were shown to have catalytic potential in the oxidation of cyclic ethers with peroxides to yield cyclic lactols:<sup>[99]</sup>



Similar results were obtained with Mn<sup>II</sup>(bpy)<sub>2</sub>Y and bentonite. Unfortunately, the very reactive 2-position of cyclic ethers does not need a highvalent metal-oxy species for fast H<sup>o</sup> abstraction. It explains why the presence of the bpy ligands hardly enhances the activity of the transition metal loaded supports.

It should be stressed that the well-known Ru(bpy)<sub>3</sub> complex formed upon addition of excess ligand to the ion exchanged FAU-type zeolite, does not form a 'dark' but a photocatalyst.<sup>[9,100,101]</sup> The photoinduced electron transfer from NaX encaged Ru(bpy)<sub>3</sub> to methylviologen occurs two orders of magnitude faster than in many other crystallites of the same size.<sup>[100]</sup> A phenomenon of 'through-framework-electron-transfer' from external Ru-polypyridyl towards the 10-MR encaged (viologen)<sup>2+</sup> cations was discovered for zeolite ITQ-2 as well.<sup>[9]</sup>

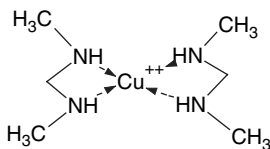


The replacement of bpy by the more rigid bidentate phen ligand (3), has a profound effect on the catalytic properties of the material, though the homogeneous chemistry has hardly been studied.<sup>[92]</sup> Alkene epoxidation, followed by acid catalysed ring opening, is much less selective, compared with the bpy case. The products from allylic oxidation (2-cyclohexenol, 2-cyclohexenon from cyclohexene) are now dominant. The hydrogen peroxide loss to O<sub>2</sub> with the zeolite occluded Mn-phen complex is probably due to a lower degree of Mn complexation, the peroxide being decomposed via radical pathways. Both the size and the geometry

probably make the ligand less suited for ligation of zeolitic  $\text{Mn}^{\text{II}}$ , resulting in an enhanced catalase activity. Similar results have been obtained with  $\text{Fe}(\text{phen})\text{Y}$ .<sup>[102]</sup> Whereas the author's claim for the presence of encapsulated  $\text{Fe}(\text{phen})_3$  complexes is exclusively based on the starting Fe/phen ratios used, the thorough washings via Soxhlet extraction possibly resulted in the formation of bis complexes.

### 10.3.2 LIGATION OF ZEOLITE EXCHANGED TRANSITION IONS WITH BIDENTATE AZA LIGANDS

The formation of ethylene diamine (en) complexes in the intracrystalline space zeolites was reported more than 25 years ago by De Wilde *et al.*<sup>[100]</sup> Recently, the issue has been addressed again<sup>[103]</sup> and the presence of encaged  $\text{Cu}^{\text{II}}(\text{en})_2$  (**4**) in zeolites NaY, KL, NaBeta, and even in NaZSM-5 was established with IR, UV-VIS, ESR spectroscopies and cyclic voltammetry. Changes of the redox potential of the complex upon encapsulation in a zeolite is clear from the different electrochemical responses. Peak broadening and changes in peak potential towards more negative values upon entrapment occurred, in parallel with the calculated increase of the HOMO and LUMO orbital energies of the  $\text{Cu}^{\text{II}}(\text{en})_2$  complex. This was attributed to the presence of charge compensating cations that decrease the intrazeolitic electric field. The significantly enhanced activity of the encaged complex in the room temperature oxidation of dimethylsulfide with HOOH showing 100 % conversion into dimethyl sulfoxide, was correlated with this enhanced redox potential. Although nature performs various electron-transfer processes manipulating the redox potential of metal-protein complexes, it cannot be excluded that in the same way a zeolite sorption effect is contributing to this phenomenon (see above). Anyway, the encapsulated  $\text{Cu}^{\text{II}}(\text{en})_2$  complexes represent at least a formal mimic of Cytochrome C.

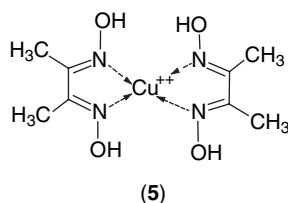


(4)

ESR parameters of the complex show its distortion upon entrapment, depending on the geometry of the intrazeolite space. In ZSM-5, the decreased effective spin-orbit coupling constants and molecular orbital coefficients for in-plane  $\pi$  binding are indicative of increased covalency between Cu and en, due to distortion from planarity upon encapsulation. This distortion from planar geometry is confirmed by a red shift in the energy-level diagrams at least for the zeolites with the smaller pores (ZSM-5; Beta). An intensity enhancement of the d-d bands occurs in parallel.

$\text{Me}^{\text{II}}(\text{dmgH})_2$  complexes were entrapped in CuY, NiY, and CoY zeolites upon addition of dimethylglyoxime (dmgH) to the zeolite via the flexible ligand

method.<sup>[104]</sup> The Cu-catalyst is moderately active in the oxidation by hydrogen peroxide of benzyl alcohol to benzaldehyde and of ethylbenzene to phenylethanol. The selectivity of the former reaction to the aldehyde exclusively, is the result of encapsulation. Low temperature X-band ESR spectra of encapsulated Cu(dmgH)<sub>2</sub> (5) are indicative of magnetically dispersed C<sup>II</sup> ions, dispersed in the zeolite matrix. The magnetic moment of the complex of 1.83–1.86 BM, implies square planar geometry. Complex formation in the present case is possible with only minor distortion.



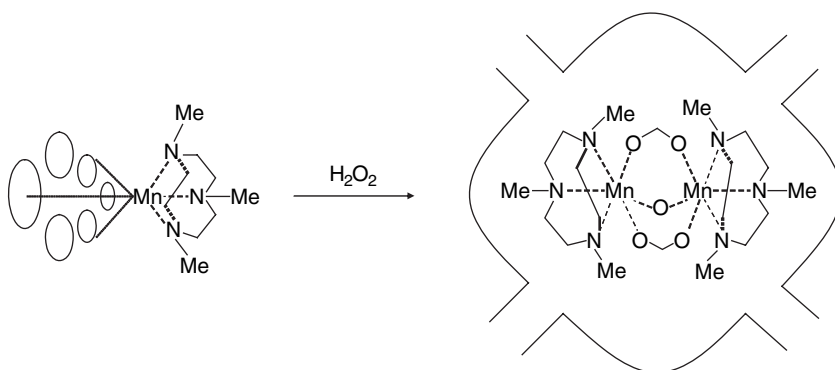
### 10.3.3 LIGATION OF ZEOLITE EXCHANGED TRANSITION IONS WITH TRI- AND TETRA-AZA(CYCLO)ALKANE LIGANDS

1,4,7-Triazacyclononane and related ligands are tridentate, facially coordinating octahedral Fe<sup>III</sup> and Mn<sup>II, III</sup>, leaving three coordinating sites in positions *trans* to the coordinating ligand N atoms free for coordination with other ligands.<sup>[105]</sup> In oxidative conditions in aqueous solution, a tetranuclear complex with a Mn<sup>IV</sup><sub>4</sub>O<sub>6</sub> core is thermodynamically most stable, though a large number of complexes is possible. Although the Mn and 1,4,7-trimethyl-1,4,7-triazacyclononane (tmtacn) complexes formed are extremely reactive in the HOOH decomposition and in an aqueous buffer at pH = 9 and were (unsuccessfully) proposed for stain bleaching,<sup>[106]</sup> the epoxidation of 1 equivalent of alkene requires a 100-fold HOOH excess.<sup>[107]</sup> In the presence of an oxalate buffer it was found that a 1:1:1 complex of Mn, tmtacn and oxalate is formed, allowing epoxidation of even strongly electron deficient alkenes (like methylvinylketone) with high activity (e.g. 1000 TON in a few hours).<sup>[108]</sup> The lack of reaction of alkanes indicates that a Groves' oxygen rebound mechanism is probably not applicable here.

It is evident that the observations summarized in the previous paragraph have triggered attempts to entrap Mn(tmtacn) complexes in zeolites.<sup>[109,110]</sup> ESR shows that upon encapsulation a mononuclear Mn<sup>II</sup>(tmtacn) complex is formed in the supercages of zeolite Y, as can be inferred from the shift in the zero field splitting.<sup>[109]</sup> Upon exposure to hydrogen peroxide, a 16-line spectrum of dinuclear complex with mixed valency [(tmtacn)Mn<sup>III</sup>-X<sub>3</sub>-Mn<sup>IV</sup>(tmtacn)] is detected (X = OH<sup>-</sup> or O<sup>2-</sup>) (Scheme 10.12). The residual positive charge of the complex will improve its retention in the zeolite host. Other spectroscopic similarities indicate that the homogeneous and encapsulated complexes in the presence of hydrogen peroxide are very similar.

The catalytic properties, in particular in acetone, are excellent and are, e.g. for cyclohexene and styrene epoxidation, comparable as well.<sup>[110]</sup> The use of a filtration experiment points to the heterogeneous nature of the catalyst. In such

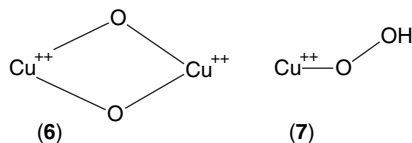




**Scheme 10.12** Representation of the dimerization of Mn(trimethyl-1,4,7-triazacyclonane) in the zeolite Y supercage (after De Vos and Jacobs<sup>[88]</sup>).

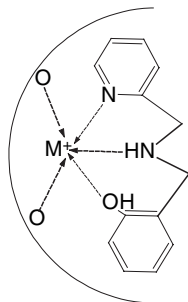
a test, the lack of catalytic activity in the partially converted feed and products, when separated from the heterogeneous catalyst, provides strong evidence for the heterogeneous nature of the latter. The stereo-retention in the epoxidation of *cis*-alkenes is more pronounced with the heterogeneous catalyst, while the allylic oxidation is even more suppressed. It is indeed likely that free radicals formed are more likely to start a radical chain in solution than in the zeolite intracrystalline space.

With the corresponding copper complexes,<sup>[111]</sup> in homogeneous conditions side-chain as well as ring oxygenation of ethylbenzene occurs with *tert*-butylhydroperoxide as oxidant (TOF 50–60 h<sup>-1</sup> at 55 °C). Upon complex entrapment in the supercages of zeolite NaY, the oxygenation activity increases, while ring alkylation is suppressed, resulting in the selective formation of acetophenone. Under the reaction conditions a band at 462 nm appears, assigned to a bis- $\mu$ -peroxo dimeric Cu complex (**6**), it can be speculated that the suppression for steric reasons of the Cu<sup>II</sup>-hydroperoxide species (**7**) is responsible for the decrease of the ring hydroxylation. The intervention of similar species in Ti chemistry with TS-1 is well-known.<sup>[31,32]</sup> This is also in line with the well-established behaviour observed with Mn(mtacn)Y.



Complexation via the ligand method of more than 70 % of the Cu and Fe ions in zeolite Y with a mixed tridentate *N,N',O*-ligand such as (2-hydroxymethyl) (2-methylpyridine)amine (Hbpa) was reported, yielding entrapped Fe(bpa) (**8**) together with residual uncomplexed rhombohedral Fe<sup>III</sup> with an ESR signal at  $g = 4.3$  and Fe–Fe interactions with  $g = 2.0$ .<sup>[112]</sup> When a more than stoichiometric amount of Hbpa

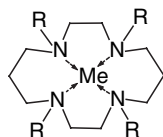
is added, apparently a  $M(\text{bpa})_2$  complex is encapsulated. In the absence of reported catalytic data, it can be speculated that as well as monooxygenase activity, significant free radical chemistry will occur with such systems. It was clearly shown that the use of larger ligands resulted in a reduced degree of metal ion complexation. The issue of ligand deprotonation upon complexation will be addressed below.



(8)

Several polydentate N-ligands form the corresponding macrocyclic poly-aza complexes in the supercages of FAU-type zeolites.<sup>[50,113]</sup> The intense d–d transition of 4-N coordinated square planar  $\text{Ni}^{2+}$  is observed between 22000 and 23000  $\text{cm}^{-1}$  depending on the exact nature of the ligand. While with SQUID Curie–Weiss behaviour was detected, showing homogeneous dilution of the  $\text{Ni}^{2+}$  paramagnetic centres, the value of the low temperature magnetic susceptibility points to an almost complete ligation of all zeolitic Ni. The shift of the d–d energies to lower wavenumbers upon water addition, shows it predominantly coordinates to Ni as axial ligand, than rather protonating the amine function and destroying the square planar N-coordination. It also follows that in absence of water, the axial position is available for ligation. In the corresponding clay encapsulated complexes, the axial positions are blocked by the clay platelets.<sup>[114]</sup>

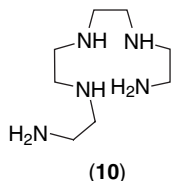
The formation of  $\text{Co}^{\text{II}}$ cyclamY (9) is clearly established, the *cis* complexes outnumbering by far the *trans*-ligated ones. This behaviour is quite general and is observed for several tetradentate ligands forming pseudo-octahedral complexes. It seems that the zeolite surface has a tendency to bind as a multidentate ligand, namely tridentate ligand, to planar metal surfaces.



(9)

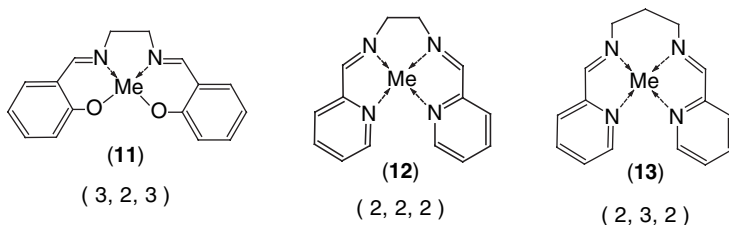
It forms a new microporous redox-solid acting as a reversible, high affinity and high capacity ( $>90 \mu\text{mol g}^{-1}$ ) dioxygen-sorbing material<sup>[3]</sup> and ranks among the best compared with  $[\text{Co}^{\text{II}}(\text{bipyridine-terpyridine})]$  and  $[\text{Co}^{\text{II}}(\text{CN})_5]^{3-}\text{NaY}$ .<sup>[115,116,117]</sup> On

$[\text{Co}^{\text{II}}(\text{tetren})]^{2+}\text{-NaY}$  oxygen sorption is irreversible, due to  $\mu$ -peroxo formation, possibly related to the presence of a ligand with extremely high electron density (tetren, **10**). In contrast to Co, with  $[\text{Ni}(\text{II})\text{cyclam}]\text{Y}$  the *trans*-form dominates, keeping the axial positions available for ligand exchange.



### 10.3.4 LIGATION OF ZEOLITE EXCHANGED TRANSITION IONS WITH SCHIFF BASE-TYPE LIGANDS

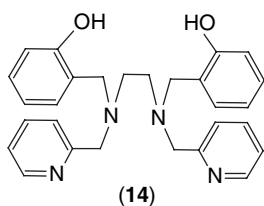
Schiff base-type ligands available are with wide structural variations, using the ligand method allowed the corresponding zeolite entrapped complexes to be synthesized for use as heterogeneous oxidation catalysts. The first reported specimens<sup>[118,119]</sup> containing immobilized Mn(salen) with *N,N'*-ethylenebis(salicylideneaminato) (salen) as a 3,2,3-ligand, show only a limited number or turnovers in the alkene oxidation with PhOI. The digits in this notation refer to the number of C atoms linking the coordinating (O and N) atoms. The inherent weakness of such complexes is due to the presence of phenolic moieties, which are very susceptible to oxidation and subsequent complex destruction. To overcome this, Schiff base analogues like Me(pyren) (**12**) and Me(pyrpn) (**13**) with four coordinating N atoms have also been used,<sup>[92]</sup> pyren and pyrpn being 2,2,2- and 2,3,2-ligands, respectively.



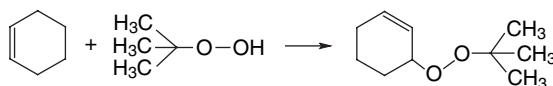
Despite the fact that more than a decade ago the formation of a square planar  $\text{Co}^{2+}$  complex was already demonstrated to be very difficult in faujasite,<sup>[119]</sup> further claims of its entrapment continued to appear. The ESR cobalt signature does not correspond to that of solution or solid  $\text{Co}(\text{salen})$ . Addition of the hexadentate  $\text{H}_2\text{bbpen}$  ligand (**14**) to  $\text{CuY}$  via the ligand method resulted in a degree of coordination with iron ions of less than 46 %.<sup>[112]</sup>

Another tedious issue is to position an axial ligand like pyridine on the zeolite encapsulated  $\text{Me}(\text{salen})$ . It is known from homogeneous catalysis that epoxide

yields can be significantly enhanced this way.<sup>[120]</sup> In the absence of an axial base, the decomposition of Mn-OO*t*Bu transiently formed from Mn(salen) and *tert*-butylhydroperoxide, occurs homolytically. The axially coordinated base enables heterolysis of this intermediate into Mn<sup>V</sup> = O and a nonradical-type reaction. The homolytic features, resulting from the lack of axial coordination by an added base are apparent in the cyclohexene oxidation with *tert*-butylhydroperoxide, where a mixed peroxide dominates the epoxide in the products:



(14)  
N,N'-bis(2-hydroxybenzyl)-N,N'-bis(2-methylpyridyl)  
ethylenediamine

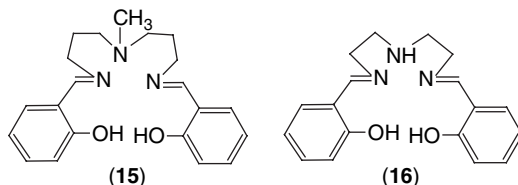


The partial radical character remains when the salen ligands are substituted for the more stable pyren and pyrpn ligands. With alkanes, the long-term stability of encapsulated Mn(salen) is low, but is very much enhanced with Mn(pyren) and Mn(pyrpn).<sup>[92]</sup> Ketone/alcohol ratios below 7/1 are achieved.

Both the difficult formation of square planar complexes and the scarcely controllable positioning of an axial base in faujasite supercage, can be circumvented when the axial base is an inherent chemical part of the salen ligand such as is the case with bis[(3-salicylideneamino)propyl]methylamine (H<sub>2</sub>smdpt) (15).<sup>[119]</sup> The eight-line hyperfine structure of square pyramidal Co(smdpt), anisotropic even at room temperature, is now easily formed. Moreover, spectral simulation yields a parameter set typical for superoxo adducts, removal of oxygen being reversible. It is not unusual to observe more pronounced spectral features when this process is repeated for Co(smdpt) in zeolite EMT, suggesting that the complexes are now being accommodated in the spacious hypercages of the hexagonal faujasite. Indeed, in the hypercage of hexagonal faujasite (EMT), more space is available and less distortion is expected compared with the supercage of cubic faujasite.<sup>[121]</sup>

Pentadentate saldien (16) complexes with Cu<sup>II</sup>, Ni<sup>II</sup>, Zn<sup>II</sup>, Cr<sup>III</sup>, Fe<sup>III</sup> and Bi<sup>III</sup> encapsulated in zeolite Y have been reported as well and have been used for the hydroxylation of phenol with H<sub>2</sub>O<sub>2</sub>.<sup>[122-124]</sup> The following sequence of decreasing activity was observed, all systems showing superior yields compared with the homogeneous case: Zn > Ni > Cu. The reported spectral features point to the

presence of a square planar structure with an unusually long Me-N bond length for the axially coordinated atom.<sup>[122,125]</sup>



VO(salen) in NaY is an effective catalyst in the room temperature epoxidation of cyclohexene with either *tert*-butylhydroperoxide<sup>[126]</sup> or hydrogen peroxide.<sup>[127]</sup> No attention, however, was paid to the long term or repeated use in batch conditions of such catalysts.

When the inclusion of complexes in NaX and Y using both the ligand and the zeolite synthesis method is compared, the former method was shown to yield higher loadings of salen complex.<sup>[128]</sup> Substitution of the aromatic H atoms of salen with Cl (Cl<sub>2</sub>salen; Cl<sub>4</sub>salen), Br or NO<sub>2</sub>, leads to an enhanced concentration of complexes, with significantly enhanced catalytic activity in the oxidation of phenol, *p*-xylene and styrene.<sup>[128]</sup> Though not understood in detail, an increased retention and stability occurs in the following sequence:

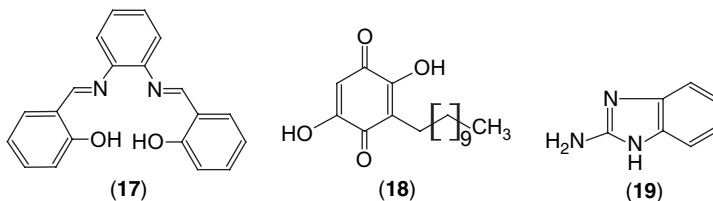


IR and UV-vis spectroscopy show that the majority of the encapsulated complexes still have structural integrity. As observed for many other oxidation catalysts, entrapment shows significantly enhanced activity. This effect is more pronounced when the degree of ligand substitution with Cl is higher. The simultaneous occurrence of two mechanisms is confirmed again, the selectivity of the encapsulated Mn(salen) complexes for the formation styrene epoxide is only 30%, the dominant product being benzaldehyde.

The mixed behaviour of such catalysts, in terms of oxo-type and allylic oxidation, was also confirmed in the oxidation of  $\alpha$ -pinene, yielding a mixture of the epoxide and the allylic oxidation product (D-verbenone). The epoxide stems from the existence of a high valent Ru(V)=O intermediate, while D-verbenone formation points to the presence of a radical chain involving peroxoruthenium as intermediate.<sup>[128,129]</sup> The activity of encapsulated H, Cl, Br, nitro-substituted Ru on and Co(salophen) (structure of ligand see insert; also known as saloph) is always at least a factor of two higher than in solution. Comparable Co/Si ratios are obtained from XPS and TGA, indicated no significant amounts of complex at the external surface.

The Co(*t*-butylsalophen) complex entrapped in zeolite Y was shown to be an essential member of electron chains designed for alcohol oxidation<sup>[130]</sup> and for the acetoxylation of 1,3-dienes with dioxygen.<sup>[131,132]</sup> The Co(*t*-butylsalophen)Y

catalyses the oxygenation of hydroquinone into quinone, which in its turn reoxidizes  $\text{Pd}^0$  formed upon diene acetoxylation with  $\text{Pd}^{\text{II}}$ .



The hybrid material consisting of  $\text{Cu}(3\text{-ethoxysalen})\text{NaY}$  prepared via the flexible ligand method, was very active for phenol and naphthol hydroxylation with aqueous hydrogen peroxide compared with the homogeneous system.<sup>[133]</sup> The deep purple colour of this pristine complex turns yellow in the zeolite intracrystalline space. Due to space restriction around the encapsulated complex, it seems to suffer from considerable distortion as substantiated by the shift to shorter wavelength of the d-d transitions around 550 nm, and the shift to higher EPR  $g_{\text{parallel}}$  values (from 2.158 to 2.186).

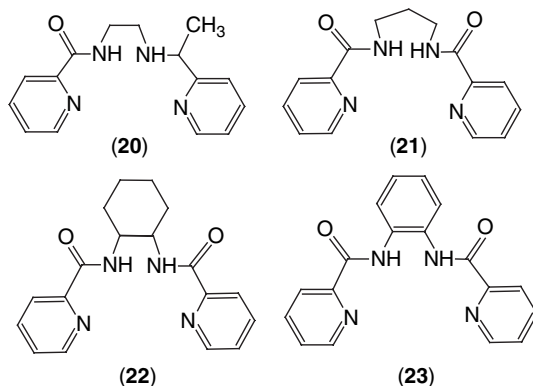
The deoxo reaction, performing the reduction of dioxygen with hydrogen, usually catalysed by a noble metal catalyst, was also reported to occur with NaY encapsulated complexes of  $\text{Cu}(\text{embelin})$  (**18**) and 2-aminobenzimidazole (**19**).<sup>[134]</sup> The  $\text{Cu}(\text{embelin})$  complex entrapped in NaY is a stable catalyst, that showing enhanced activity compared with the homogeneous case and may be reused many times, the corresponding benzimidazole complex is deactivated rapidly.

### 10.3.5 ZEOLITE EFFECTS WITH *N,N'*-BIS(2-PYRIDINECARBOXAMIDE) COMPLEXES OF MN AND FE IN ZEOLITE Y

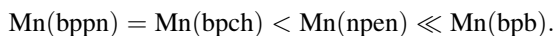
The chemical nature of the link between two 2-pyridinecarboxamide parts of several *N,N'*-bis(2-pyridinecarboxamide) complexes of Mn and Fe has been systematically changed from ethyl (bpen, **20**), to propyl (bppn, **21**), cyclohexyl (bpch, **22**), and phenyl (bpb, **23**) to examine effects, such as influence of ligand rigidity upon degree of distortion and catalyst behaviour of the complexes encapsulated in the FAU topology.<sup>[135,136]</sup>

When ligated via the flexible ligand method with the Mn ions in Y zeolite, (partial) ligand deprotonation upon complex formation occurs, resulting in hybrid catalysts which are able to oxidize alkanes and alkenes with peroxides under mild conditions with. Catalase activity, i.e. unproductive hydrogen peroxide decomposition as well as the appearance of allylic oxidation products, such as 2-cyclohexene-1-one and -1-ol, in the epoxidation of cyclohexene depend very much on the nature of the ligand. While  $\text{Mn}(\text{bpb})\text{Y}$  and  $\text{Mn}(\text{bpen})$  much decreased activity is encountered, and with  $\text{Mn}(\text{bpb})\text{Y}$  enhanced allylic oxidation is also observed the  $\text{Mn}(\text{bppn})$  and  $\text{Mn}(\text{bpch})$  encaged complexes behave as selective epoxidation catalysts. With

*tert*-butylhydroperoxide, the secondary acid-catalysed ring opening of the epoxide is suppressed as the reaction occurs in water-free conditions, though mixed ethers such as 2-*t*butoxy cyclohexan-1-ol are obtained.<sup>[135]</sup> In the oxidation cyclohexane with HOOH, Fe(bppn)Y shows enhanced activity forming cyclohexylhydroperoxide, cyclohexanone and cyclohexanol.<sup>[136]</sup>



Spectroscopic characterization of the same samples indicates that the complexes with bbpn or bpch ligands are mainly square planar ( $4 \times N$  coordination) and deprotonated, while with the bpen and bpb ligands,  $2 \times N$  coordination and double protonation is more likely.<sup>[135]</sup> The amide III band of the ligand around  $1400 \text{ cm}^{-1}$  (reflecting the C-N characteristics of C-N and N-H bending modes), is weak for Mn(bpen) and Mn(bpb), and very strong for Mn(bpch) and Mn(bppn), mirroring the degree of ligand deprotonation upon complexation. The amide II band intensity around  $1570 \text{ cm}^{-1}$  shows the same changes, being most intense for Mn(bpch) and Mn(bppn). The amide I band around  $1650 \text{ cm}^{-1}$  with mainly C=O characteristics, is very strong in each of the four cases. As the degree of ligand deprotonation and formation of undisturbed square planar  $4 \times N$  coordination occurs in parallel, the degree of complex distortion upon encapsulation is expected to increase along the sequence:



A semiquantitative indication of complex distortion is also possible with the ESR spectra of  $\text{Mn}^{\text{II}}$ . For unchelated  $\text{Mn}^{\text{II}}$  in zeolite Y, the values of the axial and rhombic parameter are small, most of the spectral intensity in X band being accumulated close to  $g_{\text{eff}} = 2$  with a broad distribution of axial sites. This is observed for the bpen and bpb complexes, while for bpch and bppn a feature around  $g = 4.3$  is prominent. The complex distortion estimated from ESR thus follows the sequence derived from IR.

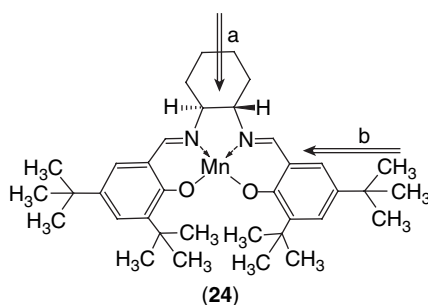
Mössbauer spectral data<sup>[136]</sup> allowed the respective amounts of complexed  $\text{Fe}^{\text{II}}$ , free  $\text{Fe}^{\text{II}}$  and Fe ions in the hexagonal prism of the faujasite structure to be

determined. The relative amount of complexed Fe again dominates for the Fe(bpch)Y system (89 %).

When the reaction mechanism is probed for adamantane oxidation, concordant information is obtained. For random attack on the 12 and 4 H atoms belonging to secondary (C2) and tertiary (C3) C atoms, respectively, a C3/C2 ratio of 0.33 should be obtained. For radical reactions, values as high as 20 have been reported due to the higher reactivity of tertiary C-H bonds, while for pure oxo chemistry reduced ratios as low as 3 were determined. With Fe<sup>II</sup>Y and Fe(bpch)Y, the respective ratios of 20 and 3.6 point to the predominant occurrence of radical and oxo chemistry, respectively.

### 10.3.6 ZEOLITE ENCAPSULATED CHIRAL OXIDATION CATALYSTS

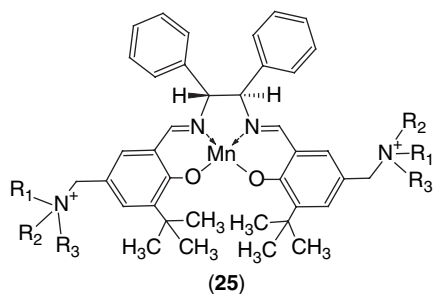
The issue of encapsulation of chiral complexes in zeolites and the retention of their enantioselective discrimination power has been reviewed recently.<sup>[1,9,137–139]</sup> Asymmetric epoxidation of prochiral olefins with substituted salen complexes perform an enantioselective oxygen transfer from mono oxygen donors, such as NaClO or PhIO, to the alkene double bond,<sup>[140]</sup> provided two factors are strictly controlled, i.e. the pathway of the approaching olefin and its conformational orientation. Based on the idea that greater steric hindrance at certain positions on the flat Me(salen) complex should result in differentiation of the approach of the alkene to the metal-oxo active site, catalysts with relatively high enantioselective inducing power were generated with a number of unfunctionalized alkenes by positioning two bulky *tert*-butyl groups at positions 5, 5' and 8, 8' of the salen plane, thus creating the preferred approach pathways a and b (**24**).<sup>[141]</sup> Although the debate is still going on as how to substitution affects stereochemistry in the epoxidation of alkenes, it is clear that the relationship is very subtle.



It is also clear that entrapment of such complexes in zeolitic cages will most likely affect the enantioselective discrimination power. Since molecular modelling predicted that the actual Jacobsen catalyst (**24**) would not fit into a supercage, an unsubstituted ligand was ligated to zeolite Mn ions (**25**).<sup>[142]</sup> Methylstyrene could be epoxidized with an epoxide yield of 4% and an ee of 58%. In analogous homogeneous conditions, a yield of 28% and an ee of 60% were achieved,



indicating that the accommodation of the complex resulted in the creation of less effective preferred pathways, compared with those of the original catalyst. Entrapment of a more congested ligand with methyl or *tert*-butyl substitution at positions 8,8' and 5,5' in the hypercage of zeolite EMT, showed results comparable to homogeneous conditions,<sup>[143]</sup> though lower activities were achieved, possibly due to diffusional limitations. With clay intercalated complexes, results comparable with homogeneous conditions were approached, although good catalyst stability was still questionable.<sup>[144]</sup> A redesigned dicationic complex, ion exchanged into the interlaminal space of montmorillonite clay, showed further enhanced ee values, (especially for styrene epoxidation) as well as enhanced stability.<sup>[145]</sup> Although it could be expected that site-isolation would reduce the vulnerability of Me(salen) towards self-oxidation, deactivation via degradation of the phenolic moieties is still at the heart of the limited operational stability.



It was also shown that mesopores surrounded by micropores, generated through ultrastabilization of ammonium-exchanged zeolite Y, were ideal hosts for transition metal salen complexes as excellent stereoselectivity was obtained in the epoxidation of  $\alpha$ -pinene with dioxygen, i.e. 100 % conversion, 96 % chemoselectivity and 91 % diastereoselective excess being obtained.<sup>[146]</sup> The catalysts were reusable and did not leach. It should be stressed that this Mukajama-type chemistry<sup>[147]</sup> is more suited to heterogeneous catalysts than Jacobsen's system.<sup>[146]</sup> To avoid extended contact and subsequent ligand destruction in the homogeneous salen complex, residing with the feed olefin in the organophilic phase, and the oxidant, NaClO is resides in the aqueous phase. In a heterogeneous triphasic system, such as with a zeolite or clay immobilized catalyst, the solid will usually prefer the aqueous phase, thus overexposing the catalyst to contact with the oxidant. The alternative use of an oxidant like *tert*-butylhydroperoxide soluble in the organic phase, will overexpose catalyst and epoxide product to the oxidant.<sup>[13,148]</sup> In the ideal case, when the solid positioned itself automatically at the interface of the aqueous and lipophilic phase, the reaction still will continue to depend on stirring rates and will be under diffusional control.

A chiral encapsulated Mn or Cu catalyst for the liquid phase oxidation of sulfides into sulfoxides or sulfones with relatively low enantioselectivity has been reported.<sup>[149,150]</sup> The catalyst is reusable and shows the generally encountered positive features, such as enhanced activity and stability, compared with the homogeneous case.

## 10.4 CONCLUSIONS

Although much of the heterogenization work of oxidation catalysts in zeolites was done in the 1990s, a recent revival in research activity is obvious.

Generally, enhanced activity of the encapsulated complex (prepared either by entrapment in zeolite micropores or mesopores or by synthesis of the zeolite around the pre-synthesized complex), is observed and assigned to zeolite sorption or concentration effects. In parallel, radical chain reactions or unproductive decomposition of hydrogen peroxide, that may occur in solution, are suppressed with the zeolite based oxidation catalysts, provided unligated transition ions are absent. Complex occlusion preferably occurs in the supercages of cubic or in the hypercages of hexagonal faujasite, yielding catalysts with thermally enhanced stability. Adaptation of the flexible guest to the rigid host in the case of space limitations results in complex distortion and incomplete coordination. Such phenomena form the basis of allylic oxidation selectivity or initiate radical chain reactions.

Zeolite encapsulated complexes catalyse the oxygenation of alkanes with peroxides according to oxo chemistry, following a mechanism very similar to the oxygen-rebound mechanism encountered in monooxygenase enzymes.

The often uncontrollable hydrolysis chemistry of Mn in aqueous solution, is attenuated by the geometry of the super- and hypercages in faujasite zeolites. This way, not only specific species are stabilized, but also new catalytically active complexes are formed.

## ACKNOWLEDGEMENTS

The authors appreciate continuous sponsorship by the Federal and Flemish Government in the frame of IAP and GOA schemes, respectively. Sponsorship by the Flemish FWO is acknowledged as well.

## REFERENCES

1. Blaser, H. U., Pugin, B., Studer, M. In *Chiral Catalyst Immobilization and Recycling*, De Vos, D. E., Vankelecom, I. F. J. and Jacobs, P. A. (eds). Wiley-VCH, Weinheim, **2000**, pp. 1–15.
2. Vankelecom, I. F. J. and Jacobs, P. A. In *Chiral Catalyst Immobilization and Recycling*, De Vos, D. E., Vankelecom, I. F. J. and Jacobs, P. A. (eds). Wiley-VCH, Weinheim, **2000**, pp. 21–28.
3. De Vos, D. E., Sels, B. F. and Jacobs, P. A. *Adv. Catal.*, **2001**, *46*, 2–87.
4. Rechavi, D. and Lemaire, M. *Chem. Rev.*, **2002**, *102*, 3495–3524.
5. Zhong-lin Lu, E., Lindner, H. A., Meyer, *Chem. Rev.* **2002**, *102*, 3543–3578.
6. Wight, A. P., Davis, M. E. *Chem. Rev.* **2002**, *102*, 3589–3614.
7. De Vos, D. E., Dams, M., Sels, B. F., Jacobs, P. A. *Chem. Rev.* **2002**, *102*, 3589–3614.
8. Corma, A., Garcia, H. *Chem. Rev.* **2002**, *102*, 3837–3892.
9. Corma, A., Garcia, H. *Eur. J. Inorg. Chem.* **2004**, 1143–1164.

10. Sheldon, R. A., Downing, R. S. *Appl. Catal., A*, **1999**, *189*, 163–183.
11. Schüth, F., Wingen, A., Sauer, J. *Microporous Mesoporous Mater.* **2001**, *44–45*, 465–476.
12. Wahlen, J., Wuyts, S., Dams, M., Jacobs, P., De Vos, D. *Stud. Surf. Sci. Catal.* **2005**, *158*, 1213–1222.
13. Jacobs, P. A. *Stud. Surf. Sci. Catal.* **2005**, *157*, 289–310.
14. McQuarry, D. In *Handbook of Green Chemistry and Technology*, J. Clark and D. McQuarry (eds). Blackwell, 2002, pp. 120–149.
15. Sels, B. F., De Vos, D. E., Jacobs, P. A. *Catal. Rev.* **2001**, *43*, 443–488.
16. De Vos, D. E., Jacobs, P. A. *Stud. Surf. Sci. Catal.* **2001**, *137*, 957–985.
17. Beneke, M., Jaeger, N. I., Schulz-Ekkloff, G. In *Host–Guest Systems Based on Nanoporous Crystals*, F. Laeri (ed). Wiley-VCH Weinheim, **2003**, pp. 165–182.
18. Guzman, J., Gates, B. C. *Dalton Trans.* **2003**, 3308–3318.
19. Hölderich, W. F., Wagner, H. H., Valkenberg, M. H. *Spec. Publ.-R. Soc. Chem.* **2001**, *266*, 76–93.
20. Brunel, D. *Spec. Publ.-R. Soc. Chem.* **2001**, *266*, 38–27.
21. Schulz-Ekkloff, G., Ernst, S. In *Preparation of Solid Catalysts*, G. Ertl, H., Knözinger, J., Weitkamp (eds). Wiley-VCH Weinheim, **1999**, pp. 405–427.
22. Louis, C., Che, M. *Preparation of Solid Catalysts*, Ertl, G., Knözinger, H., Weitkamp J. (eds). Wiley-VCH Weinheim, **1999**, pp. 341–355.
23. Bein, T. *Curr. Opinion Sol. St. Mater. Sci.* **1999**, *4*, 85–96.
24. De Vos, D. E., Sels, B. F. *Adv. Synth. Catal.* **2003**, *345*, 457–473.
25. De Vos, D., Jacobs, P. A. *Stud. Surf. Sci. Catal.* **2004**, *154A*, 66–79.
26. Raja, R., Thomas, J. M. *J. Mol. Catal., A*, **2002**, *181*, 3–14.
27. Corma, A., Garcia, H. *Chem. Rev.* **2003**, *103*, 4307–4365.
28. Dusi, M., Mallat, T., Baiker, A. *Catal. Rev.-Sci. Eng.* **2000**, *42*, 213–278.
29. De Vos, D. E., Jacobs, P. A. *Stud. Surf. Sci. Catal.* **2001**, *137*, 957–986.
30. Ziolek, M. *Catal. Today* **2004**, *90*, 145–150.
31. Clerici, M. G. *Chim. Industr. (Milan)* **2003**, *85*, 55–66.
32. Clerici, M. G. *Stud. Surf. Sci. Catal.* **1993**, *78*, 21–33; Ratnasamy, P., Srinivas, D., Knoezinger, H. *Adv. Catal.* **2004**, *48*, 1–169.
33. Reddy, J. S., Sayari, A. *Chemical Industries*. Marcel Dekker, **1997**, Vol. 69, pp. 405–415.
34. Parmon, V. N., Panov, G. I., Uriarte, A., Noskov, A. S. *Catal. Today* **2005**, *100*, 115–131.
35. Bellussi, G., Rigutto, M. S. *Stud. Surf. Sci. Catal.* **2001**, *137*, 911–955.
36. Sheldon, R. A., Wallau, M., Arends, I. W. C. E., Schuchardt, U. *Acc. Chem. Res.* **1998**, *31*, 485–493.
37. Ratnasamy, P., Raja, R., Srinivas, D. *Phil. Trans. R. Soc. London, Ser. A*, **2005**, *363*, 1001–1012.
38. Thomas, J. M., Raja, R., Sankar, G., Bell, R. G. *Nature* **1999**, *398*, 227–230.
39. Boronat, M., Concepcion, P., Corma, A., Renz, M., Valencia, S. *J. Catal.* **2005**, *234*, 11–118.
40. Corma, A., Nemeth, L. T., Renz, M., Valencia, S. *Nature* **2001**, *412*, 423–425.
41. Wahlen, J., De Hertogh, S., De Vos, D. E., Nardello, V., Bogaert, S., Aubry, J.-M., Alsters, P., Jacobs, P. A. *J. Catal.* **2005**, *233*, 422–433.
42. Wahlen, J., De Vos, D. E., De Hertogh, S., Nardello, V., Aubry, J.-M., Alsters, P., Jacobs, P. A. *Chem. Commun.* **2005**, 927–929.
43. Wahlen, J., De Vos, D. E., Jacobs, P. A., Alsters, P. L. *Adv. Synth. Catal.* **2004**, *346*, 152–164.
44. Fazio, O., Gnida, M., Meyer-Klaucke, K., Frank, W., Klaui, W., Wolfgang, *Eur. J. Inorg. Chem.* **2002**, 2891–2896.

45. [http://topaz.ethz.ch/IZA-SC/FMPro?-db=Atlas\\_main.fp5&-lay=web%20layout&-format=FWtopology.htm](http://topaz.ethz.ch/IZA-SC/FMPro?-db=Atlas_main.fp5&-lay=web%20layout&-format=FWtopology.htm) FAU&-find.
46. Romanovski, B. V. In *Proceedings of the 5th International Symposium on Relations in Homogeneous and Heterogeneous Catalysis*, Novosibirsk, Yu., Yermakoc and Likholobov, V. (eds). VNU Science Press, Utrecht, **1986**, p. 343.
47. Zakharov, V. Yu., Romanovski, B. V. *Vestik Moscow University, Ser. Khim.* **1977**, *18*, 143–151.
48. Meier, G., Wörle, D., Mohl, M., Schulz-Ekloff, G. *Zeolites* **1984**, *4*, 30–34.
49. Herron, N. *Chemtech* **1989**, *19*, 542–546.
50. Srinivas, D., Sivasanker, S. *Catal. Surv. Asia* **2003**, *7*, 121–132.
51. Parton, R. F., Thibault-Starzyk, F., Reynders, R. A., Grobet, P. J., Jacobs, P. A., Bezoukhanova, C. P., Sun, W., Wu, Y. *J. Mol. Catal., A*, **1995**, *97*, 183–186.
52. Seelan, S., Sinha, A. K., Srinivas, D., Sivasanker, S. *J. Mol. Catal., A*, **2000**, *157*, 163–171.
53. Herron, N. *Inorg. Chem.*, **1986**, *25*, 4714–4717.
54. De Vos, D. E., Thibault-Starzyk, F., Knops-Gerrits, P. P., Parton, R. F., Jacobs, P. A. *Macromol. Symp.*, **1994**, *80*, 157–184.
55. Parton, R. F., Bezoukhanova, C. P., Grobet, P. J., Grobet, J., Jacobs, P. A. *Stud. Surf. Sci. Catal.* **1994**, *83*, 371–378.
56. Fish, K. M., Avaria, G. E., John, T. J. T. *Microsomes Drug Oxid., Proc. Int. Symp.*, *7th* **1988**, 176–183; Groves, J. T. *J. Chem. Educ.*, **1985**, *62*, 928–31.
57. Parton, R. F., Vankelecom, I., Bezoukhanova, C. P., Casselman, M., Uytterhoeven, J. B., Jacobs, P. A. *Nature*, **1994**, *370*, 541–544.
58. Valente, A. A., Vital, J. *Stud. Surf. Sci. Catal.* **1997**, *108*, 461–468.
59. Thibault-Starzyk, F., Van Puymbroeck, M., Parton, R. F., Jacobs, P. A. *J. Mol. Catal., A*, **1996**, *109*, 75–79.
60. Schulz-Ekloff, G., Wohrle, D., Andreev, A. *DECHEMA Monogr.* **1991**, *122*, 205–17.
61. Iliev, V., Ileva, A. I., Bilyarska, L. *J. Mol. Catal., A*, **1997**, *126*, 99–108.
62. Seelan, S., Srinivas, D., Agashe, M. S., Jacob, N. E., Sivasanker, S. *Stud. Surf. Sci. Catal.*, **2001**, *135*, 2224–2230.
63. Langendries, G., Claessens, R., Baron, G. V., Parton, R. F., De Vos, D. E., Jacobs, P. A. *Fundam. Adsorpt.*, **1998**, *6*, 389–394.
64. De Vos, D. E., Baron, G. V., Van Laer, F., Jacobs, P. A. In *Nanostructured Catalysts*, Scott, S. L., Crudden, C. M. and Jones, C. W. (eds). Kluwer / Plenum, New York, 2003, pp. 311–328.
65. Raja, R., Ratnasamy, P. *Stud. Surf. Sci. Catal.* **1996**, *100*, 181–190.
66. Seelan, S., Siha, A. K., Srinivas, D., Sivasanker, S. *Bull. Catal. Soc. India* **2002**, *1*, 29–37.
67. Balkus Jr, K. J. *Phthalocyanines* **1996**, *4*, 285–305.
68. Balkus Jr, K. J., Eissa, M., Lavado, R. *Chemical Industries*, Marcel Dekker, **1997**, Vol. 69, 363–378.
69. Balkus Jr, K. J., Khanmamedova, A. K., Dixon, K. M., Bedioui, F. *Appl. Catal., A*, **1996**, *143*, 159–173.
70. Balkus Jr, K. J., Eissa, M., Levado, R. *J. Am. Chem. Soc.* **1995**, *117*, 10753–10754.
71. [http://topaz.ethz.ch/IZA-SC/FMPro?-db=Atlas\\_main.fp5&-lay=web%20layout&-format=FWtopology.htm&STC=VFI&-find](http://topaz.ethz.ch/IZA-SC/FMPro?-db=Atlas_main.fp5&-lay=web%20layout&-format=FWtopology.htm&STC=VFI&-find).
72. Parton, R. F., Thibault-Starzyk, F., Reynders, R. A., Grobet, P. J., Jacobs, P. A., Bezoukhanova, C. P., Sun, W., Wu, Y. *J. Mol. Catal., A*, **1995**, *97*, 183–186.
73. Parton, R. F., Bezoukhanova, C. P., Thibault-Starzyk, F., Reynders, R. A., Grobet, P. J., Jacobs, P. A. *Stud. Surf. Sci. Catal.* **1994**, *4*, 813–820.

74. Nakamura, M., Tatsumi, T., Tominaga, H. *Bull. Chem. Soc. Japan* **1990**, *63*, 3334.
75. Mansuy, D. and Battoni, P. *The Porphyrin Handbook*, Kadish, K. M., Smith, K. M. and Guillard, R. (eds). Academic Press, New York, **2000**, Vol. 4, Ch.26.
76. Wark, M. *Porphyrim Handbook*. Academic Press, San Diego, **2003**, Vol. **17**, pp. 247–283.
77. Nagiev, T. M., Gasanova, L. M., Sulfugarova, S. Z., Mustefaeva, C. A., Abbasov, A. A. *Chem. Eng. Commun.* **2003**, *190*, 726–748.
78. Khan, T. A., Hriljac, J. A. *Inorg. Chim. Acta* **1999**, *294*, 179–182.
79. Skrobot, F. C., Rosa, I. L. V., Marques, A. P. A., Martins, P. R., Rocha, J., Valente, A. A., Iamamoto, Y. *J. Mol. Catal., A*, **2005**, *237*, 86–92.
80. Zhan, B., Li, X. *Chem. Commun.* **1998**, 349–350.
81. Balkus, K. J., Gabrielov, A. G. *J. Incl. Phenom. Mol. Recogn. Chem.* **1995**, *21*, 159.
82. Poltowicz, J., Haber, J. *J. Mol. Catal., A*, **2004**, *220*, 43–51.
83. Grinstaff, M. W., Hill, M. G., Labinger, Y. A., Gray, H. B. *Science* **1994**, *264*, 1311–1313.
84. Hassanein, M., Serges, S., Abdo, M., El-Khalafy, S. *J. Mol. Catal., A*, **2005**, *240*, 22–26.
85. Crestini, C., Pastorini, A., Tagliatesta, P. *J. Mol. Catal., A*, **2004**, *208*, 195–202.
86. Bedoui, F. *Coord. Chem. Rev.* **1995**, *144*, 39–68.
87. Barloy, L., Lallier, J. P., Battioni, P., Mansuy, D., Piffard, Y., Tournoux, M., Valim, J. B., Jones, W. *New J. Chem.* **1992**, *16*, 71–80.
88. De Vos, D. E., Jacobs, P. A. *Catal. Today* **2000**, *57*, 105–114.
89. Bossek, U., Wiegardt, K., Nuber, B., Weiss, J. *Inorg. Chem. Acta* **1989**, *165*, 123–129.
90. Wiegardt, K. *Angew. Chem., Int. Ed. Engl.* **1994**, *33*, 725–728.
91. Knops-Gerrits, P. P., De Vos, D. E., Thibault-Starzyk, F., Jacobs, P. A. *Nature*, **1994**, *369*, 543–546.
92. Knops-Gerrits, P. P., De Vos, D. E., Jacobs, P. A. *J. Mol. Catal., A*, **1997**, *117*, 57–70.
93. Knops-Gerrits, P. P., Yhibault-Starzyk, F., Jacobs, P. A. *Stud. Surf. Sci. Catal.*, **1994**, *84*, 1411–1418.
94. Knops-Gerrits, P. P., Toufar, H., Jacobs, P. A. *Stud. Surf. Sci. Catal.*, **1997**, *105*, 1109–1115.
95. Fan, B., Cheng, W., Li, R. *Stud. Surf. Sci. Catal.*, **2001**, *135*, 297 (21-P-11).
96. Alizadeh, M., Farzaneh, F., Ghandi, M. *J. Mol. Catal., A*, **2003**, *194*, 283–287.
97. Knops-Gerrits, P. P., Trujillo, C. A., Zhan, B. Z., Li, X. Y., Rouxhet, P., Jacobs, P. A. *Top. Catal.* **1996**, *3*, 437–449.
98. Shul'pin, G. B., Attanasio, D., Suber, L. *J. Catal.* **1993**, *142*, 147–152.
99. Niassary, M. S., Farzanheh, F., Gandhi, M. *J. Mol. Catal., A*, **2001**, *175*, 105–110.
100. De Wilde, W., Peeters, G., Lunsford, J. H. *J. Phys. Chem.* **1980**, *85*, 2306–2310.
101. Dutta, P. K., Incavo, J. A. *J. Phys. Chem.* **1987**, *91*, 4443–4446.
102. Fan, B., Fan, W., Li, R. *J. Mol. Catal., A*, **2003**, *201*, 137–144.
103. Ganesan, R., Viswanathan, B. *J. Phys. Chem. B* **2004**, *108*, 7102–7114.
104. Xavier, K. O., Chacko, J., Yusuff, K. K. M. *Appl. Catal., A*, **2004**, *258*, 251–259.
105. Wiegardt, K. *Angew. Chem. int. Ed. Engl.* **1989**, *28*, 1153–1159.
106. Hage, R., Ibutg, J. E., Kerschner, J., Koek, J. H., Lempers, E. L. M., Martens, R. J., Racherla, U. S., Russell, S. W., Swarthoff, T., van Vliet, M. R. P., Warnaar, J. B., van der Wolf, L., Krijnen, B. *Nature* **1994**, *369*, 637–638.
107. Quee-Smith, V. C., DelPizzo, L., Jureller, S. H., Kerschner, J. L., Hage, R. *Inorg. Chem.* **1996**, *35*, 6461–6465.
108. De Vos, D. E., Sels, B. F., Reynaers, M., Subba Rao, Y. V., Jacobs, P. A. *Tetrahedron Lett.* **1998**, *39*, 3221–3224.
109. De Vos, D. E., Bein, T. *J. Am. Chem. Soc.* **1997**, *119*, 9460–9465.

110. De Vos, D. E., Meinershagen, J. L., Bein, T. *Angew. Chem. Int. Ed. Engl.* **1996**, *35*, 2211–2213.
111. Bennur, T. H., Srinivas, D., Sivasanker, S. *J. Mol. Catal., A*, **2004**, *207*, 163–171.
112. Drehsel, S. M., Kaminski, R. C. K., Nakagaki, S., Wypich, F. *J. Coll. Interf. Sci.* **2004**, *277*, 138–145.
113. De Vos, D. E., Vanoppen, D. L., Li, X. Y., Libbrecht, S., Bruynseraede, Y., Knops-Gerrits, P. P., Jacobs, P. A. *Chem. Eur. J.* **1995**, *1*, 144–149.
114. Schoonheydt, R. A., Velghe, F., Uytterhoeven, J. B. *Inorg. Chem.* **1979**, *18*, 1842–1847.
115. Imamura, S., Lunsford, J. H. *Langmuir* **1985**, *1*, 326–330.
116. Taylor, R. J., Drago, R. S., Hage, J. P. *Inorg. Chem.*, **1992**, *31*, 253–258.
117. Bowers, C., Dutta, P. K. *J. Catal.* **1990**, *122*, 271–279.
118. Herron, N. *Inorg. Chem* **1986**, *25*, 4714–4717.
119. De Vos, D. E., Thibault-Starzyk, F., Jacobs, P. A. *Angew. Chem. Int. Ed. Engl.* **1994**, *33*, 431–433; De Vos, D. E., Feyen, E. P. J., Schoonheydt, R. A., Jacobs, P. A. *J. Am. Chem. Soc.* **1994**, *116*, 4746–4752.
120. Srinivasan, K., Perrier, S., Kochi, J. K. *J. Mol. Catal.* **1986**, *36*, 297–317.
121. [http://topaz.ethz.ch/IZA-SC/FMPro?-db=Atlas\\_main.fp5&-lay=web%20layout&-format=FWtopology.htm&STC=EMT&-find](http://topaz.ethz.ch/IZA-SC/FMPro?-db=Atlas_main.fp5&-lay=web%20layout&-format=FWtopology.htm&STC=EMT&-find)
122. Maurya, M. R., Titinchi, S. J. J., Chand, S. *J. Mol. Catal., A*, **2003**, *201*, 119–130.
123. Maurya, M. R., Titinchi, S. J. J., Chand, S. *J. Mol. Catal., A*, **2003**, *193*, 165–176.
124. Maurya, M. R., Titinchi, S. J. J., Chand, S., Mishra, I. M. *J. Mol. Catal., A*, **2002**, *180*, 1201–209.
125. Maurya, M. R., Titinchi, S. J. J., Chand, S. *Appl. Catal., A*, **2002**, *228*, 177–185.
126. Balkus Jr, K. J., Khanmamedova, A. K., Dixon, K. M., Bedioui, F. *Appl. Catal., A*, **1996**, *143*, 571–579.
127. Kozlov, A., Asakura, K., Iwasawa, Y. *Microporous Mesoporous Mater.* **1998**, *21*, 571–579.
128. Jacob, C. R., Varkey, S. P., Ratnasami, P. *Microporous Mesoporous Mater.* **1998**, *22*, 465–474.
129. Joseph, T., Sawant, D. P., Gopinath, C. S., Halligudi, S. B. *J. Mol. Catal., A*, **2002**, *184*, 289–299.
130. Zsigmond, A., Ntheisz, F., Frater, Z., Bäckvall, J. E. *Stud. Surf. Sci. Catal.* **1997**, *108*, 453.
131. Wöltinger, J., Bäckvall, J. E., Zsigmond, A. *Chem. Eur. J.* **1999**, *5*, 1460.
132. Zsigmond, A., Notheisz, F., Szegetes, Z., Bäckvall, J. E. *Stud. Surf. Sci. Catal.* **1994**, *94*, 728.
133. Saha, P. K., Koner, S. *Inorg. Chem. Commun.* **2004**, *7*, 1164–1166.
134. Abraham, R., Yusuff, K. K. M. *J. Mol. Catal., A*, **2003**, *198*, 175–183.
135. Knops-Gerrits, P. P., L'Abbé, M., Jacobs, P. A. *Stud. Surf. Sci. Catal.* **1997**, *108*, 445–452.
136. Knops-Gerrits, P. P., L'Abbé, M., Leung, W. H., Van Bavel, A. M., Langouche, G., Bruynseraede, Y., Jacobs, P. A. *Stud. Surf. Sci. Catal.*, **1996**, *101*, 811–118.
137. Corma, A. *Catal. Rev.* **2004**, *46*, 369–417.
138. McMorn, P. C., Hutchings, G. J. *Chem. Soc. Rev.* **2004**, *33*, 108–122.
139. Li, C. *Catal. Rev.* **2004**, *46*, 419–492.
140. Zhang, W., Loebach, J. L., Wilson, S. R., Jacobsen, E. N. *J. Am. Chem. Soc.* **1990**, *112*, 2801–2802.
141. Zhang, W., Jacobsen, E. N. *J. Org. Chem.* **1991**, *56*, 2296–2299.
142. Sabater, M. S., Corma, A., Domenech, A., Forneés, V., Garcia, H. *Chem. Commun.* **1997**, 1285–1286.
143. Ogunwumi, S. B., Bein, T. *Chem. Commun.* **1997**, 901–902.

144. Fraile, J. M., Garcia, J. I., Massam, J., Mayoral, J. A. *J. Mol. Catal., A*, **1998**, *123*, 136–144.
145. Kursehy, R. I., Khan, N. H., Abdi, S. H. R., Singh, A. S., Jasra, R. V. *Catal. Lett.* **2003**, *91*, 207–210.
146. Schuster, C., Hölderich, W. F. *Catal. Today* **2000**, *60*, 193–207.
147. Mukaijama, T., Yamada, T., Imagawa, K., Nagata, T. *Chem. Lett.* **1992**, *11*, 2231–2232.
148. De Vos, D. E., Sels, B. F., Van Rhijn, W. M., Jacobs, P. A. *Stud. Surf. Sci. Catal.* **2000**, *130A*, 140.
149. Alcon, M. J., Corma, A., Iglesias, M., Sanchez, F. *J. Mol. Catal.* **2002**, *178*, 253–266.
150. Alcon, M. J., Corma, A., Iglesias, M., Sanchez, F. *J. Mol. Catal.* **2003**, *194*, 137–152.

---

# Subject Index

---

- Acetylation 16, 45, 53, 57, 59, 60, 63,  
69–83, 85, 89–91, 95, 99  
mechanism 57, 76  
of anisole 16, 57, 71, 75, 76, 90, 99  
of 2-methoxynthalene 57, 70  
of veratrole 81
- Acid sites 16, 39, 49, 60, 76, 89, 96, 102,  
107, 108, 111, 117, 118, 126, 128–130,  
133, 166, 172  
accessibility 16  
strength 15, 49, 79, 130, 172
- Acidity 11, 14, 16, 49, 102, 112, 116, 127,  
129, 133, 148, 163–165, 167, 177, 182,  
187, 210, 214, 218, 221
- Acylation 54, 69, 70, 75, 80–82, 85–87,  
89, 95–99, 101, 102
- Adsorbent properties 143
- Adsorption 18, 21, 27, 41, 43, 45,  
47–50, 53–61, 78, 79, 87, 89, 97,  
99, 100, 111, 117, 130, 141,  
172–175, 190, 194, 208, 209,  
214–216
- Alkoxylation 126, 180
- Alkylation 43, 98, 151, 187, 226
- Aromatization 126
- Base catalysis 172, 194  
catalyst characterization 172  
hydrotalcite 172, 183  
layered double hydroxides 183, 209  
metal oxides 175, 177  
probe molecules 174  
test reactions 172
- Batch catalysis 45
- BEA (zeolite Beta) 58
- Beckmann rearrangement 167
- Benzoylation 95–98, 101, 102
- Bifunctional catalysis 157  
hydrogenation 158, 165, 182  
one-pot transformations 158,  
166  
oxidation 166
- Carbohydrates 141, 153–154  
dehydration 145, 146, 147  
hydrolysis 142, 143, 144, 150  
hydrogenation 151–153  
isomerization 144  
oxidation 153
- Catalyst 11, 17, 19, 20, 22–30, 39,  
42–53, 55, 58, 60–63, 69, 75, 76, 79,  
81, 82, 85, 89–91, 96–99, 101, 102,  
106–118, 125–135, 143–149, 151,  
153, 154, 157, 158, 163–167, 175–182,  
187–190, 192–195, 207, 208, 209,  
211, 214, 216, 218, 219, 225, 230,  
231, 233–235  
deactivation 61  
preparation 2, 4, 13, 16, 19, 28, 29, 69,  
90, 166, 176, 179, 182, 188  
activation 44, 46, 90
- Chiral 10, 19, 23–25, 33, 35–38, 188, 194,  
202, 205
- Coking 62
- Competitive adsorption 57, 60, 79, 100,  
173



- Confinement effects 61  
Crystallite size 43, 78, 80, 148, 177
- Deactivation 61, 118  
  pore blockage 41  
Deacylation-acylation mechanism 78  
Dealumination 28, 43, 62, 80, 117,  
  128  
Diels-Alder reactions 29  
Disproportionation 126, 184
- Electronic effects 101  
Esterification 47, 83, 84, 183,  
  187  
Ethylbenzene 96, 225, 226  
Extra-framework aluminium species 47,  
  62, 80  
Extra-large pore zeolites 11–13
- FAU (zeolite Y) 58  
Fixed bed reactor 41, 44, 51, 52, 76, 79,  
  80, 82–84, 87, 90, 158, 164  
Flow mode catalysis 51  
Fries rearrangement 53, 56, 69, 82–84, 87,  
  97, 98
- Hydration 3  
Hydrogenation 21, 24–26, 129, 151–153,  
  158, 163–166, 182  
Hydrolysis 4, 41, 44, 58, 87, 101, 142–144,  
  149–151, 153, 164, 165, 177, 191, 214,  
  235  
Hydrolysis-condensation reaction 4  
Hydrotalcites 144, 145, 172, 179, 181,  
  183  
Hydroxylation 60, 61, 210, 215, 226,  
  229, 231
- Ion-exchange 7, 18, 21, 25, 87, 133,  
  143, 144, 146, 163, 166, 184, 209,  
  214, 221  
Isomerization 56, 77–79, 81, 126, 134,  
  172–174, 178, 181, 214
- Knoevenagel reaction 179
- MCM22 50  
MCM41 8, 18, 25, 61, 76, 131, 135, 151,  
  181, 190
- Medium pore zeolites 78, 127, 167  
Meerwein Ponndorf Verley reduction 185  
Mesoporous catalysts 11, 141, 142,  
  144  
Mesoporous materials 2, 7, 8, 11, 13, 16,  
  19–21, 25, 26, 29, 141, 148, 154, 158,  
  167, 191, 194  
Metal complexes encapsulation of 27  
MFI 4, 47, 70, 77, 89, 131, 135, 153, 163,  
  166  
Modified zeolites 133, 164  
  by Ti 167  
  by Zn 113  
Molecular sieves 39, 43, 50, 60–64,  
  72, 77, 131, 135, 153, 158, 163,  
  167, 210  
MOR (zeolite mordenite) 47, 79, 95
- Nitration 105–107, 109, 113  
  of deactivated aromatic compounds 109  
  liquid phase 107  
  vapour phase 116  
Nitronaphthalene 113
- Olefin conversion 126, 129  
  aromatization 126  
  catalytic membranes 131  
  epoxidation 60, 184, 188, 194, 220–223,  
  225, 226, 230, 233  
  oligomerization 125, 127  
Oxidation 50, 60, 61, 153, 166, 167,  
  190, 209, 211, 214, 219, 223, 228,  
  233  
  aza ligands 224, 225  
  chiral 233–235  
  encapsulated complexes 215, 216,  
  220  
  metallo-phthalocyanines 211, 215  
  Schiff base-type ligands 228
- Photocatalyst 223
- Redox catalysis 40, 158
- SAPO catalysts 129, 163  
Selective reduction 184  
Shape selectivity 15, 43, 72, 79, 96, 108,  
  117, 128, 141, 148  
Solvent effects 88  
Stereoelectronic effects 143, 149, 151

- Synthesis 1-4, 6-10, 14, 15, 17-19, 24, 27,  
29, 39, 40, 43-47, 51, 60-64, 70, 74,  
76, 81, 83, 84, 89-91, 105, 115, 131,  
132, 141, 144, 147, 150, 151, 154, 158,  
163, 165, 167, 168, 171, 177, 179, 183,  
184, 186, 190-194, 215-219, 230
- of alcohols 129
- of aromatic ketones 95
- of fragrances 168
- of esters, *See* Esterification
- Template effects 7
- zeolite synthesis 2, 215, 217, 219,  
230
- mesoporous oxides synthesis 7
- VPI-5 12, 215
- Zeolite synthesis 1-3, 215, 217, 219,  
230
- ZSM5 133, 146